THESIS

MAXIMIZING THE UTILITY OF AVAILABLE ROOT ZONE SOIL MOISTURE DATA FOR DROUGHT MONITORING PURPOSES IN THE UPPER COLORADO RIVER BASIN AND WESTERN HIGH PLAINS, AND ASSESSING THE INTERREGIONAL IMPORTANCE OF ROOT ZONE SOIL MOISTURE ON WARM SEASON WATER BALANCE

Submitted by

Peter Goble

Department of Atmospheric Science

In partial fulfillment of the requirements

For the Degree of Master of Science

Colorado State University

Fort Collins, Colorado

Spring 2016

Master's Committee:

Advisor: Russ Schumacher

Scott Denning
José Chávez

ABSTRACT

MAXIMIZING THE UTILITY OF AVAILABLE ROOT ZONE SOIL MOISTURE DATA FOR DROUGHT MONITORING PURPOSES IN THE UPPER COLORADO RIVER BASIN AND WESTERN HIGH PLAINS, AND ASSESSING THE INTERREGIONAL IMPORTANCE OF ROOT ZONE SOIL MOISTURE ON WARM SEASON WATER BALANCE

Root Zone Soil Moisture (RZSM) data have both drought monitoring and seasonal forecasting applications. It is the lifeblood of vegetation, an integral component of the hydrologic system, a determining factor in irrigation requirements, and works to govern the means by which energy imbalances are settled between land and atmosphere. The National Integrated Drought Information System (NIDIS) has worked in conjunction with the Colorado Climate Center to improve regional drought early warning through enhanced monitoring and understanding of RZSM. The chief goals of this research have been as follows: 1. Examine regional drought monitoring in the Upper Colorado River Basin and eastern Colorado with specific inquiry as to soil moisture's role in the process. 2. Develop operational products that can be used to improve the weekly drought monitoring process in the Upper Colorado River Basin and eastern Colorado with an emphasis on utilization of soil moisture data. 3. Review in-situ soil moisture data from high elevation Snow Telemetry measurement sites in Colorado in order to understand the descriptive climatology of soil moisture over the Colorado Rockies. 4. Compare output from soil sensors installed by the Snow Telemetry and Colorado Agricultural Meteorological Network using current calibration methods in order to better understand application of direct comparison

between output from the two different sensor types. Engineer a soil moisture core measurement protocol that is reliable within ten percent of the true volumetric water content value. This protocol, if successful on a local plot, will be expanded to alpha testers around the United States and used by the USDA for drought monitoring as well as NASA for ground validation of the Soil Moisture Active Passive (SMAP) Satellite. 5. Expose the seasonality and spatial variability of positive feedbacks that occur between RZSM and the atmosphere across the Upper Colorado River Basin and western High Plains using reanalysis data from the North American Land Data Assimilation System Phase-2 (NLDAS).

Regional drought monitoring was found to involve assimilation of data from a bevy of sources. The decision-making process includes assessment of precipitation, soil moisture, snowpack, vegetative health, streamflow, reservoir levels, reference evapotranspiration, surface air temperature, and ground reports from the regional agricultural sector. Drought monitoring was expanded upon in this research through the development of several products intended for future Colorado Climate Center use. In-situ soil moisture timeseries are now being created from select SNOTEL and SCAN measurement sites. Reservoir monitoring graphics are being produced to accompany spatial analyses downloaded from the bureau of reclamation. More soil moisture data is being used, and now come from an ensemble of models rather than just the VIC model.

While only ten years of data were collected in analyzing the descriptive soil moisture climatology of the Colorado Rockies, these data were telling in terms of the expected seasonal cycle of soil moisture at high elevations. SNOTEL measurements reveal that soil moisture levels peak prior to snowmelt, large decreases in soil moisture are expected in June and early July, a slight recovery is anticipated in association with the North American Monsoon, and the sign of near-surface water balance flips back to positive in the first two weeks of September before soils freeze. Seasonal variance and distribution of volumetric water content varies in ways that are useful to understand from a drought monitoring standpoint. The data show that measurements are affected when soil freezes.

Comparing output from soil sensor relays using sensor types and calibration methods consistent with current SNOTEL and CoAgMet specifications revealed large differences in output regardless of being subject to the same meteorologic conditions.

Soil moisture measurement protocol development proved to be a trial and error process. The data collected at Christman Field was not sufficient proof that soil coring results did come within ten percent of ground truth perhaps due to microscale variations in infiltration. It was possible to develop a protocol of an acceptable standard that could be followed by citizen scientist for an estimated cost of $50.

Results from statistical modeling of post-processed NLDAS data from the last 30 years point primarily to a time frame between May and July in which soil moisture anomalies become significantly correlated with seasonal temperature and precipitation anomalies. This time of year is partially characterized by a climatologic maximization of downwelling solar radiation and a northward recession of the polar jet, but also precedes the anticipated arrival of the North American Monsoon. Correlations appear to be due to a climatologically-expected transition between energy-limited and moisture-limited evaporation regimes that propagates from south to north and from low elevations to high elevations over the course of the first half of the summer. Coupling between RZSM and precipitation exudes a substantial amount of interregional variation, but if issued at the optimum time of year, seasonal precipitation forecasts can be improved by 4-14%. Furthermore, careful monitoring of RZSM before and during this time of year can improve drought early warning capability by flagging areas that are at risk of experiencing exacerbated drought through soil moisture feedbacks.

ACKNOWLEDGEMENTS

SPECIAL THANKS TO:

COLORADO STATE UNIVERSITY

OUR FUNDERS: THE NATIONAL INTEGRATED DROUGHT INFORMATION SYSTEM (NIDIS) AWARD NUMBERS NA09OAR320074 AND NA14OAR43201, PRISM CLIMATE GROUP, COLORADO AGRICULTURAL EXPERIMENT STATION

MAJOR DATA SOURCES: THE NATIONAL ATMOSPHERIC & OCEANIC ADMINISTRATION (NOAA), AND THE NATIONAL AERONAUTICS & SPACE ADMINISTRATION (NASA)

ADVISOR: NOLAN J. DOESKEN

ADVISOR: DR. RUSS S. SCHUMACHER

COMMITTEE MEMBERS: DR. JOSÉ CHÁVEZ AND DR. SCOTT DENNING

NOTABLE OUTSIDE CONTRIBUTORS: DR. GREG BUTTERS (CSU) AND DR. MIKE HOBBINS (NOAA BOULDER)

COLORADO CLIMATE CENTER

SCHUMACHER RESEARCH GROUP

FAMILY, FRIENDS, AND COLLEAGUES

TABLE OF CONTENTS

THE DROUGHT MONITORING PROCESS

Monitoring Drought Across the United States: The American Meteorological Society defines drought as "A period of abnormally dry weather sufficiently long enough to cause a serious hydrological imbalance (American Meteorological Society 2015)." The glossary goes on to say the following:

> "Drought is a relative term; therefore any discussion in terms of precipitation deficit must refer to the particular precipitation-related activity that is under discussion. For example, there may be a shortage of precipitation during the growing season resulting in crop damage (agricultural drought), or during the winter runoff and percolation season affecting water supplies (hydrological drought) (American Meteorological Society 2015)."

Established in 1999, the U.S. Drought Monitor is a weekly effort to appraise drought conditions. The organizations responsible for producing and maintaining the United States Drought Monitor (USDM) are the National Oceanic and Atmospheric Administration (NOAA), the United States Department of Agriculture (USDA), and the National Drought Mitigation Center (NDMC), but there are over 350 organizations nationwide that contribute (U.S. Drought Monitor 2015).

The socioeconomic gravity of the data provided by the USDM is substantial. In the period from 2008 to 2011 the Department of Agriculture used USDM data in order to distribute $1.64 billion in drought relief to suffering agricultural entities. Following the crippling summer drought of 2012 the USDA made receiving relief funds nearly automatic for counties which the USDM deem have suffered from a drought classification labeled as severe or worse for eight or more consecutive weeks (U.S. Drought Monitor 2015).

If dry conditions are present for a given area, it is ranked by the USDM using one of the following classifications: D0, D1, D2, D3, or D4. D0 is the least severe drought classification, and corresponds to conditions generally ranging from the 20th to 30th percentile, or more colloquially, "abnormally dry" conditions, a condition one might expect every three to five years. D1 indicates moderate drought conditions, or conditions between the 11th and 20th percentile. Some expected signs of D1 conditions are damage to crops and pastures, or low streams and reservoirs. D2 is the least serious classification of drought that is still considered severe drought, and makes counties therein for periods of eight weeks or longer eligible for federal relief as suggested above. D2 is assigned when conditions are reflective of the 6-10th percentile, a condition only expected roughly once in 10-20 years. This is the point at which water restrictions are often imposed. The second most dangerous classification of drought is D3, or extreme drought. This corresponds to conditions reflective of the 2-5th percentile, which is often characterized by major crop and pasture losses, and widespread water shortages. D4, or exceptional drought is the worst of all drought classifications. D4 is assigned to conditions reflective of the 2nd percentile or worse, or water shortage emergencies. If an area of the United States does not have a current drought classification that means that conditions correspond to the 30th percentile or higher, or "normal" to wet.

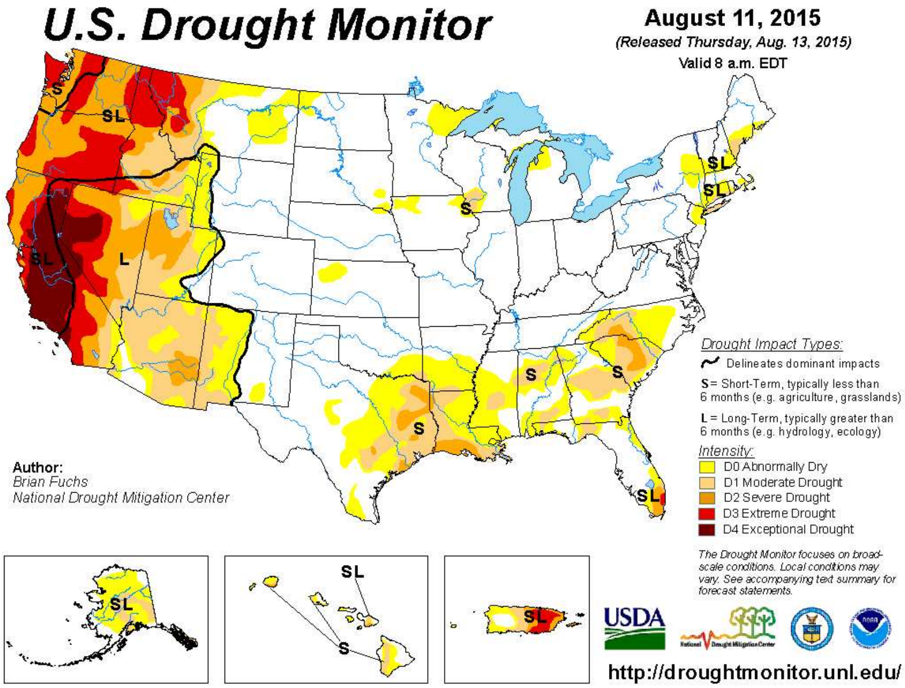

Figure 1.1: Here mid-August 2015 conditions are depicted as deemed by the US Drought Monitor. At this time exceptional drought, or water emergency is declared for California's San Joaquin Valley, Owens Valley, and Sierra Nevada range extending southward down to the Pacific Coast from Long Beach and Santa Ana to northwest of San Luis Obispo. Areas depicted in orange, red, or dark red color are eligible for federal relief if such a state has persisted for greater than eight weeks.

As can be seen in figure 1.2, more extreme drought classifications may describe a large amount of area in measurement space, but are fixed to only a small amount of area in probability space. It is worth noting that not all variables used to quantify drought characteristically follow a normal distribution. For instance, rainfall tends to follow a Gamma Distribution (McKee et al. 1993).

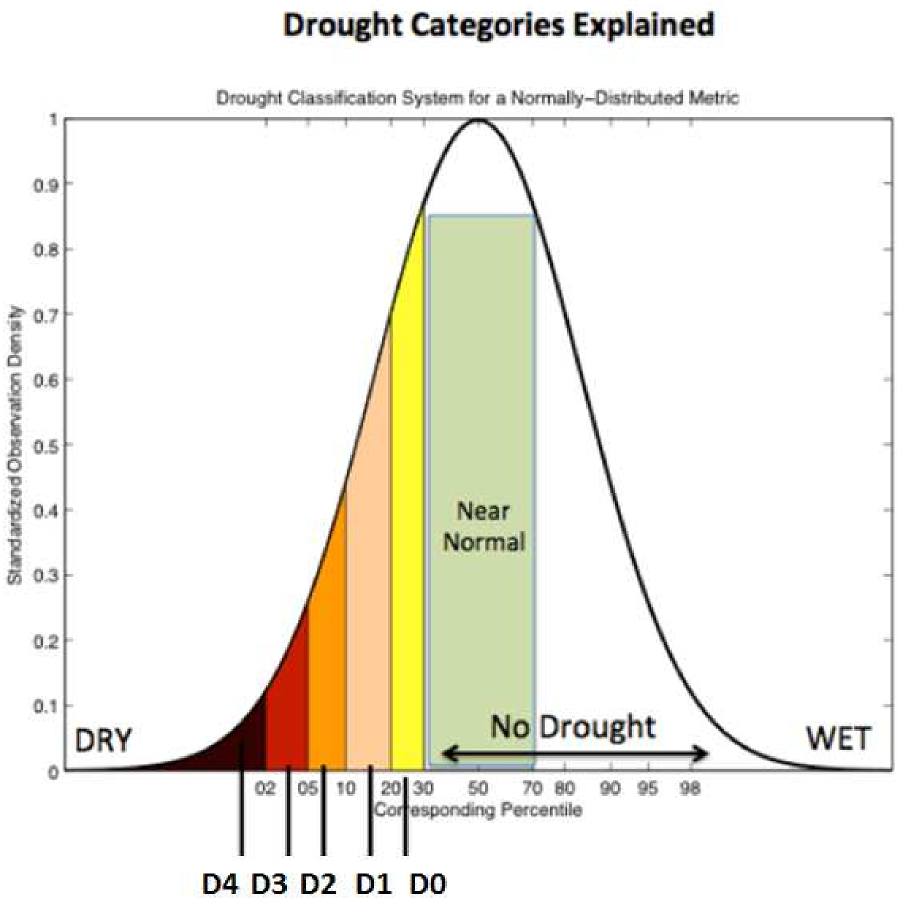

Figure 1.2: The image above shows an example of how drought classifications would be assigned for a normally-distributed variable that may be used to quantify drought. The area under the curve is close to, but not necessarily to scale.

The role of the Colorado Climate Center in the drought monitoring process is to provide weekly summaries to the USDM of changes in conditions across the Upper Colorado River Basin from the headwaters of the Upper Green River all the way down to Lake Powell, and the remainder of Colorado east of the continental divide. If the changes in conditions over the past week merit a change in drought classification these changes are outlined and sent to USDM's weekly drought monitor author. These recommendations have been highly regarded at the national level. Though there has not been an effort to archive push-back from the USDM on regional recommendations, anecdotally, the Colorado Climate Center's recommendations have always been accepted with limited or no revisions.

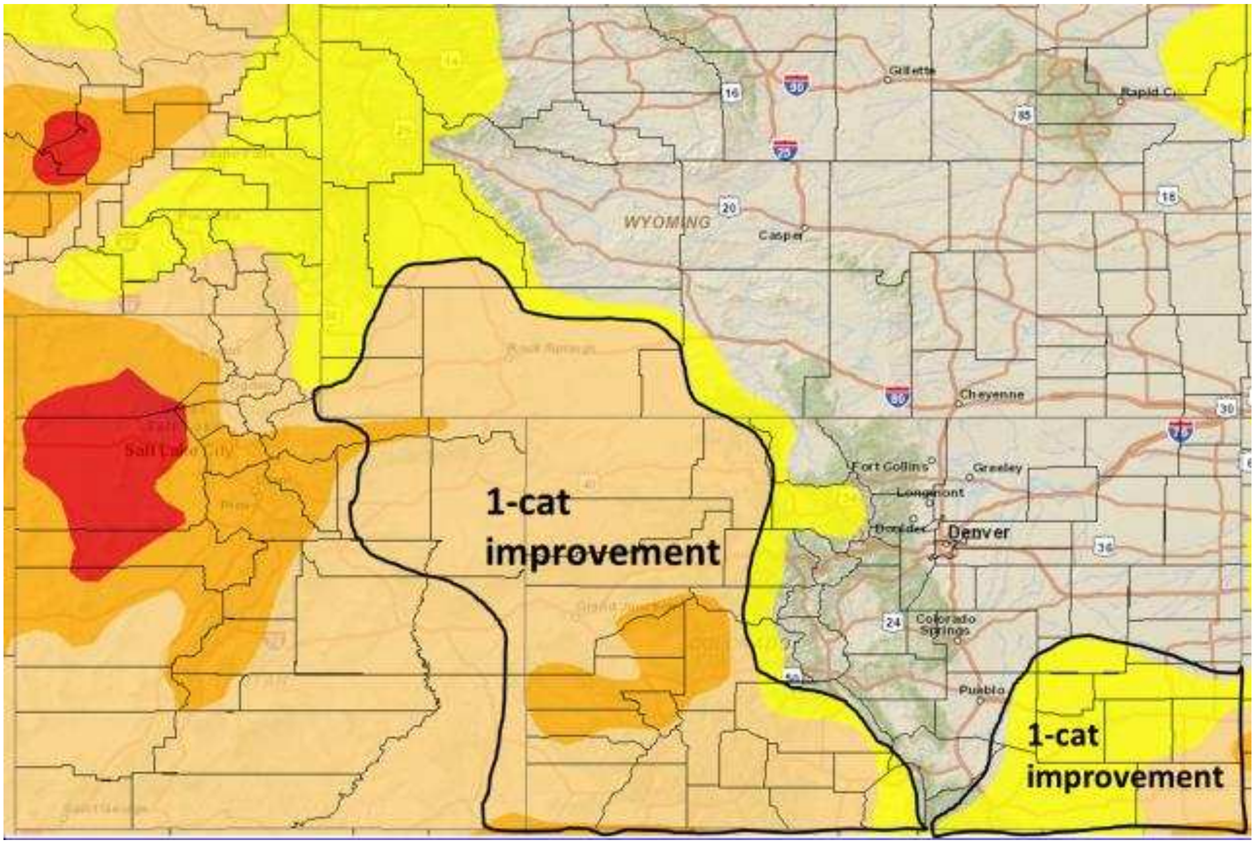

Figure 1.3: Here is an example of a regional recommendation from the Colorado Climate Center to the US drought monitor. The color scheme here represents the different drought classifications listed above and is consistent in pigmentation with figures 1.1 and 1.2. This specific recommendation was made on May 26th, 2015 following a very wet week and month for the state of Colorado and the Upper Colorado River Basin.

In order to assign a drought classification that is based on a percentile ranking it is necessary to have a set of applicable metrics. Many of the indicators that are used by the Climate Center and the drought community at large as metrics of drought can be assessed quantitatively. Precipitation, temperature, soil moisture, snowpack, streamflow, and even potential evapotranspiration would all be examples for this (Colorado Climate Center 2015). However, the importance of any given drought indicator is neither necessarily spatially nor temporally-constant. Because the weights of each component are not something explicitly solved for, assignment of drought classification for a region is still a semi-qualitative process in spite of the vast increases of numerical input to the process.

Components of the hydrologic system respond to changes via interface with the atmosphere on different timescales. A perturbation to the normal precipitation – evaporative demand balance will materialize on a characteristic timescale of days or more quickly in streams, small rivers, and mountain snowpack. For components of the system such as root zone soil moisture, vegetative health, large rivers, and small reservoirs weeks may be a more appropriate timescale. Large lakes and reservoirs and underground aquifers may take months to years to respond to such perturbations (Vicente-Serrano et al 2010). Negative effects from financial loss caused by drought-related damage may linger for years as well. These timescale estimates are once again regionally-dependent, and very dependent on the size of the component of the system. Managed rivers and streams, and reservoirs managed for irrigational and mixed uses are more resilient to climatic drought in the short term at the cost of lengthening the recovery process (Lorenzo-Lacruz 2013).

Regionally-Implemented Drought Monitoring Techniques: Regional drought monitoring has been done primarily based on regional Precipitation, SPI, Streamflow, Snowpack, Temperature, Surface Water, Evapotranspiration, and Forecast data. Each of these drought monitoring techniques will be outlined below. Drought monitoring techniques implemented but the USDM are similar to what is used regionally, but do not match exactly. Along the way some of the lingering weaknesses of regional drought monitoring will be addressed, specifically in areas where there is an aim in later chapters to make improvements.

Precipitation: On a weekly basis, precipitation maps are generated to depict absolute precipitation over the past seven days, absolute precipitation for the month to date, precipitation for the prior month as a percent of normal, and precipitation for the water year to date (starting October 1st) as a percent of normal. Primary precipitation data sources used to produce contour maps such as figure 1.4 include the National Weather Service's Cooperative Observing Network (COOP), the Natural Resources Conservation Service's Snow Telemetry Network (SNOTEL), Colorado's Agricultural Meteorology Mesonet (CoAgMet), and the nation-wide citizen science Community Collaborative Rain, Hail, and Snow Network (CoCoRaHS). Percentages of normal are derived by comparing these precipitation maps against PRISM climatology (PRISM 2015).

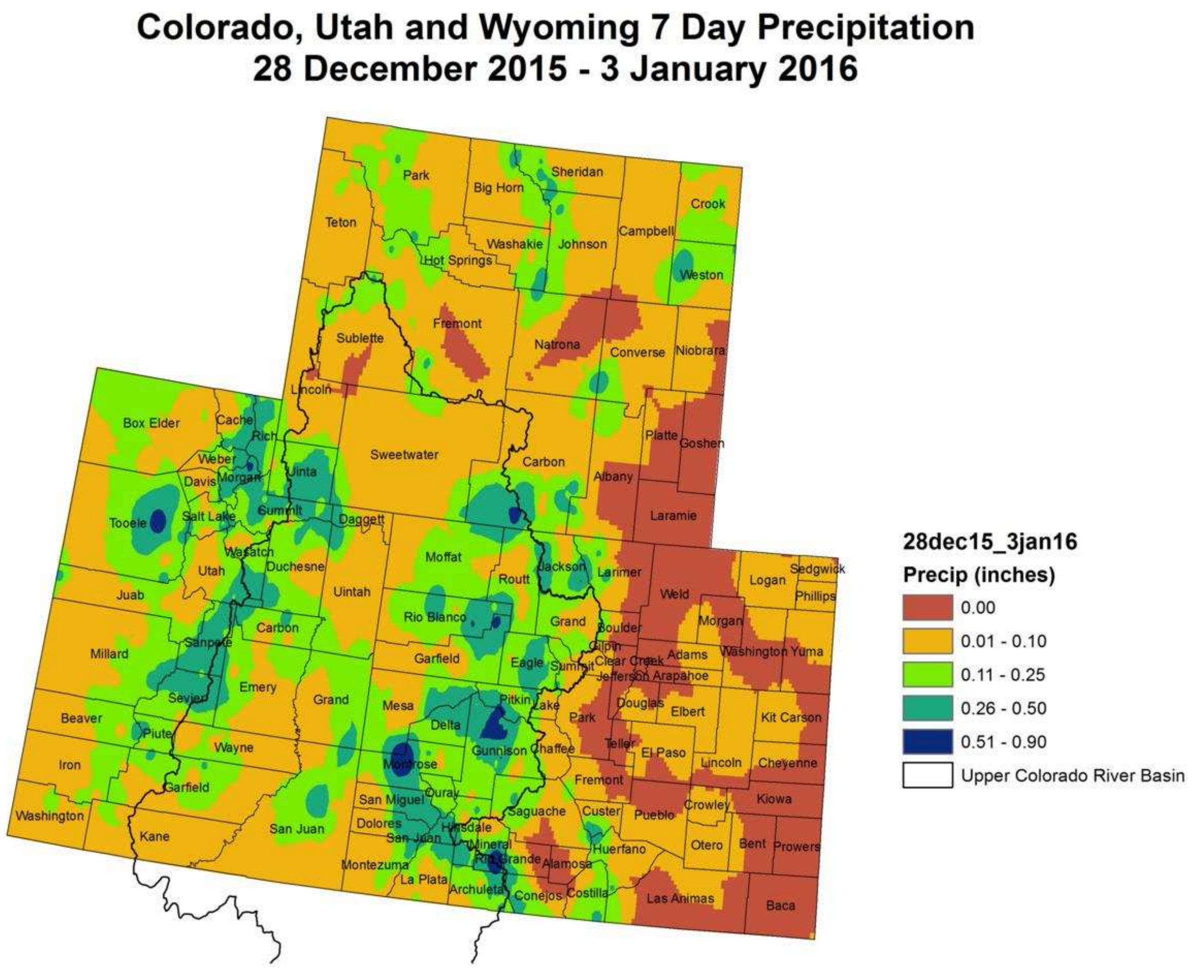

Figure 1.4: The amount of precipitation that fell between December 28th, 2015 and January 3rd, 2016 is contoured above for the tri-state area of Colorado, Utah, and Wyoming. The Upper Colorado River Basin has been outlined in black.

The Standardized Precipitation Index (SPI) maps are not produced in-house, but rather by the High Plains Regional Climate Center (HPRCC 2015). SPIs are determined based on gamma-fitted precipitation data that were recorded during the period used to establish climate normals, which for the time includes data between 1981 and 2010. SPIs are a measure of how many standard deviations above or below the climatological mean precipitation has been over a given time frame if precipitation were a normally-distributed metric (McKee et al. 1993). SPIs can be evaluated at any timescale, and the mathematical technique can be used on other metrics of drought. This will be discussed at more length in chapter two.

SPIs are fundamental in determining a drought classification, but the data used to produce SPI maps comes from only COOP and ADWN weather stations (HPRCC 2015). Due to lack of consistent long-term data in some areas these maps are of lower resolution than the in-house precipitation maps such as in figure 1.4. They are likewise problematic in determining SPIs for high elevation terrain since these areas are under-sampled by COOP and ADWN. This elevation under-sampling is highlighted by the difference in SPIs over northeast Utah's Uintah Range in figures 1.5 and 1.6. Using NLDAS Phase-2 data of 1/8th latitude by 1/8th longitude resolution much drier than average conditions for April of 2015 are pinpointed over the Uintah Range.

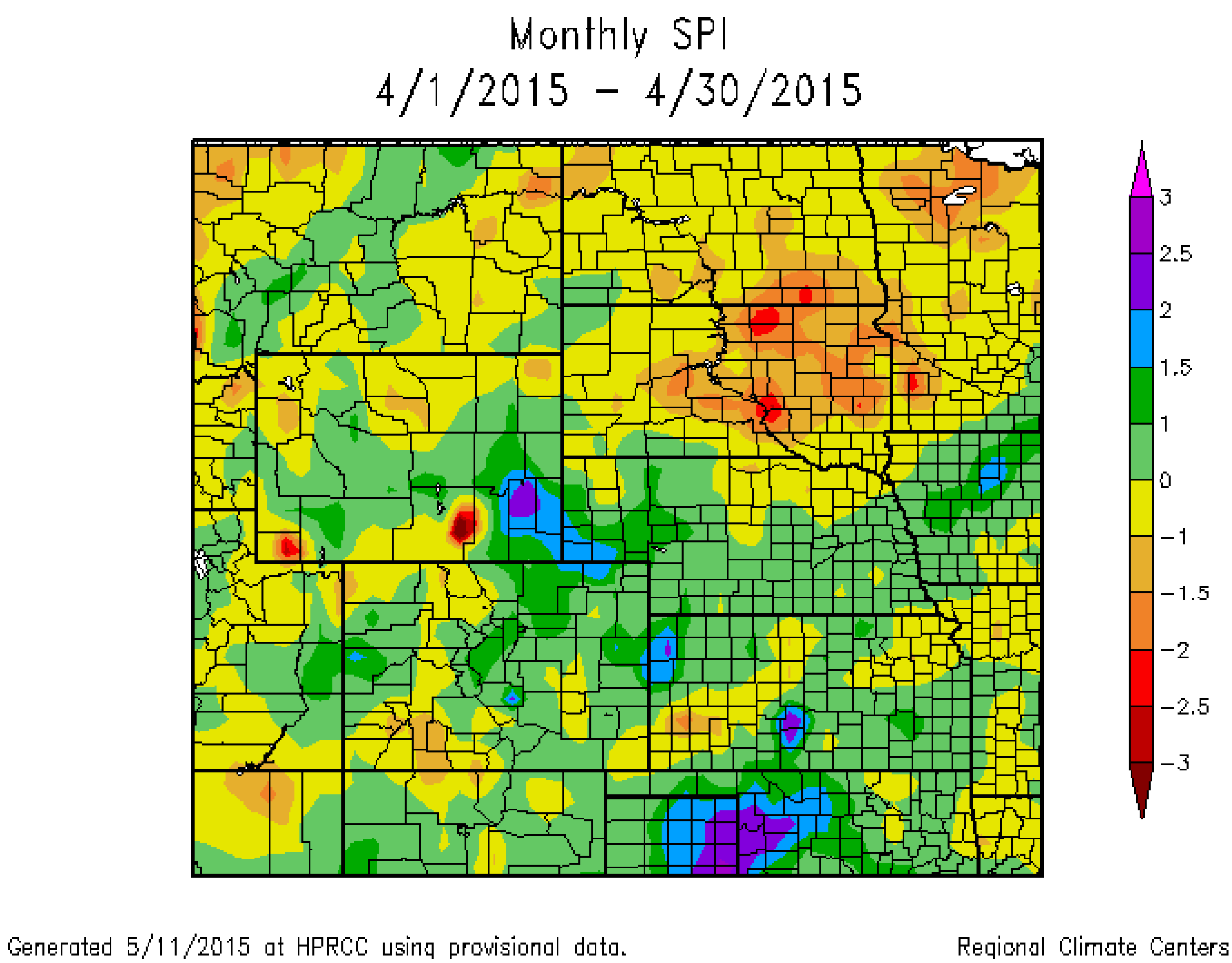

Figure 1.5: 30-Day SPI data ending on April 30th, 2015 are depicted above for the high plains region provided by the High Plains Regional Climate Center.

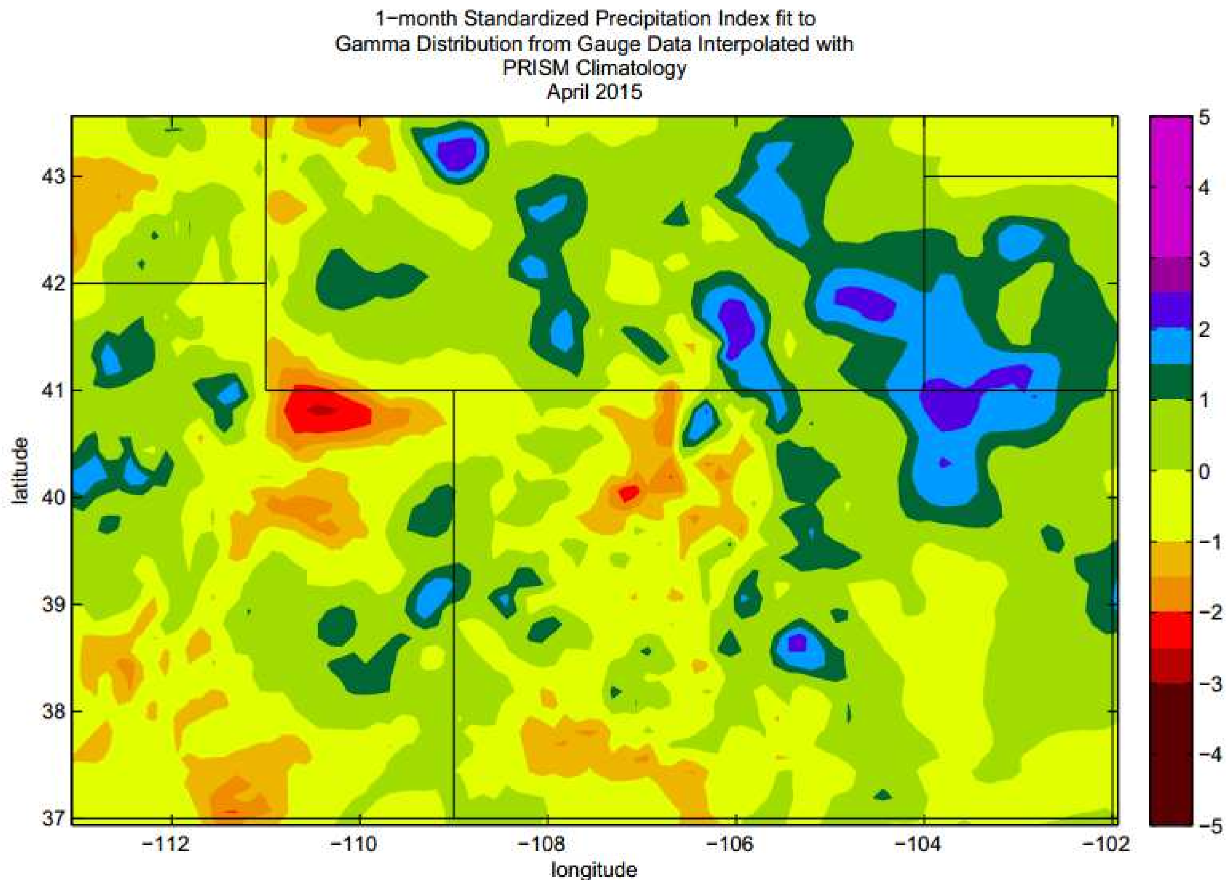

Figure 1.6: 30-Day SPI data ending on April 30th, 2015 are depicted above for the Upper Colorado River Bain and Western High Plains from NLDAS Phase-2 data.

Streamflow: Streamflow data are compiled weekly courtesy of the United States Geological Survey (USGS). Gage data are considered from the Upper Colorado, Upper Arkansas, and Upper South Platte River Basins. All USGS gage data are color-coded by percentile making them well-tailored for drought monitor use. Hydrographs that show streamflow trend for the past two years plotted against the station's background climatology are also made available by USGS. These are very telling as to how the changes in streamflow that have occurred scale against what is expected at that time of year. The Colorado Climate Center pulls hydrographs weekly from the following gages: Colorado River near CO-UT state line, Green River at Green River, UT, and San Juan near Bluff. These sites were chosen as indicator sites as they provide a robust sample of flows of the largest rivers in the Upper Colorado River Basin (UCRB) into the bottom of the region at Lake Powell. No efforts will be made in this study to improve upon streamflow monitoring techniques.

Snowpack: During the winter snowpack evaluation becomes one of the most important tools, if not the most important tool, for evaluating whether or not parts of the intermountain west are suffering from drought. According to Oregon State's PRISM climatology group some of the areas within the Upper Colorado River Basin and eastern Colorado that receive the most precipitation annually are high in elevation and on the windward (west) side of mountain ranges. This precipitation primarily falls as snow though the winter and spring, and recharges the basin's rivers, soils, and reservoirs upon melt. This input to the hydrologic system is used regionally as a means of justifying widespread improvements or degradations. Snowpack data used during the cold season in the weekly drought monitor process come from the Natural Resource Conservation Service (NRCS).

Temperature: Temperature data used in weekly drought monitor updates, like SPI data, come from the HPRCC. Temperature departures from normal are assessed for the past week, the month to date, and the previous month. The data source for these temperature readings are once again the same as the SPI data, and come from COOP and ADWN stations. Anomalies are reported with respect to 1981-2010 climatology. It's important to monitor temperature anomalies in order to monitor drought effectively, but this is one component of the current drought monitoring scheme that could be improved upon greatly. This idea will be expanded upon in chapter two.

Temperature anomalies are important for drought monitoring because they do carry an inverse relation to water storage, but temperature anomaly graphics currently used in the regional drought monitoring process have several faults. For one, temperature anomaly spread is not spatially or temporally constant, so for most effective decision making temperature anomalies should be standardized. Secondly, since these data are pulled from the same source as SPI maps high elevations are under-sampled. Perhaps most problematically for drought monitoring, temperature is only one factor governing the flux of water back from land to atmosphere (evapotranspiration). Potential evapotranspiration (PET) can be decomposed into anomalies in four atmospheric conditions: surface temperature, vapor pressure deficit, downwelling solar radiation, and near-surface wind speed (Bonan 2008). Measuring actual evapotranspiration (AET) requires that available water for ET is known. In both sustained and flash droughts there is an inverse relationship between PET and AET (Hobbins 2015). An ideal drought monitoring system would track PET and AET in a spatially distributed sense along with all the components of PET so that anomalies can be properly attributed.

Potential Evapotranspiration: ET is now being addressed in two ways: in terms of cumulative growing season ET from indicator CoAgMet Stations, and in a spatially-distributed sense using the Evaporative Demand Drought Index (EDDI). CoAgMet growing season ET provides a telling comparison between the current warm season and those of the last 20-25 years by comparing cumulative ET realized in the current year to those of the mean year, and highest and lowest years on record. The amount plotted represents the number of inches of water a well-watered alfalfa crop would use in a growing season. This is also known as reference ET (Colorado Climate Center 2015). Similarly, potential evapotranspiration is modeled using data from the NLDAS-2 project (which will be discussed more in the surface water section of chapter one as well as in chapter two) via EDDI. These data are presented in terms of percentile rankings that correspond to the drought monitor's percentile ranking system, and are available for timescales of 1-12 weeks. One of EDDI's primary functions is to help identify warm season flash drought events.

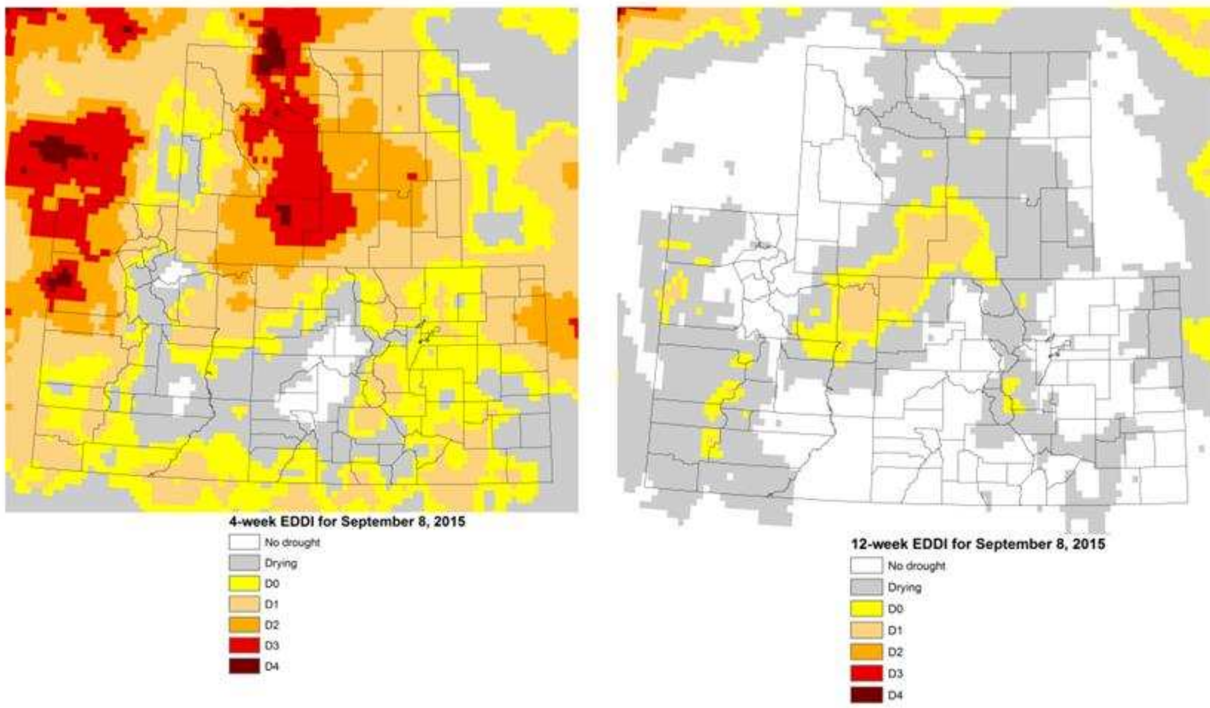

Figure 1.7: Here we see EDDI's depiction of evapotranspiration on 4-week (left) and 12-week (right) timescales ending on September 8th, 2015. This image shows that over the four weeks leading up to September 8th potential evapotranspiration was above the 95th percentile for much of the middle of Wyoming with respect to background climatology, but the entire 12-week period leading up to the same date shows more typical, less severe conditions.

Surface Water: In the context of the Colorado Climate Center drought monitoring website "Surface Water" refers to reservoir levels, soil moisture, and vegetative health. Surface water conditions are assessed by looking at soil moisture, vegetative health, and reservoir levels. Soil moisture data used in weekly analysis come from the University of Washington's Hydrology department using their model run of the Variable Infiltration Capacity (VIC) model. This model outputs a spatially-distributed soil moisture map in terms of percentiles corresponding to a 5-day windowed period with reference to background climatology at each gridpoint. Soil moisture data are pulled during the warm season, but soil moisture plus snow-water equivalent (SWE) data are pulled during the cold season.

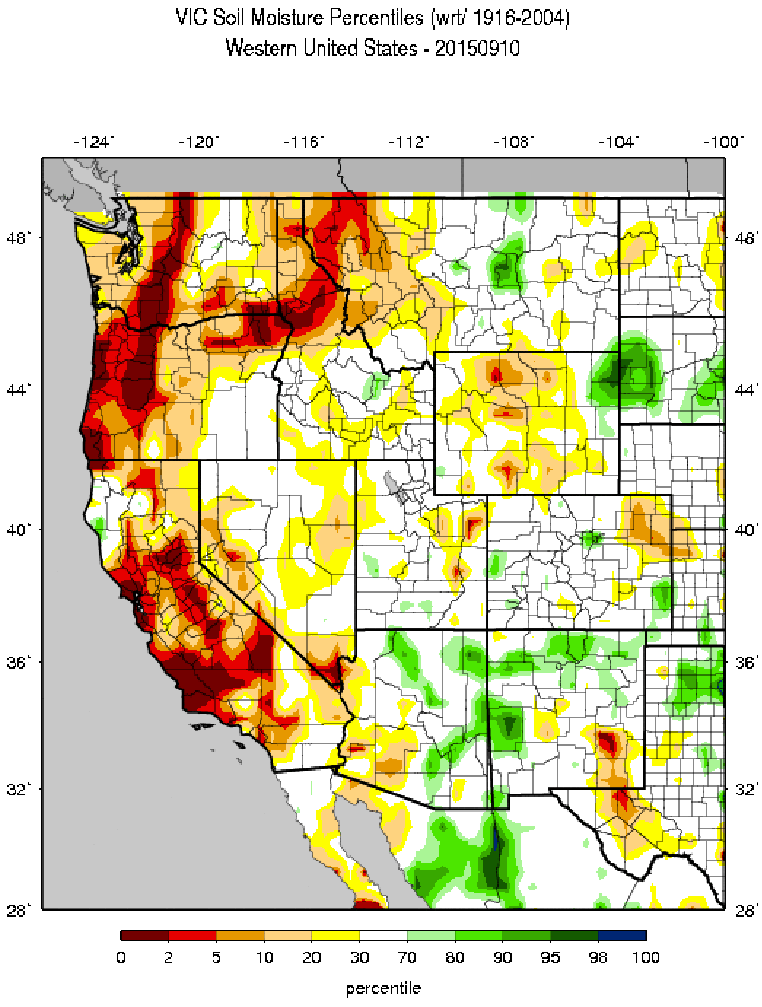

Figure 1.8: The image above is a depiction of VIC model output from September 10th, 2015. Some disturbingly dry root zone soils plague the west coast at this time.

The reservoir situation in the Upper Colorado River Basin has traditionally been addressed by pulling data from key indicator sites using daily data from the United States Bureau of Reclamation. The indicator sites used are Flaming Gorge, Green Mountain, Lake Granby, Lake Dillon, Blue Mesa, Navajo, McPhee, and Lake Powell Reservoirs (see figure 1.5). These reservoirs were chosen as indicators for their size. The following reservoir capacity statistics come from the United States Department of Agriculture: Lake Powell is the giant of the bunch. With a capacity of over 24 million acre-feet it has nearly eight times the potential size of any other reservoir in the Colorado River Basin. Flaming Gorge and Navajo Reservoirs are the other one million plus acre-feet bodies of water in the system with capacities of 3.75 and 1.4 million acre-feet respectively. Blue Mesa is the largest reservoir in the Gunnison Basin by a factor of seven over Marrow Point Reservoir. Lake Granby, Lake Dillon, and Green Mountain Reservoirs are the first, second, and third largest reservoirs respectively along the Upper Colorado River mainstem. McPhee is the second largest reservoir to Navajo Reservoir along the San Juan River, and beats out third place by a factor of over ten. In summary, massive amounts of water are stored in reservoirs in the Upper Colorado River Basin. These reservoir levels are tracked with respect to monthly averages and with respect to their capacity.

Tracking reservoir levels is an integral component of tracking long-term drought in Colorado and the Upper Colorado River Basin, but there are a few challenges associated with appropriating these data for drought monitoring purposes. For one, reservoirs are heavily managed by the United States Bureau of Reclamation, so this is not a naturally-varying component of the hydrologic system. As a consequence of management, this is not a metric of the hydrologic system that is spatially-distributable. Reservoir levels have far-reaching implications on the amount of usable water downstream, but are not always reflective of natural areas in the immediate vicinity.

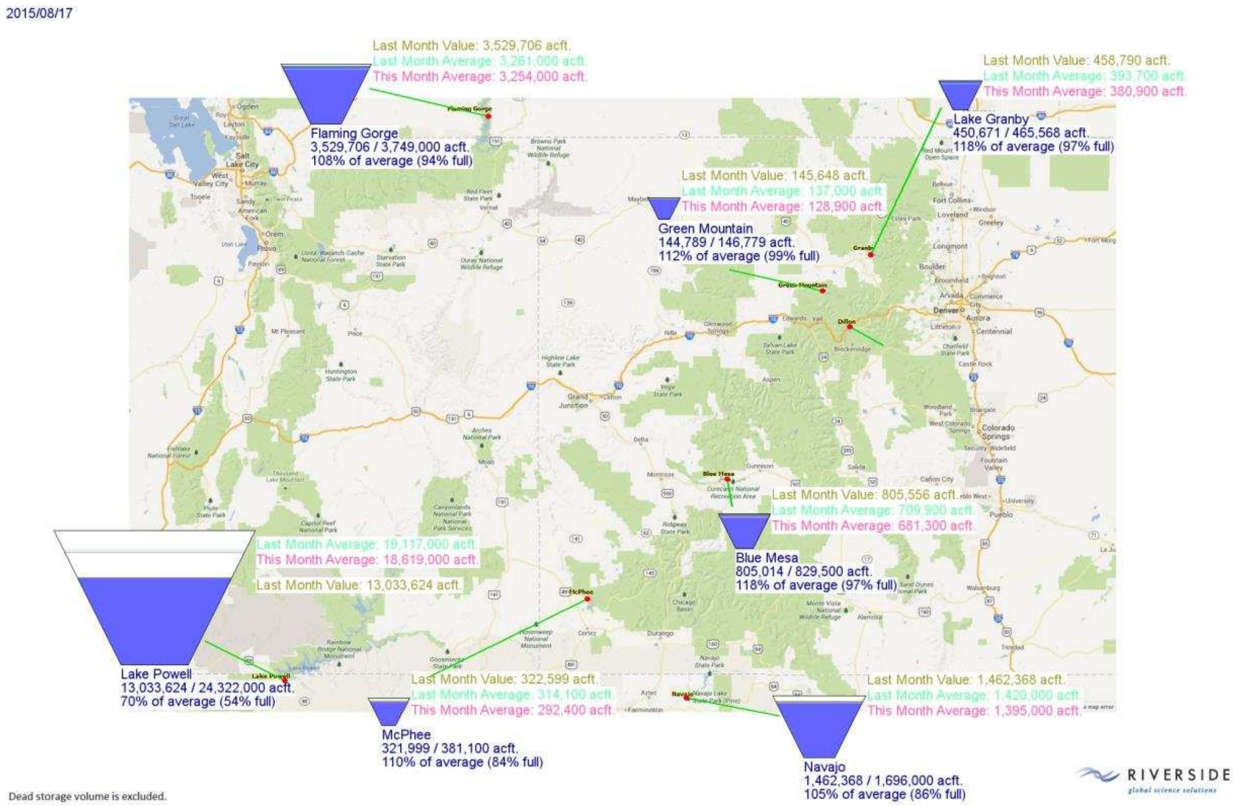

Figure 1.9: Here reservoir locations are shown with respect to more familiar geographic features such as state borders and U.S. interstates 25 and 70.

The final product used in assessing the state of the hydrologic system at ground level in the Colorado Climate Center's weekly drought monitoring process is the MODIS satellite VegDRI product. VegDRI assesses health of flora from space at a resolution of 1km. Vegetation conditions are ranked as "extremely moist," "very moist," "slightly moist," "normal," "pre-drought," "moderate drought," "severe drought," or "extreme drought." Rankings are based on satellite returns of normalized difference vegetation index, or NDVI (Brown and Wardlow 2009). The principle behind NDVI is quite simple actually. Live vegetation strongly absorbs radiation in the visible spectrum that impinges on it giving plants their dark appearance. Near-infrared radiation from the sun is damaging to plant life, and is reflected by vegetation. NDVI is just the ratio of difference between the radiation reflected through these two channels over the sum of the two [NDVI = (NIR - VIS)/(NIR + VIS)] (Weier 2000). VegDRI output is created by running this NDVI data, along with local climate data and biophysical data through a tree regression model (Brown and Wardlow 2009). Anecdotally, stakeholders in the agricultural sector, such as Farm Service Agency employees, have praised this product's performance. The exceptional drought that plagued southeast Colorado from 2011 to 2014 was a good example of this. The Colorado Climate Center uploads new MODIS VegDRI imagery weekly. It is synthesized as a part of the week's surface water data though NDVI doesn't explicitly fit the category of "surface water."

As suggested above, all this weekly information is then synthesized by climate center personnel. Recommendations for drought improvements or degradations are then drafted and distributed to regional stakeholders. Any stakeholder input is then compiled and carefully considered before releasing a final recommendation to the week's US Drought monitor author.

Soil Moisture Monitoring: As drought is "A period of abnormally dry weather sufficiently long enough to cause a serious hydrological imbalance." Even in the Upper Colorado River Basin and western High Plains where a high proportion of the surface area can be characterized as a semi-arid climate soil moisture is the largest part of the surface hydrologic system (Bailey, 1994). Soil moisture monitoring is thus a focal point of drought monitoring. In the agricultural sector soil moisture's importance is elevated as keeping root zone soils between wilting point and field capacity levels is key to a healthy crop yield. Furthermore, as will be discussed in great detail later in this study, the status of soil moisture has the potential to alter the earth's surface energy balance in ways that impact both temperature and precipitation.

Criticisms of Current Soil Moisture Monitoring Techniques: The University of Washington's VIC soil moisture model is not an easily-defensible one-stop shop for soil moisture data in the Upper Colorado River Basin and eastern Colorado. The VIC's output should be compared and contrasted against mechanisms with the capability of taking physical, observational measurements such as satellites, reflectometers, and core measurements. Root zone soil moisture is largely dependent on soil type (Crosby et al. 1984), and soil type varies on scales smaller than that of synoptic, and even most mesoscale atmospheric processes (USDA 2015). Modeled soil moisture is a valuable tool for drought monitoring in the sense that models allow for a combination of spatial and temporal resolution that isn't rivaled by satellites, in-situ electronic measurements, or direct measurements from soil cores.

Currently, the Colorado Climate Center is only utilizing data from the University of Washington's Variable Infiltration Capacity (VIC) Model, and only using one soil moisture model is less defensible as it does not give a sense of soil moisture model spread. The VIC model's value in assessing soil moisture percentiles is limited by its reference to a climatology of 1916-2004 as well. With the last decade being the hottest on record, and hotter weather expected in future years (IPCC 2014), this climatology may be outdated. It is possible that long-term shifts in the climate regime may be causing the VIC to bias soil moisture percentiles either high or low at times. The VIC model is limited in accuracy by the quality of its input data as well. If inaccurate precipitation data are assimilated the quality of subsequent soil moisture data suffers.

OPERATIONAL DROUGHT MONITORING TOOLS DEVELOPED

While this section is not explicitly devoted to showcasing new experiments that produce scientific discoveries it must be noted that a non-trivial portion of the effort involved in this research project was devoted to creating new products for drought monitoring use from data that are currently publically available. Not all of this work was directed at soil moisture monitoring. The products reviewed here will be reservoir timeseries graphics, station-based growing season continuous ET drivers monitor, a station-based soil moisture/precipitation tracker, and a SPI/percentile map generator that has potential to work for any field available from the NLDAS-2 land data assimilation project.

Reservoir Graphics: The first new product examined will be the reservoir timeseries graphics. These graphics were designed to supplement but not replace data obtained from Riverside Global Science Solutions (RGSS). RGSS supplies the Colorado Climate Center with data from seven major reservoirs in the Upper Colorado River Basin on a weekly basis, Flaming Gorge, Green Mountain, Lake Granby, Blue Mesa, Navajo, McPhee, and Lake Powell. These data include current reservoir volume information, and current volume with respect to full volume and with respect to average at monthly resolution. These numbers are displayed for both the current month and the past month.

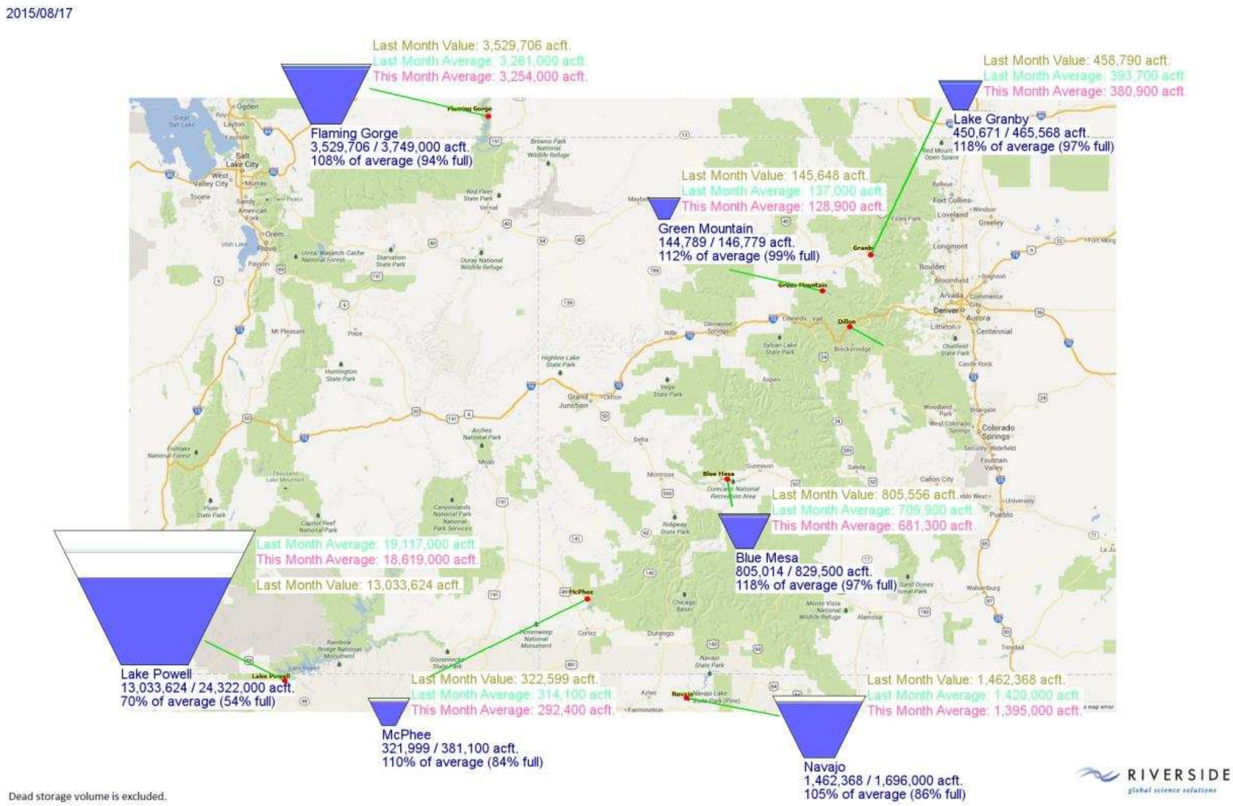

Figure 2.1: Reservoir teacup data used by Colorado Climate Center in drought monitoring process

These data have been handy in past decision-making, but lack several qualities that are essential to drought monitoring. It is worth restating that drought classifications ultimately are designed to express the state of the hydrologic system in terms of a percentile range. The data above do not provide any sort of percentile context, let alone show a trend in percentile ranking from one day, or even week, to the next. Monthly resolution for reservoir data is also somewhat troubling. Bureau of Reclamation data indicate that reservoirs in the Upper Colorado River Basin tend to follow a schedule of high inflow rates in the late spring when snow melts and large outward fluxes via both releases and evaporation in the summer and early fall. This signal tends to be most pronounced in smaller reservoirs. As a result, looking at the percent of average volume a reservoir is occupying is much more useful at daily resolution than monthly in months such as May and September.

Data Acquisition: All data used for reservoir timeseries graphics are obtained from measurements taken and made publicly available by the United States Bureau of Reclamation. Specifically, data for Lake Powell, Flaming Gorge, Navajo Reservoir, McPhee Reservoir, and Blue Mesa Reservoir are obtained at http://www.usbr.gov/uc/water/rsvrs/ops/r40day.html. Data for Lake Granby are obtained at http://www.dwr.state.co.us/SurfaceWater/data. Green Mountain and Lake Dillon were not included in the reservoir timeseries graphics project. Dillon was excluded due to missing data. Green Mountain was omitted because of size and proximity to Lake Granby.

Data Quality Control: The first step to reservoir data QC was to remove jumps in the data that do not appear to be representative of any sort of physical process. For instance, if a reservoir elevation (level) is consistently listed at right around 8000ft, experiences a one-day jump from 8000 to 8020 feet, and then returns to a level of 8000 feet the next day, that's probably a data error.

A reservoir smoothing function was applied to each timeseries that does not allow daily changes in reservoir volume that exceed 5% of the reservoir's capacity value. This value was not chosen based on any past research. The 5% barrier was applied because it did not cause any reservoirs to lose data from levels changing relatively quickly during late Spring and early Fall, but did remove most values that appeared to be errors. The raw data were not manipulated much as it is likely that the Bureau of Reclamation did some data quality control of their own.

End Product Amenities: The reservoir timeseries graphics developed have been a successful and useful addition to the Colorado Climate Center drought monitoring webpage ccc.atmos.colostate.edu/~drought/. One crucial slice of information that this product easily makes privy to users is that some reservoirs, such as McPhee, Granby, and Blue Mesa, can be expected to fill to capacity during the early summer at least 10% of the time. For McPhee Reservoir has filled to capacity over 30% of the time between 1985 and 2015. While teacup graphics do a stellar job shedding light on the relative scale of reservoir volumes, timeseries graphics shed such light on the seasonal and interannual variation that major reservoirs in the Upper Colorado River Basin are prone to. Since 1985 Flaming Gorge Reservoir has never dipped below roughly two thirds of its capacity. In contrast, Lake Granby was drained of all but its dead storage following the extreme drought of 2002. Dead storage refers to water below the lowest level that has been engineered for drainage.

A careful examination of these graphics reveals that percentiles do not line up at the beginning of the year. This break in the data is startling at first glance but exists because of differing reservoir levels at the start and end of the background climatology period. In other words, the dataset is not a closed loop. If the current year was substituted in for the initial year in calculation of quantiles the dataset would make a closed loop and there would not be a break at the new year.

The summer of 2015 turned out to be an excellent case study for these graphics, and a fortunate time for their inclusion in the drought monitoring process. Reservoir levels in the southern portion of the basin started 2015 below or near the 10^{th} percentile, reflecting the continuation of long-term drought conditions. Levels at Navajo and McPhee Reservoirs jumped well back into the normal range (between the 30^{th} and 70^{th} percentiles) whereas the wet spring raised Lake Powell only a small amount with respect to its capacity. Even after conditions became drier later in the summer Navajo and McPhee held onto seasonally-normal reservoir levels.

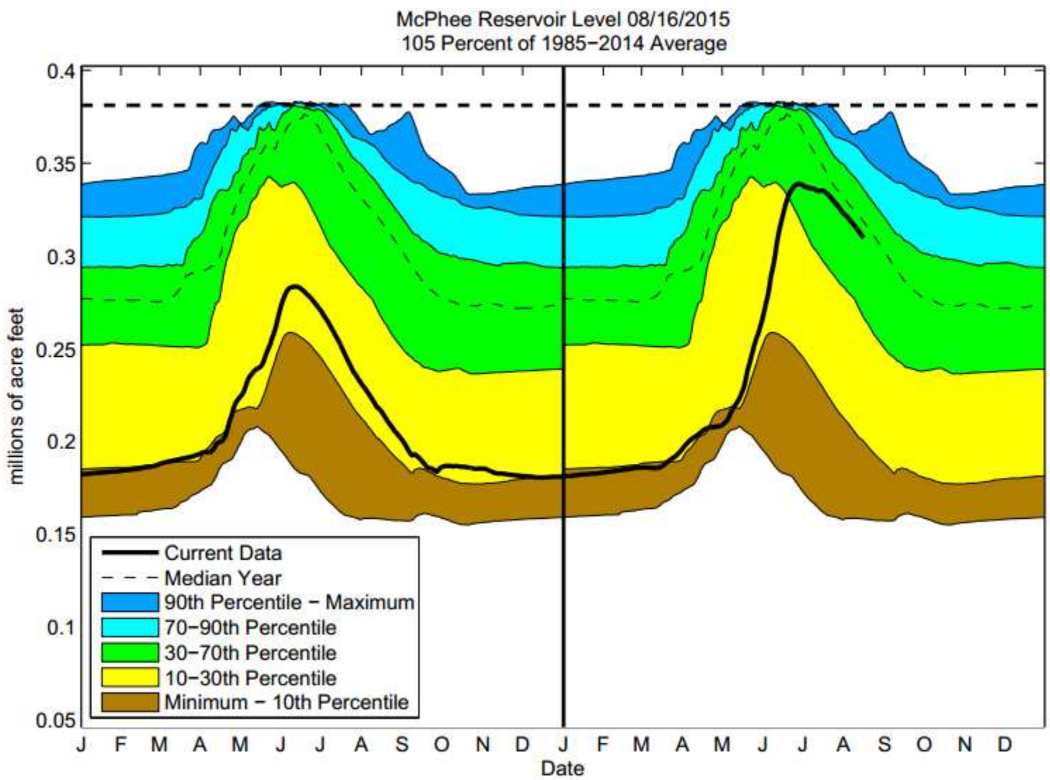

Figure 2.2: Here we see an example of one of the new reservoir timeseries plots from McPhee Reservoir in August. We see here that McPhee Reservoir rallied nicely from March to July of 2015 going up from below the 10^{th} percentile to near average level. The reservoir did not fill to capacity following the snowmelt season as it has 30% of the time between 1985 and 2014.

SNOTEL Soil Moisture: The next product added to the drought monitoring process, and the first to tie into the overarching theme of soil moisture monitoring in this work, is the SNOTEL station soil moisture/precipitation tracker.

Data Acquisition and Attributes: All data used for the soil moisture/precipitation tracker tool are publically available courtesy of the Natural Resource Conservation Service, which falls under the umbrella of the United States Department of Agriculture. Currently, data are being collected weekly from eight SNOTEL (Snow Telemetry) sites. These sites were chosen out of 144 SNOTEL sites in Utah and Colorado. Six of these sites fall within the Upper Colorado River Basin, and two are on the Front Range just east of the divide, and are part of the South Platte River Basin. The stations included are Burro Mountain, East Willow Creek, Lone Cone, Lost Dog, Michigan Creek, Park Cone, Trout Creek, and Wild Basin. These particular stations were chosen for their spatial distribution pattern, elevation range, length of soil moisture record, and relatively low amount of data that needed to be quality controlled.

Station elevations are between 8300 and 10600 ft with six of the eight stations being between 9000 and 10000 feet. This creates a sampling bias if one's goal is to determine the state of soil moisture basin-wide as the average elevation of these stations is higher than the basin at large. The logic behind choosing to closely monitor stations at this elevation is that they fall in the montane and subalpine plant zones, which can be characterized by forests of pine and spruce (Ramley1907). This region has been the target elevation of some of Utah's historic fires (Brown 2008), is prone to severe fires, and in a region where confidence is high in the increase in fire activity over the next 50 years (Rocca 2014). Stations chosen have a record of data anywhere from nine to sixteen years in length. Relative to common atmospheric variables like temperature and precipitation, there is a dearth of historic root zone soil moisture volumetric water content data that are available to the public. In terms of in-situ soil moisture measurements in the area ten years of data is above average. Distribution is not perfect through Colorado and eastern Utah. Ideally there would also be key stations in Wyoming near the headwaters of the Green River, one or more on the other side of the San Juan Mountain Range, and one in the Sangre de Cristo Range in southern Colorado.

Soil moisture conditions are not homogeneous as for each individual mountain range. Including multiple samples in each mountain range would also be desirable, but is not realistic at the time. The proportion of stations that have at least a ten year data record and are consistently devoid of quality errors is low.

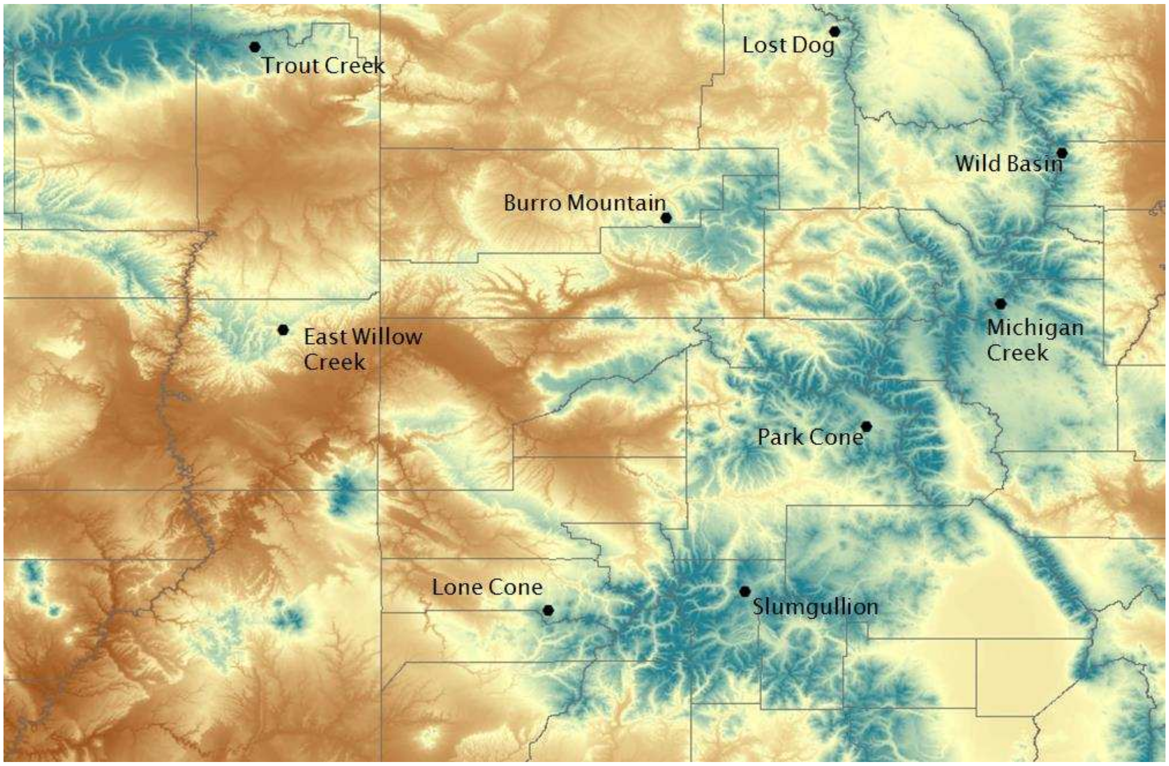

Figure 2.3 shows the key SNOTEL sites now used for weekly soil moisture trend plotting to be used for drought monitoring. The San Juan, Uintah, Sawatch, Mosquito, and Front Ranges all are represented. East Willow Creek, Burro Mountain, and Lost Dog form a transect of stations at similar elevations between these ranges. Slumgullion was included only because it will be referenced in a figure.

Data Quality Control and Analysis: The end product produced by the soil moisture/precipitation tracker tool displays vertically integrated soil moisture through the root zone. That is to say, rather than charting the readings of sensors at each depth separately, a weighted average is plotted for each day where the weighting is determined by a linear interpolation between the surface and the depth of the lowest soil probe. In the case of the majority of these stations soil probes have been installed at 2, 8, and 20”. The weighting scheme applied to this scenario would be Vertically Integrated Mean $V = [5 * (2'' \, depth) + 9 * (8'' \, depth) + 6 * (20'' \, depth)]/20$. Lost Dog and Michigan Creek have sensors at 2, 4, 8, 20, and 40” depth. This adjusts the weighting scheme to be Vertically Integrated Mean…

$$V = [3 * (2'' \, depth) + 3 * (4 \text{ depth}) + 8*(8'' \text{ depth}) + 16*(20'' \text{ depth}) + 10*(40 \, depth)]/40.$$

In this case 4” and 40” measurements can also be omitted in order for the first interpolation scheme to be applied if homogeneity is desired.

The QC process for soil moisture proves tricky because there are a number of factors with potential to skew the data that must be accounted for. Firstly, volumetric water content is a strong function of soil type (Clapp and Hornberger 1978) and soil type may change with soil depth. Therefore, even by taking a weighted average of the available data, comparison to data that involves all sensors is not appropriate because the physical constraints on the upper and lower limits of measurement have been altered. On top of this, if one sensor goes out a trend in RZSM will be registered that does not represent a real change in the physical system. Because these types of changes would produce misleading data if one sensor is in the relay is not operational data from the whole relay are removed from consideration.

Volumetric water content values are removed from consideration if they are below zero since this is not physically possible, and if they are above 55% as even saturation for silty clay should be below this by a considerable margin of error (Clapp and Hornberger 1978). When the temperature of the soil is 0 C or below the data are removed large differences in measured volumetric water content occurred as well. These data were removed.

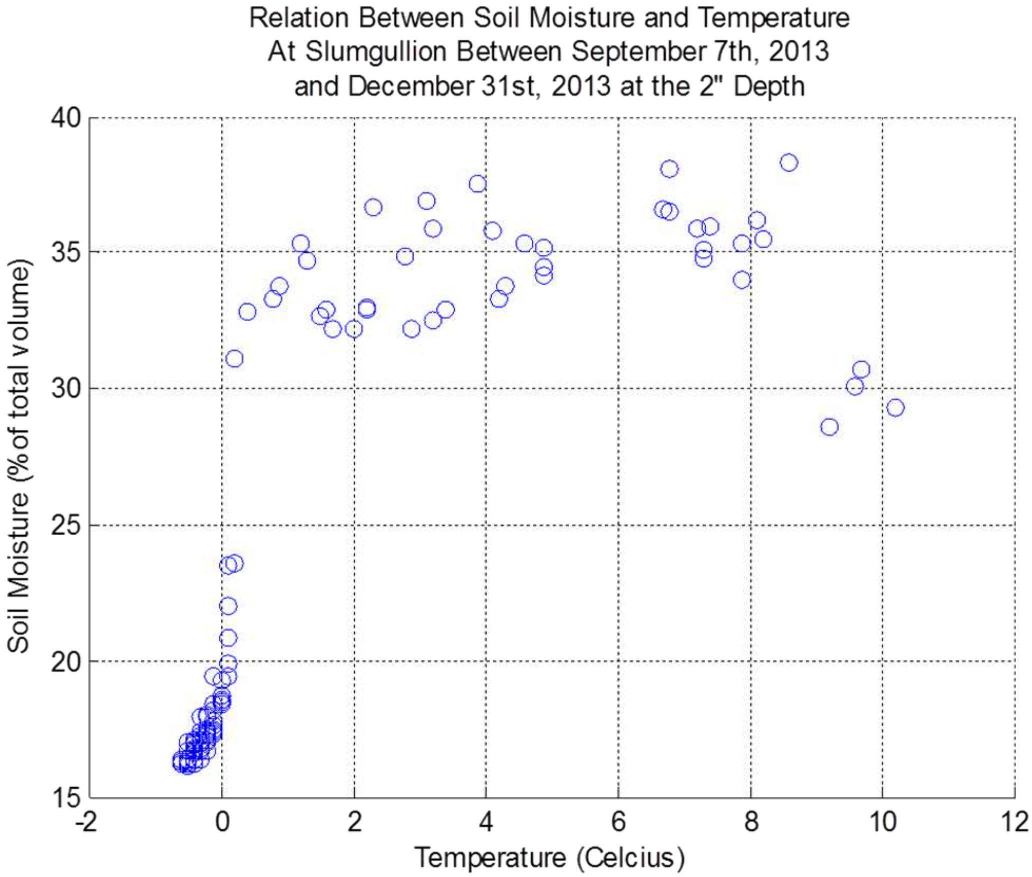

(Celsius)

Figure 2.4 displays daily soil moisture data at the SNOTEL Slumgullion station. It shows the clear discontinuity in volumetric water content readings between when soil is frozen and when soil moisture takes liquid form. Slumgullion is the highest SNOTEL station in all of Colorado, and spends much of the year with its near surface soil frozen.

End Product Amenities: The resultant product is one that effectively shows the rises and falls of root zone soil moisture associated with precipitation events, and enhances understanding of what it takes to maintain healthy root zone soil moisture levels throughout the growing season. Much like with new reservoir timeseries graphics, the warm season of 2015 ended up being a very effective case study involving soil moisture timeseries graphics. Precipitation was above, to much above average throughout the basin through the months of May and June extending into the first half of July in some areas. Through late July, August, and September precipitation was much below normal. As of mid-September stations that did not miss their monsoonally-driven late summer precipitation surge maintained healthy root zone soil moisture levels whereas the memory of the wet late spring was lost from stations that were much drier than normal through the late summer.

As addressed above, one clear criticism of these data is the period of record. Figure 2.5 shows how especially in the middle of the warm season there is a lot of day-to-day variation in the maximum Root Zone Soil Moisture level measured. These peaks correspond to times directly following a precipitation event. As the length of the timeseries goes to infinity one could expect that the maximum line would stay on par with saturation, and the minimum line would stay on par with wilting levels. Assignment of a percentile ranking will increase in meaning with time for these datasets as well.

Figure 2.5 is a demonstration of the soil moisture/precipitation tracker at work for East Willow Creek, UT. This station was in D0 drought, or just abnormally dry, at the time the figure was produced. It well characterizes the back-and-forth behavior of the 2015 growing season in eastern Utah. The plot is generating data at the beginning of April. While it looks like conditions are above average, it is actually a bad sign that snow it is already producing data because that means snow has melted early. It looks like East Willow Creek is on an unhealthy track early in the growing season, but then climatologically uncharacteristic rains strike in late May and early June propping up soil moisture levels. A subpar monsoon season knocks conditions back down below normal by the beginning of August.

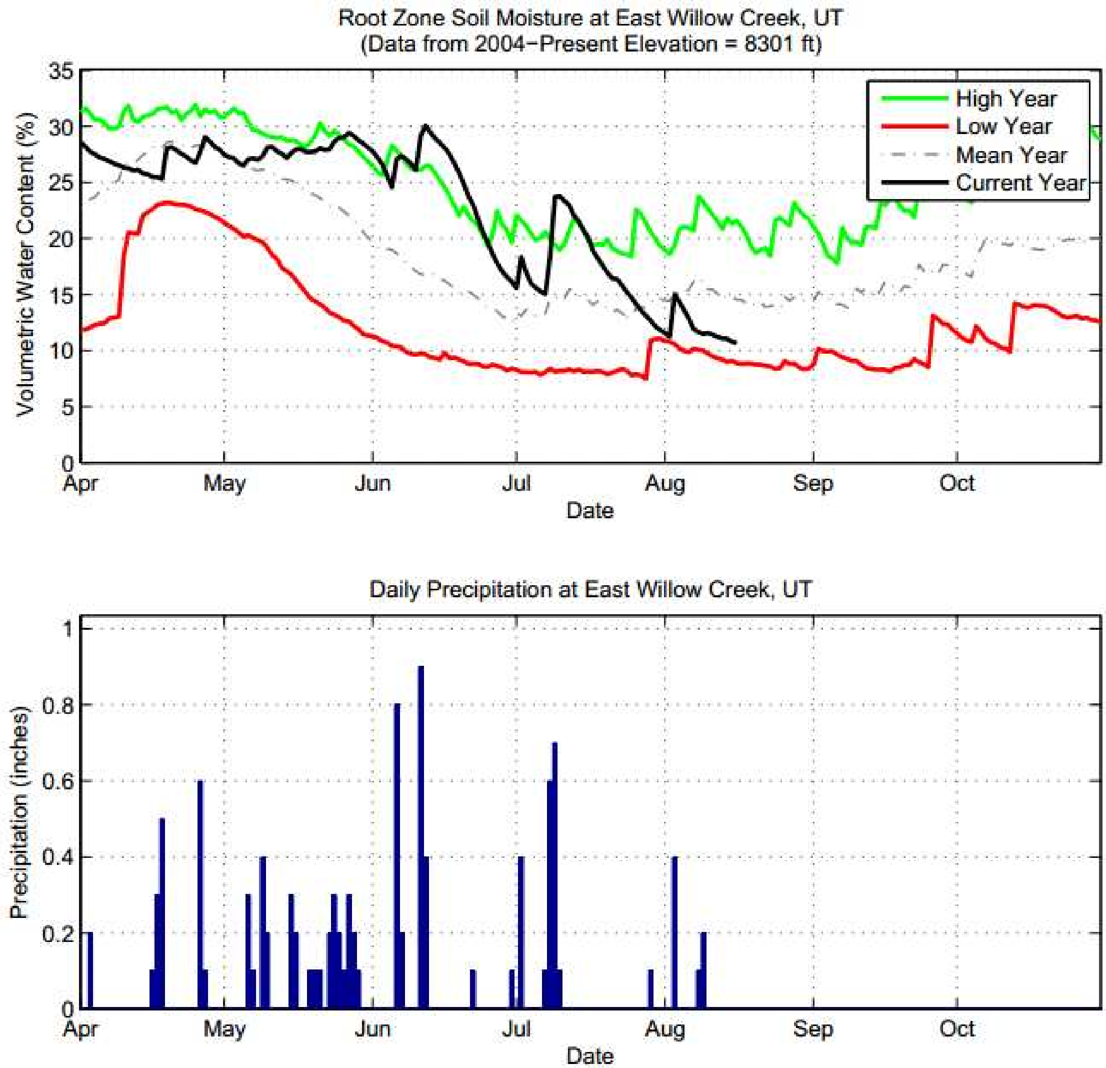

Figure 2.5: The top figure shows vertically integrated volumetric water content from 2-20" depth for the East Willow Creek SNOTEL station in eastern Utah as a function of time. The current year is depicted in black, the highest year on record in green, and the lowest year on record in red. The bottom figure shows daily precipitation totals.

NLDAS-2 Percentiles and SPIs: There are several challenges associated with the current drought classification decision-making process which are unrelated to soil moisture, but merit some discussion here: One challenge associated with the current drought monitoring process is that not all data assimilated for decision-making come either in a percentile format, or standardized against climatology. Also while ET is explicitly addressed on the Colorado Climate Center Drought Monitoring webpage, not all drivers of ET are addressed. While temperature maps are produced every week using HPRCC no such thing is done for downwelling solar radiation, wind run, or atmospheric vapor pressure deficit. Furthermore, spatial interpolations of HPRCC precipitation and temperature data are faulty as high elevation area is under sampled by COOP and ADWN networks over the domain. This makes attribution of anomalies in the hydrologic system more difficult than need be.

That's where the NLDAS-2 monthly data can be put to use. Forcing data for this application are primarily North American Regional Reanalysis (NARR) data. The exception to this is precipitation, which comes from gauge data that is disaggregated into hourly measurements using radar estimates, and then interpolated using PRISM climatology (Hualan 2014). Forcing data used for the following product include temperature, precipitation, wind run, and surface downwelling solar radiation data. Each month data for each and every gridpoint are fitted to their respective distribution. For instance, both temperature and solar radiation characteristically follow normal distributions. Precipitation follows a Gamma distribution (McKee et. al 1993), and wind follows a Weibull distribution (Justus et. al 1976).

Once monthly data are ftp'd these data are all processed in one all-inclusive function called "modelMonthlyDroughtSituation." This function will automatically create graphs of gridded precipitation, temperature, wind run, and incoming shortwave radiation in terms of both monthly and yearly percentiles and SPIs. One of the best things about this function is that it's nowhere near its value ceiling. With some work, this function could not only integrate more time frames, but also be expanded to other metrics that are output by NLDAS-2. Snow water equivalent (SWE) is one example that could enhance cold-season drought monitoring. Vapor pressure deficit could be used to enhance drought monitor capabilities during the warm season.

It could also be expanded to newer, more holistic drought metrics using the Kimberly-Pennman, or Pennman-Monteith equations to calculate potential evapotranspiration (PET). Some of the more highly-reviewed metrics of drought include the Standardized Precipitaiton-Evapotranspiration Index (SPEI), and Aridity Index (Vicente-Serrano 2010). SPEIs are calculated as Precipitation – PET, and Aridity is calculated as Precipitation/PET. This opens the door for making plots of PET, SPEIs, Aridity. For instance, SPEIs can be calculated as Precip – PET traditionally follows a log-logistic distribution (Vicente-Serrano 2010). In research done by Tsakiris et al. 2006 Precipitation/PET is assumed to follow a lognormal distribution.

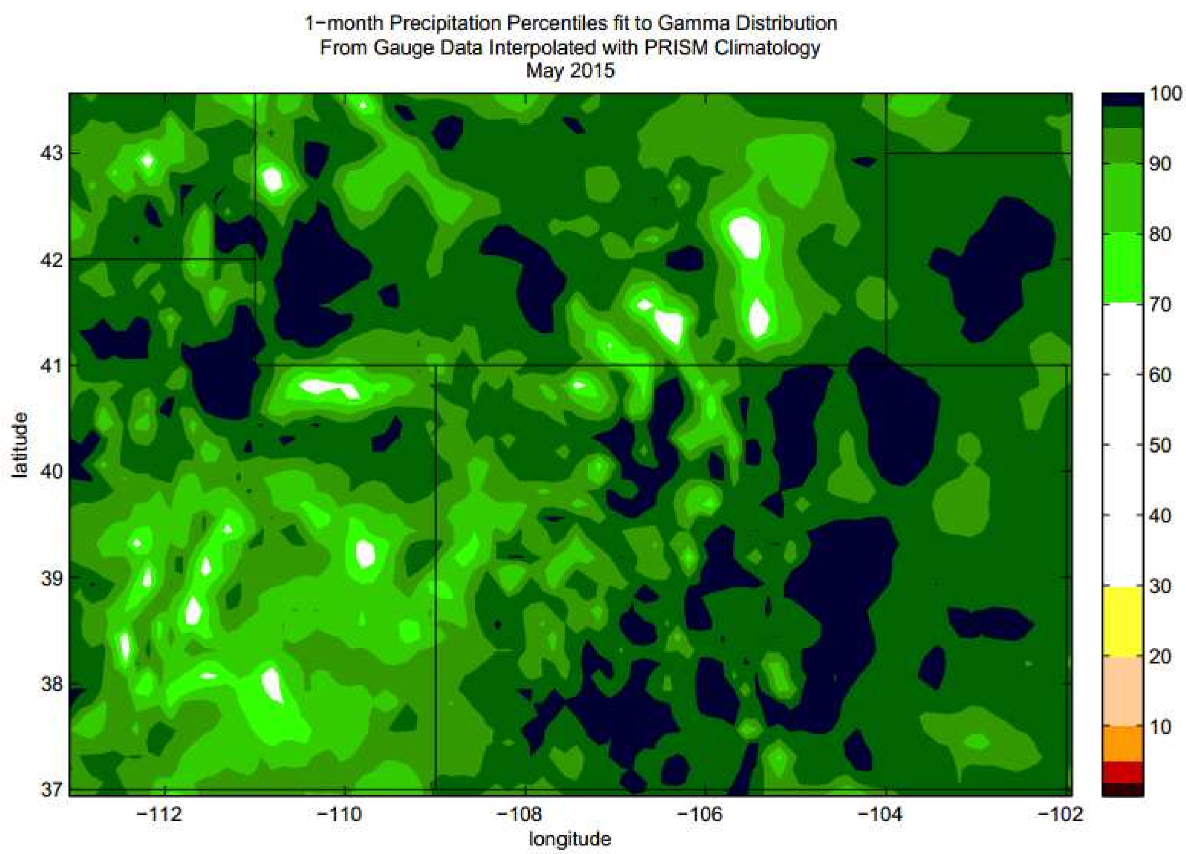

Figure 2.6: 1-month precipitation accumulation percentiles are contoured here for the Upper Colorado River Bain and western High Plains for the month of May, 2015. NLDAS Phase-2 data were used here in order to determine a precipitation percentile ranking for each grid cell for the month of May 2015, a very wet month. Percentiles are assigned according to where the value

falls on a cumulative density function of the associated Gamma distribution from years 1985-2014. Some areas, such as the Wasatch and Uintah Mountain Ranges in Utah, did not fare as well with respect to normal.

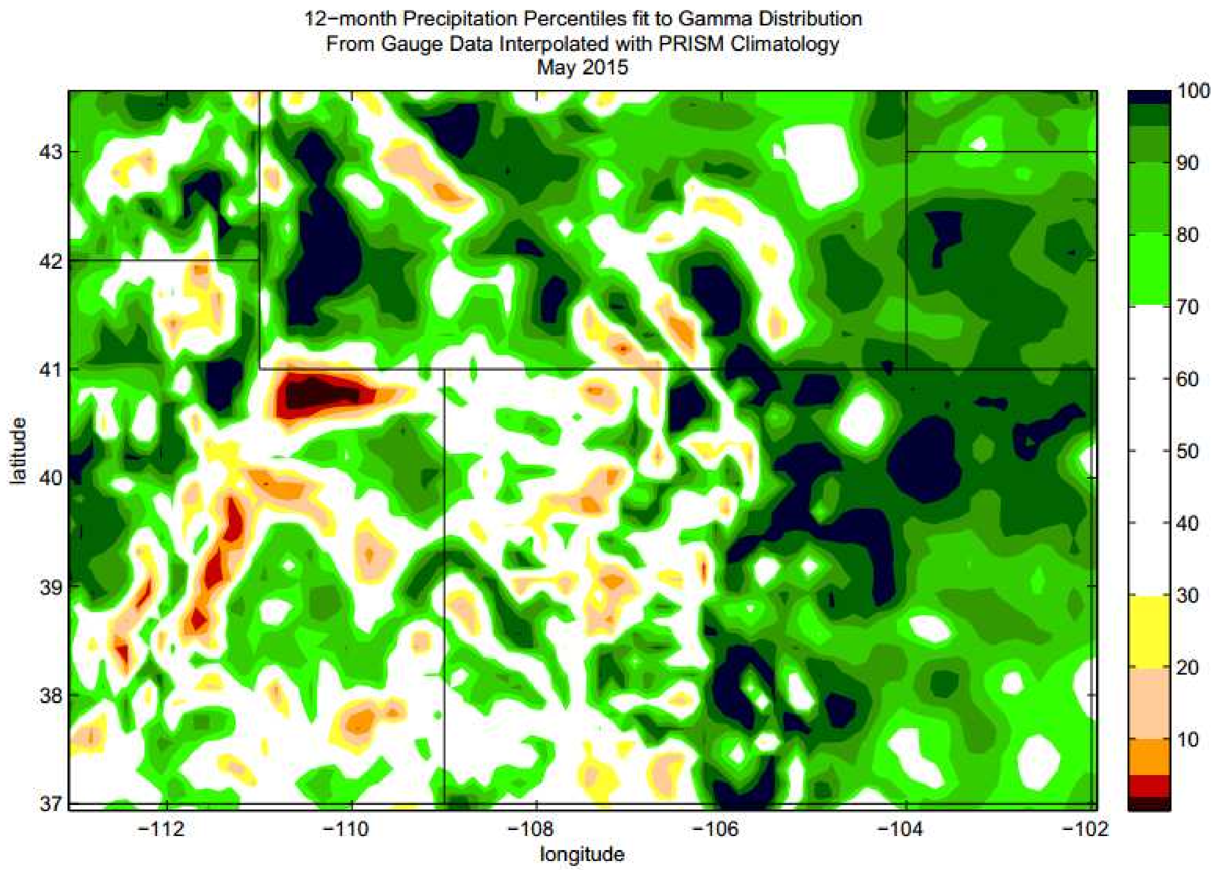

Figure 2.7: Looking at the bigger picture (12 months) this example gives us an evident view of how the wet late April and May of 2015 balanced against a poor snow season for the Upper Colorado River Basin. Higher elevations, which climatologically receive a greater fraction of their precipitation in the wintertime, are still drier in areas such as the Wasatch and Uintah Mountain Ranges in Utah. This kind of depiction is not as easily conjured up using High Plains Regional Climate Center Data as building precipitation maps for the area with stations with long, consistent periods of record may under sample high terrain. This comes with the tradeoff of a shorter period of record and the precipitation totals not being direct observations of precipitation.

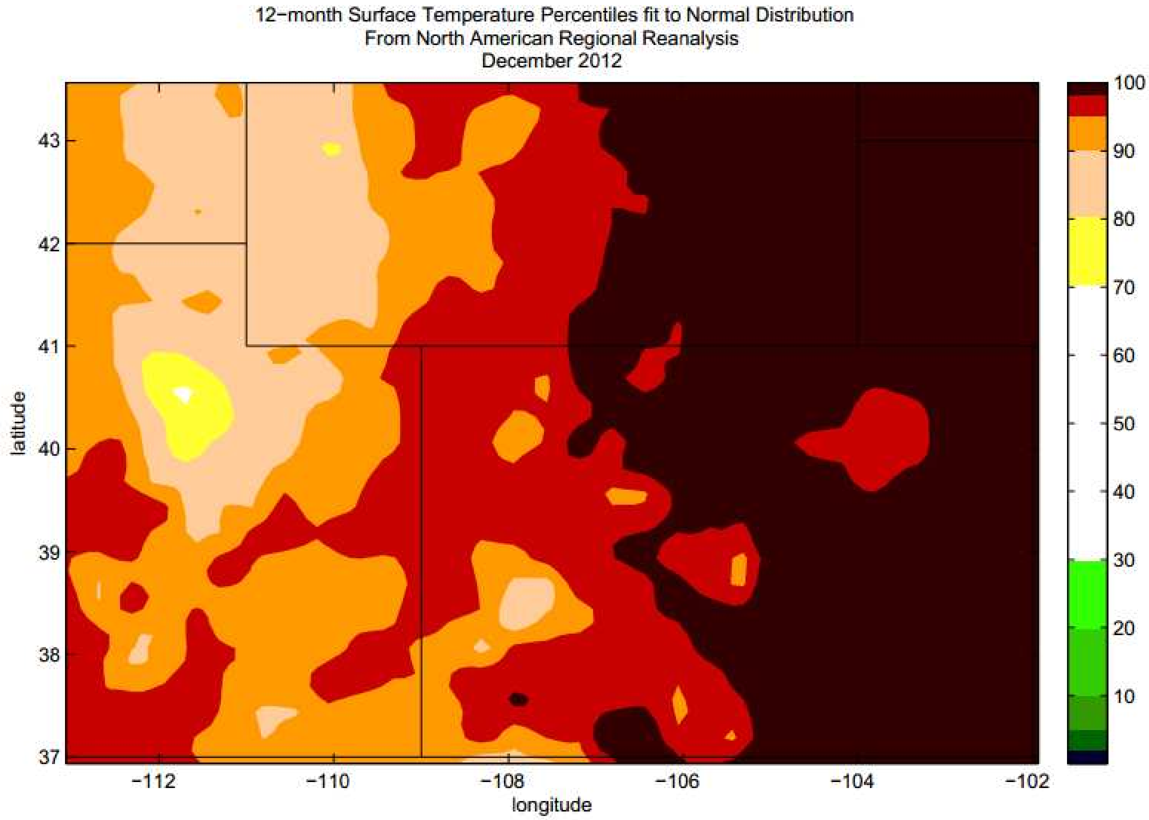

Figure 2.8: Temperature percentiles using NLDAS-2 data have been contoured here for the Upper Colorado River Basin and western High Plains. The year of 2012 was hotter than the 98th percentile expected based on 1985-2014 climatology for most of eastern Colorado and Wyoming.

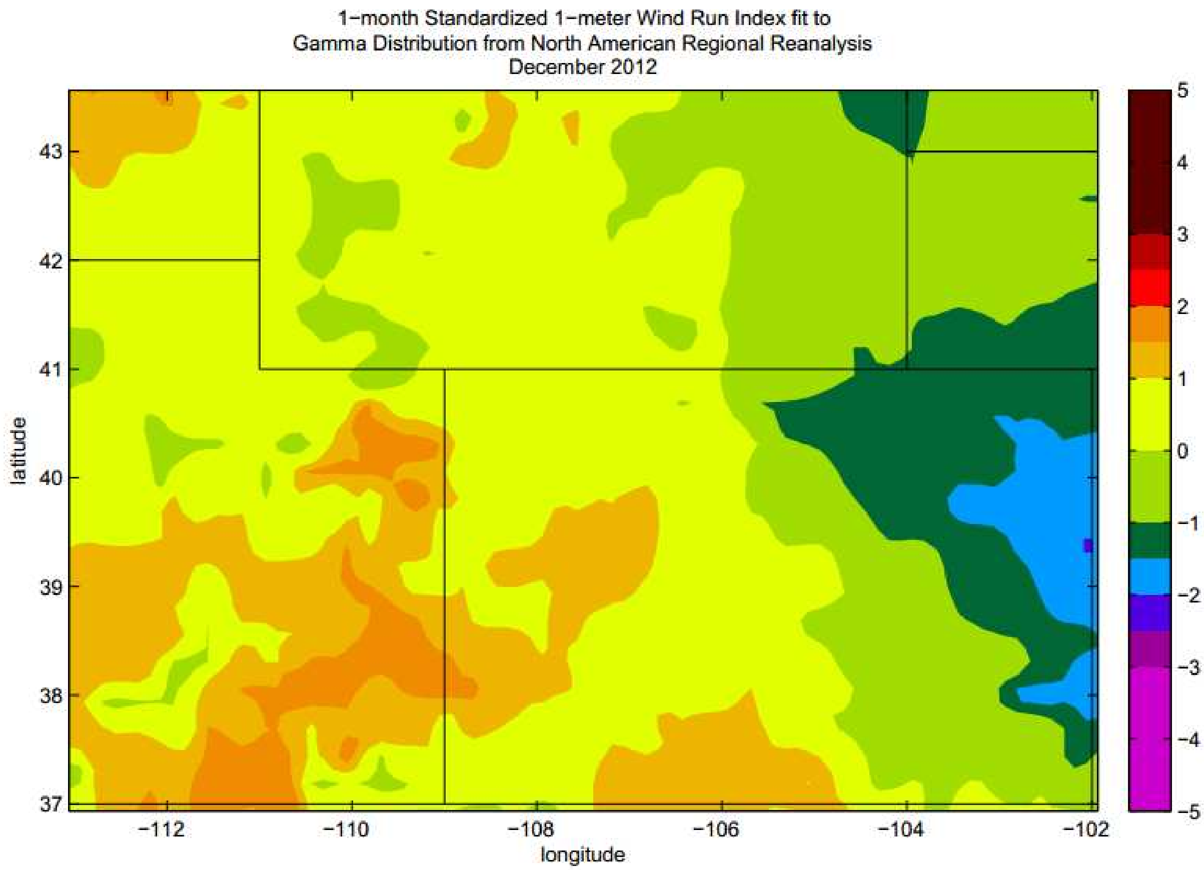

Figure 2.9: SUIs are depicted here for the month of December, 2012. SUIs are essentially a version of the SPI for wind. There is an error in the title. Wind run was fit to a Weibull Distribution. This month was characterized by above average wind run west of the Continental Divide and below average wind run east of the Continental Divide.

AN INVENTORY OF TOOLS AVAILABLE FOR SOIL MOISTURE MONITORING

Root zone soil moisture can be monitored in a number of ways. Each method has its limitations. There is lots of value to be had in combining several RZSM monitoring techniques. In this chapter the tools available for monitoring soil moisture in Colorado and the Upper Colorado River Basin are briefly explored, and a roadmap is laid out for how it will be used in this research.

Gravimetric Measurements: Soil moisture all starts with quality ground validation. Gravimetric measurements are taken by removing a known volume of soil from the earth, drying that sample thoroughly at 100 Celsius, and then calculating the volume of water removed divided by the total volume. The cost of both the materials and time necessary for gravimetric measurements is considerable, but no other measurement techniques are possible without them.

In-situ Reflectometer and Hydraprobe Measurements: While the spatial distribution is not ideal in-situ soil moisture measurements are gradually becoming quite plentiful in the Upper Colorado River Basin. In eastern Colorado the number of available measurements drops off quite a bit as neither SCAN nor SNOTEL have a presence in this area, and CoAgMet is yet to really establish a widespread soil moisture monitoring network. In-situ measurements offer better temporal resolution than gravimetric, satellite, or modeled soil moisture measurements. The primary limitation of in-situ measurements is spatial distribution. Soil type changes on characteristic length scales of less than one km^2, so the cost of installing enough stations for interpolations of RZSM to be accurate would be exorbitant. This can be corrected for by lab-testing soil samples from each measurements site, and reporting measurements as “Available Plant Water,” or amount of water in surplus of the soil moisture wilting point. This is the strategy employed by the Oklahoma Mesonet.

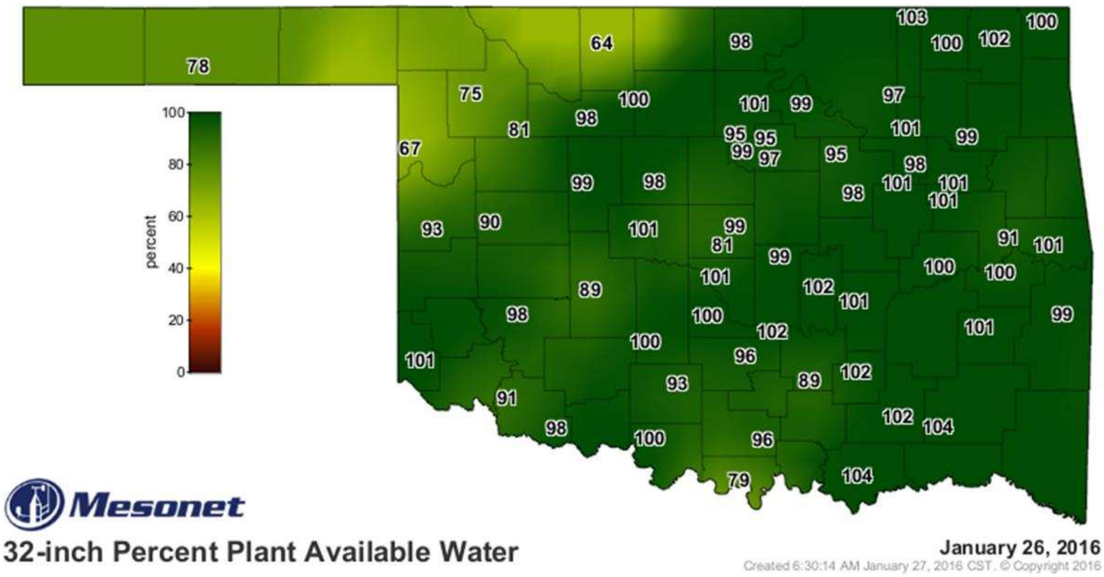

Figure 3.1: A spatial interpolation of available plant water is offered here by in-situ soil moisture measurements from the Oklahoma Mesonet. A value of 100 is representative of field capacity. A value zero is representative of wilting point.

Satellite Observations: The highest spatial resolution measurements of all tend to come from satellites. Starting in the 1990s this has traditionally been done with microwave radiation because the atmosphere is mostly transparent to microwave radiation, vegetation is semi-transparent, and the dielectric properties of soil are a function of its volumetric water content (Jackson 1993). LandSat and WindSat have both been utilized for global soil moisture data reconnaissance in the past. The latest satellite to hit the sky is the Soil Moisture Active Passive (SMAP) satellite, which launched in February of 2015. The "active" component of the sensor has experienced some technical difficulties.

Numerical Land Surface Models: Parameterizations of root zone soil moisture in land surface models are important in the numerical weather prediction community both on operational forecasting and seasonal forecasting timescales. Soil moisture models offer a combination high-resolution spatial and temporal analysis. It is the combination of measurement techniques discussed above that makes drought monitoring with numerical soil moisture models possible. These data are, of course, derived fields, and therefore only as good as the land survey and atmospheric data that are used in the assimilation process.

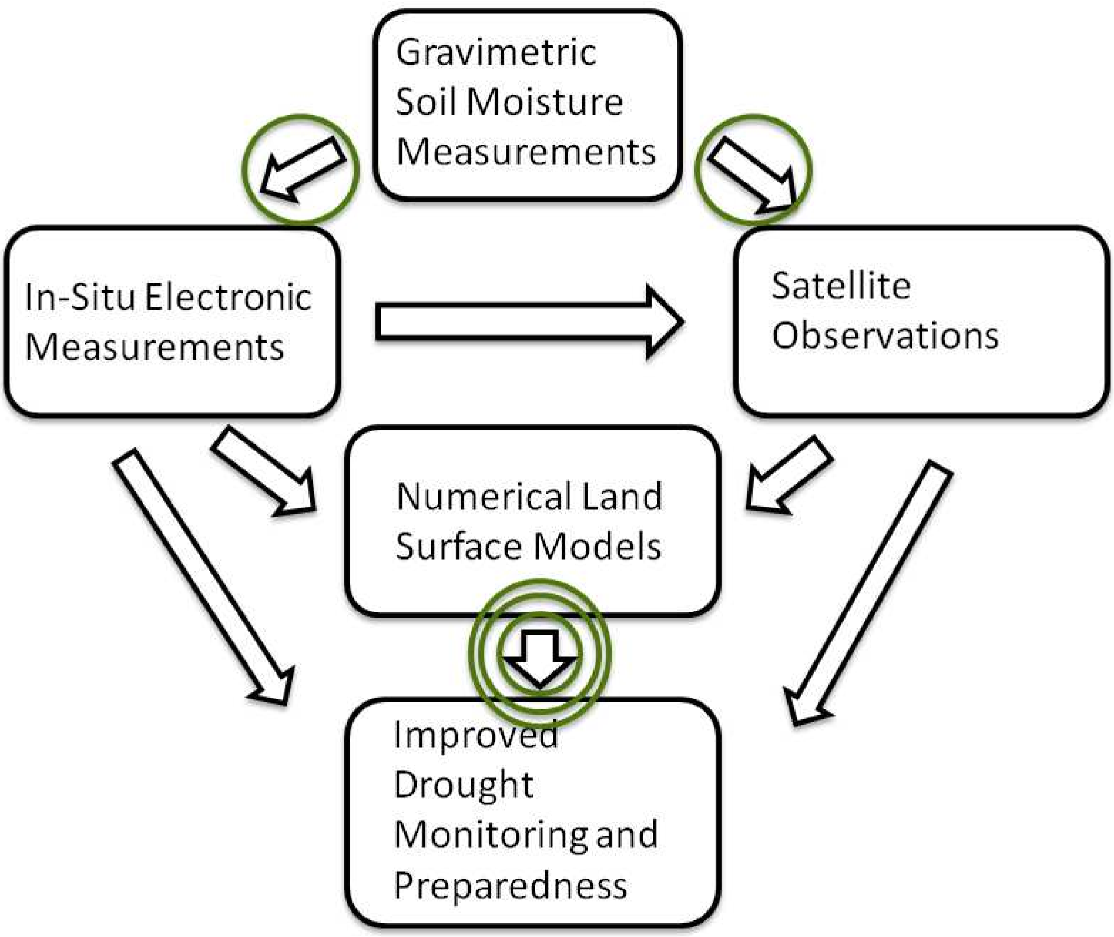

Figure 3.2 illustrates the pathways by which soil moisture data from one source can be used to improve the quality of others. The green circles are representative of the proportion of discussion this study will include for each arrow.

Now that concepts paramount to drought monitoring and soil moisture monitoring have been thoroughly introduced the remaining results from this research will focus exclusively on soil moisture data of different kinds. The development of a volunteer (citizen scientist) gravimetric soil moisture measurement protocol designed to help ground validate drought impacts and satellite measurements will be discussed. Later results will focus heavily on the use of numerical soil moisture modeling results for the improvement of drought monitoring and early warning. Firstly, the relationship between root zone soil moisture, and temperature and precipitation averages for subsequent Julian days will be explored from a domain-averaged perspective for the Upper Colorado River Basin and western High Plains. Then, these relationships will be quantified as a function of space. Ultimately, a statistical model will be engineered to improve precipitation and water balance forecasts by basin for the late spring and early summer to contribute to drought early warning efforts.

COMPARISON BETWEEN COMMONLY-USED IN-SITU ELECTRONIC SOIL MOISTURE SENSORS IN COLORADO AND THE UPPER COLORADO RIVER BASIN

Motivation: According to the North American Soil Moisture Database soilmoisture.tamu.edu there are 181 automated electronic soil moisture measurement stations in Colorado and Utah that are part of the Soil Climate Analysis Network SCAN, or the Snow Telemetry (SNOTEL) Network, which both fall under the umbrella of the Natural Resources Conservation Service (NRCS). There are several more within the Upper Colorado River Basin when including the portion of the Upper Green River Basin in southwest Wyoming. The Colorado Agricultural Meteorological Network (CoAgMet) has installed soil sensors at 14 sites around Colorado, primarily at low elevations relative to the state as a whole.

The two sensor types primarily used to collect measurements from SCAN and SNOTEL sites are the SDI-12 Volt Hydra Probe soil sensor, a Stevenswater product. The CoAgMet sites make use of data from CS650 Water Content Reflectometers, a Campbell Scientific product. Both of these instruments derive volumetric water content by generating an electric current over the sensor and measuring the dielectric permittivity of the soil around it (CS650 and CS655 Water Content Reflectometers 2011) (The Hydra Probe Soil Sensor 2007). Since water is a naturally-polarized molecule due to its hydrogen bonding, the fraction of soil pore space taken up by water can be derived by running a small current across the sensors and gauging the response of the electric field.

Data from these stations do not come without their share of limitations: Firstly, they do not offer an avenue for creating a reliable spatially-distributed overlay of soil moisture. Even if soil type were homogenous, which it is certainly not as a web soil survey from the NRCS will readily show, these stations under-sample low elevations as well as area in Colorado east of the Continental Divide. As is demonstrated in chapter two, soil moisture measurements are no longer reliable once the water in the soil freezes. The application of these data for drought monitoring is currently limited by the length of the datasets as well. The majority of the sensors have been installed since the turn of the millennium with new sensors coming online each and every year from both NRCS and CoAgMet. Drought monitoring intrinsically relies on comparing current data against background climatology, and climate normals are established based on continuous 30-year periods of record. Thus, our understanding of anomalies measured by these soil sensors is currently limited. The silver lining to this problem is as long as these sensors stay active this problem will diminish over time.

These soil sensors do offer perks that make them worth integrating in the drought monitoring process. Soil sensors allow for a physical measurement of soil moisture at rapid and regular intervals through the entire root zone, a feature not offered by numerical models, satellite observations, or soil cores. This allows dielectric permittivity sensors to provide valuable data about the state of the hydrologic system, feedbacks between the soil and the atmosphere, and fire weather danger.

Having all these pros and cons laid out; the motivation of this chapter is to test the applicability of direct comparisons between Steven's Water SDI 12-Volt sensors to Campbell's Scientific 650 reflectometers for drought monitoring applications.

Methods: Sensor comparison was conducted at the Christman Field Weather Station in Fort Collins, Colorado located 0.48 miles northeast of the Colorado State University Atmospheric Science Department on west La Porte Avenue. The first experiment simply compares the readings of CS650 sensors to Hydra Probe sensors at 8 and 20” depths throughout the growing season and shoulder seasons of 2015. These observations will be compared with gravimetric observations in a later chapter. This comparison was performed for Climate Center internal usage. One can imagine that similar comparisons at many different sites across many different soil types would make for a more interesting study, but would also be too expensive an offshoot of this research in terms of both time and money.

Installation: Hydra Probe and CS650 sensors were installed at Christman Field as of the second week of December 2014, but Hydra Probes were not made operational until the 10th of March, 2015. Though neither of these sensor types matches the types of sensors installed in the Oklahoma Mesonet (229-L heat dissipation) the installation protocol was designed in a very similar way, particularly when it comes to avoiding preferential flow through the cables. Sensors are powered using an on-site solar panel. A hole was dug down to just past 40” below ground level. Hydra Probes were placed at depths of 2, 4, 8, 20, and 40”. These intervals were chosen because they are the standard installation intervals at SCAN sites in the Upper Colorado River Basin, and are used at some of the SNOTEL sites. CS650 sensors were only placed at 8 and 20”. This is partially in attempt to mimic the setup at CoAgMet stations where there are only two soil sensors (one close to the surface, and one deeper), and so that the sensors are aligned with Hydra Probes for direct comparison. It was desired that there be a CS650 at the 2” depth, but because CS650 sensors are long, thin, and somewhat fragile this installation was omitted.

The hole dug to install these sensors included a face on the east side that is normal to the ground surface and shaved flat. The sensors were then installed into the undisturbed soil up and down the face orthogonal to the surface. Cables leading back to the data logger were looped below the sensor level in order to avoid problems with preferential flow to the sensor during percolation. The hole was then backfilled with an honest effort to keep the removed dirt at the level it previously resided at and similarly compacted.

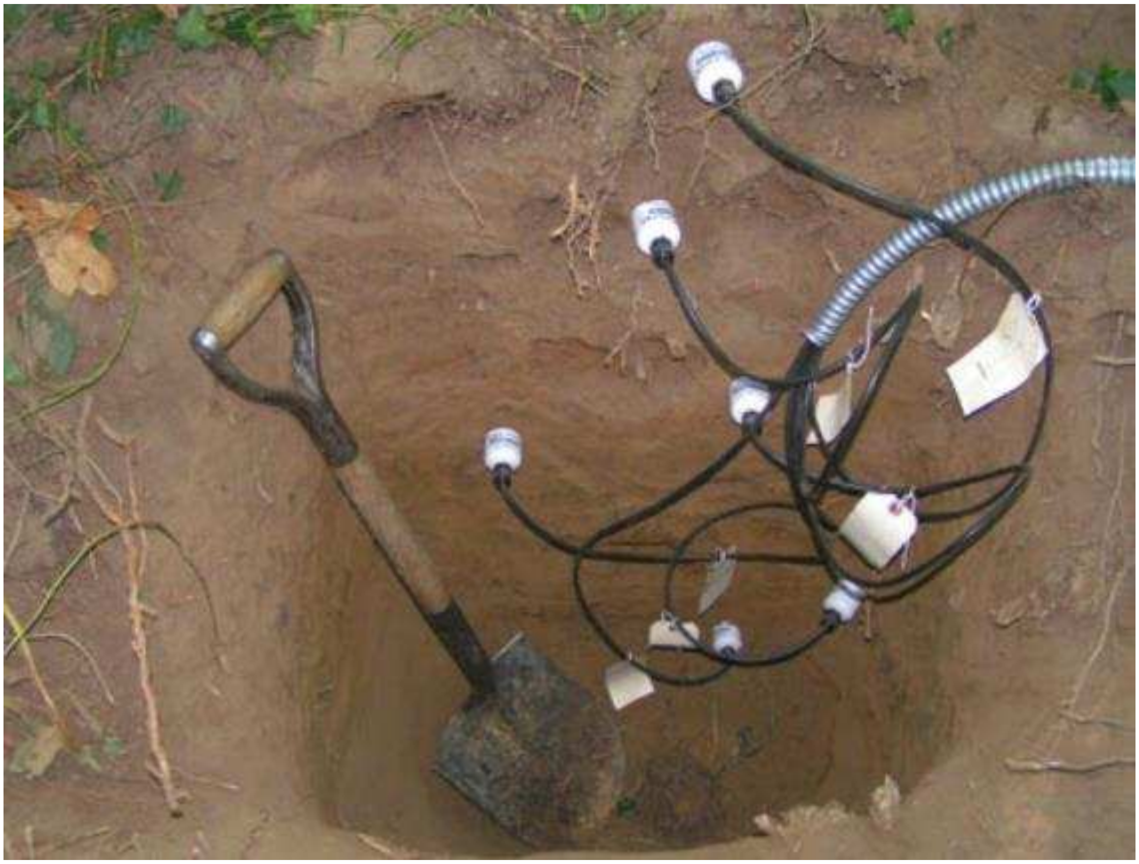

Figure 4.1: The image above courtesy of Stevenswater (The Hydra Probe Soil Sensor 2007) shows the distinct horizons soil sensor installation process that was used in this experiment.

It is important to note that dielectric permittivity sensors should be calibrated to the soil type in which they are installed in order to obtain the most reliable volumetric water content measurements possible. The Stevens Hydraprobes used in this experiment were set to the default factory LOAM calibration, which is the calibration setting used at most SNOTEL stations, and has been proven as a calibration accurate for most soil types by Seyfried et al 2005. CoAgMet soil sensors that have been installed thus far have not undergone field calibration, but soil samples have been gathered from each site, and volumetric water content is currently derived using the Topp Equation (CS650 and CS655 Water Content Reflectometers 2011).

Results: Interesting information is stored in the soil moisture readings taken from the Stevenswater Hydra Probe relay from 2-40" that were taken for the growing season and shoulder seasons of 2015. The same can be said for the Campbell's Scientific Relfectometers that were installed at 8 and 20". Unfortunately while the two sensor types did show in-phase responses to precipitation, there were large differences between measurements from the two sensor types. In general, the CS650 sensors showed more amplified responses to changes in VWC than the hydra probes. Differences between the two sensors were as much as plus or minus 80%. It is not known with certainty that the CS650's amplified response is an exaggeration, but given the hydra probes make use of a well-tested calibration setting it is reasonable to hypothesize that hydra probes' measurements may be more accurate.

Hydra probe volumetric water content measurements were receptive to the anomalous late spring moisture of 2015. The sensor relay data show evidence of a wetting front propagating from 2-20" over the course of several days starting with precipitation on April 16th. It took nearly a month over the course of which over three additional inches of precipitation fell for soil at 40" depth to be replenished. Soil type at Christman field is unlikely to be homogenous with depth. This is evidenced by the gradient in volumetric water content from 2-20" during both wet and dry periods. Volumetric water content readings decreased through all layers from June to late August as this period was quite dry. Fall rain replenished the soil down to 8", but sensors at 20 and 40" were unaffected.

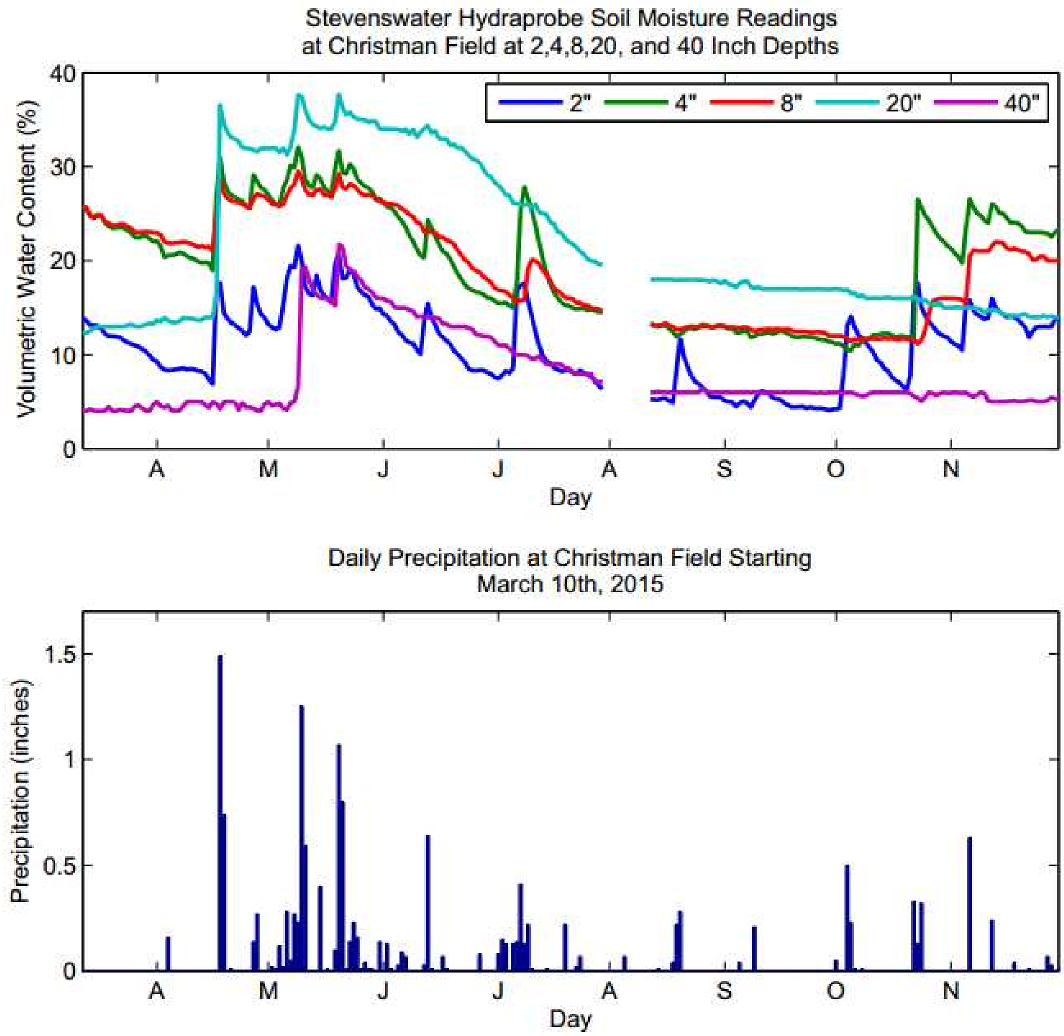

Figure 4.2: Volumetric water content is displayed (top panel) from the Stevenswater Hydra Probe Relay with sensors at 2, 4, 8, 20, and 40 inches. Daily precipitation measurements from Christman Field (bottom panel) are displayed in inches for the March 10th-November 29th of 2015.

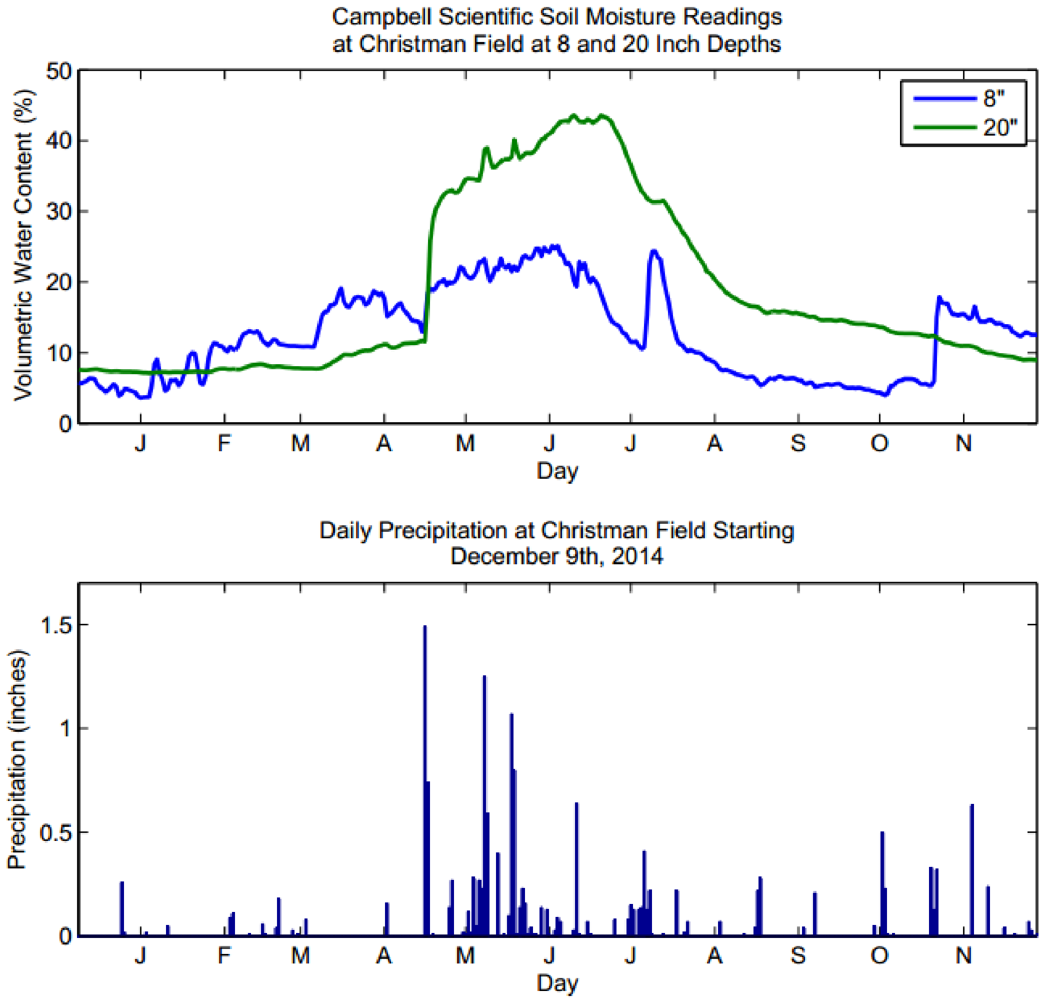

Figure 4.3: Volumetric water content is displayed (top panel) from the Campbell's Scientific Relay with sensors at 8, and 20 inches. Daily precipitation measurements from Christman Field (bottom panel) are displayed in inches for December 9th of 2014 to November 29th of 2015.

Much akin to the hydra probe readings from 2015, the CS650 reflectometer data showed a marked response to a wet April and May season. Soil drying through the month of June was more drastic as shown by the reflectometer data than the hydraprobe data. The response to rainfall occurring in the first ten days of July was also more drastic. Reflectometer response to late October rain occurred several days ahead of the hydraprobe response at 8".

One of the more puzzling aspects of the volumetric water content data gathered from both sensors is that both reveal a diurnal cycle that appears to be in phase with temperature measurements. The Stevenswater manual vouches for a lack of need for temperature correction expressing that “The Hydra Probe’s soil moisture and electrical conductivity measurements are temperature corrected providing temperature independent data year round,” but the presence of a diurnal oscillation in the data is undeniable. If the measurements are skewed as a function of temperature this raises several questions: is the relationship is linear, or higher order? What temperature should be used as a baseline for normalization? Is the amount of temperature dependence realized by the sensor a function of the true volumetric water content? The CS650 sensor at 8” oscillates in reported volumetric water content by as much as $0.047\,\frac{cm^3}{cm^3}$ in July when base state soil moisture was high and temperatures were relatively high. It is important to mention here that CS650 sensors were likely not calibrated as they should be.

This raises concern about temperature’s influence over the sensor’s seasonal cycle as well. With the exception of instances in early July and mid-October where water from the same precipitation event clearly reached the 20” depth CS650 sensor before the 20” hydra probes sensor the difference between the two sensors does one smooth three-quarters-wave oscillation from March to November that lines up with the seasonal temperature cycle, and reads as much as 40% higher than the hydra probe in mid-summer and 40% below the hydra probe at the beginning and end of the measured period. Furthermore, focusing on late April through early July, both sensors show volumetric water content increasing by over 20% following a large precipitation event on April 16^{th}-19^{th}, but respond very differently after. The hydra probe at 20” plateaus at about 34% VWC with a few small spikes in May as conditions remained wet. The CS650 sensor continues to report increasing VWC values all the way to the beginning of July up to 45%. These increases as soil temperature rises are consistent with the daily temperature sensitivity exposed at 8” depth.

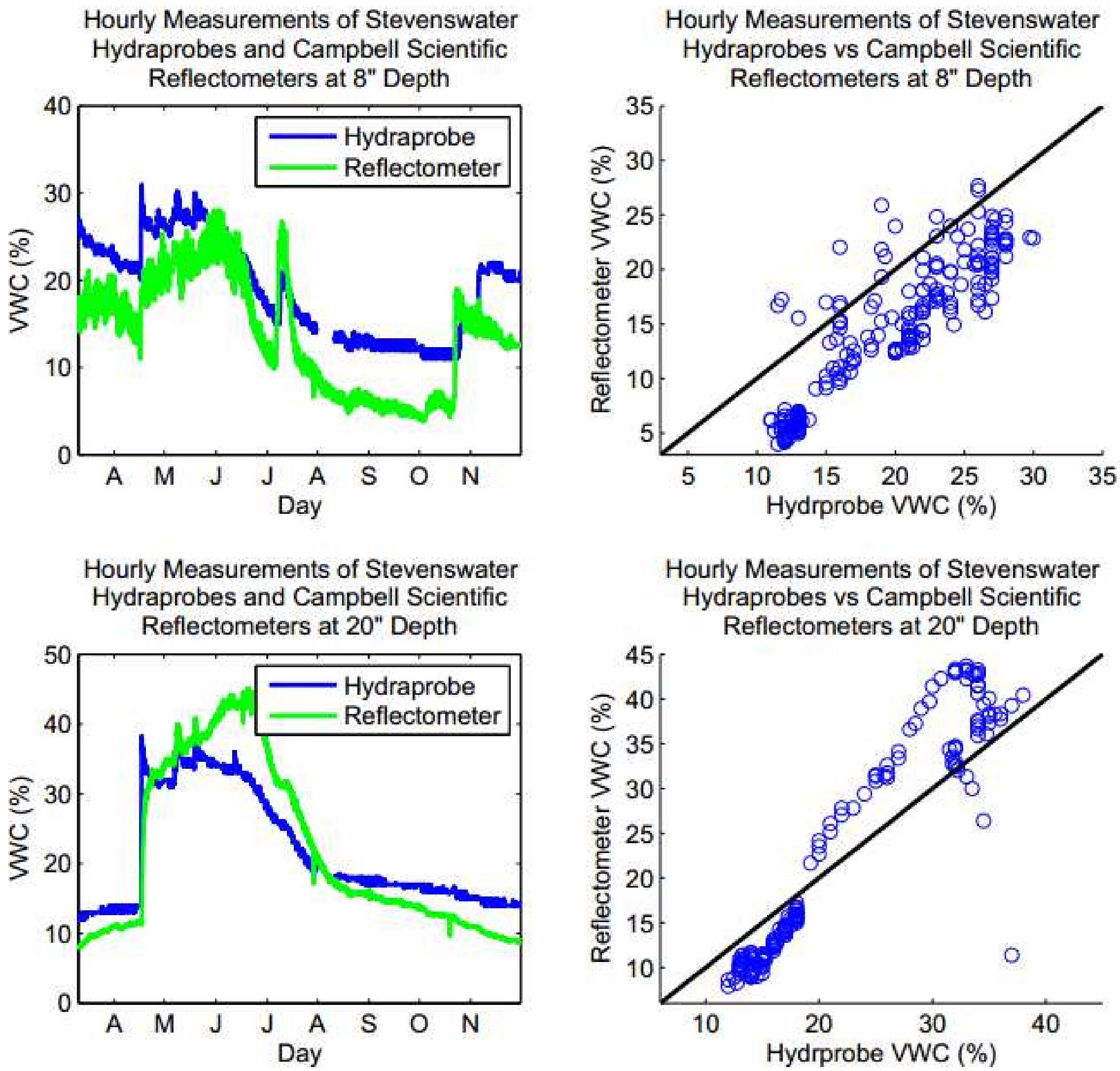

Figure 4.4: Volumetric water content is displayed for both Stevenswater Hydra Probes and CS650 Reflectometers at 8” (upper left) and 20” (lower left) for every hour from March 10th to November 29th for the year of 2015. A random sample of this data was pulled to make scatterplots of the measured volumetric water content from both sensors at 8” (upper right) and 20” (lower right) with a 1:1 comparison line included in black.

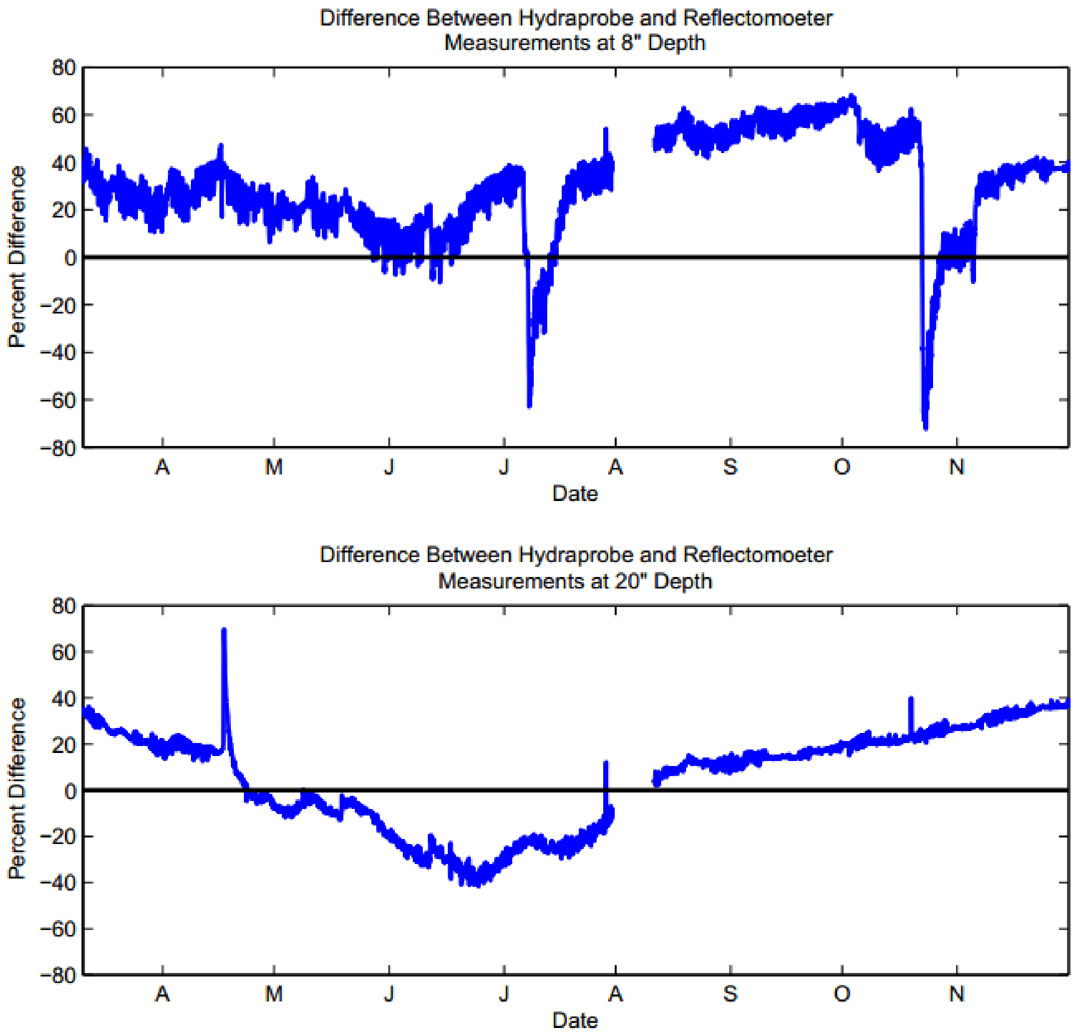

Figure 4.5: The percent difference between Hydra Probe and Reflectometer measurements are displayed here for every hour from March 10th-November 29th of 2015. Positive values indicate higher Hydraprobe readings and negative values indicate higher Reflectometer measurements.

It should not go without mention that Stevenswater probes showed a diurnal cycle that is independent of true hydraulic fluxes and appears to be temperature-dependent as well. This is a concern, but less of a concern, because these oscillations did not exceed 0.01 $\frac{cm^3}{cm^3}$ from trough to ridge on a daily basis.

The other potential problem in comparing these two sensors is that there may be some preferential flow reaching the reflectometers. Because of the long, narrow build of CS650 sensors they are harder to protect from preferential flow, especially when installed under very dry soil conditions. This was the case when the sensors were installed on December 9th of 2014.

The soil moisture trends measured by the two different sensor types showed similar responses to late spring moisture, dried through the late summer and early fall, and were recharged at depths above 10" by rain in October and November. The sensor types did not compare as favorably in volumetric water content magnitude as they did in volumetric water content trend. Sensor responses from the CS650 sensors used by CoAgMet from hydraulic fluxes were potentially too rapid and exaggerated, though it would be difficult to say for sure without a large sample of reliable gravimetric measurements at 8 and 20 inches. It is clear that CS650 data are troublesomely connected to temperature. This research is not sufficient for declaring one sensor type superior. It only demonstrates differences in current output given current calibration techniques. Campbell's Scientific and CoAgMet need to converse for CoAgMet soil moisture data to be improved. This will happen.

ESTABLISHING A CITIZEN SCIENCE-FRIENDLY SOIL MOISTURE CORING PROTOCL CABAPBLE OF PRODUCING ACCURATE GROUND VALIDATION THAT IS ALPHA-TEST READY

Motivation: One of the primary goals of this project was to help establish the citizen science community as an integral part of the soil moisture monitoring, and drought monitoring process in upcoming years. The Community Collaborative Rain, Hail, and Snow network (Reges et al 2016) serves as a potential vehicle for doing so. CoCoRaHS routinely receives over 10,000 daily rainfall reports. These reports come in from all 50 states in the USA, and from most Canadian provinces. Observers have the option not only to report daily rainfall, but also hail, snow, evapotranspiration, and drought impacts or significant weather events if any of these events happen. CoCoRaHS is slated to expand to include a soil moisture measurement protocol in 2016. In the words of Nolan Doesken, Colorado's state climatologist and founder of CoCoRaHS, had the following to say:

> "Our goal is to come up with a protocol that is affordable and citizen science-friendly, but ensures that volumetric water content measurements within 10% (as per the NASA SMAP team's request) of the true value are possible. Future uses of these data would include, but are not limited to satellite ground validation, drought monitoring, and assimilation into numerical weather prediction software."

There were two primary experiments conducted in order to develop a protocol allowing citizen scientists to contribute to the soil moisture monitoring process by taking soil cores. Both experiments were conducted at the Christman Field weather station (see chapter five for location.) Experiments ultimately lead to a draft of a protocol that may be expanded to alpha testers around the United States, but cannot be proven to meet all the quoted goals listed above, specifically, we cannot guarantee accuracy within 10% of the true volumetric water content based on the experiments to follow. The first experiment took place in the first two weeks of June in 2015, and the second throughout the fall of 2015 from September into the fourth week of November. The first experiment ended up serving as a jumping off point for creating the first draft of a potential soil moisture coring protocol, and the second to test if any of the variations of the protocol drafted are sufficient to be deployed in a nationwide alpha test coming soon. In order for the protocol to be expanded to a nationwide alpha testing group, experiments must be conducted in order to convincingly satisfy the following criteria:

1. Interested citizen scientists around the United States will be able to take soil cores and provide volumetric water content measurements to end data users that are within a 10% margin of error.
2. Participants from all over the United States will be able to participate regardless of soil type if they have legal access to dig in unirrigated soil in areas reasonably representative of surrounding prevailing soil and vegetation conditions.
3. Time committed by participants must be "reasonably minimal" if choosing to take soil cores with a regularity of at least once a month.
4. Observers must be able to enter data for soil cores not just from the top two inches of soil, but also from a depth that approximates conditions lower in the root zone (ie 7-9").
5. Soil samples from soil cores must be greater than 100g in weight.
6. Participation must be inexpensive and non-excluding of any demographics that are underserved in the citizen science community.

Disclaimer: While the first soil coring experiment done in the first two weeks of June 2015 was a valuable educational lesson it should be noted up front that the experiment was flawed due to only taking one measurement at the end of the experiment where the volume was known. Results from this particular portion of the chapter will in no way be considered for subsequent publication.

Experiment One Methods: The first of these two experiments was designed to test the covariance of the Stevenswater Hydra Probes and core measurements in handling the dynamic topsoil drying process in the first two weeks of June of 2015. This period was thought to have the potential to include a wide variety of volumetric water content measurements over a small time frame. 30-day SPIs for southeast Larimer County on May 31st of 2015 were between 1.5 and 2 standard deviations above the mean (HPRCC 2015). On top of this, May is the wettest month climatologically in the area. Root zone soil moisture as of May 31st was above the 80th percentile in the region as recorded by the Variable Infiltration Capacity model run through the University of Washington with respect to 1916-2004 soil moisture climatology. With potential in the forecast for higher temperatures, lots of incoming solar radiation, and possible thunderstorms in forecast, this two week period was ripe with exciting potential for dynamic wetting and drying of the top two inches of soil in the area.

For the early June experiment soil core measurements at depths of 0-2, and 7-9" were taken around midday on June 2nd-5th, and June 8th-12th. June 1st was unfortunately omitted from the experiment because of jury duty.

One major source of error that merits mention in the methods portion of this write-up is that the soil canisters were not full for each and every core measurement. One full sample was taken at both 0-2" and 7-9" depth, and then bulk density was assumed to be constant for all samples taken at the same depth throughout the two week period in order to allow volumetric water content values to be backed out in the cases where the canister was not full. This was the main source of error on the part of the experimenter, but other important sources of error, even when following the protocol properly were discovered in this experiment.

Hydra probe data from the sensor at 2” depth was compared to the 0-2” core measurements. The assumption was therefore built into the experiment that the 2” volumetric water content as measured by the SDI 12 sensors would make for a good approximation of layer average volumetric water content for 0-2” depth despite being an end point. This was a compromise between making sure the sensor is buried enough as to go undisturbed, and taking test soil cores of the layer that is ultimately intended to be sampled by CoCoRaHS volunteers. As is the case in a running sense, measurements from the Hydra Probes and Campbell’s Scientific sensors were compared directly against one another. The protocol used for soil coring in this experiment was inspired by NASA’s GLOBE soil moisture measurement protocol, but is not an identical protocol (GLOBE 2014). Both the oven drying and heat lamp drying methods outlined in the protocol below were tested in this experiment. It is as follows:

CoCoRaHS Soil Moisture Measurement Protocol (Experiment One):

Site Requirements:

1. The location which you choose to dig must be flat, or close to flat, as must the area around it. Because of runoff, soil moisture may be lower than representative of average at the top of mounds or hills, and higher than representative of average at local minima in elevation.
2. THE SITE CANNOT BE IRRIGATED: This is not to say there’s no benefit in soil coring irrigated land as this can help track if lawns/plants/crops are receiving appropriate water levels, but CoCoRaHS aims to depict conditions representative of a natural environment, and help to ground validate NASA’s new SMAP satellite.
3. Your dig site does not have to be baron, but surface vegetation should be pulled before taking a core sample. This helps to keep the proportion of organic matter in the sample as low as possible.

Sampling Depths:

1. 0-2”
2. 7-9”

Necessary Materials:

1. Pad, paper, and pencil/pen
2. Ruler
3. Level, or straight edge
4. Official CoCoRaHS Sampling canister
5. Metric Scale (precision to at least the nearest gram)
6. Trowel
7. Tin foil, cookie sheet, or pot pie holder
8. Oven or heat lamp
9. Graduated Cylinder (optional)
10. Gloves (optional)
11. Sharpie (or similar labeling device)
12. Masking Tape (optional)
13. Rag or paper towel

Measuring the Volume of your Canister:

- The volume of the standard CoCoRaHS canister is 8 oz, but in case of slight variance in either the manufacturing process, or your canister’s volume being slightly modified in taking past samples it can be a good sanity check to measure the volume with a graduated cylinder.
- Set your canister flat on either a rag or a surface you don’t mind getting wet. Remove the lid and fill the canister with water as full as you can get it.
- Set the top portion of your canister lid up-side-down on top of the canister itself to help remove any water falsely contributing to the canister’s volume through the formation of a meniscus. Then carefully wipe down the outside of the canister.
- Carefully pour the water into some sort of measuring device. A funnel should be placed underneath as some of this water will try to stick to the side of the canister rather than being poured. A graduated cylinder, or something that measures volume in milliliters or cm^3 (1 mL = 1 cm^3) is ideal because fresh water has the unique property of weighing one gram/cm^3 of volume. If you are using another measurement device to find the volume the following conversions may be useful:

$$8\ fluid\ ounces = 236.6\ cm^3$$

$$1\ gram\ H_2O = 1\ cm^3\ H_2O$$

The Coring Process:

1. Bring your pencil, paper, ruler, level (straight edge), sampling canister, scale, sharpie, masking tape, and trowel to your selected dig site.
2. Remove surface vegetation from your dig site as well as possible by pulling it from the ground. You only need to do this right where you are digging. You do not need to clear a large area around the dig site. About one square foot should be fine.
3. Use your ruler to make a mark on the trowel 2” above the nose. Make this mark as straight and as parallel to the nose of your trowel as possible.
4. Weigh your CoCoRaHS sampling canister and mark down the weight, so it can be subtracted from your later measurement.
5. Sink the trowel to the 2” mark in the soil. Chisel a cylindrical pattern out of the soil to this depth as close to the circumference of your sampling container as can be managed. Leverage this soil out of the ground and put it in your sampling container.
6. Remove as much of the organic matter from your soil sample as possible as well as any rocks that are larger than a pea.
7. Weigh your soil sample from the 0-2” depth and record it. Be sure to subtract out the weight of the container.
8. At this point you may want to label your canister with the date, time, and depth of measurement. You may prefer doing this with masking tape, and a sharpie or pen to avoid marking directly on the canister.
9. Clean off your trowel with a dry rag or paper towel to avoid sample cross-contamination.
10. In order to help sanity check measurements we do prefer that 2, or better yet, 3 samples be taken from each depth, so now you’re ready to repeat steps 5-11 one, or two times if desired. Keep the samples separated by several feet to avoid cross-contamination of samples, but close enough that all dig sites meet the site finding guidelines outlined above.
11. Now it’s time to get your 7-9” depth samples. It’s unlikely that you will be able to core straight down from the surface to 9”, so plan on digging out about a square foot of surface area down to 7” in order to take the measurement. These measurements should be taken directly below where you took your 0-2” measurements.
12. Be conscientious of how far you’ve dug. You can use the ruler to measure the depth, and a level, or just a straight edge, to make sure the ruler is lined up perpendicular to the ground.
13. Once you have dug out soil to 7” depth repeat steps 5-11 for your deeper samples. It is more crucial now that you have dug out a significant amount of soil to take samples that are actually representative of that depth rather than including chunks of soil that have fallen into your hole from the surface. Remember to weigh samples quickly after coring so that as little moisture escapes as possible. This is especially important for the deeper samples as this soil is not exposed to sunlight at all in its natural environment.

The Drying Process (Oven):

1. After collecting and weighing your soil samples the goal is to dry all the water out of them without igniting any of the leftover organic material. For this, make sure to have the following materials on hand: pencil and paper, drying surface (ie tin foil, cookie sheet, pot pie holder), and scale.
2. Set and your oven to 210-215 F and let it preheat.
3. Weigh the flat surface you wish to dry your soil sample on, so that this weight can be subtracted in your calculation.
4. Carefully pour your soil sample from the canister onto the drying surface, and spread it out. If you are using aluminum foil, fold up the corners before pouring the soil to avoid spilling. Drying the sample in the canister will lead to a very slow, and likely incomplete, drying process.
5. Weigh your sample again. Before placing it in the oven. A small amount of water may have already been lost having evaporated and condensed on the canister.
6. Once the oven has preheated place the soil sample in the oven, and wait!
7. Remove the soil from the oven occasionally to weigh it. Intervals of every half hour are recommended, but you may develop a more efficient system where the soil is weighed less frequently at first, and more frequently as it reaches its dry weight.
8. Once the soil weight no longer changes over at least a half hour period it is done.
9. Repeat steps 1-8 as needed in order to dry all your samples. There's no limit to how many you're allowed to oven-dry simultaneously so long as it can be done without sample cross-contamination. The average oven probably won't hold more than two on each rack.

The Drying Process (Heat Lamp):

1. Some folks may be hesitant to put soil in their oven, and in some regions of the country drying soil in the oven may leave a bit of a funky smell. Soil samples can also be dried under a heat lamp. Links to a CoCoRaHS-tested heat lamp and bulb can be found here: http://www.amazon.com/gp/product/B0066L0YJE?psc=1&redirect=true&ref_=oh_aui_detailpage_o03_s00
   http://www.amazon.com/gp/product/B0061MZ4Q6?psc=1&redirect=true&ref_=oh_aui_detailpage_o03_s01
2. Make sure to have the following materials on hand: pencil and paper, drying surface (ie tin foil, cookie sheet, pot pie holder), heat lamp, and scale.
3. Set up your heat lamp so that soil samples can be placed directly underneath it, and within a foot and a half of the bulb. DO NOT use the heat lamp over carpet, or any flammable surface. A hard, reflective surface will work best.
4. Weigh the flat surface you wish to dry your soil sample on, so that this weight can be subtracted in your calculation.
5. Carefully pour your soil sample from the canister onto the drying surface, and spread it out. If you are using tin foil, fold up the corners before pouring the soil to avoid mass

loss. Soil has very low conductivity, so drying the sample in the canister will lead to a very slow, and likely incomplete, drying process.

6. Weigh your sample again before placing it underneath the heat lamp. A small amount of water may have already been lost having evaporated and condensed on the canister.
7. Place your soil underneath the heat lamp, and wait!
8. Remove the soil from underneath the lamp occasionally to weigh it. Intervals of every half hour are recommended, but you may develop a more efficient system where the soil is weighed less frequently at first, and more frequently as it reaches its dry weight.
9. Once the soil weight no longer changes over at least a half hour period it is done.
10. Repeat steps 1-9 as needed in order to dry all your samples.

Bulk Density and Volumetric Water Content Calculations:

- A density is simply a mass divided by a volume. The bulk density of your sample is the weight of the contents of the canister once dried divided by the volume of the canister.

  Bulk Density = dried soil mass/container volume

- Since fresh water has a density of 1 gram/cm^3 the volumetric water content can be obtained by dividing the difference in wet and dry weight by the volume of your canister, and then multiplying by 100. This is expressed in the following simple formula:

  VWC (%) = 100*[(wet weight)-(dry weight)]/(container volume)

  Make sure you have converted your container volume to cm^3 so that the expression is unitless!

Experiment One Results: Correlations between gravimetric and hydra probe measurements were strong (0.723 and 0.717) at both 0-2” and 7-9”. A much closer relationship to 1:1 was desired. Only four of the nine core measurements from 0-2” differed from the closest to simultaneous hydra probe measurement by less than 10%, and only one of the nine gravimetric measurements at 7-9” differed from the 8” depth hydra probe measurement at the nearest time stamp by less than 10%. Neither gravimetric nor hydra probe measurements were consistently higher at just below surface, but at the 7-9” zone gravimetric measurements were consistently lower by 20-40%.

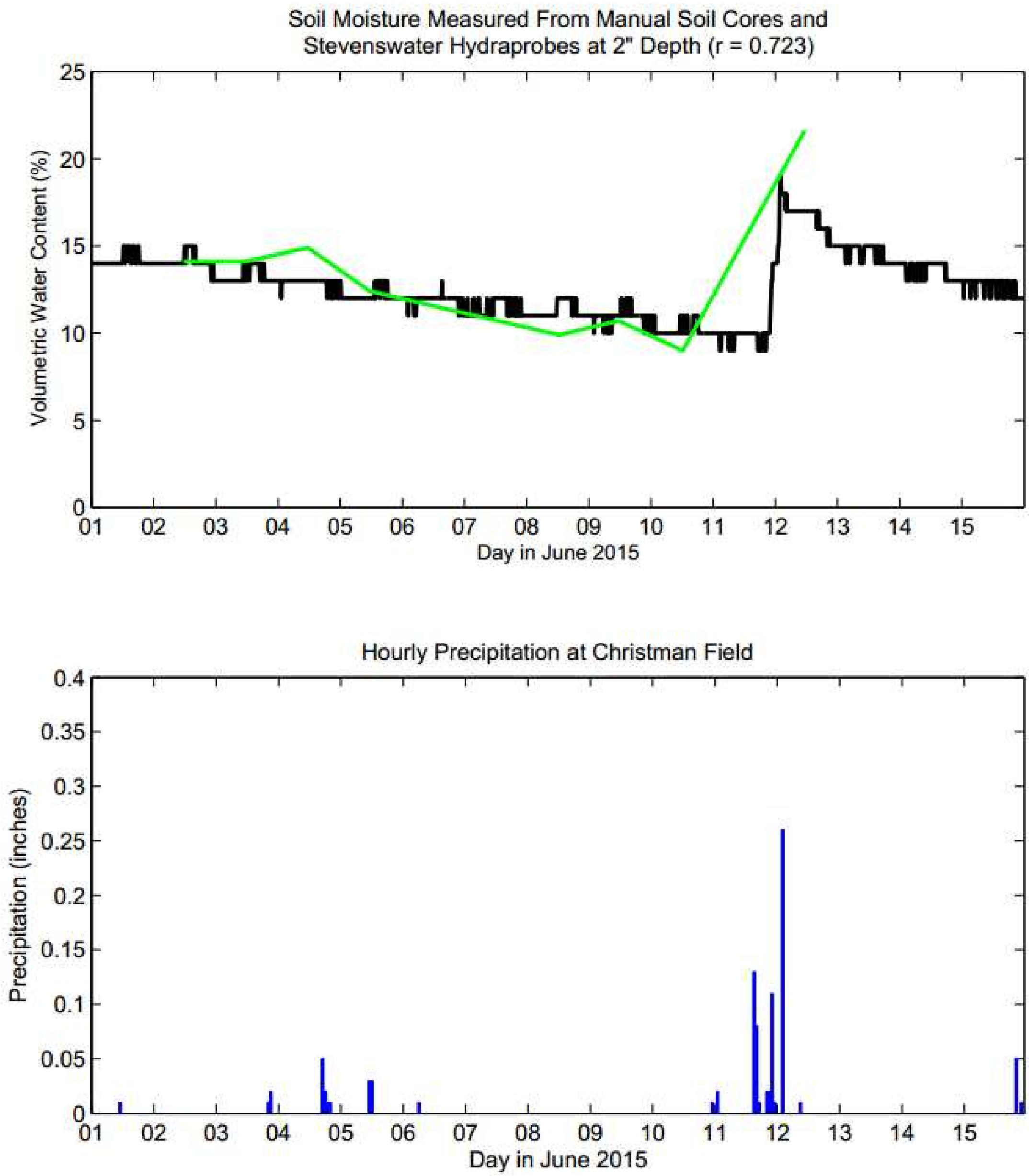

Figure 5.1: In the top panel measurements from the hydra probe installed at 2” depth are shown in black and a line connecting the gravimetric measurements is shown in green. There were only nine gravimetric measurements, and over 1,000 electronic sensor readings over this time, so interpolation in the green line makes less sense. The bottom panel shows hourly precipitation measured at the Christman Field weather station.

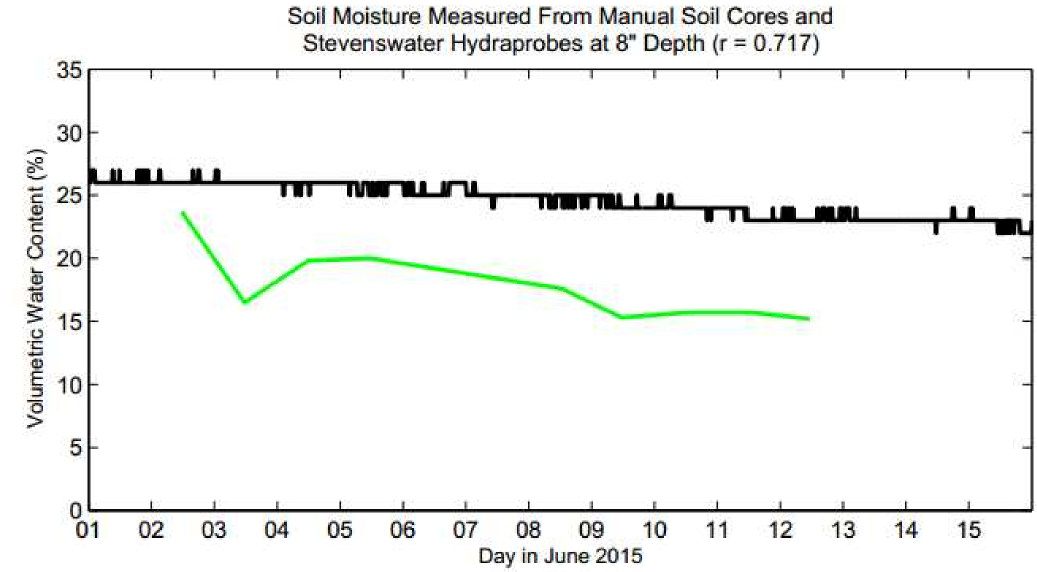

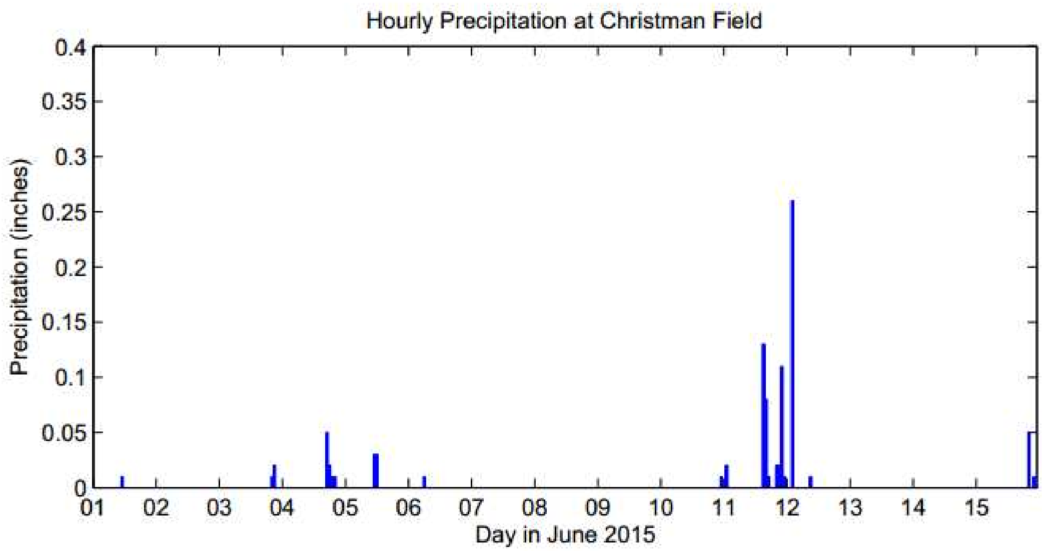

Figure 5.2: In the top panel Stevenswater Hydra Probe measurements are shown in black and a the green line interpolates between gravimetric measurements. There were only nine core measurements, and over 1,000 electronic sensor readings over this time, so there's much more interpolation in the green line. The bottom panel shows hourly precipitation measured at the Christman Field weather station.

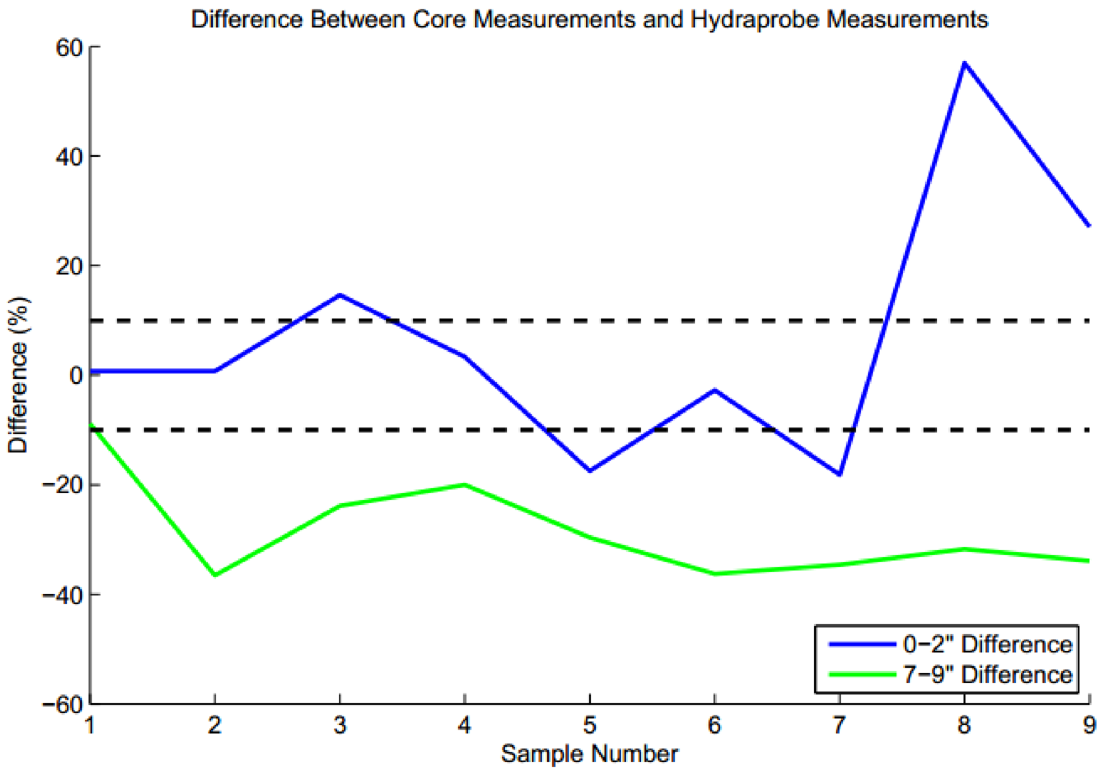

Figure 5.3: Using the protocol in this preliminary experiment confidence is very low in getting measurements within 10% of the true value. Only four of the nine samples dug in the 0-2" range were within 10% of the sensor reading value at 2". Only one of the core measurements at 7-9" came within 10% difference of the sensor simultaneous sensor reading taken at 8".

In analyzing these results it is first and foremost necessary to reiterate that there was a potentially problematic assumption that was used in order to make use of the data in spite of an experiment set-up error. All samples at 0-2" were assumed to have the same bulk density, and all samples at 7-9" were assumed to have the same bulk density. This assumption may okay as the USDA Web Soil Survey does not indicate a demarcation between soil types at the measurement site.

Startlingly-large sources of error were identified in this experiment beyond the assumption of constant bulk density at 0-2" and 7-9" that was used. For one, even measuring the volume of a canister using a graduated cylinder, a meniscus forms as a result of the surface tension between the canister and the water. This meniscus is concave as the canister is being filled and becomes convex if water is poured in beyond the true volume of the canister. This leads to a potential error in the volume calculation of -30 to +30 grams against a background value of somewhere on the order of 250 grams depending on soil density. This source of error in and of itself offers potential for a more than 10% difference in the volumetric water content measurement.

The other big problem with this trowel cut method is that it does not provide an exact soil core. As a back of the envelope estimate the cores dug out by the trowel probably averaged between 80-90% of the container volume. Even for the core measurement in which an exact volume was to be cored it is difficult to cut out a core with a trowel the exact size of the container used, and there is guess work involved in how densely to pack soil into the container to best replicate the true density.

The heat lamp method dried soil to its maximum potential faster than the oven did. It is not possible from this sample size to say for certain whether the heat lamp dries soil to the same degree as the oven or not. Gravimetric soil moisture readings were lowest with respect to the sensor measurements at 0-2" depth for samples taken June $8^{th\text{-}10th}$, but this relation did not hold at the lower depth. Because soil moisture trends were strongly correlated at 8" depth between sensor readings and core measurements, but core volumetric water content measurements were consistently 20-40% lower at this depth there is reason to suspect that both the oven and heat lamp drying methods may have been under-drying that soil type. It's also possible that this issue could stem from the coring side of things, more experimentation is needed.

This experiment made for a quality preliminary dabble in the citizen science soil coring process, but the results did not yield certainty that any protocol drafted around the aforementioned methods could meet NASA's criterion of soil samples producing volumetric water content within 10% of the true value. This result spurred on a follow-up experiment to be conducted throughout the months of September through November in 2015.

Experiment Two Methods: Due to the shortcomings of the first gravimetric measurement protocol experiment a new, more sophisticated experiment was designed with the help of Dr. Butters (a soil physics professor at Colorado State) and by drawing inspiration from NASA's GLOBE protocol (GLOBE 2014). Once again, the goal is to converge on one soil moisture measurement protocol to be extended to interested CoCoRaHS volunteers for testing nation-wide. Two new protocols would be tested against the official GLOBE (GLOBE 2014) measurement protocol making for a three-pronged coring experiment. The basic approaches behind coring techniques one, two, and three would be to follow the GLOBE protocol to the letter (1), follow the GLOBE protocol, but use a brass ring coring device as per Dr. Butters' consultation (2). Core out enough soil with a trowel to fill an 8oz container (3). The experiment was to include a much large sample size than experiment one, and to be completed over the months of September, October, and November in 2015.

The heat lamp vs oven drying aspect of the protocol was put on the back burner for the time being in order constrain sources of error. All samples were oven dried at 215 degrees Fahrenheit until the weight of the sample did not change for at least one half hour.

On top of the laundry list of requirements for this project that went with the first protocol draft, a criterion was added to the creation of the new protocol drafts that "observers must be taking soil cores with a standardized coring device of known volume that does not change during the soil coring process." This criterion is not necessarily satisfied by the GLOBE protocol. The coring device used for the GLOBE protocol methods was an eight ounce tin sampling canister provided from forestry-suppliers.com. These canisters can be bent by rocks or even dry soils during the soil coring process. This keeps the meniscus source of error discussed in experiment one, which could make obtaining volumetric water content measurements within 10% of the true value more challenging.

The hypothesis leading into this experiment was that the brass ring coring measurement would be favored as it should, hypothetically, eliminate the two problematic sources of error identified in the early June coring experiment. The volume of the brass rings is known absolutely and should not change. Thanks to the density of brass (8.70 g/cm^3) as compared with a typical dry soil density (1.1-1.6 g/cm^3) (Hillel 1980) the ring maintains its structural integrity when struck with a hammer. This method also produces an in-tact core and removes the need to fill any artificial void space with loose soil from the core's surroundings and pack it in until the density is approximately representative of an in-tact core by feel, which is the chief problem with the trowel cut method. Below is an outline of the two variations of the coring processes being compared to the GLOBE protocol.

CoCoRaHS Soil Moisture Measurement Protocol Experiment Two

Sampling Depths:

1. 0-2"
2. 7-9"

Necessary Materials:

1. Pad, paper, and pencil/pen
2. Ruler
3. Level, or straight edge
4. 2” (50.8 mm) height 3.125” (69.4 mm) diameter brass ring available from onlinemetals.com
5. Metric Scale (precision to at least the nearest gram)
6. Trowel
7. Tin foil, cookie sheet, or pot pie holder
8. Oven
9. Graduated Cylinder (optional)
10. Gloves (optional)
11. Sharpie (or similar labeling device)
12. Masking Tape (optional)
13. Rag or paper towel
14. Bucket Scoop
15. Ziploc bag
16. Wood block
17. Shovel

Soil Coring: (Brass Ring)

1. Measure the cut height of your brass ring to the nearest millimeter. Rings should have been cut to 2” (50.8mm), but the ring you ordered may vary slightly.
2. The ring has a radius of 39.69mm, so you can find the total volume your core will be given by the formula for the volume of a cylinder ($V = h\pi r^2$). If your cylinder was cut to exactly 50.8mm it will have a volume of 251.4 cm^3.
3. Bring your pencil, paper, ruler, level (straight edge), brass ring, bucket scoop (or similar thin, flat surface), scale, Ziploc bag, sharpie, masking tape, hammer, wooden block, and trowel to your selected dig site.
4. Weight the bag with which you wish to contain your soil core, so that this weight can be subtracted when weighing the sample.
5. Uproot surface vegetation to make the dig site as bare as possible. You only need to do this right where you are digging. You do not need to clear a large area around the dig site. About one square foot will suffice.
6. Place the brass ring on a flat portion of soil and twist it into the ground a bit to clearly designate a core site.
7. Put the wood block on top of the brass ring, and then hammer it into the ground until it is flat against the surface.

8. Using the trowel, remove enough soil on one side of the brass ring such that it can be excavated without mass loss using the bucket scoop.
9. Slide your soil core contained by the brass ring horizontally over the surface of the bucket scoop. Be careful not to lose any of your soil core out of the bottom, especially if soils are dry or of coarse material.
10. Wipe down the outer wall of the brass ring with a rag or paper towel.
11. Slide the soil core into your Ziploc bag. Make sure all soil sticking to the inner wall of your brass ring is added to the bag.
12. Weigh your soil sample from the 0-2” depth and record it being sure to tare the weight of the bag.
13. Break up the soil core, and remove any rocks larger than a pea, or any relatively large roots. Weight the contents that have been removed. If the weight of the removed content is more than 2% of the weight of the entire sample you’ll need to ditch the sample and repeat from step 5.
14. At this point you may want to label your sample with the date, time, and depth of measurement. You may prefer doing this with masking tape, and a sharpie or pen to avoid marking directly on the bag.
15. Clean off your trowel with a dry rag or paper towel to avoid sample cross-contamination.
16. In order to help sanity check measurements we do prefer that 2, or better yet, 3 samples be taken from each depth, so now you’re ready to repeat steps 5-14 one, or two times if desired.
17. Now it’s time to get your 7-9” depth samples. It’s unlikely that you will be able to core straight down from the surface to 9”, so plan on digging out about a square foot of surface area down to 7” in order to take the measurement. These measurements should be taken directly below where you took your 0-2” measurements. Especially if soils are dry this dig may require use of a real shovel.
18. Be conscientious of how far you’ve dug. You can use the ruler to measure the depth, and a level, or just a straight edge to make sure the ruler is lined up normal to the ground.
19. Once you have dug out soil to 7” depth repeat steps 5-14 for your deeper samples. It is more crucial now that you have dug out a significant amount of soil to take samples that are actually representative of that depth rather than including chunks of soil that have fallen into your hole from the surface. Remember to weigh samples quickly after coring so that as little moisture escapes as possible. This is especially important for the deeper samples as this soil is not exposed to sunlight at all in its natural environment.

Soil Coring: (Trowel Cut)

1. Bring your pencil, paper, ruler, level (straight edge), sampling canister, scale, sharpie, masking tape, and trowel to your selected dig site.
2. Remove surface vegetation from your dig site as well as possible by pulling it from the ground. You only need to do this right where you are digging. You do not need to clear a large area around the dig site. About one square foot should be fine.
3. Use your ruler to make a mark on the trowel 2" above the nose. Make this mark as straight and as parallel to the nose of your trowel as possible.
4. Weigh your CoCoRaHS sampling canister and mark down the weight, so it can be subtracted from your later measurement. Expect a weight of 45 grams with the lid included and 32 grams without the lid included.
5. Sink the trowel to the 2" mark in the soil. Chisel a cylindrical pattern out of the soil to this depth as close to the circumference of your sampling container as can be managed. Leverage this soil out of the ground and put it in your sampling container.
6. Remove as much of the organic matter from your soil sample as possible as well as any rocks that are larger than a pea.
7. Top off your container by scraping more soil off the sides of the hole you dug. Repeat step six as needed. You may find that the soil core you dug was more conical in shape than cylindrical when removed from the ground. If this is the case, try to top of your container using soil from the lowest half inch over your sampling depth. Try to get soil that is still attached to the wall of the hole you dug rather than loose dirt that has fallen in from above.
8. It is important that your sampling container be full for conversion to volumetric water content to work. Pat down, but do not pack or press down soil to make sure the container is full. (This is probably the biggest source of error in the experiment.)
9. Weigh your soil sample from the 0-2" depth and record it. Be sure to subtract out the weight of the container.
10. At this point you may want to label your canister with the date, time, and depth of measurement. You may prefer doing this with masking tape, and a sharpie or pen to avoid marking directly on the canister.
11. Clean off your trowel with a dry rag or paper towel to avoid sample cross-contamination.
12. In order to help sanity check measurements we do prefer that 2, or better yet, 3 samples be taken from each depth, so now you're ready to repeat steps 5-11 one, or two times if desired. Keep the samples separated by several feet to avoid cross-contamination of samples, but close enough that all dig sites meet the site finding guidelines outlined above.
13. Now it's time to get your 7-9" depth samples. It's unlikely that you will be able to core straight down from the surface to 9", so plan on digging out about a square foot of

surface area down to 7” in order to take the measurement. These measurements should be taken directly below where you took your 0-2” measurements.

14. Be conscientious of how far you’ve dug. You can use the ruler to measure the depth, and a level, or just a straight edge, to make sure the ruler is lined up normal to the ground.
15. Once you have dug out soil to 7” depth repeat steps 5-11 for your deeper samples. It is more crucial now that you have dug out a significant amount of soil to take samples that are actually representative of that depth rather than including chunks of soil that have fallen into your hole from the surface. Remember to weigh samples quickly after coring so that as little moisture escapes as possible. This is especially important for the deeper samples as this soil is not exposed to sunlight at all in its natural environment.

Cores were dug in a pattern consistent in shape with GLOBE’s block pattern (GLOBE 2014), but dimensions of the pattern were expanded such that each digging event was spaced one meter apart from the previous dig pattern rather than 25cm apart. This was necessary since three measurements were being taken at each dig site instead of just one. This pattern was not followed absolutely, but used as a guideline wherein cores could be dug slightly out of place to avoid rocks, patches of higher concentration of organic matter, and highly local elevation maxima and minima.

The time of sampling was not on a strictly-regimented schedule, but was rather designed to try to obtain a dynamic soil moisture timeseries. In the cases of rainfall or snowmelt sampling frequency was increased in order to attempt to capture the movement of wetting fronts.

Experiment Two Results: Not one of the three gravimetric measurement methods produced even close to a 1:1 relationship to simultaneous hydra probe measurements. Only six of the 54 gravimetric measurements taken between the three different protocols were within 10% of the simultaneous measurement recorded by the hydra probe at 2” depth. Three of these came from the trowel cut method, two from the brass ring coring method, and one following GLOBE protocol with a tin can. Strangely, despite the much more carefully considered methods, this represents a decrease in soil core-sensor agreement from experiment one.

Possible sources of error include, but are not limited to, a low bias in measurements by the hydra probe, change in soil type with space right around the measurement site, and soil compression, particularly when soil is wet. Core samples taken at 0-2” depth are being compared to a sensor reading at a depth of 2”. The assumption of homogeneous volumetric water content from 0-2” may be problematic.

Because of the work published in Seyfried et al 2005 vouching for the universal loam calibration of the Stevenswater sensors it is being given the benefit of a doubt in being considered truth. This is interesting because it’s more conventional to use gravimetric measurements as a means of calibrating soil sensors and ultimately satellites such as SMAP.

Another shortcoming of this experiment is that the three gravimetric measurement techniques failed to produce 1:1 relationships with one another. The trowel cut protocol is not a scientifically-viable way to find volumetric water content because there is no definite volume being used to take the measurement, so it wouldn’t have been an issue if this method had been an outlier. The other two techniques follow strict and well-established guidelines previously laid out for taking gravimetric measurements, but the percent difference in measurement between the two was still over 10% for two thirds of measurements from 0-2”, and differed by 65% at worst. Given that these two measurement techniques are very similar, and all measurements were taken right next to one another the lack of consensus between the tin can and brass ring coring methods is both alarming and puzzling.

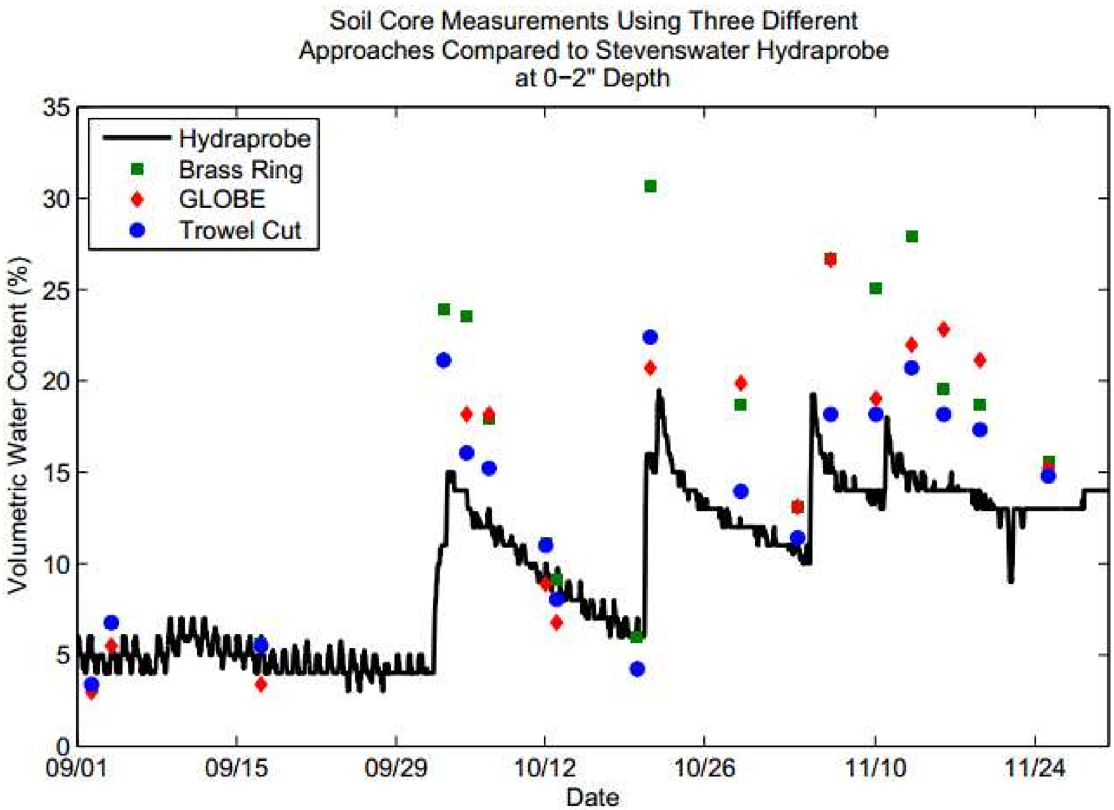

Figure 5.4: Volumetric water content of soil (%) is displayed above as a function of date for each of the three tested soil core measurement protocols for a coring depth of 0-2". For reference, measurements from the Stevenswater Hydra Probe sensor at 2" depth have been included in black.

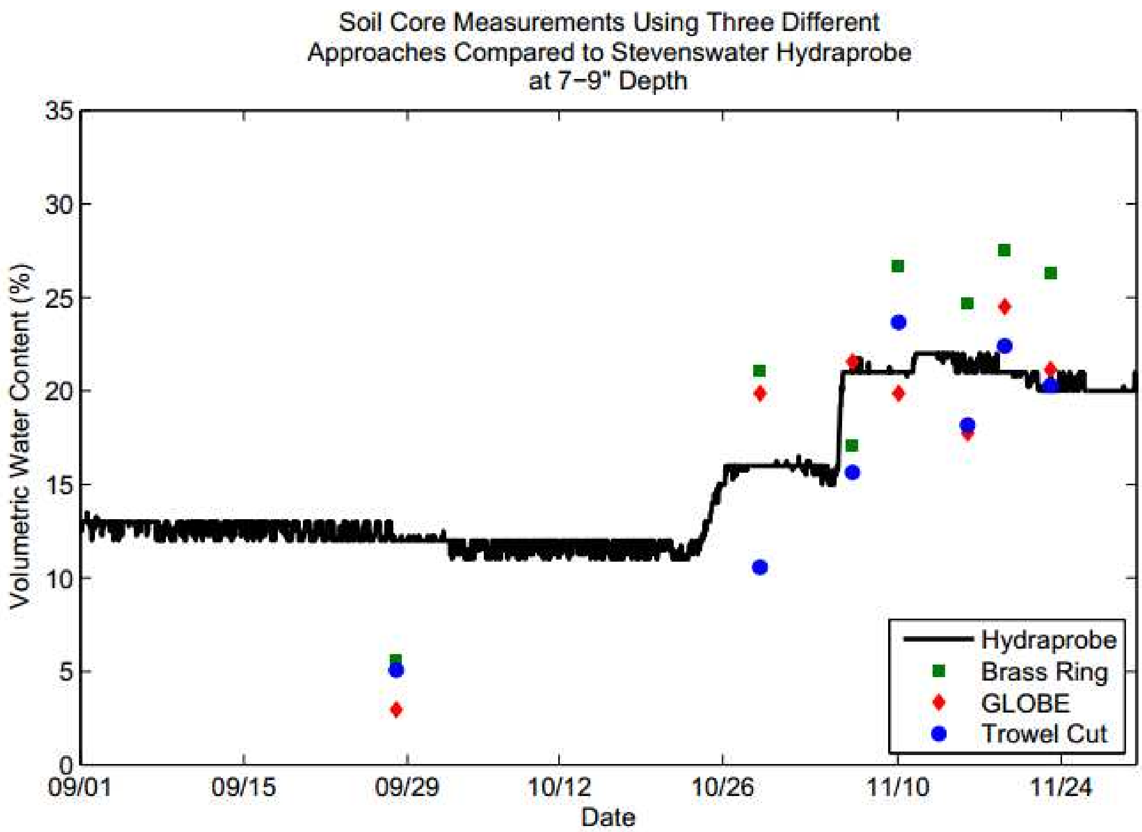

Figure 5.5: Volumetric water content of soil (%) is displayed above as a function of date for each of the three tested soil core measurement protocols for a coring depth of 7-9". For reference, measurements from the Stevenswater Hydra Probe sensor at 8" depth have been included in black.

It is possible that measurements from the hydra probe were too low, especially for wet soils. If the benefit of ground truth is given to the hydra probe what may have gone wrong with the gravimetric measurements? To rehash, here are some sources of error between the soil sensor and the gravimetric measurements:

1. The sensor is not at the midpoint of the gravimetric measurement for the 0-2" range. Even though only a thin, 2" layer of soil is being cored, this could have an impact.

2. While measurements are no more than ten meters away from the soil sensor it hasn't been proven explicitly that soil type is uniform along the site surface. Based on both gravimetric

measurements and sensor measurements soil type does not appear to be homogenous with depth. A web soil survey for the dig site agrees with the assumption of homogeneity of soil type with length and width but not with depth.

3. If soil type is constant along the surface and all soil cores were correctly filled the dry weight of gravimetric samples from both the brass ring cores and tin can cores should be constant. These results hint at soil cores either being compressed or under-filled at times. Based on bulk density numbers dry weights on the heavy side of these ranges appear more practical, which supports the hypothesis that samples in drier conditions could have been under-filled.

4. Vegetation is a factor in determining how much water infiltrates on a very small spatial scale. Vegetation is a determining factor in both infiltration and transpiration rates. At Christman Field vegetation is primarily grass with some cactus, but it inhomogeneous and clumpy on a meter-to-meter basis. The fall of 2015 was actually the warmest fall on record for Fort Collins with the latest frost on record, so evapotranspiration was occurring even into November (Colorado Climate Center 2015).

One potential source of error that remains impossible to ignore is operator error. It would be foolish to overlook the fact that soil cores were taken by a graduate student with a previous background in Atmospheric Science and not Soil Physics. In the 7-9" gravimetric samples particularly there appears to be convergence between gravimetric and sensor measurements as I improved at taking the readings and as soil became wetter and easier to core. On the positive side, this is a good mock trial for a protocol designed to be used by citizen scientists. Operator error will be an important source of error if measurements are being taken by citizen scientists around the country who may not be professional soil scientists, or even professional scientists at all.

Bulk density measurements from gravimetric samples indicate that coring devices were likely consistently under-filled, especially at 0-2” depth where there is lots of organic material. At 0-2” depth differences between hydra probe and gravimetric measurements maximized during times when soils were wet. The dry weight of samples taken using the tin can was anywhere from 162g to 278g, and the dry weight of samples taken using the brass ring was anywhere from 221g to 303g. Failure to ensure that dry bulk density measures passed the reasonability test early on in the coring experiment was probably the largest mistake in the design of this experiment, a lesson that will be applied to proper protocol development. This is especially problematic because if coring devices were filled such that bulk densities resembled anticipated bulk densities from web soil survey and soil type by feel tests more water would have dried from the samples. This would imply a larger difference in VWC readings between hydra probe measurements and gravimetric measurements in most cases.

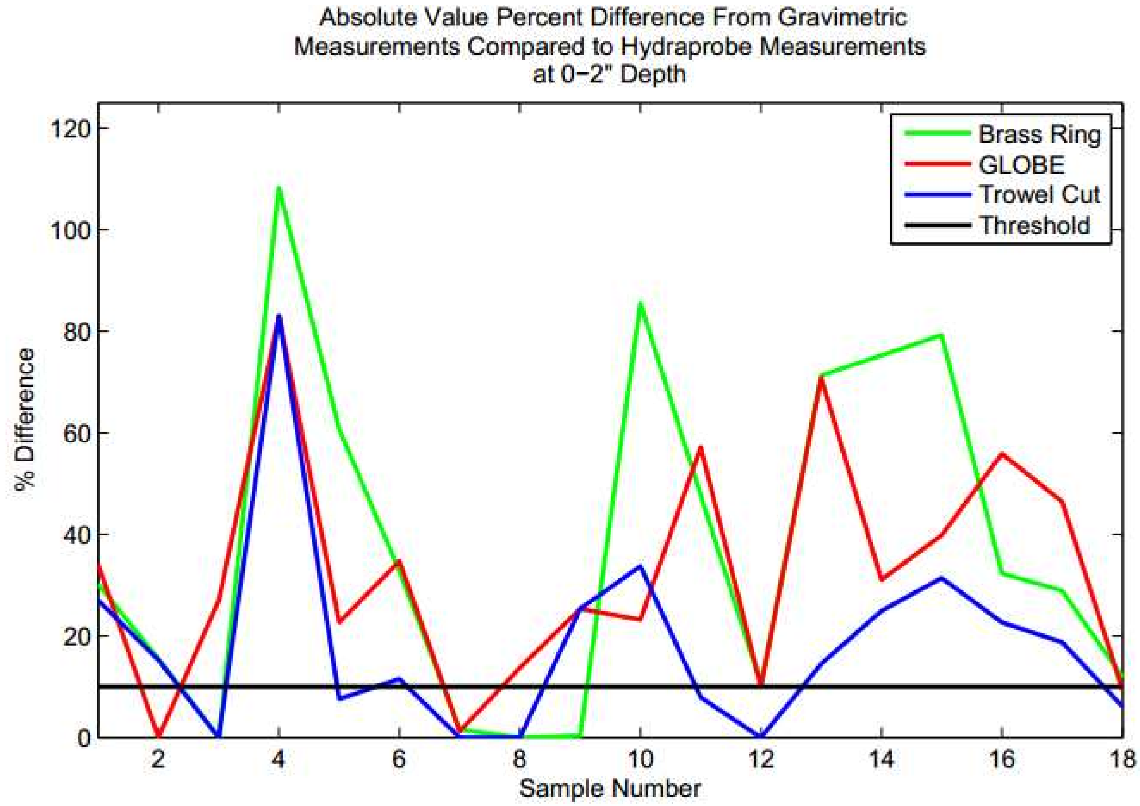

Figure 5.6: The differences in absolute value of volumetric water content measurements are given here between each of the three gravimetric measurement techniques implemented at 0-2" depth and the hydra probe at 2" depth. Based on hydra probe output a tolerance of 0.01 $\frac{cm^3}{cm^3}$ *was included, so only differences in measurement greater than that were counted.*

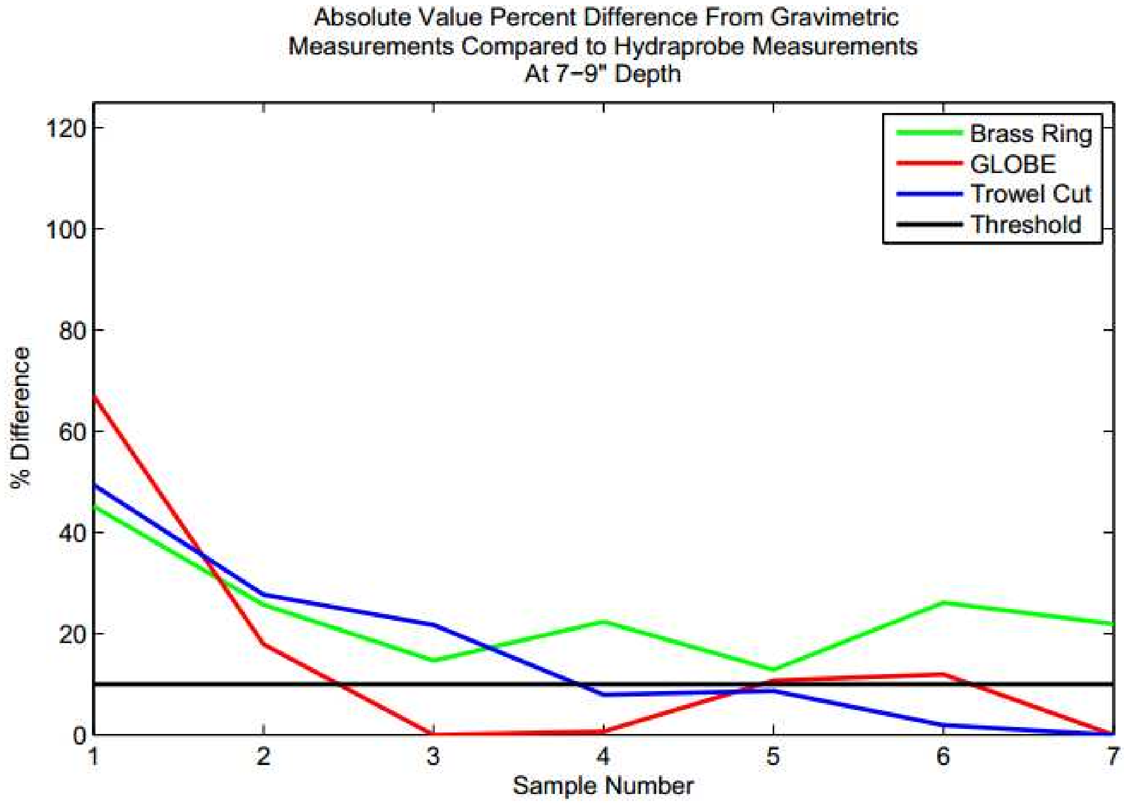

Figure 5.7: The differences in absolute value of volumetric water content measurements are given here between each of the three gravimetric measurement techniques implemented at 7-9" depth and the hydra probe at 8" depth. Based on hydra probe output a tolerance of 0.01 $\frac{cm^3}{cm^3}$ *was included, so only differences in measurement greater than that were counted.*

Perhaps the best silver lining offered by this experiment comes from the last four brass ring core measurements at 7-9" depth. These measurements were all of a dry bulk density within the 1.35-1.45$\frac{g}{cm^3}$ range, which is what was predicted by the soil type by feel test (sandy clay). Even so, none of these readings come within 10% of the volumetric water content measured by the hydra probe with a pre-considered tolerance of 0.01$\frac{cm^3}{cm^3}$ applied to the sensor readings. Both the tin can coring method and the trowel cut curing method came closer to the sensor reading at 7-9" depth, but this may only be because the samples contained an artificially high amount of pore space. If pore space of these measurements were constrained to the true amount of pore space in undisturbed soil the dry density readings would almost certainly be higher.

Protocol Recommendation: Despite differences between gravimetric measurements and sensor readings the lead protocol of the three explored here still would have to be the brass ring coring method. Supplies are cheap and durable, and the bulk densities measured from dry samples, especially at 7-9" were the closest. Should this protocol be released any time in the near future it would be with the utmost transparency that measurements within 10% of the true volumetric water content cannot be guaranteed; rather it can only be guaranteed that measurements released appear reasonable.

Leading Protocol:

Current Gravimetric Protocol: Before beginning taking soil cores estimate the dry density of your soil samples in two ways as a cross check for one another: using the web soil survey provided by the United States Department of Agriculture, and using the field soil texture test from the Colorado Master Gardener Program. The bulk density obtained by your soil samples will likely be lower than your estimated bulk density near the surface due to the presence of organic material. Dry bulk densities of soils (density of solids plus air with no water in pore space) should typically range between 1.1 and 1.6 $\frac{g}{cm^3}$. You won't be able to determine to any remarkable precision what the density of your samples when dried should be, but the main takeaway from a soil type calibration is to narrow down your expected range. Generally, more coarse soils with larger particles have less pore space and thus higher dry bulk densities. Clay-heavy soils can be expected to have dry densities closer to 1.2, loams average 1.36, and sandy soils can have dry densities over 1.5 (Hillel 1980). If your soil sample dry density is not within + or – 0.2 $\frac{g}{cm^3}$ of what is predicted by your soil type this likely indicates a problem with the sample.

Estimation of soil type by web soil survey:

1. Navigate to websoilsurvey.sc.egov.usda.gov/App/HomePage.htm. This should be the first result from most internet search engines if you type in "web soil survey."
2. Once on the page click on the green button labeled "Start WSS."

3. At the upper left portion of the page you should see five tabs labeled "Area of Interest (AOI)," "Soil Map," "Soil Data Explorer," "Download Soils Data," "Shopping Cart (Free)." Make sure you are on the "Area of Interest (AOI)" tab.
4. Zoom in on the map to the plot where you plan to take soil samples (this may take a few minutes).
5. Click on the tool labeled "AOI" at the top of your screen under the heading "Area of Interest Interactive Map." Using this tool outline the area of the map in which you intend to take soil cores and then release the mouse. The area you have selected should appear in cross hatching now. Once again, this may take a minute.
6. At the top of the page switch from the "Area of Interest (AOI)" tab to the "Soil Map" tab. The area you highlighted should now appear on the left-hand side of your screen in a box marked "Map Unit Legend." There should be a soil type listed under "Map Unit Name" with a link provided. Click on it.
7. This link should provide some estimated specifics about your soil type at both above and below 7". This is useful since you will be taking soil samples at 0-2" and 7-9". Mark down the soil types for the 0-7" and 7-60" range.

Estimation of Soil Type by Master Gardner Field Test:

1. Soil Texture by Feel instructions can be found at www.ext.colostate.edu/mg/gardennotes/214.pdf. Print these instructions.
2. Go to your measurement site with a trowel when conditions have been wet, or bring a coffee mug with some water if soils are dry.
3. Dig out a sample of roughly golf ball size from the top two inches of soil and then follow the flow chart instructions from Figure 5.4 of the "Estimating Soil Texture" printout to determine soil type.
4. Repeat the process for soil of 7-9" depth.

If both of the soil type estimation techniques indicate that there is a significant amount of clay or silt in your soil (ie clay, silty clay) expect dry density of your samples to be < 1.3 $\frac{g}{cm^3}$. If both of the soil type estimation techniques indicate that there is a large amount of sand (ie sand, loamy sand) in your soil expect dry density measures to be > 1.4 $\frac{g}{cm^3}$. For loam-heavy types such as loam, clay loam, and silt loam a range between about 1.25-1.45 $\frac{g}{cm^3}$ is to be expected, once again weighting things on the more dense side if you see "sand" in the name, and on the less dense side if you see "clay," or "silt" in the name. If there is disagreement between the two estimation techniques on your soil type you may proceed, but with less confidence about what dry density measurements you may obtain.

Site Requirements:

1. The location which you choose to dig must be flat, or close to flat, as must the area around it. Because of runoff, soil moisture may be lower than representative of average at the top of mounds or hills, and higher than representative of average at local minima in elevation.
2. THE SITE CANNOT BE IRRIGATED: This is not to say there's no benefit in soil coring irrigated land as this can help track if lawns/plants/crops are receiving appropriate water levels, but CoCoRaHS aims to depict conditions representative of a natural environment, and help to ground validate NASA's new SMAP satellite.
3. Your dig site does not have to be barren, but surface vegetation should be pulled before taking a core sample. This helps to keep the proportion of organic matter in the sample as low as possible.

Sampling Depths:

1. 0-2"
2. 7-9"

Necessary Materials:

1. Pad, paper, and pencil/pen
2. Ruler
3. Level, or straight edge
4. 2" (50.8 mm) height 3.125" (69.4 mm) diameter brass ring available from onlinemetals.com
5. Metric Scale (precision to at least the nearest tenth of a gram desired)
6. Trowel
7. Tin foil, cookie sheet, or pot pie holder
8. Oven
9. Gloves (optional)
10. Sharpie (or similar labeling device)
11. Masking Tape (optional)
12. Rag or paper towel
13. Shovel
14. Bucket scoop
15. Ziploc bag
16. Wood block
17. Water bottle
18. Graduated cylinder

Soil Coring Instructions:

1. Measure the cut length of your brass ring to the nearest millimeter. Rings should have been cut to 2” (50.8mm), but the ring you ordered may vary slightly in length.
2. The ring has a radius of 39.69mm, so you can find the total volume your core will have using the volume of a cylinder is $V = h\pi r^2$. If your cylinder was cut to exactly 50.8mm it will have a volume of 251.4 cm^3.
3. Bring your pencil, paper, ruler, level (straight edge), brass ring, bucket scoop (or similar thin, flat surface), scale, Ziploc bag, sharpie, masking tape, hammer, wooden block, and trowel to your selected dig site.
4. Weigh the bag with which you wish to contain your soil core, so that this weight can be subtracted when weighing the sample.
5. Remove surface vegetation from your dig site as well as possible by pulling it from the ground. You only need to do this right where you are digging. You do not need to clear a large area around the dig site. About one square foot should be fine.
6. Place the brass ring on a flat portion of soil and twist it into the ground a bit to clearly designate a core site.
7. Put the wood block on top of the brass ring, and then hammer it into the ground until it is flat against the surface.
8. Using the trowel, excavate the soil on one half of your brass ring down to the depth of the bottom of your sample. Make sure you have excavated enough area to lay the bucket scoop flat in the pit.
9. Slide your soil core contained by the brass ring horizontally over the surface of the bucket scoop. Be careful not to lose any of your soil core out of the bottom, especially if soils are dry.
10. Slide the soil core into your Ziploc bag.
11. Weigh your soil sample from the 0-2” depth and record it being sure to tare the weight of the bag.
12. Break up the soil core, and remove any rocks larger than a pea, or any relatively large roots.
13. Squirt some water from your water bottle into your graduated cylinder, and measure that volume.
14. Now drop the rocks and roots you removed into the graduated cylinder and read the volume again. The difference in volume between these two measurements will be subtracted from your container volume when determining bulk density and volumetric water content.
15. At this point you may want to label your canister with the date, time, volume of rocks and roots removed, and depth of measurement. You may prefer doing this with masking tape, and a sharpie or pen to avoid marking directly on the bag.
16. Clean off your trowel with a dry rag or paper towel to avoid sample cross-contamination.

17. In order to help sanity check measurements we do prefer that 2, or better yet, 3 samples be taken from each depth, so now you're ready to repeat steps 5-14 one, or two times if desired. Keep the samples separated by several feet to avoid cross-contamination of samples, but close enough that all dig sites meet the site finding guidelines outlined above.
18. Now it's time to get your 7-9" depth samples. It's unlikely that you will be able to core straight down from the surface to 9", so plan on digging out about a square foot of surface area down to 7" in order to take the measurement. These measurements should be taken directly below where you took your 0-2" measurements.
19. Be conscientious of how far you've dug. You can use the ruler to measure the depth, and a level, or just a straight edge, to make sure the ruler is lined up perpendicular to the ground.
20. Once you have dug out soil to 7" depth repeat steps 5-14 for your deeper samples. It is more crucial now that you have dug out a significant amount of soil to take samples that are actually representative of that depth rather than including chunks of soil that have fallen into your hole from the surface. Remember to weigh samples quickly after coring so that as little moisture escapes as possible. This is especially important for the deeper samples as this soil is not exposed to sunlight at all in its natural environment.

The Drying Process (Oven):

1. After collecting your soil samples the goal is to dry all the water out of them without igniting any of the leftover organic material. For this, make sure to have the following materials on hand: pencil and paper, drying surface (ie tin foil, cookie sheet, pot pie holder), and scale.
2. Set and your oven to 210-215 F and let it preheat.
3. Weigh the flat surface you wish to dry your soil sample on, so that this weight can be subtracted in your calculation.
4. Carefully pour your soil sample from the canister onto the drying surface, and spread it out. If you are using tin foil, fold up the corners before pouring the soil to avoid mass loss. Soil has very low conductivity, so drying the sample in the canister will lead to a very slow, and likely incomplete, drying process.
5. Weigh your sample again before placing it in the oven. A small amount of water may have already been lost having evaporated and condensed on the canister.
6. Once the oven has preheated place the soil sample in the oven, and wait!
7. Remove the soil from the oven occasionally to weigh it. Intervals of every half hour are recommended, but you may develop a more efficient system where the soil is weighed less frequently at first, and more frequently as it reaches its dry weight.
8. Once the soil weight no longer changes over at least a half hour period it is done.

9. Repeat steps 1-8 as needed in order to dry all your samples. There's no limit to how many you're allowed to oven-dry at once so long as it can be done without sample cross-contamination. The average oven probably won't hold more than two on each rack.

Bulk Density and Volumetric Water Content Calculations:

- A density is simply a mass divided by a volume. The bulk density of your sample is the weight of the contents of the canister once dried divided by the volume of the canister.

  Bulk Density = dried soil mass/(container volume-volume of rocks and roots)

- Since fresh water has a density of 1 gram/cm^3 the volumetric water content can be obtained by dividing the difference in wet and dry weight by the volume of your canister, and then multiplying by 100. This is expressed in the following simple formula:

  VWC (%) = 100*[(wet weight)-(dry weight)]/(container volume-volume of rocks and roots)

  Make sure you have converted your container volume to cm^3 so that the expression is unitless!

Motivation: When RZSM becomes sufficiently low plants are no longer able to overcome the suction force holding water in the soil. This skews the partitioning of latent and sensible heating in favor of sensible heating (Bonan 2008). This excess warming of the surface can potentially invoke a positive feedback wherein evaporative stress is increased and hydrologic reserves are further depleted (Koster et. al 2004).

$$1.\quad R_n = (1-\alpha)S\downarrow + (L\downarrow - L\uparrow) = H + \lambda E + G$$

$$2.\quad H = -\rho c_p \frac{(T_a - T_s)}{r_H}$$

$$3.\quad \lambda E = -\frac{\rho c_p}{\gamma}\frac{(e_a - e_*[T_s])}{r_W}$$

The equations above (6.1-3) are from Gordon Bonan's Ecological Climatology textbook. They describe earth's net radiative energy balance (1), sensible heat flux between the surface and atmosphere (2) and latent heat flux between the surface and atmosphere (3).

To show the potential for a temperature feedback more explicitly the above equations can be referenced. The Top equation is merely a representation of Earth's surface energy balance. R_n is the net surface radiative energy balance given by the non-reflected portion of downwelling solar energy in addition to the downwelling longwave from Earth's atmosphere minus the radiative energy emitted by the surface. Any imbalances here must be satisfied by phase change of water, or thermal energy exchange between the surface and atmosphere. When soils in the root zone are depleted the flux of latent energy decreases via decreased transpiration by vegetation, and the land surface gives more of its excess energy over to the atmosphere in the form of thermal energy. These increased temperatures drive up the potential for evapotranspiration, and thus the cycle goes.

In terms of RZSM-precipitation feedbacks, findings from Koster et al published in 2004 indicate that not only is there potential for the improvement of seasonal forecasts through tracking RZSM, but also that RZSM feedbacks are strongest in what can be thought of as wet-dry transitional zones. These are zones where surface evaporation rates average high enough to be expected to have an important influence on precipitation, and where available soil moisture is still an important constraint on how much surface evaporation takes place. In the Upper Colorado River Basin and eastern Colorado climate varies rapidly with space due to differences in elevation, and these transitional zones do exist in some elevation layer. In this section NASA Land Data Assimilation Modeled RZSM is used to assess the potential for added marginal seasonal forecast skill in various regions of the Upper Colorado River Basin and eastern Colorado using RZSM anomalies.

It is important to note that even during the growing season high correlations between root zone soil moisture and temperature, precipitation, etc are not necessarily expected, and this research is not geared towards improving numerical weather forecasts for short lead times (timescales of less than a week). Relationships between soil moisture and the atmosphere do offer potential for advances in forecasts on the timescale of months, and thus drought early warning as well, because the state of the land surface varies more slowly than the atmosphere (Koster et al. 2004). If statistically-significant relations are found between root zone soil moisture and factors that can enhance or mitigate drought then the experiment in this section has served its purpose of aiding in revealing when soil moisture monitoring is of enhanced importance for drought early warning in the Upper Colorado River Basin and Colorado east of the Continental Divide.

Methods: For this section forcing data used by NASA as well as three different land data assimilation models were used in order to better quantify the tie between soil and atmosphere in the Upper Colorado River Basin and Western High Plains. The forcing data used are primarily North American Regional Reanalysis (NARR) data. The exception to this is precipitation, which comes from gauge data that is disaggregated into hourly measurements using radar estimates, and then interpolated using PRISM climatology (Hualan 8). These forcing data are fed into three similar land surface models, the Mosaic Model (MOS), NOAH Model, and Variable Infiltration Capacity (VIC) model. It is important for this section that the NARR model does make use of NOAH model physics in order to help close surface water and energy budgets (Fador 2006). This is hypothesized not to make a large difference in the relationship between ensemble root zone soil moisture and reanalysis data, but to be safe against research that simply begs the question, data with and without the NOAH model will be included.

A number of avenues will be explored to further understand RZSM's role in determining the future state of the atmosphere on seasonal timescales. In this chapter standardized RZSM anomalies are correlated with anomalies in future maximum daily surface temperatures, minimum daily surface temperatures, mean daily surface temperatures, diurnal temperature swings, and precipitation. The relationship between RZSM and future maximum daily temperatures will be explored in greater detail. The variation in correlation strength between standardized RZSM anomalies is examined as a function of grid elevation, soil type, and what soil depth is being used to approximate the root zone. The relationship between RZSM and future precipitation anomalies is further scrutinized as well. An investigation is done as to how the correlation between standardized RZSM anomalies and seasonal precipitation anomalies changes as a function of grid resolution.

Results of analysis in this chapter will serve as an overview of domain-wide relationship between RZSM and the future state of the atmosphere. The whole domain is large and by no means does it have a spatially homogenous climate. In later chapters this will be broken down into smaller, more homogenous regions that make seasonal forecasts from a statistical model more applicable.

The first round of tests applied to the data was a comparison study between model ensemble mean soil moisture anomalies in the top meter of soil and maximum temperature anomalies. The logic behind testing the predictive skill on maximum temperature is that dry soils will constrain surface evaporation, skewing the Bowen Ratio in favor of sensible heating, and potentially limiting convective heat transport, so maximum 2m surface temperatures could be expected to be higher on average. This was chosen as the first key atmospheric variable to test firstly because it is hypothesized to be more strongly correlated to RZSM than any other atmospheric variable for reasons outlined above.

A linear correlation analysis between ensemble mean top meter soil moisture anomaly and NARR maximum daily temperature anomaly was applied to each and every grid space (a total of 4860) on a domain stretching from -113.063 to -101.938 degrees in longitude and from 36.938 to 43.563 degrees in latitude. Resolution was 1/8 lat by 1/8 lon. This process was initially applied between root zone soil moisture level at midnight and the maximum temperature on that same day for each Julian day. The sample size for each correlation is 30 (years 1985-2014). This process was then iterated another 89 times to show the correlation between soil moisture at midnight and maximum temperature 2,3,4…90 days into the future.

This test was repeated after reshaping the maximum temperature anomaly array such that each point represents the running 5-day temperature average high temperature anomaly. This window was converged on empirically in order to optimize between removing day-to-day variations in correlation that are seemingly depended on synoptic variation over the 1985-2014 period, and preserving resolution in changes of climate as a function of Julian Day. The rationale here was that in a 30-year period some Julian days are bound to receive inordinately high or low advectional activity, which adds noise to the signal. This excess background noise may artificially inflate or deflate the correlation between RZSM and maximum temperature depending on the day. Referencing the results section, windowing the temperature anomalies cuts down on "striping" behavior that does not represent a physical link between RZSM and maximum temperature.

The next step taken was to determine the statistical significance of the derived domain-averaged correlations between RZSM and maximum temperature for each Julian Day and lead time. To do this, a Fischer-Z transformation was applied to the correlation analysis at each gridpoint for each day of the year over the 30-year period. Each year's sample was assumed to be independent of the other years. The mean of these Z-scores was then taken for the entire domain at each day and each lag value to determine where the predictive skill of soil moisture is significant.

$$4.\quad Z = \frac{1}{2}\ln\left(\frac{1+r}{1-r}\right)$$

$$5.\quad \mu_z = \frac{1}{2}\ln\left(\frac{1+\rho_0}{1-\rho_0}\right)$$

$$6.\quad \sigma_z = \frac{1}{\sqrt{N-3}}$$

Equations 6.4-6.6 were used to transform an array of linear correlations bound between values of -1 and 1 into a Gaussian dataset.

In order to properly determine for which days and lead times statistical significance exists it becomes necessary to determine some sort of effective sample size in domain space. While there may be 4860 points included on the grid, it is ridiculous to consider each measurement independent given they average ~13*8km, and the length of a Rossby wave scales as 10^3 km (Holton 1972). This step can be a bit tricky, and involves some engineering on the side of the tester, but just as a back of the envelope calculation to help motivate this section, even if the whole domain was assumed to be just one independent sample for each day and lead time, correlations with an absolute value greater than 0.42 would be considered statistically significant at the $\alpha = 0.99$ level. Correlations of this magnitude were realized within the domain in the area where RZSM and maximum temperature were hypothesized to have the greatest coupling (during summer months for shorter lead times).

The effective sample size was measured by running a type of Monte Carlo experiment. A random permutation of the standardized five-day windowed maximum temperature anomaly matrix was created with the assumption that the non-permuted standardized soil moisture anomaly matrix would have no predictive power over the permuted temperature dataset. Not all dimensions of the maximum temperature anomaly matrix were permutated. Anomalies were held to their true position in lat-lon space, but were ordered randomly in year, and Julian Day space.

In algebraic terms, if the original dataset "X" has dimensions of "i,j,k,l" the new dataset "Xrand" has dimensions of "i,j,m,n" where "m" is a random permutation of the "k^{th}" dimension and "n" is a random permutation of the "l^{th}" dimension.

A correlation analysis between ensemble standardized soil moisture anomalies and the permuted maximum temperature dataset in the same way as outlined between the real soil moisture and maximum temperature datasets. The Fischer-Z transformation was then applied to the domain average correlation at each point in Julian Day-lag space. The effective sample size was then solved for by rearranging the Z-test equation to read "$N = [\frac{Z\sigma}{(\mu - \mu_x)}]^2$." Here Z represents the Z-score corresponding to the 0.5^{th} or 99.5^{th} percentile of a Gaussian (2.58), σ is the standard deviation, which is $\frac{1}{\sqrt{Nyears-3}}$, or 0.1925, μ is the hypothesized mean correlation of 0, and μ_x is the mean correlation that corresponded to the correlation at the 0.5^{th} or 99.5^{th} percentile. The data were very close to, but not perfectly symmetrical about 0, but the average absolute value of μ_x was 0.2471. This brought the grid of 4860 points down to an effective sample size of 4.04. While this effective sample size is laughable, the results that came from the experiment did not disappoint.

Before continuing on to results with such methodology it is important to address two weaknesses of comparing soil moisture to atmospheric variables such as precipitation and temperature using a linear correlation analysis. Firstly, on the scale at which transpiration actually occurs (a single root interacts with neighboring soil) the transpiration will either occur at a rate corresponding to its potential, or not occur at all (ref). If this process is integrated over a depth of soil and over a large cross-sectional surface area using a first-order approximation does reveal connection between RZSM and the future state of the atmosphere, but with a large signal to noise ratio.

Secondly, the amount of parametrized and actual transpiration as a function of gridspace soil moisture can be markedly different since $f(\bar{x}) \neq \overline{f(x)}$ where x can be thought of as volumetric water content and f(x) can be thought of as transpiration. For example, consider a given grid cell where in reality 80% of area is grass plains, and 20% of area is situated in a riparian zone tracking a river valley. Prescribing one vegetation type and one volumetric water content value to the grid cell will lead to uncharacteristically high transpiration rates prior to depleting available plant water reserves and lower transpiration rates thereafter. This is a weakness both in assessing soil moisture's role in the exacerbation of dry conditions using reanalysis data as was done here, and in modeling soil moisture feedback.

Results (Soil Moisture vs Daily Minimum Temperatures): Week to week variation is consistent with the hypothesis that 30 years of data is not enough to remove synoptic variability from the equation. The peak in predictive skill during summer in both magnitude and lead time is consistent with the hypothesis that soil moisture's impact on the Bowen Ratio carries the most weight during convective season. The magnitude of this correlation maxes out at a value of -0.5352. This is a promising initial result as it confirms the hypothesized sign and seasonality of correlation between RZSM anomalies and maximum temperature anomalies. There is also clearly some background noise, and the areas where negative correlations are of the greatest magnitude are pretty clearly the result of noise interfering constructively with a real physical relationship.

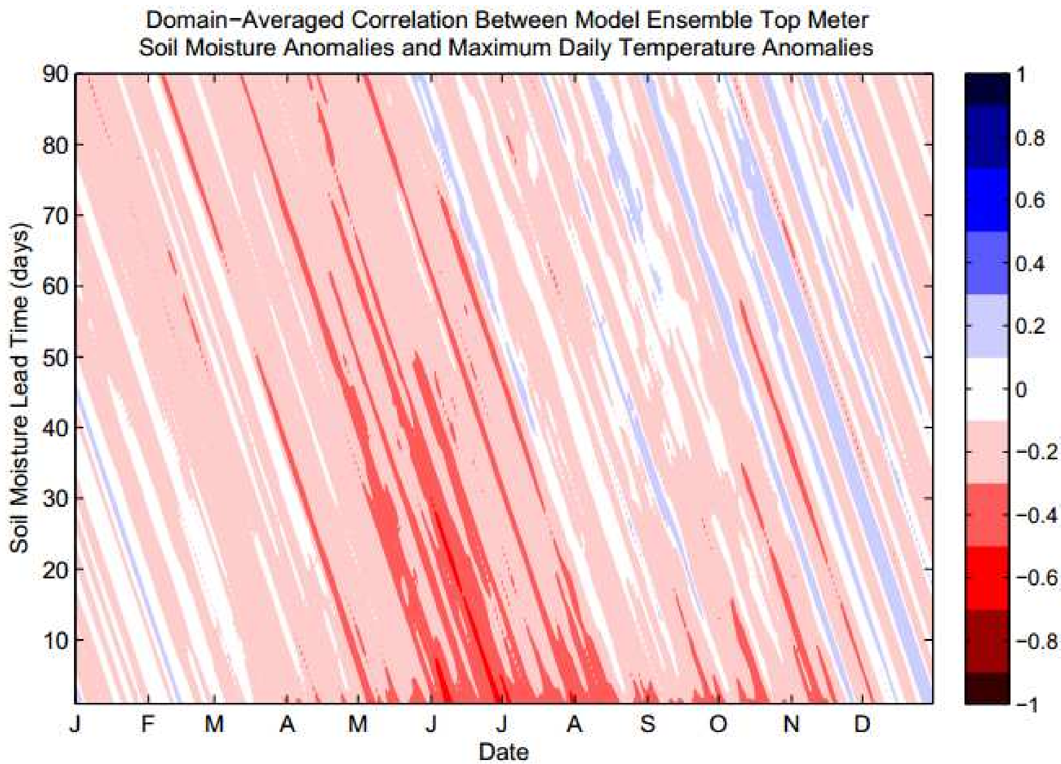

Figure 6.1 shows the existing correlation between top meter RZSM as measured at midnight, and the maximum temperature the amount of days in the future as given by the y-axis. This comes from NLDAS-2 data using the models consistent with what has been outlined in the methods section. The domain covered by this figure extends from -113.063 to -101.938 degrees in longitude and from 36.938 to 43.563 degrees in latitude. Grid resolution is 1/8 lat x 1/8 lon. The years of data included were 1985-2014.

While results from different elevations do hint at some variation of soil moisture's ability to predict future maximum temperatures with elevation, the only relationship found statistically significant at 99% confidence is that RZSM is a less reliable tool for predicting future maximum temperatures at elevations over 10,000ft during April and May. While it was not found to be significant at 99% confidence, there is a likely-related higher average predictive skill at these elevations later in the season (June/July). It's likely that this can be attributed to the snowmelt cycle. Until snow cover is gone root zone soil moisture will not have an impact on temperature.

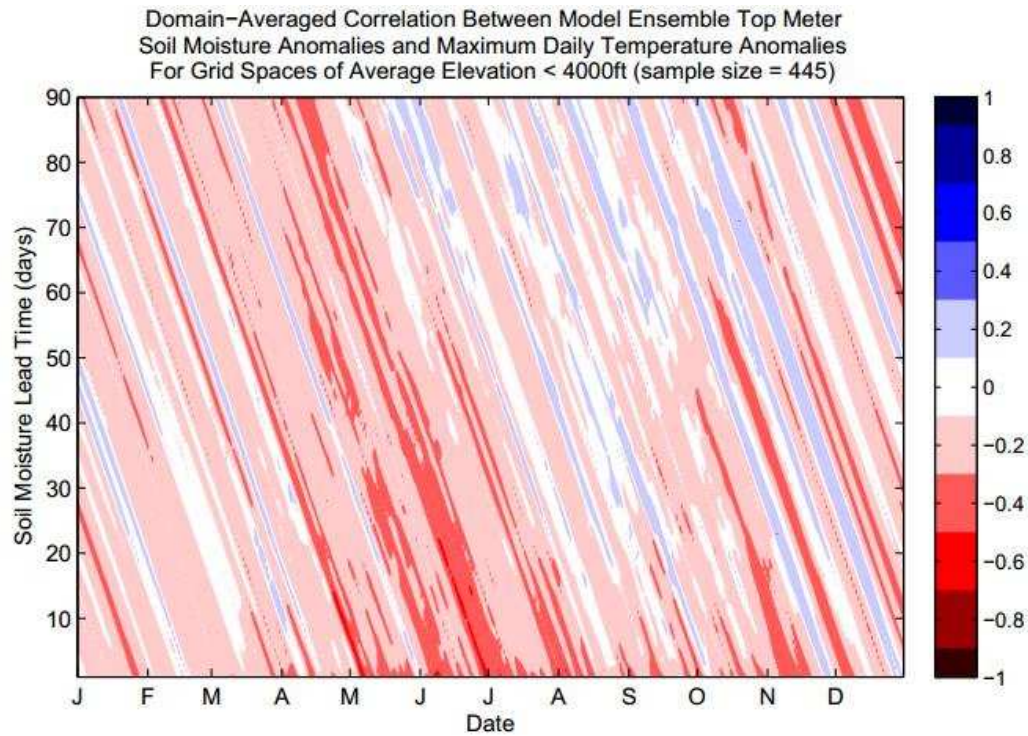
Domain−Averaged Correlation Between Model Ensemble Top Meter
Soil Moisture Anomalies and Maximum Daily Temperature Anomalies
For Grid Spaces of Average Elevation < 4000ft (sample size = 445)
Soil Moisture Lead Time (days)
90
80
70
60
50
40
30
20
10
J F M A M J J A S O N D
Date
1
0.8
0.6
0.4
0.2
0
−0.2
−0.4
−0.6
−0.8
−1

Figure 6.2

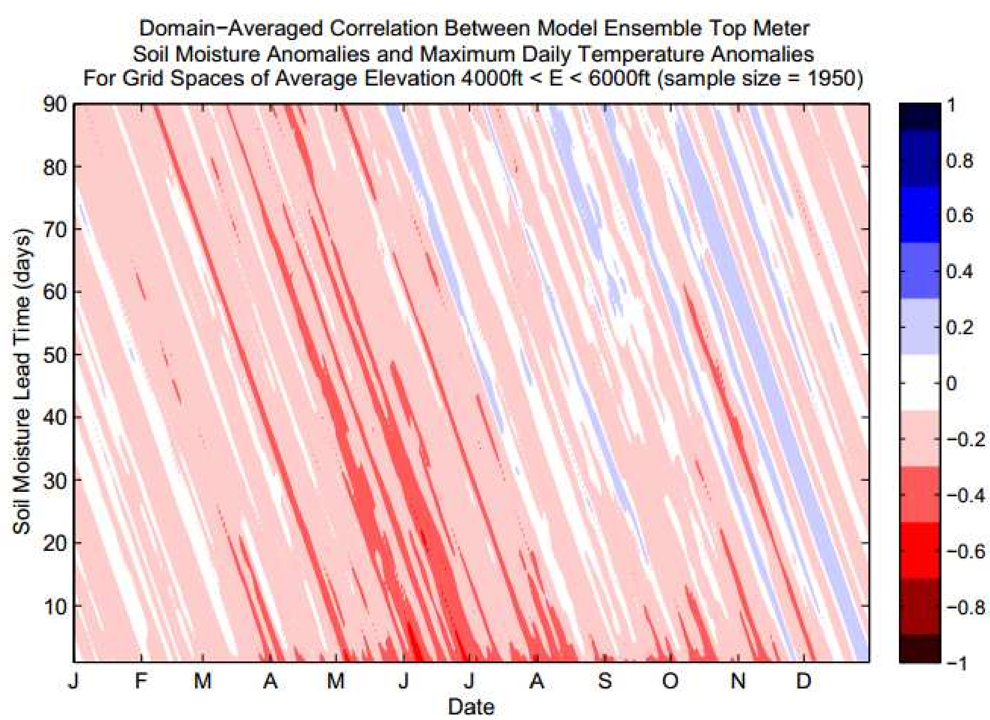
Domain−Averaged Correlation Between Model Ensemble Top Meter
Soil Moisture Anomalies and Maximum Daily Temperature Anomalies
For Grid Spaces of Average Elevation 4000ft < E < 6000ft (sample size = 1950)
Soil Moisture Lead Time (days)
90
80
70
60
50
40
30
20
10
J F M A M J J A S O N D
Date
1
0.8
0.6
0.4
0.2
0
−0.2
−0.4
−0.6
−0.8
−1

Figure 6.3

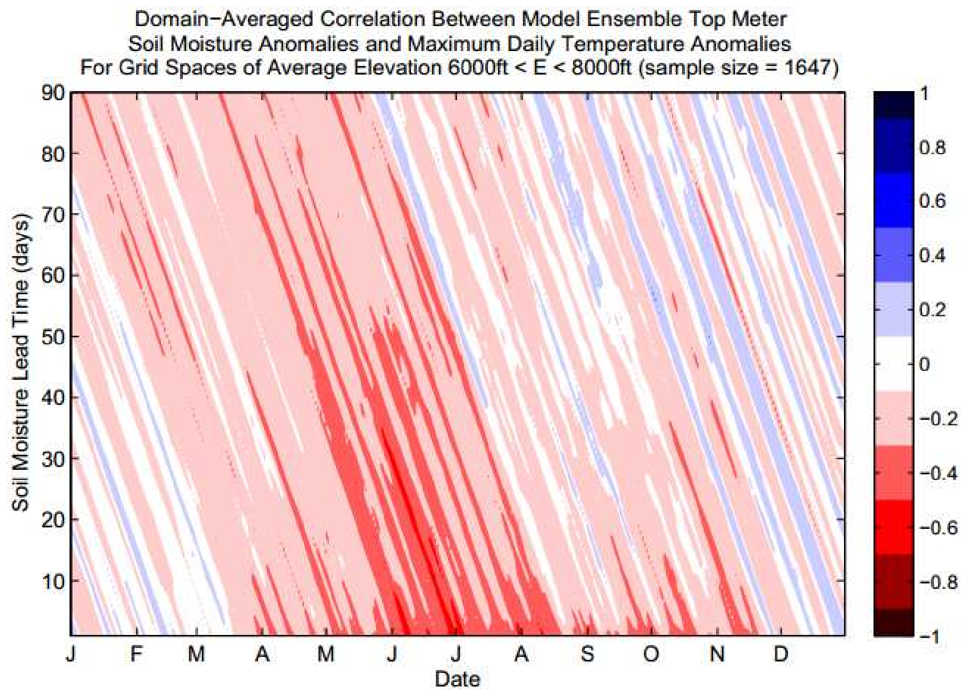

Figure 6.4

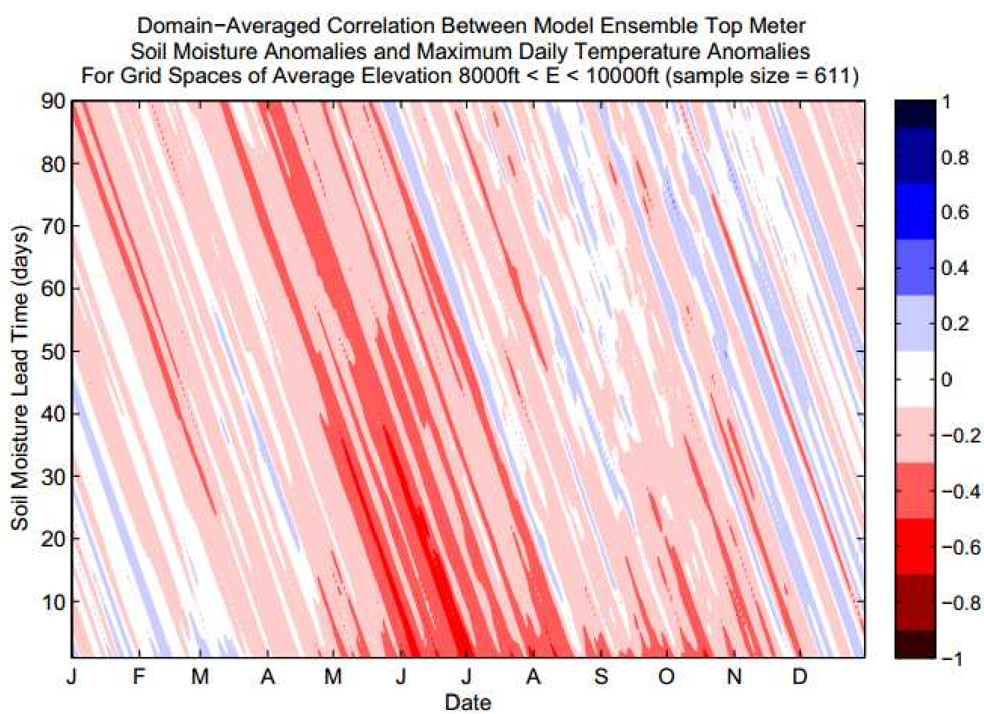

Figure 6.5

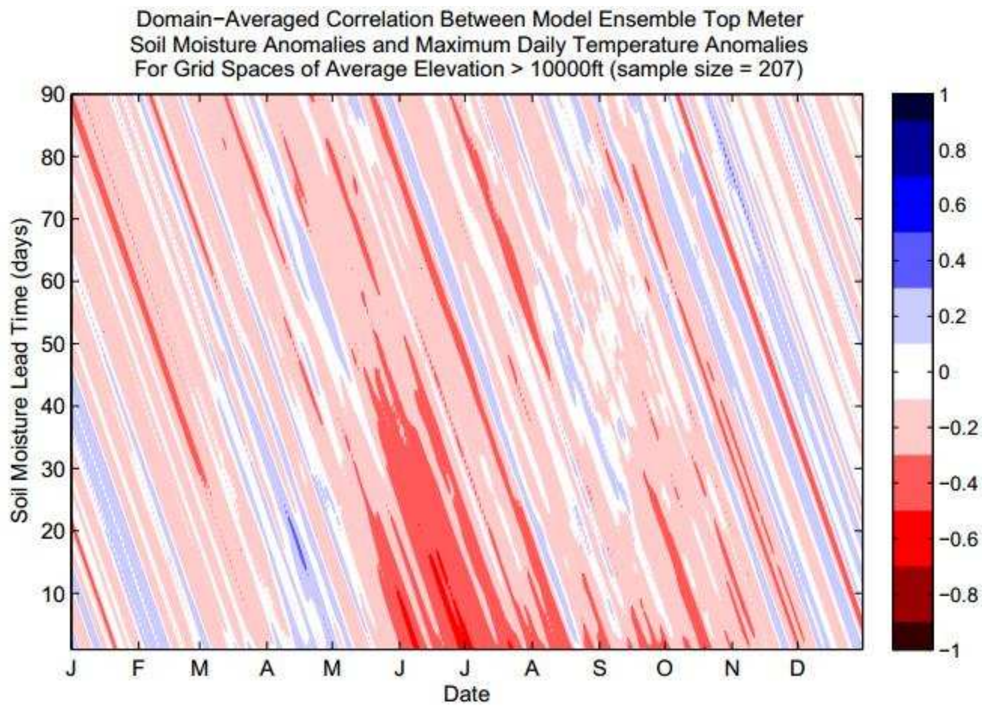

Figure 6.6

Figures 6.2-6 show the existing correlation between top meter RZSM as measured at midnight, and the maximum temperature the amount of days in the future as given by the y-axis. The domain and period of record used are still the same as in figure 6.4, but results have been parsed into separate grid elevation domains (< 4,000 ft (2), 4,000-6,000 ft (3), 6,000-8,000 ft (4), 8,000-10,000 ft (5), > 10,000ft (6)).

Applying a 5-day running average to the temperature field removes most of the “striping” behavior. Essentially, a large proportion of the synoptic variability remaining from a relatively small sample of years has been largely removed. This supports the hypothesis that the striping is caused by the element of randomness of calendar days in which major changes in the weather occurred over the 1985-2014 period, and that the striping is entirely unrelated to soil moisture. One thing to be careful of with these results is now soil moisture lead times of one and two days include information about temperatures before the soil moisture measurement. It is expected that higher temperatures lead to higher evapotranspiration and therefore lower soil moisture, so with at 5-day running average applied only results for lead times of three or more days should be considered. It is also possible that using a 5-day running average maximum temperature removes some of the correlation strength that comes from a true relationship between RZSM and future maximum temperatures.

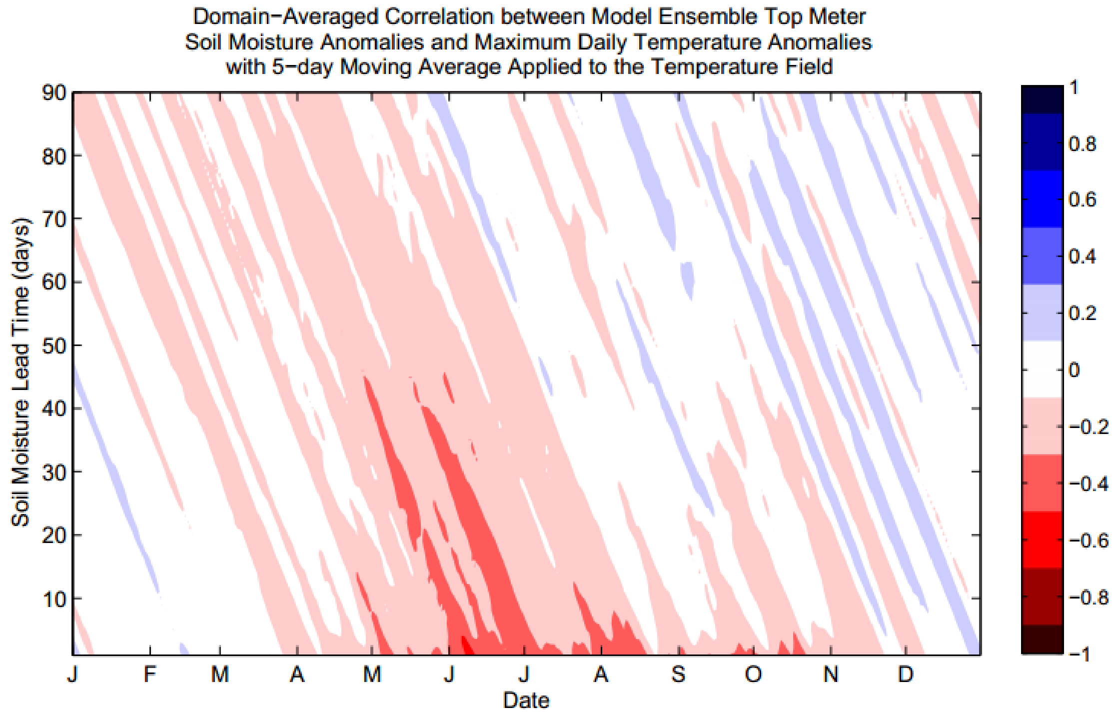

Figuere 6.7 shows the correlation between standaridzed top meter RZSM anomalies and standardized, 5-day moving averaged daily maximum temperature anomalies. Domain and period of record match figure 6.1.

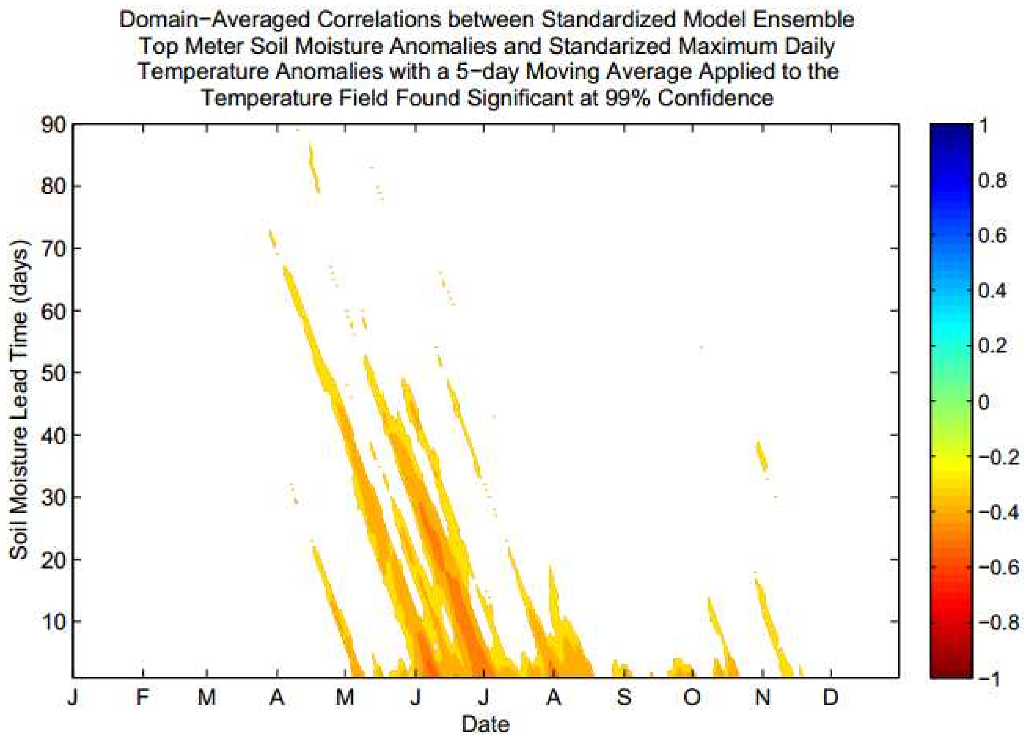

Figure 6.8 shows the same results as figure 6.7 with all correlations not significantly less than zero at 99% confidence masked.

Figures 6.9-11 tie the results for correllation between standardized root zone soil moisture anomalies and standardized maximum temperature anomalies back to physical units. A one degree Celsius (1.8 F) daily maximum temperature increase is expected on average for every one standard deviation decrease in RZSM. Figure 6.9 illustrates that even in situations where there is very high confidence in a statistically significant relationship between RZSM and maximum temperatures there is still lots of scatter. It is, however, uncommon for maximum temperatures to be above average when soils are very wet (> +1 standard deviations), or for maximum temperatures to be below average when soils are very dry (< -1 standard deviations). One standard deviation is only being considered a large anomaly here because it is difficult to find situations where the domain average soil moisture anomaly is greater in absolute value than one.

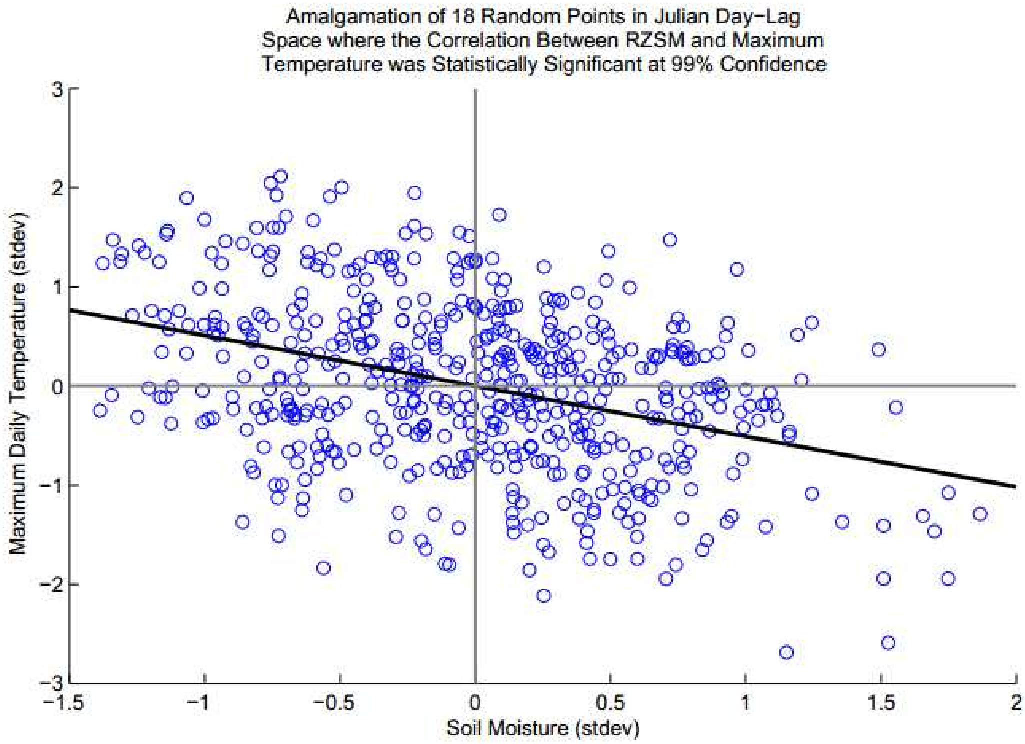

Figure 6.9: Every gridspace in figures 6.1-6.8 is a correlation between RZSM and maximum temperatures over the last 30 years, so each point was derived from its own, unique scatterplot. Here 18 different gridpoints from figure 6.8 have been randomly plotted with standardized RZSM on the x-axis and standardized maximum daily temperatures on the y-axis.

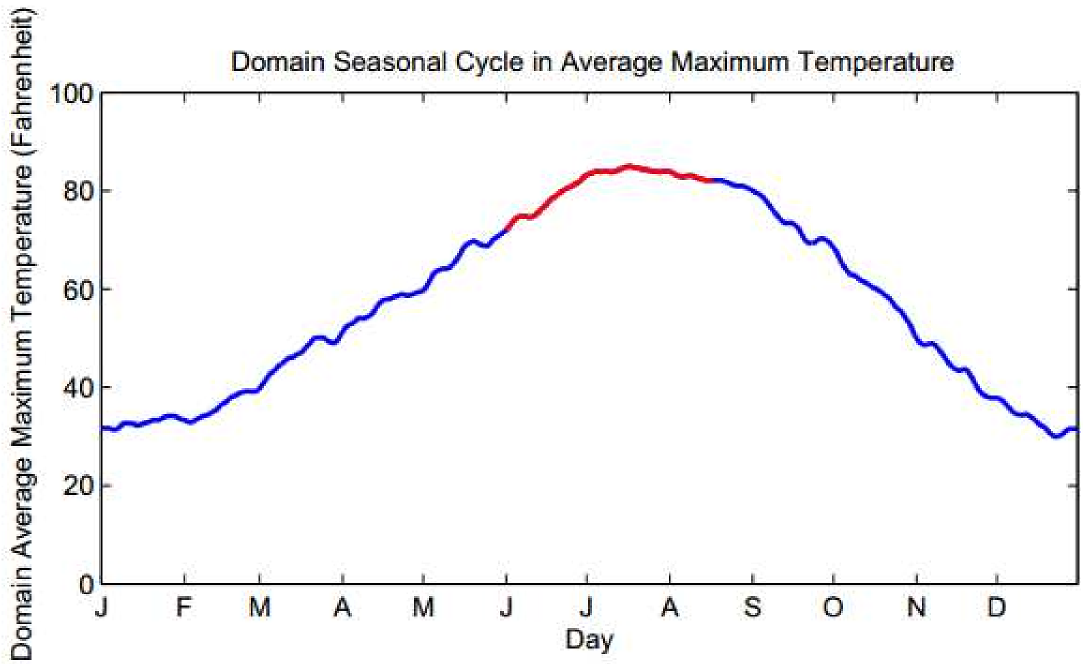

Figure 6.10:Domain average maximum temperature over the 1985-2014 period is shown here as a function of Julian Day. Once again, the red line represents the time of year in which data indicates that top meter soil moisture has the most influence on daily maximum temperatures based on correlation strength integrated over all lead times. The red line does not indicate any specific level of significance.

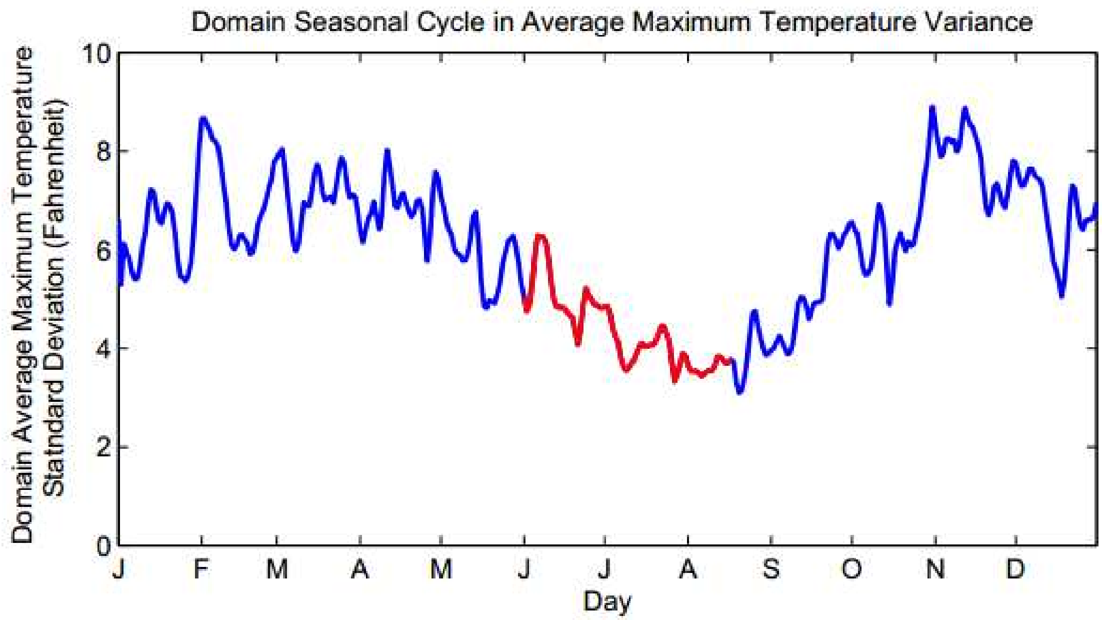

Figure 6.11: Domain average maximum temperature standard deviation over the 1985-2014 period is shown here as a function of Julian Day. Once again, the red line represents the time of year in which data indicates that top meter soil moisture has the most influence on maximum temperatures based on correlation strength integrated over all lead times. The red line does not indicate any specific level of significance.

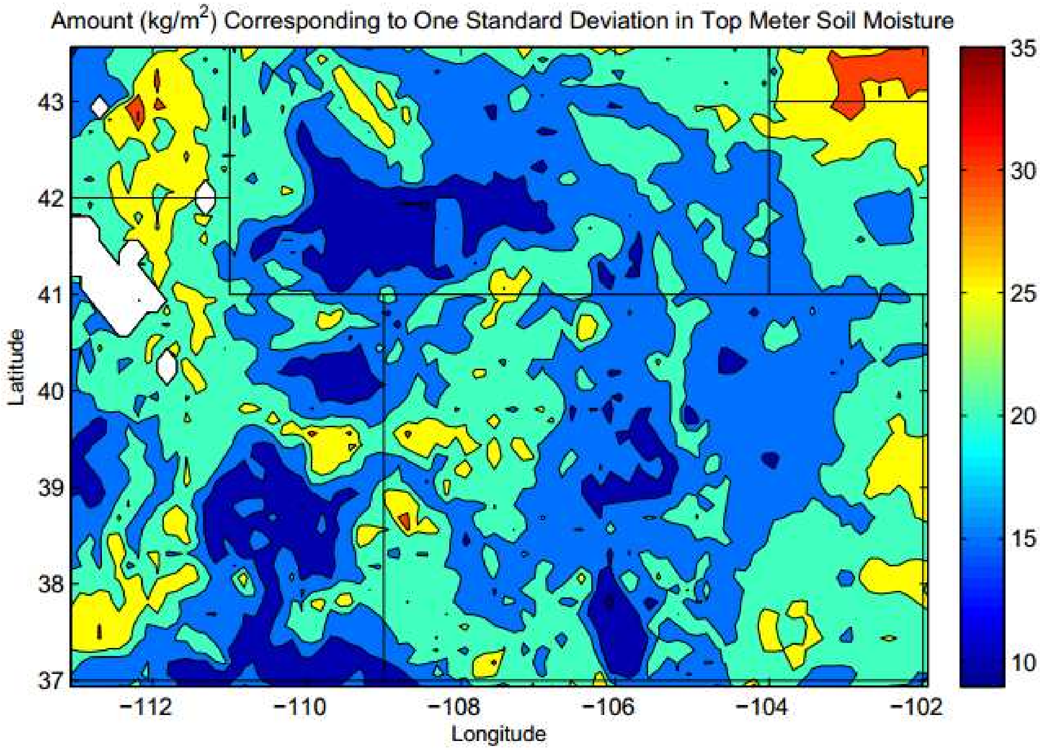

Figure 6.12 can be thought of as a proxy for soil type. Since one of the ways to distinguish between soil types is how great a variance of capacity they have for water storage, showing how much water mass corresponds to one standard deviation in soil moisture gives an indication of where different perdominant soil types exist. Note: soil type does vary quite a bit on a subgrid scale. Some terrain, such as mountain tops, may not have any soil at all. No statistically significant relationships between RZSM variance, and RZSM-max temperature feedback were unveiled by partitioning the data by percentile ranking in RZSM variance and comparing results to the domain average.

A read of the seminal paper on the North American Regional Reanalysis Model indicates that physics from NOAH model are, in fact, programmed in to help close the surface water balance (Fedor 2006). A jackknife experiment where NOAH data were removed from the land data assimilation model ensemble revealed very little change in the solution from the complete ensemble. This means that the correlation is not just an artifact of the NARR model's interaction with a surface that includes NOAH data.

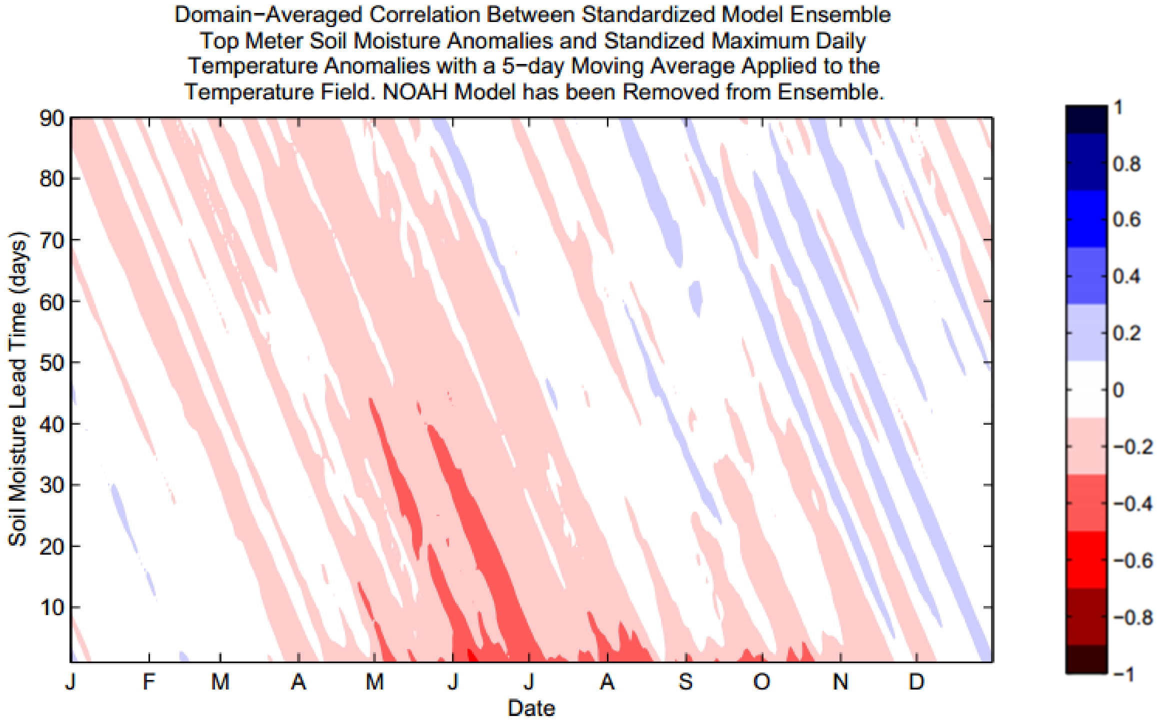

Figure 6.13: Correlation between standardized top meter RZSM anomalies and daily maximum temperature anomalies of lead times of 3-90 days are contoured here. This is the same information as figure 6.7, but without the NOAH model included in the land surface model ensemble. The domain and period of record used remain the same.

Model results do indicate that there is a statistically significant correlation between top meter root zone soil moisture and maximum temperature across the domain of the Upper Colorado River Basin, the high plains of Colorado and Wyoming east of the divide, and small connected portions of Idaho, Nebraska, and South Dakota. This correlation maximizes in the early and mid-summer in both strength and lead time. Low volumetric water content in the top meter of soil should be heeded for drought monitoring purposes in early May through mid-August as higher temperatures lead to increased potential transpiration rates, acting to further deplete soils and create a drought-enhancing feedback.

Strength of correlation between root zone soil moisture and maximum temperature was not found to be dependent on the variance of water storage capacity in the root zone. Evidence from this experiment also does not support the hypothesis that strength of correlation between RZSM and maximum daily temperatures is largely independent of elevation. The notable exception to this with a readily apparent, justifiable, physical explanation was the statistically significant decrease in root zone soil moisture's predictive skill over future maximum temperatures for high elevations as compared to the rest of the domain prior to the end of snowmelt season.

Domain-wide maximum temperature variance peaks in the early winter and reaches a minimum in the late summer. The time of year during which correlations are highest between standardized root zone soil moisture anomalies and maximum temperature anomalies is the greatest is right on the early side of this minimum in temperature variance.

In situations where the correlation between root zone soil moisture and maximum temperature is statistically significant at 99% confidence there is an average of a 0.414 decrease in standard deviation of maximum daily temperature for every one standard deviation increase in soil moisture over the entirety of the domain. This corresponds to an average of a 1.8 degree F fall in maximum temperature for every one standard deviation rise in top meter soil moisture. This relation could be as high as 3.6 degrees Fahrenheit/standard deviation in late May and early June, or as low as 1.5 degrees Fahrenheit/standard deviation in late July and early August. The time in which the most statistically significant correlation is present between root zone soil moisture and temperature corresponds to the first half of the summer season. At this time temperatures are in the first half of their seasonal maximum and downwelling solar radiation is at a zenith for the year.

Results (Soil Moisture vs Maximum Daily Temperature at Varying Root Zone Layer Depths): It came as no surprise that the main difference in predictive skill of varying thicknesses of soil moisture layers on the future temperature of the atmosphere was increased signal strength for more shallow layers on short timescales at the expense of less skill at longer timescales. Magnitude of domain-averaged correlation between soil moisture and five-day windowed average temperature topped out at 0.696 for the 0-10cm soil moisture layer of the mosaic model.

If domain averaged correlations are averaged once more across Julian Days within the growing season, and the growing season is approximated to be April 1st through September 30th (figure 6.14) there is a decay in these correlation averages as a function of soil moisture lead time that resembles exponential decay. The e-folding time for correlations between root zone soil moisture and maximum temperature as a function of lead time is not the same from 1 to $\frac{1}{e}$ as it is from $\frac{1}{e}$ to $\frac{1}{e^2}$. Correlations between RZSM and maximum temperature decayed from their day one value to $\frac{1}{e}$ times their day one value for 10 cm, 40 cm, one meter, and two meter-thick layers on timescales of 24, 33, 45, and 51 days respectively. Decreases to $\frac{1}{e^2}$ times their day-one values were 78, 79, and 87 days for 10 cm, 40 cm, and one meter-thick layers. This decrease fell beyond 90 days when a two meter thick layer was used to approximate RZSM.

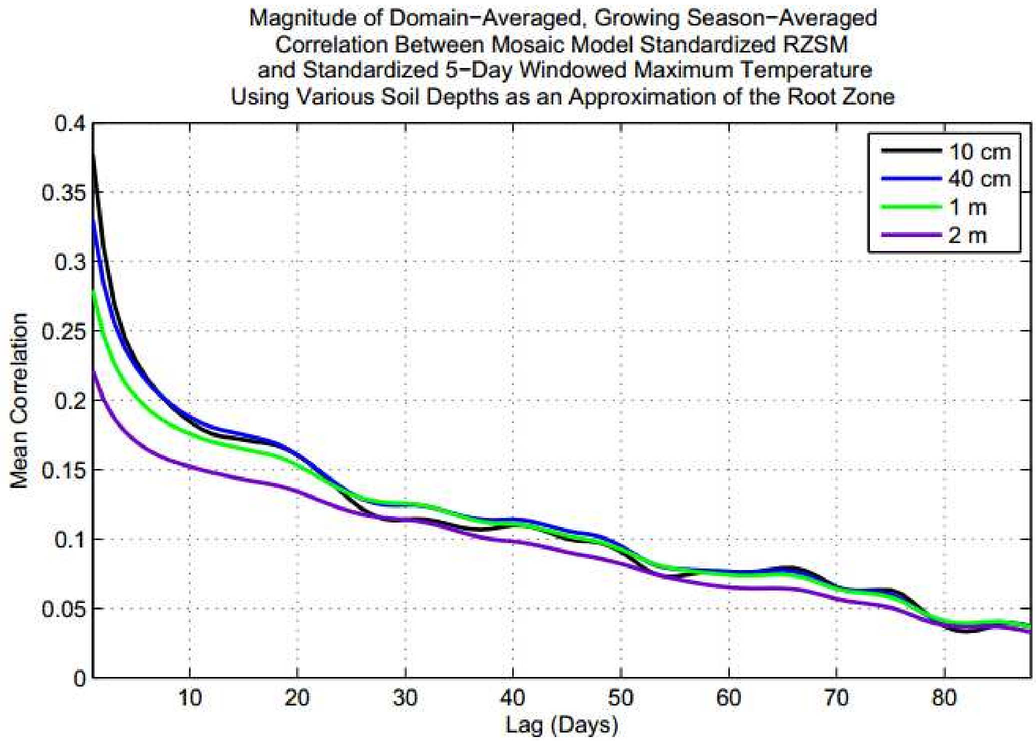

Figure 6.14: Here the relationship is quantified between standardized RZSM and Standardized 5-day Windowed Maximum Temperature as an April 1st-October 31st average. All correlations are negative in actuality, but their absolute values have been plotted here. The legend displays the depth below surface where the root zone ending has been approximated in each case.

The plot above shows the magnitude of soil moisture's predictive skill during the growing season on future maximum daily temperature levels for lead times of three days through 90 days. One and two-day lead times were omitted because of the five-day window applied to the temperature field. Looking at lead times of one and two days shows correlation between maximum daily temperatures and future RZSM, which is not a goal of this study. There exists a break-even point close to 80 days where magnitude of correlation becomes larger for deeper root zones. This stands to reason as fluxes in and out of the layer will change the anomaly of a thicker layer more slowly if the fluxes scale the same. If anything, fluxes may be quicker for the more shallow layers as wetting fronts move more quickly (Darcy 1856) and a greater proportion of flora has access to these shallow layers to pull water out of the system for transpiration.

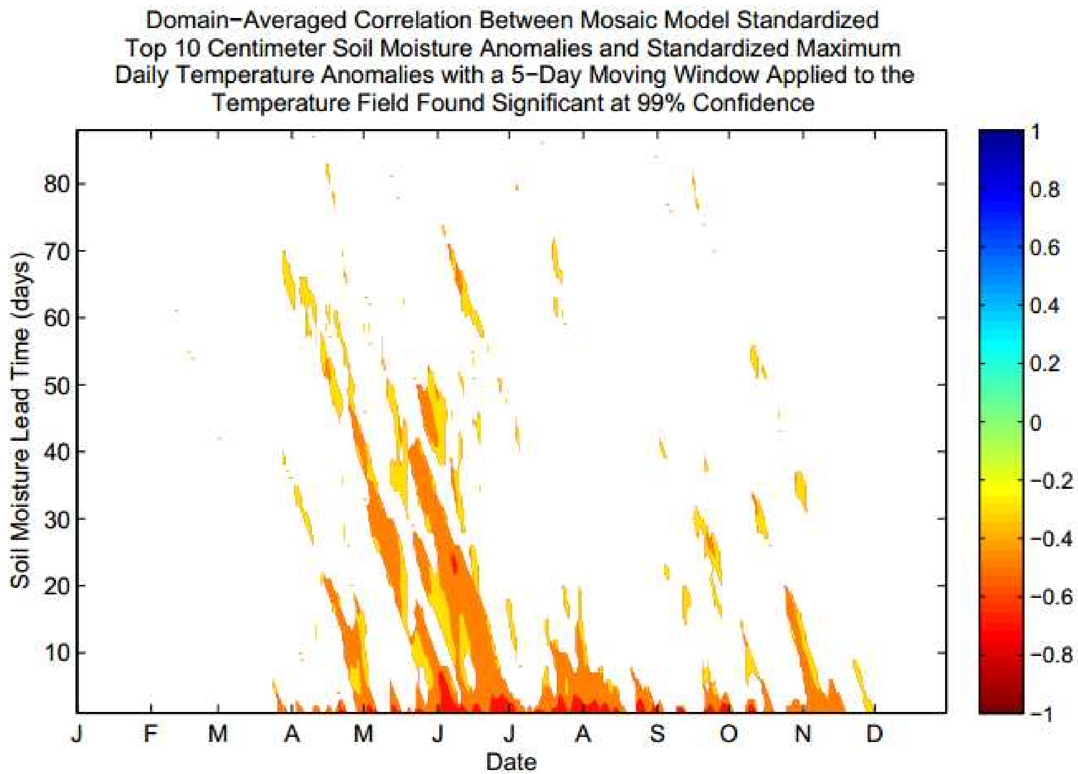

Figure 6.15: Correlations between standardized RZSM anomalies and standardized daily maximum temperature anomalies are contoured above as a function of Julian Day and days in advance of the middle of the 5-day temperature window that RZSM was used. Here the root zone was approximated as 0-10 centimeters. Values not significantly lower than 0 at 99% confidence have been masked. 9.36% of area in the contour domain met the significance threshold.

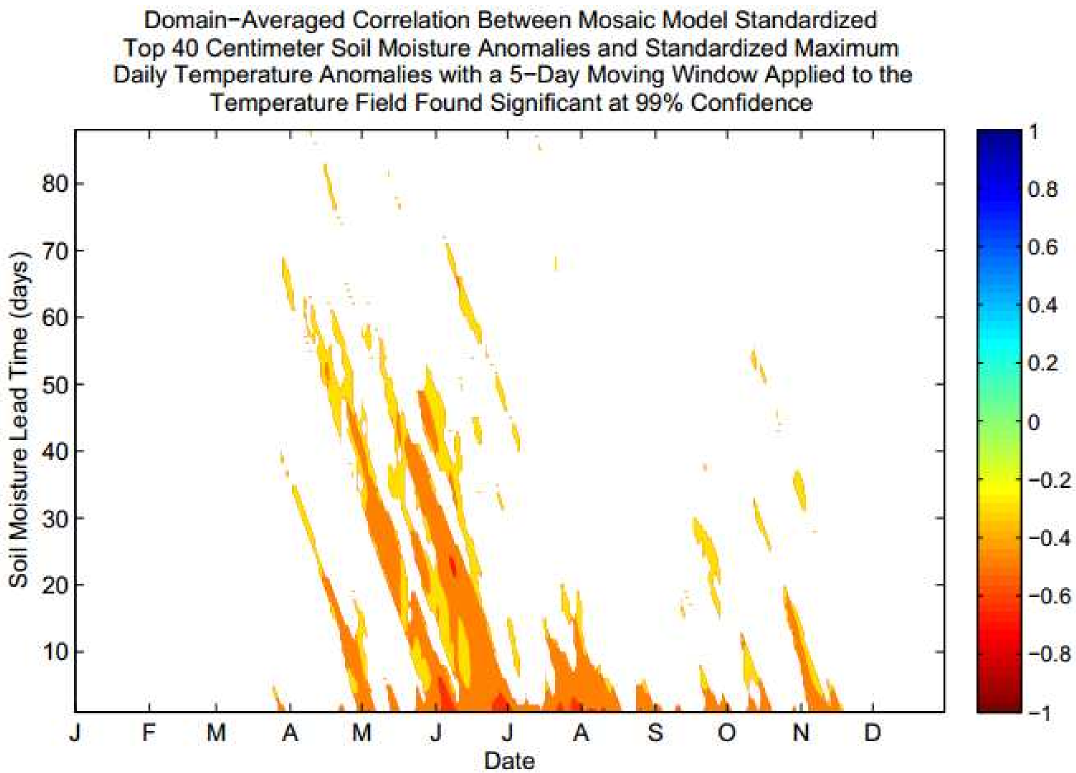

Figure 6.16: Correlations between standardized RZSM anomalies and standardized daily maximum temperature anomalies are contoured above as a function of Julian Day and days in advance of the middle of the 5-day temperature window that RZSM was used. Here the root zone was approximated as 0-40 centimeters. Values not significantly lower than 0 at 99% confidence have been masked. 9.35% of area in the contour domain met the significance threshold.

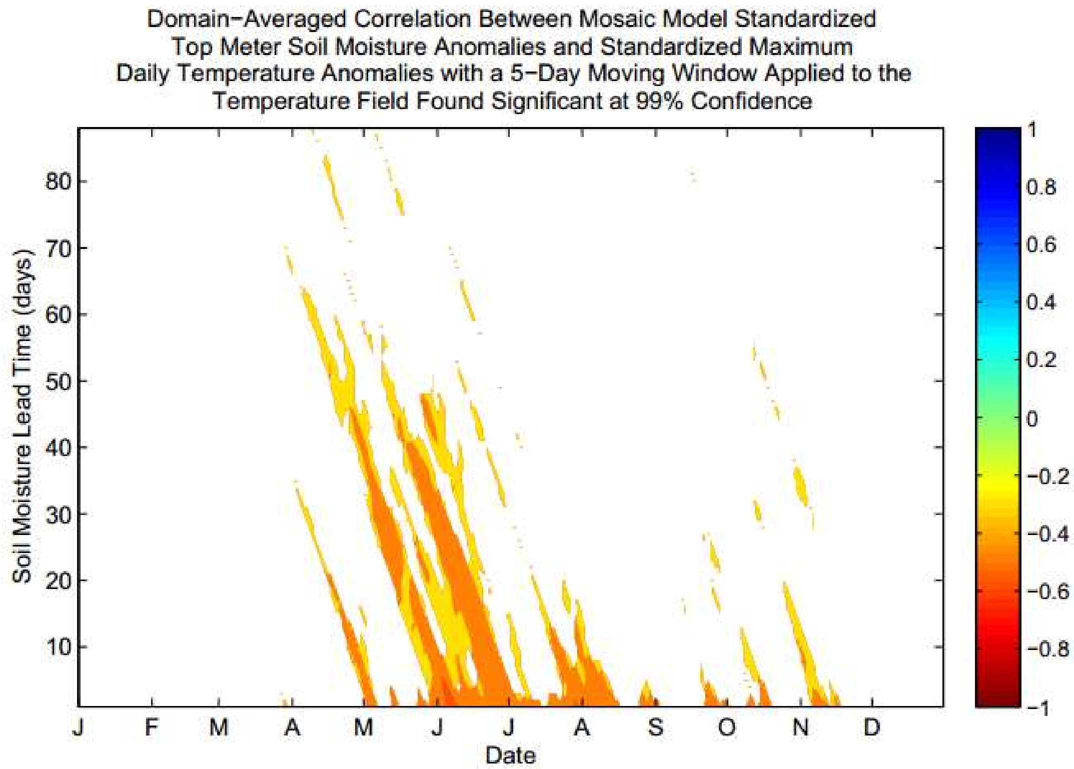

Figure 6.17: Correlations between standardized RZSM anomalies and standardized daily maximum temperature anomalies are contoured above as a function of Julian Day and days in advance of the middle of the 5-day temperature window that RZSM was used. Here the root zone was approximated as one meter thick. Values not significantly lower than 0 at 99% confidence have been masked. 8.27% of area in the contour domain met the significance threshold.

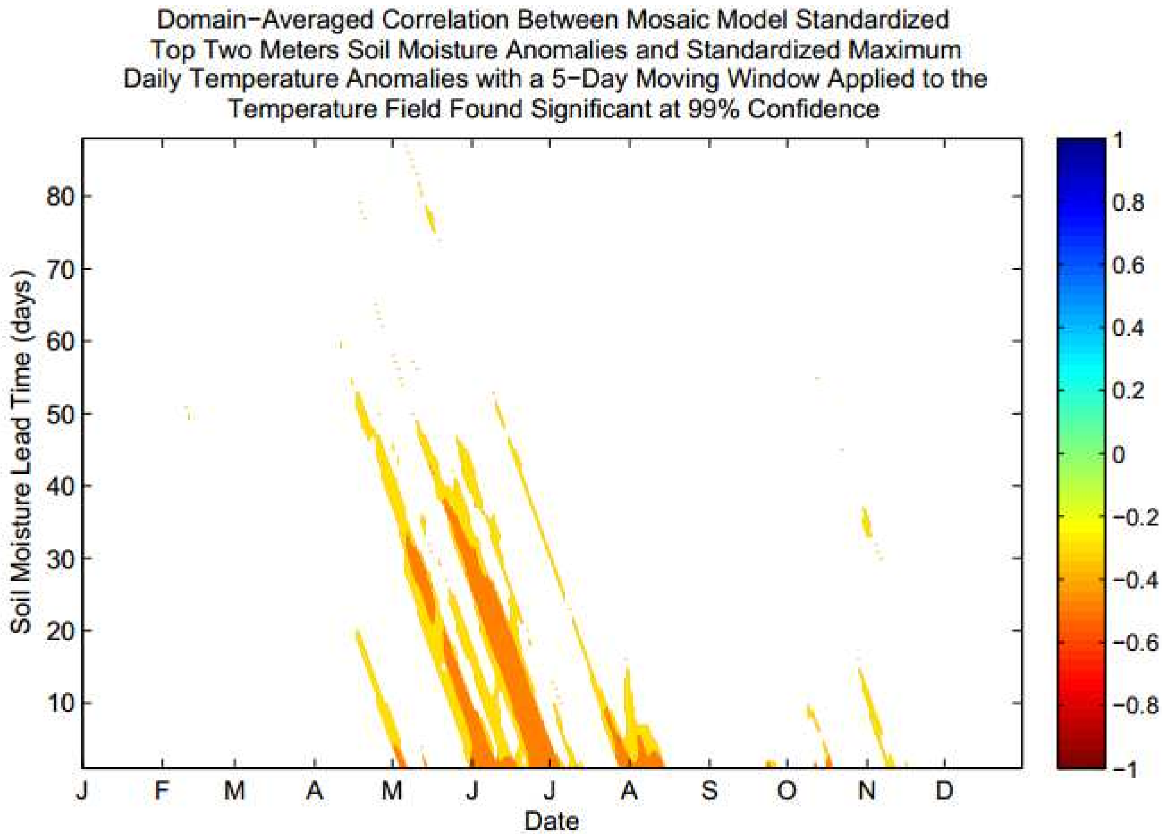

Figure 6.18: Correlations between standardized RZSM anomalies and standardized daily maximum temperature anomalies are contoured above as a function of Julian Day and days in advance of the middle of the 5-day temperature window that RZSM was used. Here the root zone was approximated as two meters thick. Values not significantly lower than 0 at 99% confidence have been masked. 5.51% of area in the contour domain met the significance threshold.

Making use of the Mosaic Model's suite of root zone soil layer thickness options and North American Regional Reanalysis data correlations between soil moisture and future temperatures have been strongest over the past 30 years when considering shallower soil depths (0-10,0-40 layer thicknesses). This is especially true at short lead times (10 or less days). There is reason to be concerned that these correlations may be artificially inflated as thinner layers of soil will undergo more dynamic anomaly changes during a precipitation event, and maximum temperatures are often lower during and after synoptic precipitation events because of the way weather systems propagate (Bjerknes and Solberg 1922). These results aren't particularly meaningful for drought monitoring since numerical weather prediction should be trusted over these types of seasonal relationships on short timescales. All layers showed a peak in correlation significant at 99% confidence where it was anticipated. This occurs in the middle of meteorologic summer, and for lead times of 0 to 60-70 days. For the 10cm, 40cm, one meter, and two meter-thick layers 9.36, 9.35, 8.37, and 5.51 percent of correlations in Julian Day-lag space was significantly less than zero at 99% confidence respectively. The numbers for 95% confidence were 21.41, 21.22, 20.56, and 17.26 respectively.

Results (Soil Moisture vs Daily Minimum Temperatures): The relationship between root zone soil moisture anomalies and minimum temperature anomalies was markedly weaker than the relationship between root zone soil moisture anomalies and maximum temperature anomalies. It also carried the same sign as the relationship between RZSM and max temperature anomalies. This goes against the hypothesis that high soil moisture can be related with high dew points thus keeping temperatures warmer at night and leading to a positive correlation. Instead, it is consistent with the hypothesis that higher temperatures mean the atmosphere can hold more water, and thus dew points are higher, and minimum temperatures are higher.

Only 2.35% of the gridpoints in Julian Day-lag space qualified as statistically significant at 99% confidence using the methods outlined above. This area is nearly unanimously negative in sign, and relates absolutely with where negative correlation between maximum temperatures and soil moisture peaked.

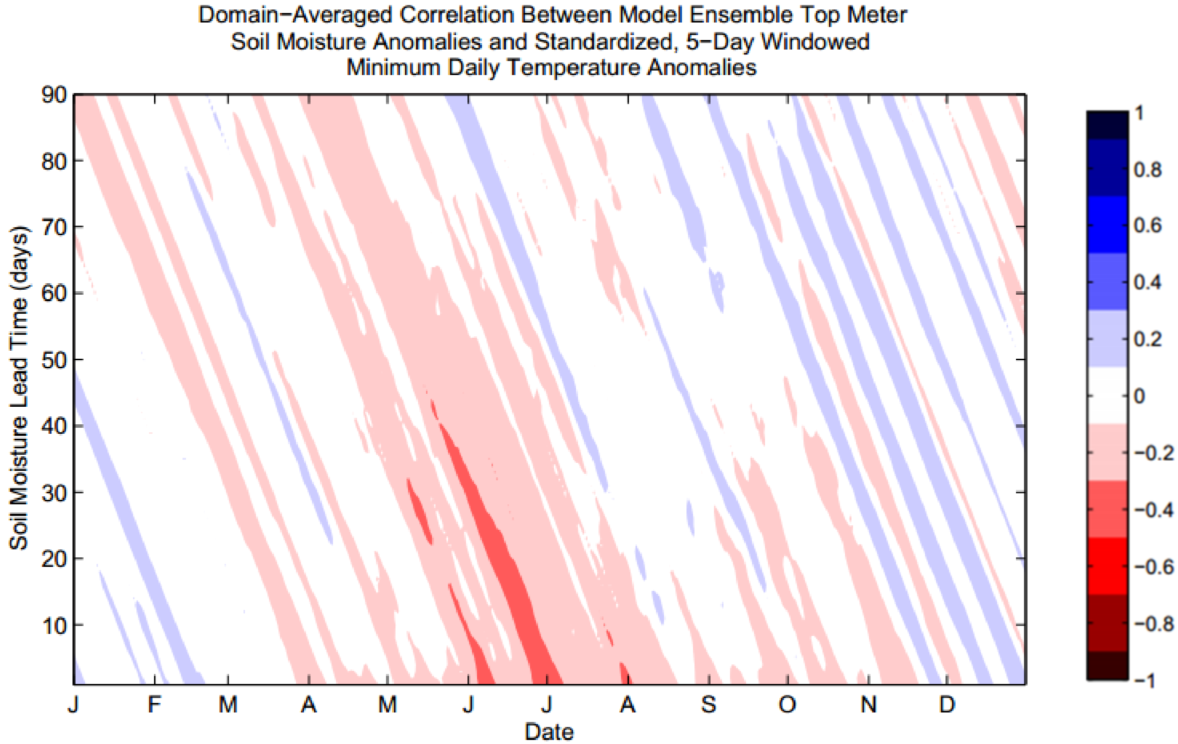

Figure 6.19 shows the correlation between standardized model ensemble RZSM anomalies and standardized, 5-day windowed temperature anomalies in Julian Day-lag space where the y-axis represents how may days in advance soil moisture is being used to predict temperature. The correlations were weaker than between RZSM and maximum temperature, but there is a peak in the summer and it does indicate higher minimum temperatures when soil moisture is low.

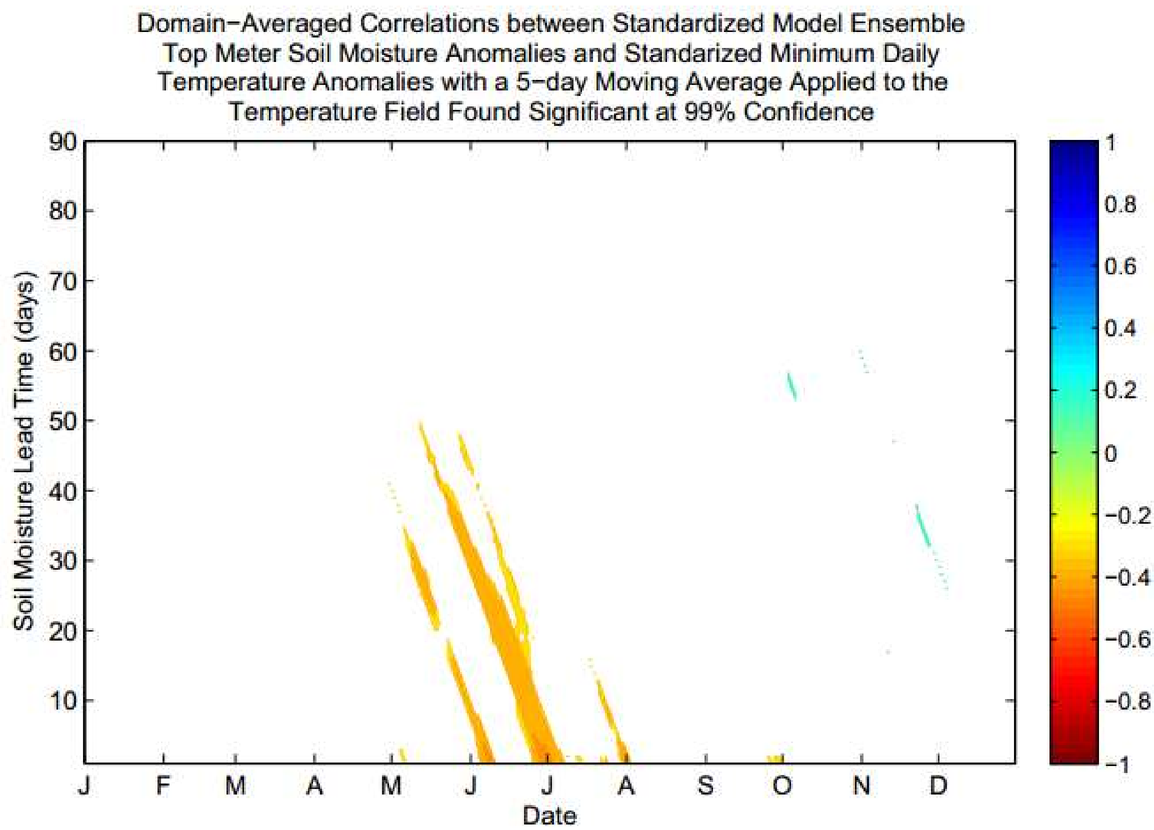

Figure 6.20 shows the same results as figure 6.15, but masks all data that aren't statistically significant at a 99% confidence level. Far less area was found to be significant on the Julian-Day lag space surface between RZSM and minimum temperature as between RZSM and maximum temperature, and the areas are aligned with the areas of greatest significance on the maximum temperature surface. This implies that there is a relationship between RZSM and diurnal temperature swings.

Results (Soil Moisture vs Diurnal Temperature Swings): There was a solid relationship found between RZSM and diurnal temperature swing with low RZSM implying larger diurnal swings in temperature. Over 10% of the area in Julian Day-lag space was found to be statistically significant at the 99% confidence level. Confidence was highest at small lead times in the middle of summer, with a large number of smaller peaks later in the fall. This is probably due in large part to RZSM's partial control of the near-surface, or boundary layer water vapor budget. The surface water vapor budget can be thought of in the following way: $\frac{dq}{dt} = E - \nabla \cdot (\overrightarrow{V_H} q) - \Delta q \uparrow$

Where E is the surface evapotranspiration rate $\nabla \cdot (\overrightarrow{V_H} q)$ describes convergence or divergence of the moisture field, and $\Delta q \uparrow$ describes moist convective transport to the upper atmosphere. The missing element that closes this system is, of course, condensation/precipitation.

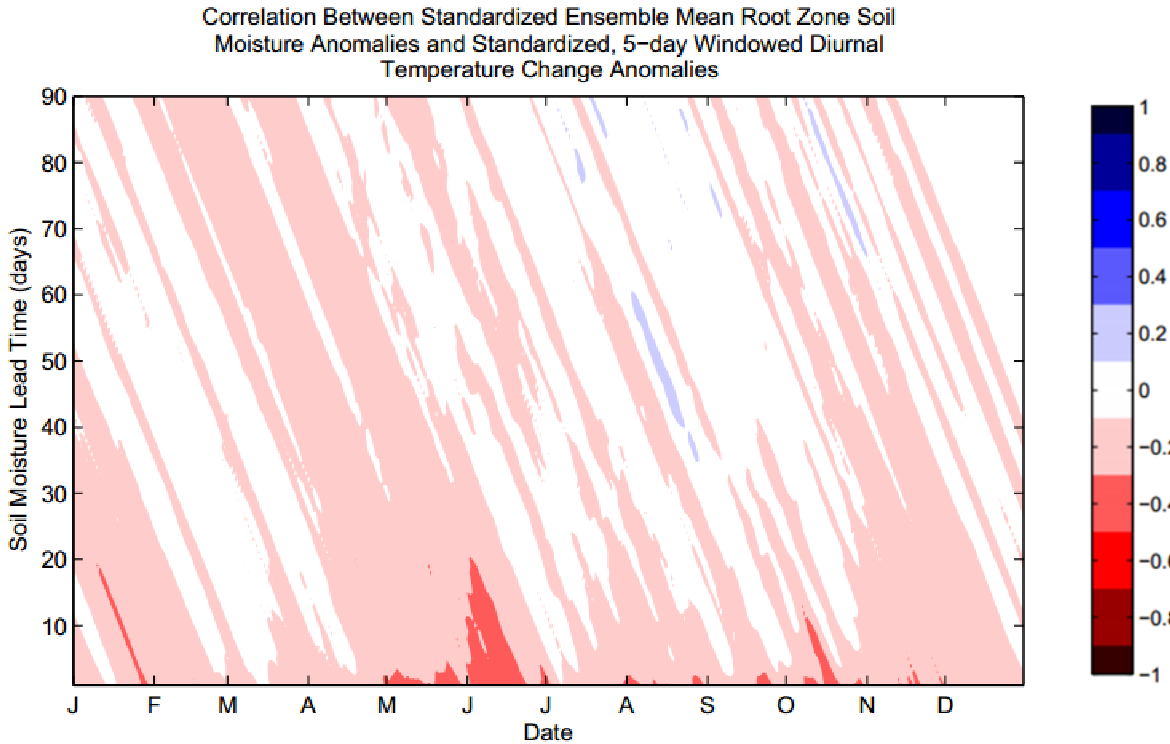

Figure 6.21: Correlations between standardized model ensemble RZSM and diurnal temperature swings are shown above. The x-axis represents the day of the year in which measurements are taken and the y-axis represents the number of days ahead of the middle of the temperature window RZSM was measured.

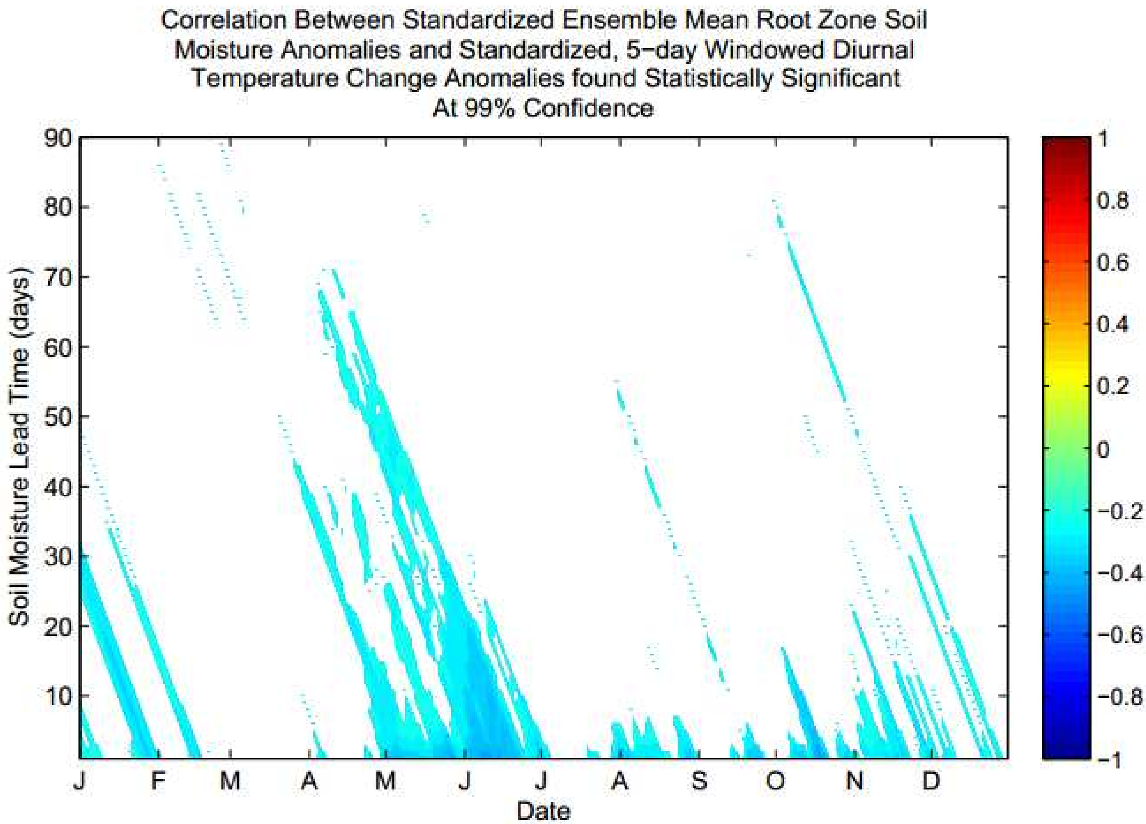

Figure 6.22:The same information as in figure 6.21 is depicted here, but all correlations not significant at 99% confidence have been masked.

Results (Soil Moisture vs Precipitation): As hypothesized, there was a domain-averaged positive relationship between standardized root zone soil moisture anomalies and standardized nine-day running average precipitation anomalies throughout the majority of the spring and summer. The first week of July proved an anomalous exception to this relationship. Correlations were not as significant between root zone soil moisture and precipitation as they were between root zone soil moisture and temperature when using the NLDAS-2 grid at its full resolution. While effective sample size was on the order of four times as high for correlations between RZSM and future precipitation as for RZSM and future maximum temperature this was not enough to make up for the decrease in correlation in order to keep the same level of statistical significance.

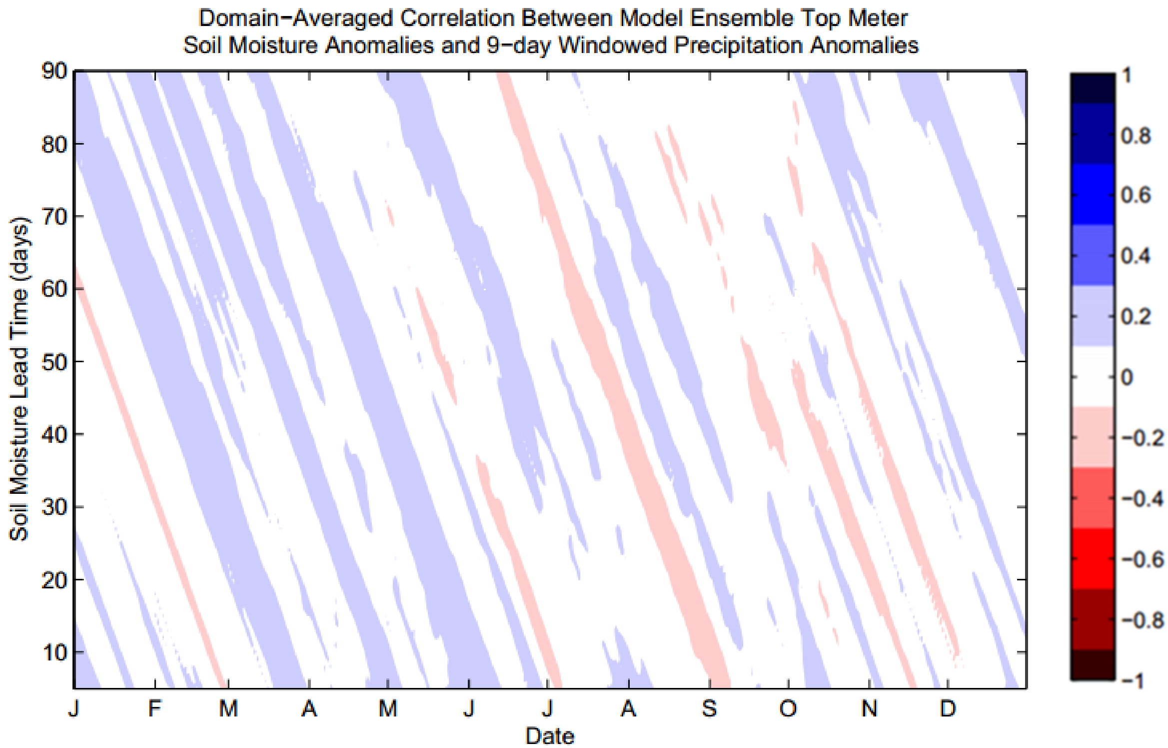

Figure 6.23: Correlations have been plotted above between standardized root zone soil moisture anomalies and standardized 9-day running average precipitation anomalies for every day of the year. The x-axis represents the day of the year with months labeled by their first letter. The y-axis denotes the amount of days in advance of the center of the precipitation window soil moisture was being used as a predictor from five up to 90.

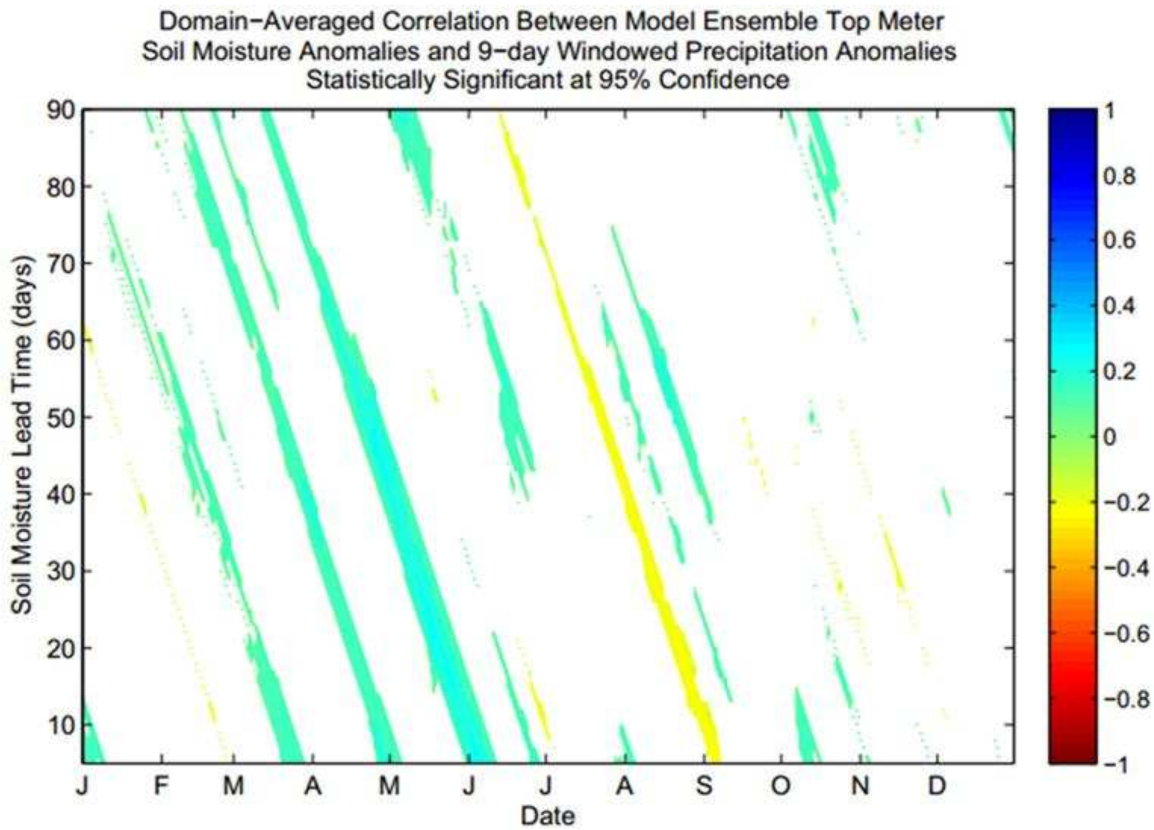

Figure 6.24: The data above are the same results as figure 6.1, however all values that were not determined to be statistically significant at 95% confidence (|correlation > 0.117|) have been masked. Like figure 6.7 the x-axis represents the day of the year with months labeled by their first letter, and the y-axis represents the number of days in advance of the center of the precipitation window that root zone soil moisture is being used to forecast precipitation.

For correlations that met the criteria for statistical significance at 95% confidence there was an average of a 0.317 standard deviation increase in precipitation for every standard deviation increase in root zone soil moisture. Correlations between standardized root zone soil moisture anomalies and standardized precipitation anomalies tended to be highest in the late spring from mid-April until mid-June. For the domain as a whole this is the time of year in which one standard deviation of precipitation has the greatest magnitude in physical units. Between mid-April and mid-June a one standard deviation increase in root zone soil moisture would correspond to an average of 0.019” of precipitation/day.

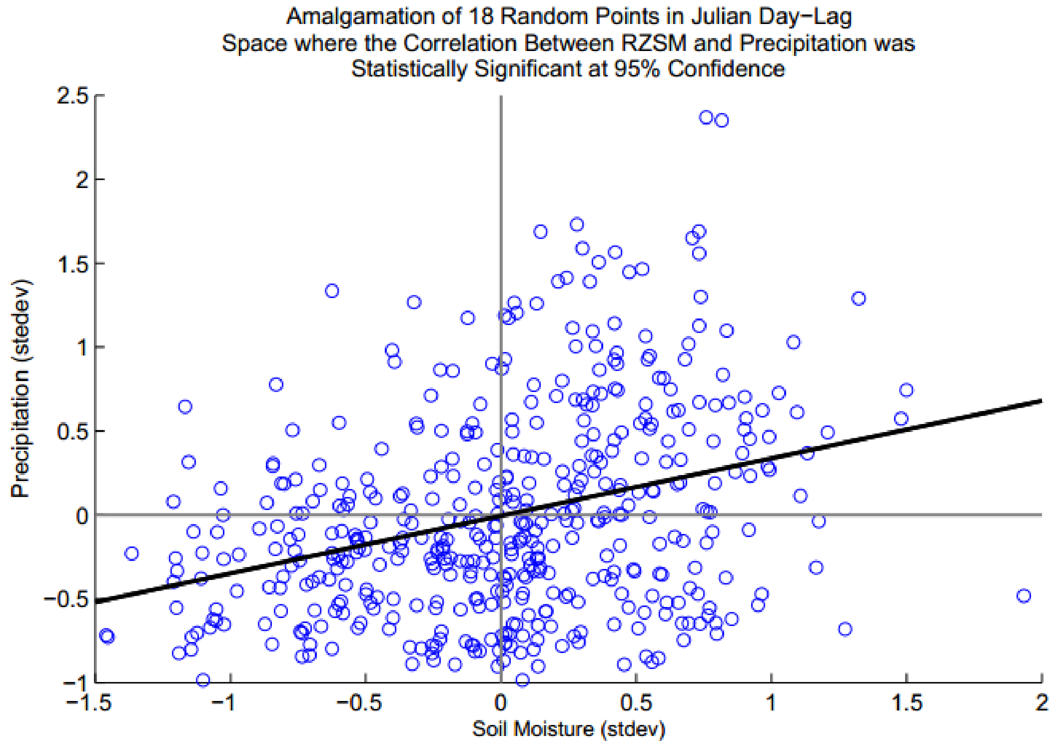

Figure 6.25: Here 18 randomly-selected scatterplots within the domain that were found to be statistically significant at the 95% confidence level have been plotted as one. The bolded line represents the average of all linear regression slopes 0.317 sigma increase in precipitation for every one sigma increase in root zone soil moisture that was realized from statistically significant situations.

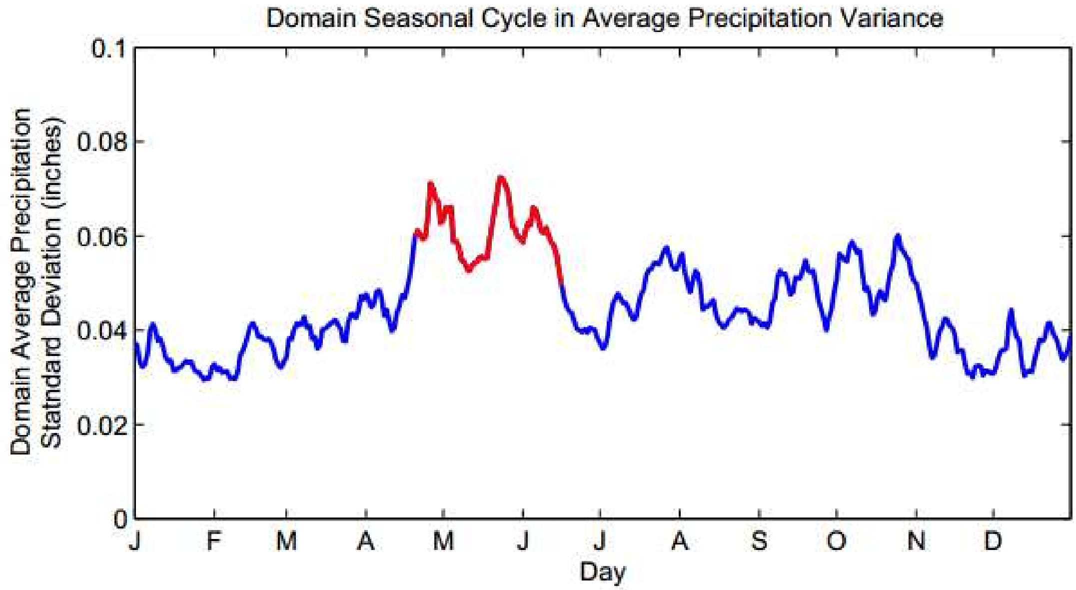

Figure 6.26: The domain-average value corresponding to one standard deviation in daily precipitation is plotted here as a function of Julian Day. The time of year in which RZSM has the greatest influence on future precipitation is highlighted in red.

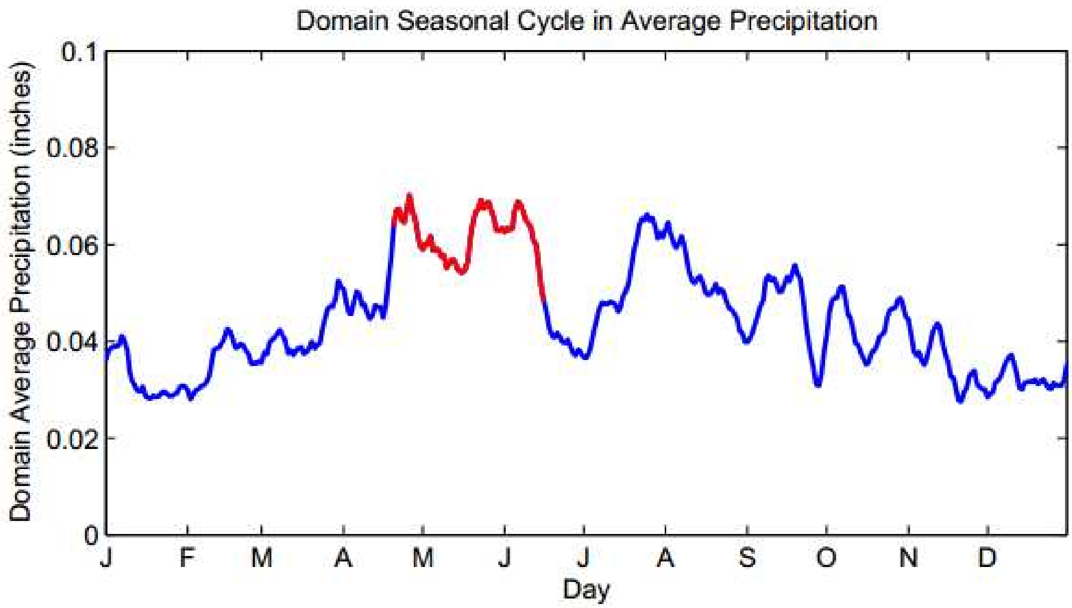

Figure 6.27: The domain-average value corresponding to the mean daily average precipitation is plotted here as a function of Julian Day. The time of year in which RZSM has the greatest influence on future precipitation is highlighted in red.

Perhaps the most important finding about RZSM's relationship with future precipitation is that it changes as a function of grid resolution. In coarsening the grid resolution correlations between root zone soil moisture and precipitation did rise. This will be revisited in great detail in later chapters as it appears that a much better job could be done of quantifying the relationship between RZSM and precipitation for the Upper Colorado River Basin and the Western High Plains. Much more discussion about the link between top meter soil moisture and future precipitation will follow in later chapters where the relationship is examined using different statistical techniques.

WET AND DRY YEAR DEPENDENCE OF ROOT ZONE SOIL MOISTURE-MAXIMUM DAILY TEMPERATURE FIT

Results for several chapters of this thesis make use of a linear approximation for the relationship between root zone soil moisture and seasonally-projected temperatures, precipitation, and water balance. A first-order approximation is used because of the expected heterogeneity within the domain and or over the period of record analyzed in variables such as precipitation, soil type, land slope, and downwelling shortwave radiation that the overall relationships between RZSM and temperature will be visible in a linear framework. Given results from chapter six this hypothesis appears to be robust. Experiments were not performed this way because temperature and precipitation are expected to be linear functions of RZSM. If fact, as shown in Clapp and Hornberger 1978, the suction force holding water to plants increases exponentially. One would not expect the partitioning of land surface energy received in excess of radiative equilibrium between sensible and latent heat fluxes to be linear based on this information.

In this chapter the magnitude of non-linearity of the domain-wide relationship between RZSM and high temperatures will be explored. The same will be explored for precipitation using different methods in the chapter nine. If correlations are truly linear in nature then correlations should hold when a piece of the data are removed, so in this chapter correlation will be reevaluated between RZSM and temperature when extreme soil moisture values have been removed. One experiment will be conducted where RZSM and temperature datasets are re-standardized and correlations are recalculated after removing the three driest soil years on record for each Julian Day. Another experiment will be conducted doing the same, but after removing the three wettest years in terms of standardized soil moisture anomalies on record for each Julian Day. This method has the added benefit of showing whether correlations are more dominantly lead by wet or dry anomalies.

Results: Findings here indicate that even given the spatial heterogeneity of the land surface and the temporal heterogeneity of the atmosphere the RZSM-maximum temperature feedback was decidedly non-linear for the Upper Colorado River Basin and western High Plains over the last thirty years of record as shown by NLDAS Phase-2 data. Both the wet and dry years had a pronounced effect on the correlation between RZSM and future maximum temperatures. The wettest years have a less concentrated, but fairly ubiquitous effect of lessening the magnitude of correlation at all lead times from March through August and at shorter lead times in September and October.

Removing the three driest years of data had a bigger effect on the correlation between RZSM anomalies and temperature anomalies through the beginning of June and short and long lead times for the most part. Using the full dataset it is anticipated that for short lead times RZSM has a domain-wide expected impact on 5-day running average maximum temperatures of 1.5-3.5 Fahrenheit/standard deviation for the month of June. When either the three wettest or driest years are removed not only is the confidence in the relationship between RZSM and future maximum temperatures reduced, the regression slopes are on the order of half as steep.

While droughts are expected to increase both in intensity and duration (IPCC 2014) in a warming climate there is no guarantee that dry anomalies of the magnitude of 2002 or 2012 will manifest in any given 30-year period. Likewise, there is no guarantee wet anomalies of the magnitude of 1995, 1998, or 2013 will show up in any given 30-year period. Growing season projections made based on a 30-year period are therefore subject to an over-fitting bias from only using a 30-year data record. Using a longer dataset also has potential complications as removing the climate change signal from the relationship between RZSM and temperature, or another variable like precipitation, is not as simple as removing a linear trend. For instance, one of the drivers of evapotranspiration is vapor pressure deficit. This does not increase in a linear fashion as temperature increases.

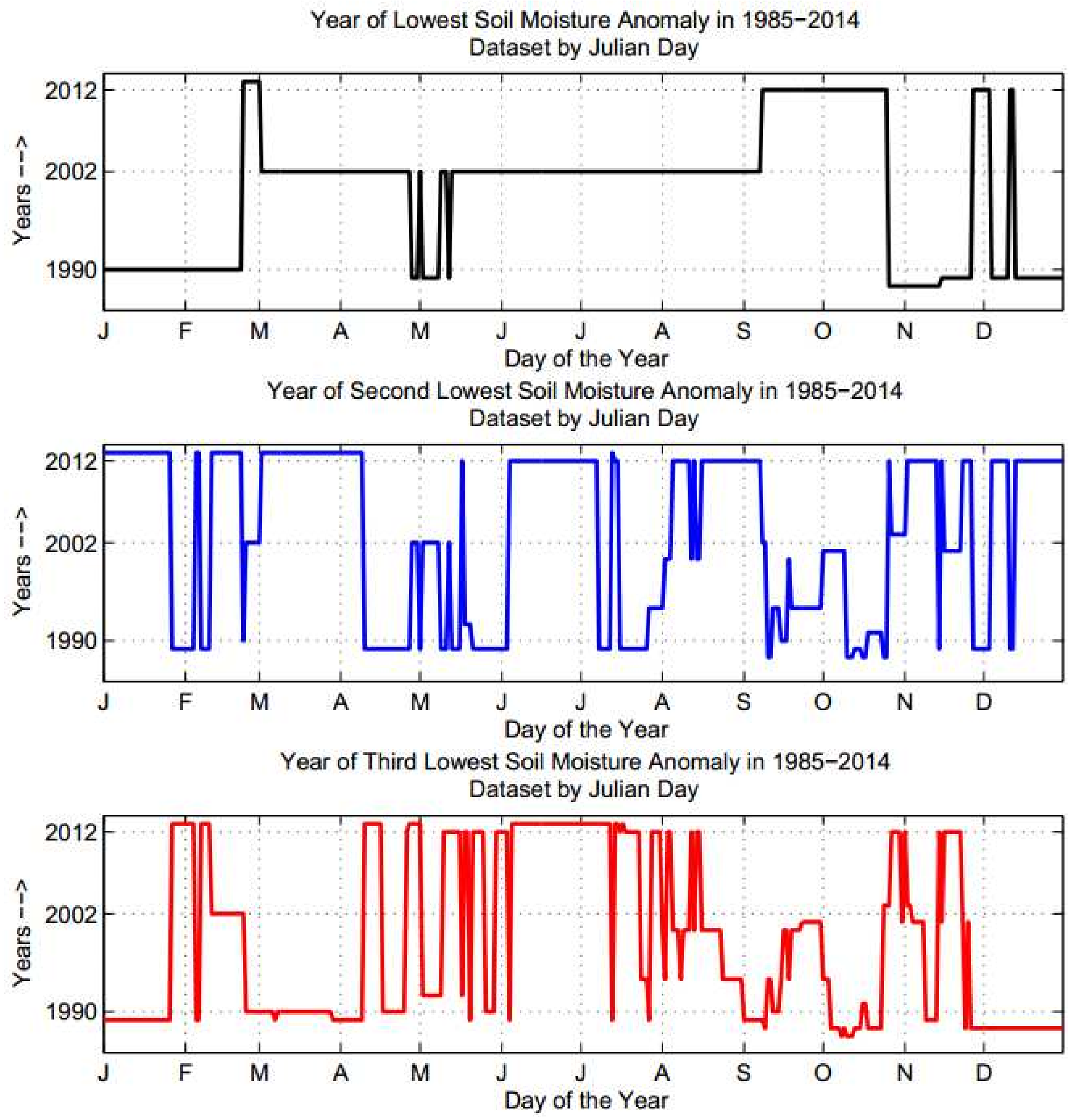

Figure 7.1: In the three plots above the three driest years of data are depicted for each Julian Day. Plots are ordered from most to least extreme with the driest year (top), second driest year (middle), and third driest year (bottom) shown.

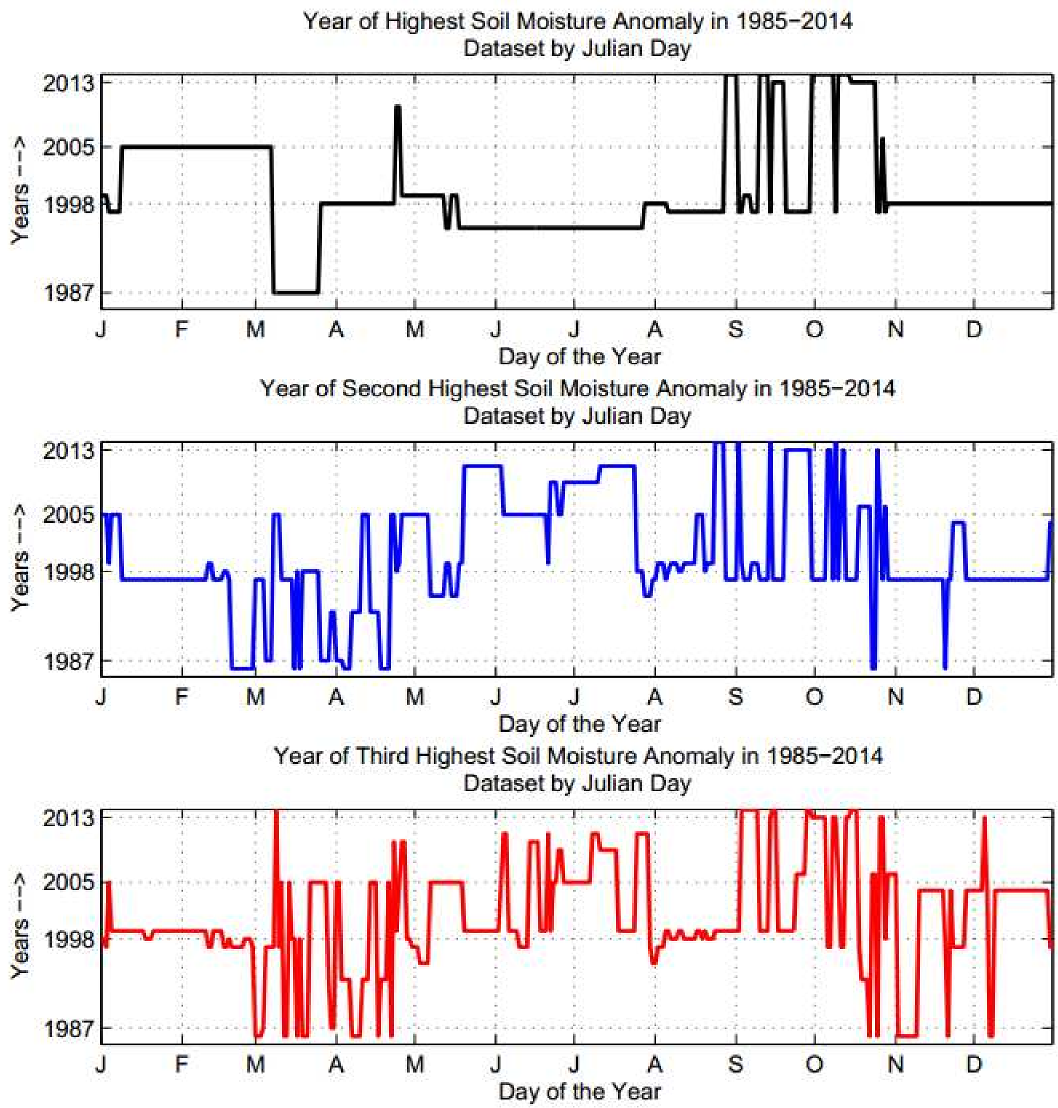

Figure 7.2: In the three plots above the three wettest years of data are depicted for each Julian Day. Plots are ordered from most to least extreme with the wettest year (top), second wettest year (middle), and third wettest year (bottom) shown.

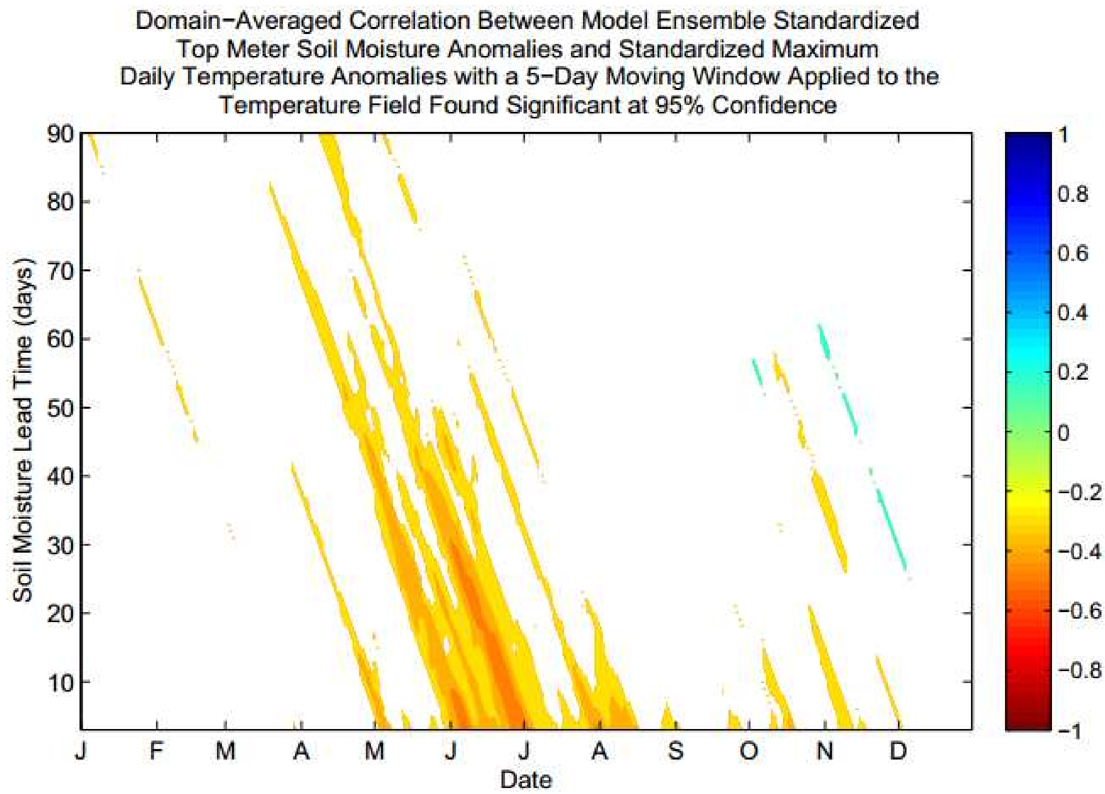

Figure 7.3 shows the linear correlation between Model Ensemble Standardized Root Zone Soil Moisture Anomalies and Maximum Temperature Anomalies where values that are not significantly different than zero at 95% confidence have been masked. 10.5% of area is shaded and negative in sign.

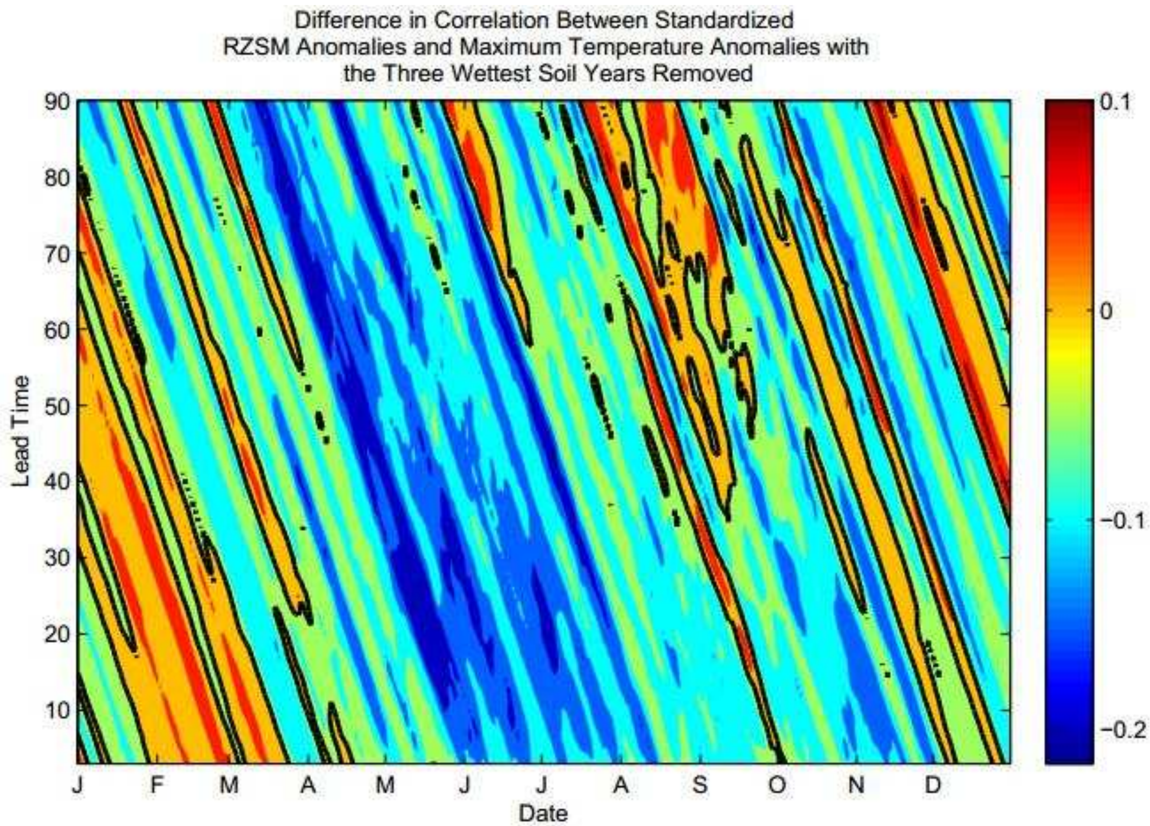

Figure 7.4 shows the difference in correlation between standardized model ensemble RZSM and future maximum temperatures in Julian Day-Lag space between when all 30 years are used for correlation and when the three wettest years are removed. The thick, black contour represents the zero line.

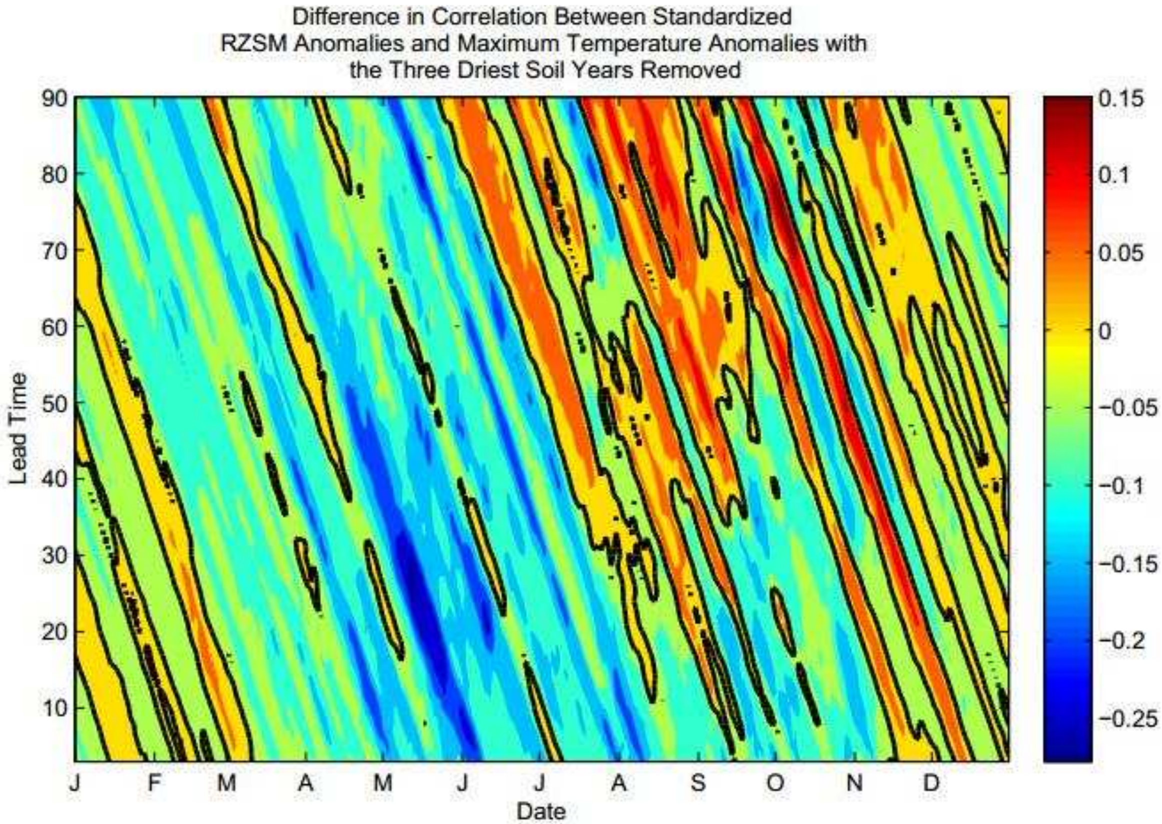

Figure 7.5 shows the difference in correlation between standardized model ensemble RZSM and future maximum temperatures in Julian Day-Lag space between when all 30 years are used for correlation and when the three driest years are removed. The thick, black contour represents the zero line.

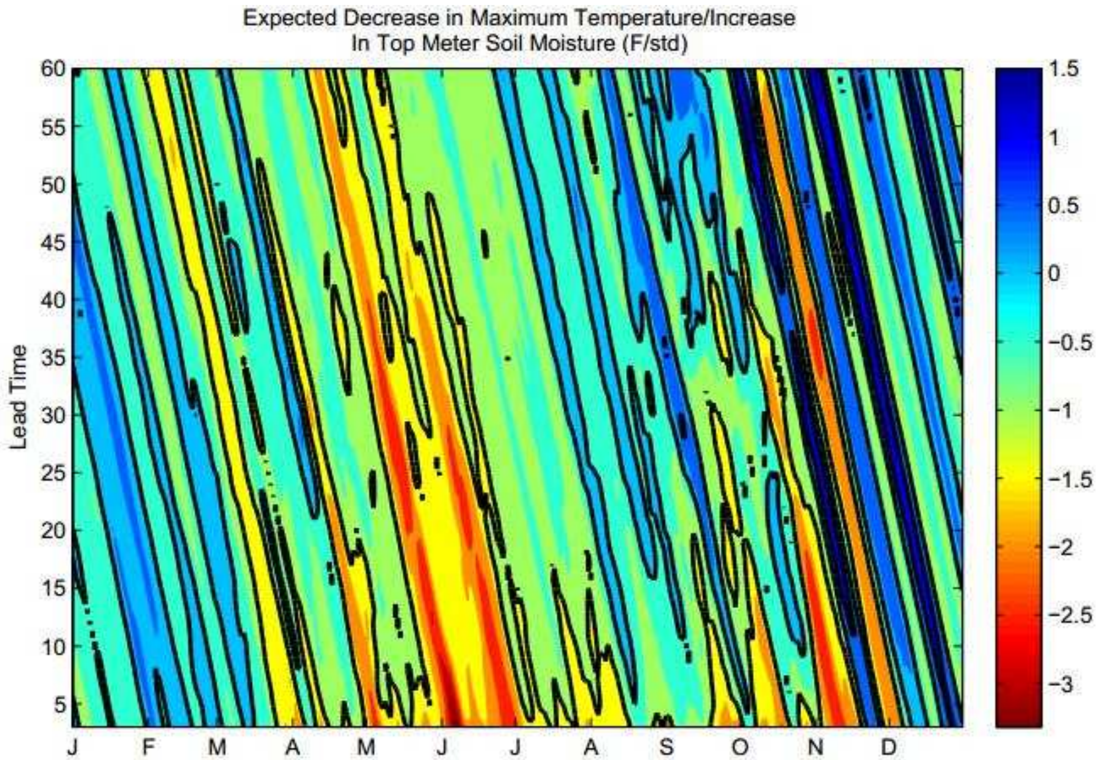

Figure 7.6 shows the domain-averaged expected decrease in 5-day running average maximum temperature anomaly (F) per unit decrease in standardized top meter soil moisture anomaly using data from the entire 1985-2014 record.

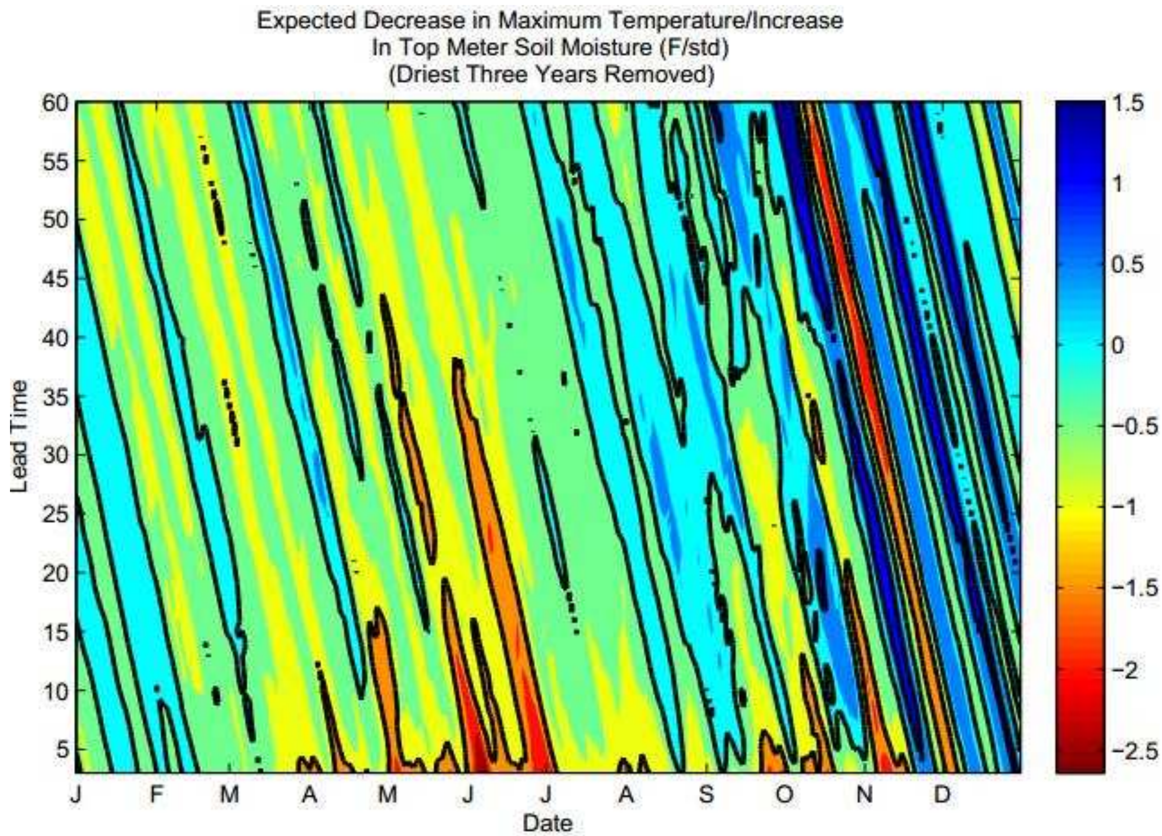

Figure 7.7 shows the domain-averaged expected decrease in 5-day running average maximum temperature anomaly (F) per unit decrease in standardized top meter soil moisture anomaly using all the data from the 1985-2014 record except for the three years where root zone soil moisture is the highest.

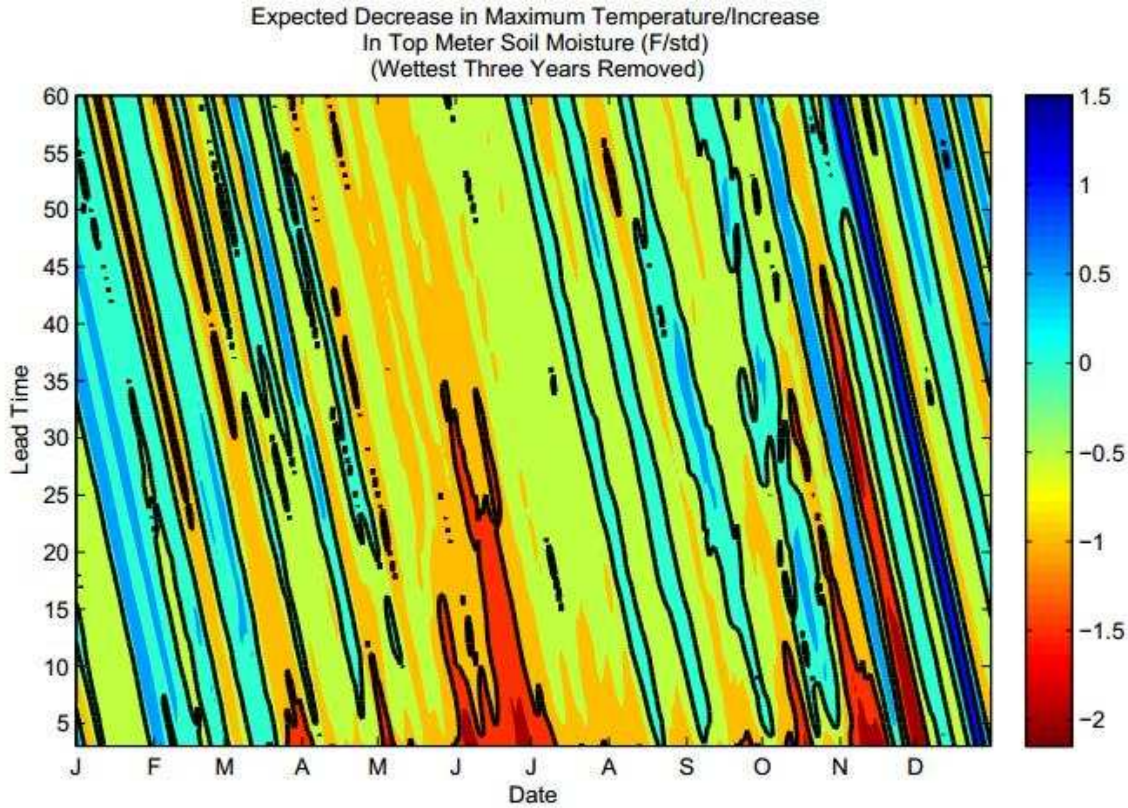

Figure 7.8 shows the domain-averaged expected decrease in 5-day running average maximum temperature anomaly (F) per unit decrease in standardized top meter soil moisture anomaly using all the data from the 1985-2014 record except for the three years where root zone soil moisture is the lowest.

BREAKDOWN OF FEEDBACKS BETWEEN ROOT ZONE SOIL MOISTURE AND THE ATMOSPHERE FOR DROUGHT EARLY WARNING BY MAJOR SUBBASINS WITHIN THE DOMAIN

Methods: Results in chapter six obtained by parsing the full domain by soil type and by elevation revealed very little about how correlation between root zone soil moisture levels and the future state of the atmosphere varies with space. This is because statistics were examined as domain averages. On top of this, different parts of the domain experience very different seasonal temperature and precipitation patterns, so the mean state and its variance is a function of space. As such, it is natural to be curious about correlation between root zone soil moisture and atmospheric variables such as temperature and precipitation with space within the domain. These correlations will be linked back to expected seasonal changes in temperature and precipitation, and how this changes within the overall domain of 36.938 to 43.563 degrees latitude by -113.063 to -101.938 degrees longitude (figure 8.1).

Sub regions within the domain were chosen largely based on river basin. Using this division scheme, feedbacks between RZSM and the atmosphere can be quantified as a function of watershed, which is well-suited to the overarching goal of drought early warning.

The divisions are not perfectly drawn by watershed, but deviations from this scheme were not arbitrary. Larger subbasins were broken up either by political boundary or natural breaks from topography. For instance, the Colorado River main stem runs through the north side of the Colorado Headwaters region marked in figure 8.1 into the Colorado Plateau Region, so these two regions are part of the same basin. The Uncompahgre Plateau serves as the major dividing line between the two regions. Likewise, the Green River feeds into the Colorado River in southeast

Utah and drains to the same location, but there is a demarcation between zones along the Roan Cliffs. Sampling the entire Upper Colorado River Basin as one zone would lead to having a zone that is too large and diverse in climate relative to the others. For this same reason the northeast corner of the map is not split into just the portions of the North and South Platte Basins existing within the domain, but rather partially divided based on political boundary.

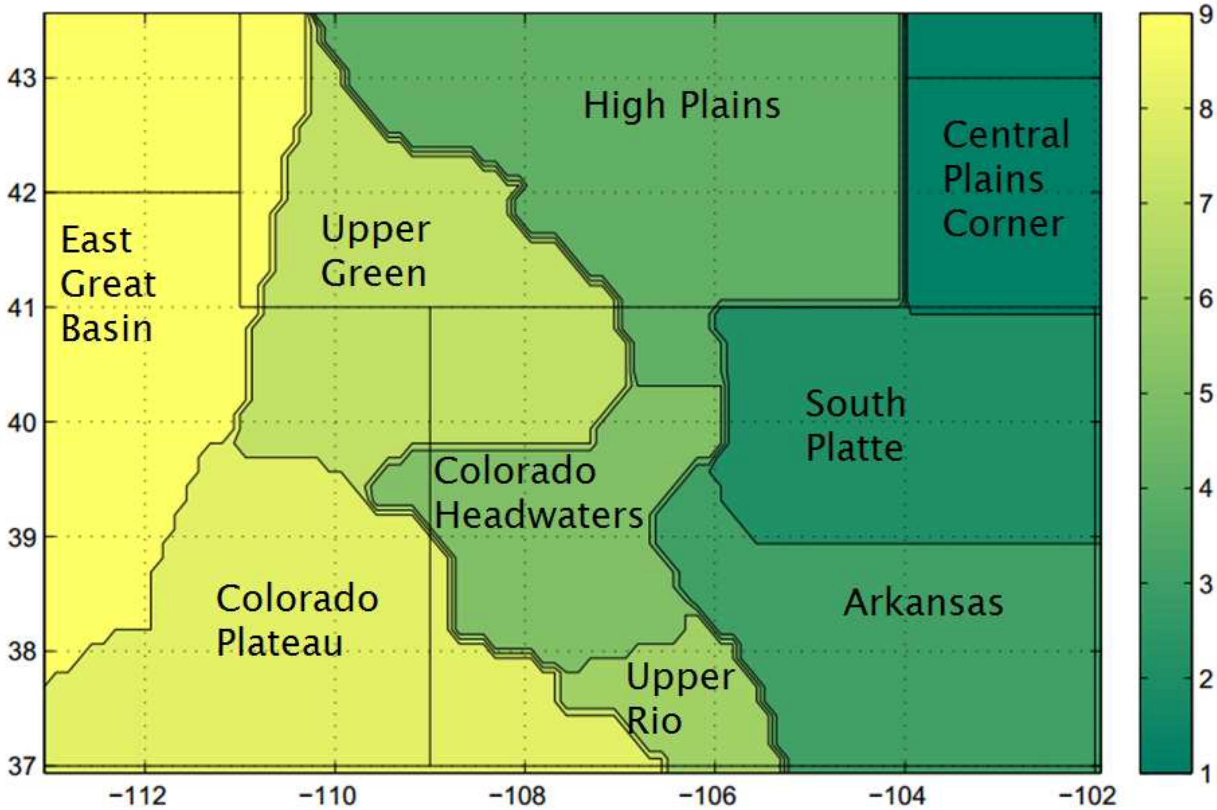

Figure 8.1: The results shown in the section below that represent soil moisture's energy balance connection to temperature and precipitation are divided based on the nine regions contoured here.

Root Zone Soil Moisture vs Maximum Daily Temperature: Once the subbasin grid had been established pulling results for subbasins was done by first decomposing ensemble root zone soil moisture and maximum temperature matrices according to which watershed the center point of each grid cell fell within. Once again using data from 1985 through 2014, the same correlation analysis procedure outlined in chapter six was followed to obtain results. Just like for the full field, correlation was analyzed between standardized ensemble soil moisture anomalies and standardized five-day moving average maximum temperature anomalies. This was done for every day of the year, and with soil moisture lead times over the center of the five-day temperature window from three all the way to 90 days.

In the panels below the subbasin-wide mean of these correlations are mapped in the upper left much as was seen in chapter six. To save text space in displaying subbasin panels these contour maps are affectionately referred to as “fire plots,” a name that was chosen because of their shape and because of their demonstration of low RZSM leading to higher maximum temperatures. Areas where subbasin mean correlation exceeded 99% confidence in being significantly lower than zero were set aside, and the increase in maximum temperature (standard deviations) was quantified per unit decrease in RZSM (standard deviations). The upper right of the panels below will show an amalgamation of ten random points in Julian Day-lag space for the displayed subbasin (at 30 years (points) a piece) where this was applicable. These plots also include the least squares line for all points within the subbasin in Julian Day-Lag space that exceeded 99% confidence.

Using the methods outlined in chapter six to assess statistical significance the magic number for the domain- mean correlation between RZSM and maximum temperature to be statistically significant with 99% confidence using a one-tailed test was $\rho < -0.2471$. Splitting the domain into subbasins this value was reassessed for each subbasin separately as effective sample sizes for smaller sub-domains should be smaller than for the whole domain. This was done in the same way by randomizing the date and year dimensions of the maximum temperature matrix and correlating the standardized ensemble RZSM matrix with these randomized matrices.

In order for correlation to be declared significantly lower than 0 at 99% confidence the new thresholds that must be met by basin are as follows: Central Plains Corner: $\rho < -0.3101$, South Platte Region: $\rho < -0.3292$, Upper Arkansas Region $\rho < -0.3328$, Upper High Plains Region: $\rho < -0.3238$, Colorado Headwaters Region $\rho < -0.3504$, San Luis Valley Region: $\rho < -0.3619$, Upper Green River Region: $\rho < -0.3289$, Wasatch to San Juan Region: $\rho < -0.3378$, East Great Basin Region: $\rho < -0.3388$. The magnitude of these thresholds is inversely, but not monotonically related to subbasin spatial extent.

The two bottom plots for each panel are a little simpler. These plots merely show the mean (left) and standard deviation (right) of maximum temperature within the subbasin for each day of the year. Areas where the line is red correspond to areas where the average subbasin correlation for all soil moisture lead times between three and 90 days was less than the tenth percentile in correlation of the randomized matrix for the subbasin for the period of time starting four days before the center of the window to the period four days after the center of the window. This doesn't imply any given level of significance, but was chosen for two reasons: 1. Since effective sample size was determined using a randomly-permuted matrix, the percentile ranking of a value with respect to the randomized matrix is directly linked to significance. 2. This method standardizes the red line by basin. The same correlation value has less significance for smaller regions than for large ones. This value was a bit more arbitrarily chosen, but it effectively highlights the season in which drought early warning could be boosted through more advanced knowledge of RZSM-atmosphere feedback strength. This area makes a parallelogram shape on the upper-left diagrams, and a visual example has been included in figure 8.2.

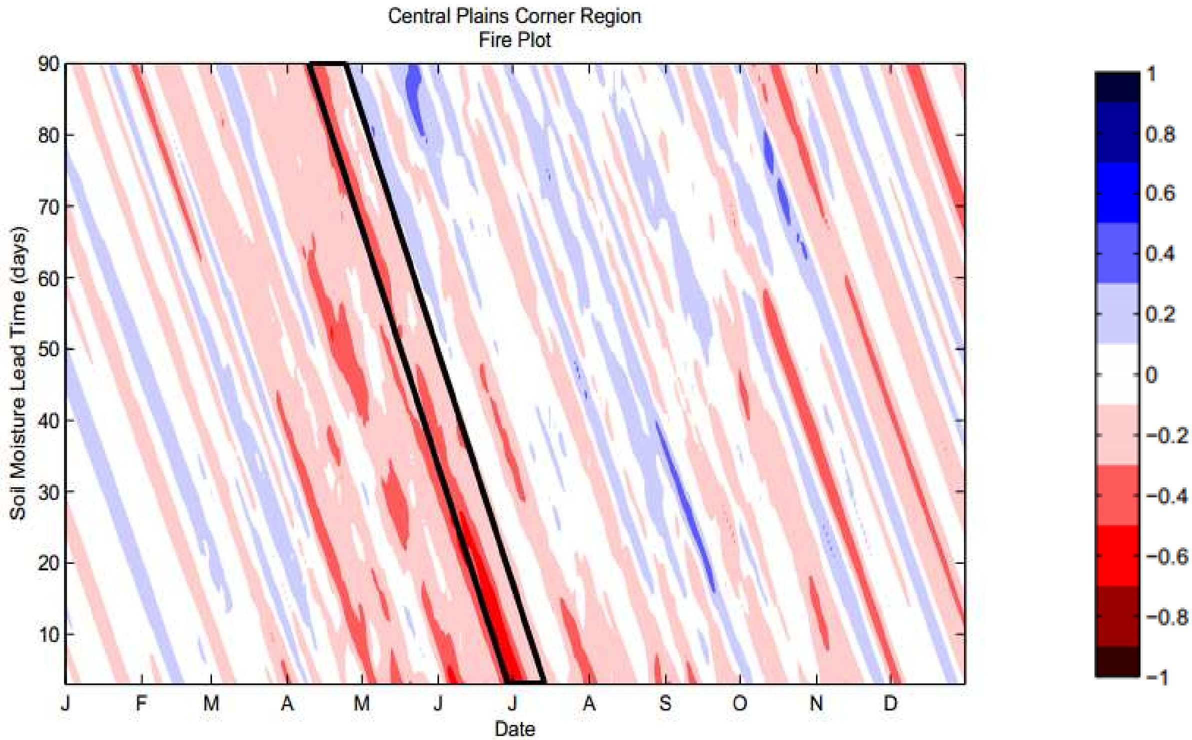

Figure 8.2 is an example of the area averaged together that must meet thresholds outlined above in order to highlight lower-right and lower-left lines red in the panels below. These plots were generated using a 5-day moving average maximum temperature, so these results represent nine days of consecutive data. The colorbar shown in figure 8.2 will be used for the upper-left corner of all panels below for both RZSM vs maximum daily temperature and RZSM vs future SPIs below.

For the Central Plains Corner Region at the far northeast end of the domain a relatively small amount of area in Julian Day-lag space showed up as statistically significant at 99% confidence with 5.8% of the area meeting the threshold. Of the area that met the 99% confidence threshold there was an average slope of -0.458, so almost half a standard deviation decrease in temperature for every one standard deviation increase in top meter soil moisture is to be anticipated. The statistical significance was centered in the early June to early July time frame. A drop-off is evident between these two peaks, which both have fairly narrow ranges in Julian Days. There is anticipated decrease in temperature of 2.77 degrees Fahrenheit for every one standard deviation increase in RZSM in portions of the growing season where significant coupling appears to exist. (The period of time from April 1st – October 31st will sometimes be used to approximate the growing season). Areas highlighted in the bottom two panels represent times when the average correlation in Julian Day-lag space is below -0.177, which corresponds to the tenth percentile of the region's temporally-randomized matrix, in the area from three to 90 day lead time and from four days before and after the middle of the window.

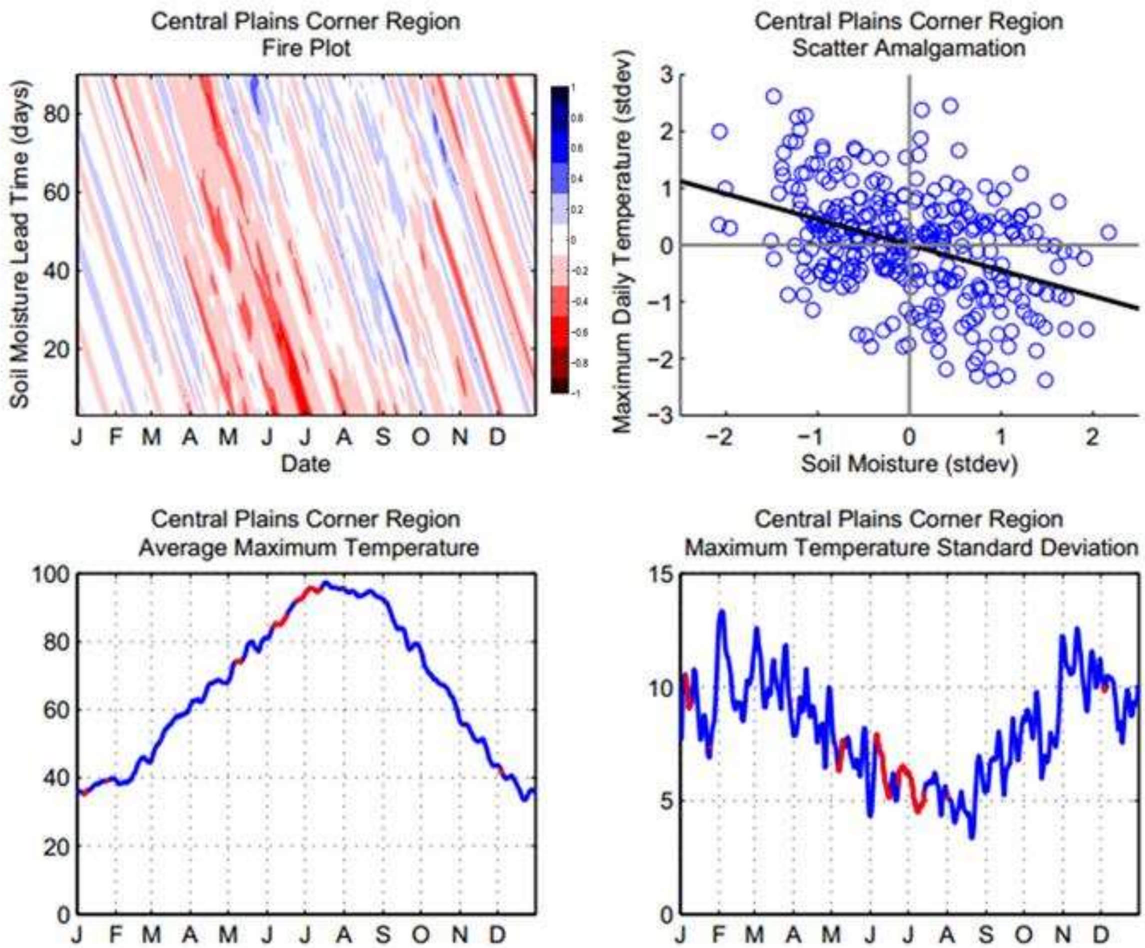

Figure 8.3: Central Plains Corner Region Maximum Temperature Panel

Much like other areas within the overall domain, soil moisture's predictive power over future maximum temperatures maximized in June and July, and did generally decrease at longer lead times for the South Platte Region. This region exhibited the lowest amount of statistically significant correlations with a mere 1.9% of the area in Julian Day-lag space showing significance at 99% confidence. Only a few days showed a nine-day running average RZSM-maximum temperature correlation of less than -0.189 (red line threshold). This included anomalous days outside of the growing season in the first week of December. For the periods within the growing season where this negative correlation was lower than -0.189 an average of a 3.60 Fahrenheit decrease in maximum temperatures can be expected for every one standard deviation increase in RZSM. This occurs only in early and mid-June. These data provide strong evidence that RZSM does not play a large role in governing maximum temperatures in northeastern Colorado outside of late May and early June at short lead times.

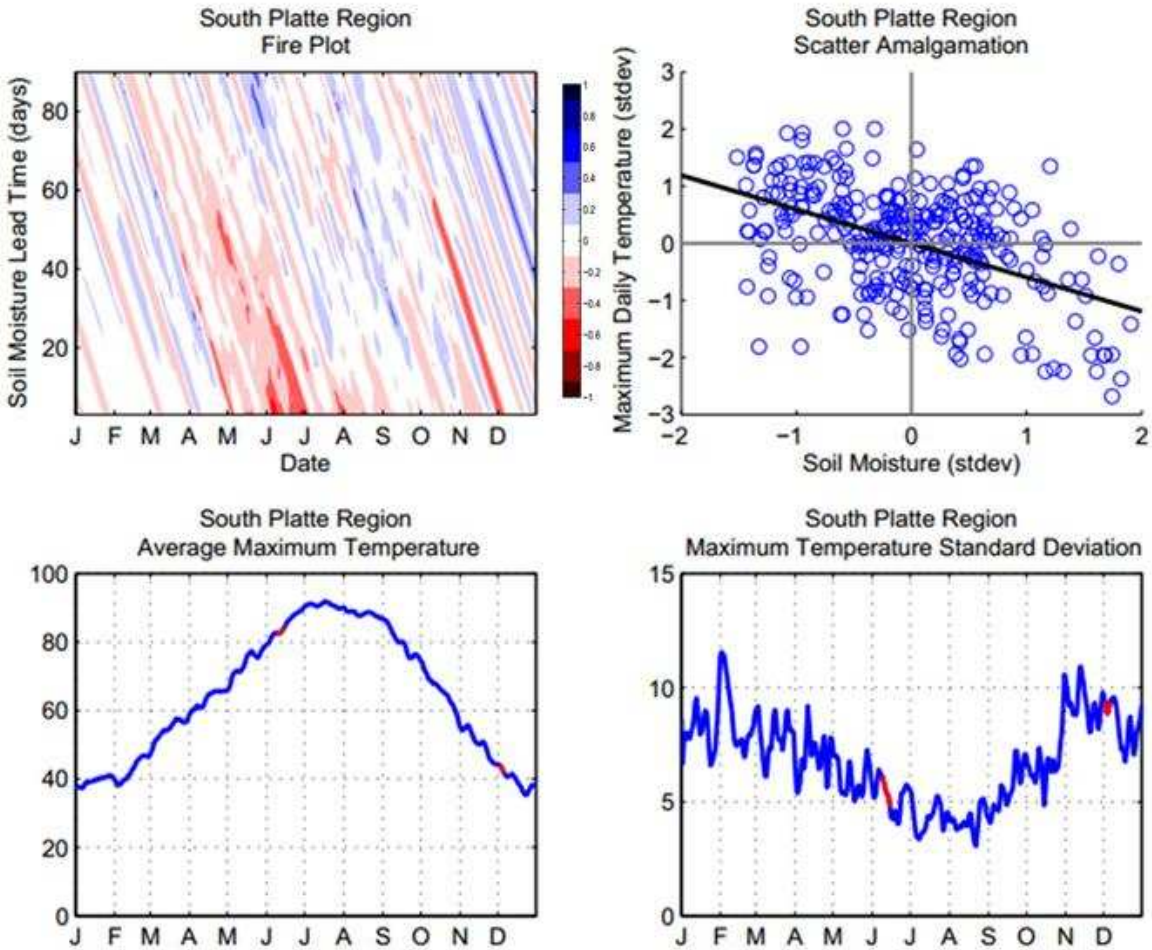

Figure 8.4: South Platte Region Maximum Temperature Panel

The Upper Arkansas Region saw more seemingly anomalous correlation outside of the expected growing season than any other basin. It is less clear for these areas whether the correlation represents something truly physical or is just an artifact from too small a sample of years. The fact that there is a signal of consistent sign not just in the warm season but all the way from the middle of February through early September is nonetheless interesting, and should be noted for drought early warning in this region. 4.6% of the area in Julian Day-lag space exhibits a negative linear correlation between standardized RZSM anomalies and standardized maximum temperature anomalies that are significantly lower than 0 at 99% confidence. This area includes late March soil moisture being used to predict mid-June maximum temperatures. Not many basins saw this strong a correlation at such long lead times in advance of the warm season. For areas within the growing season where the nine-day running average correlation was less than -0.19 a region average decrease in maximum temperature of 3.43 Fahrenheit is predicted for every one standard deviation increase in RZSM.

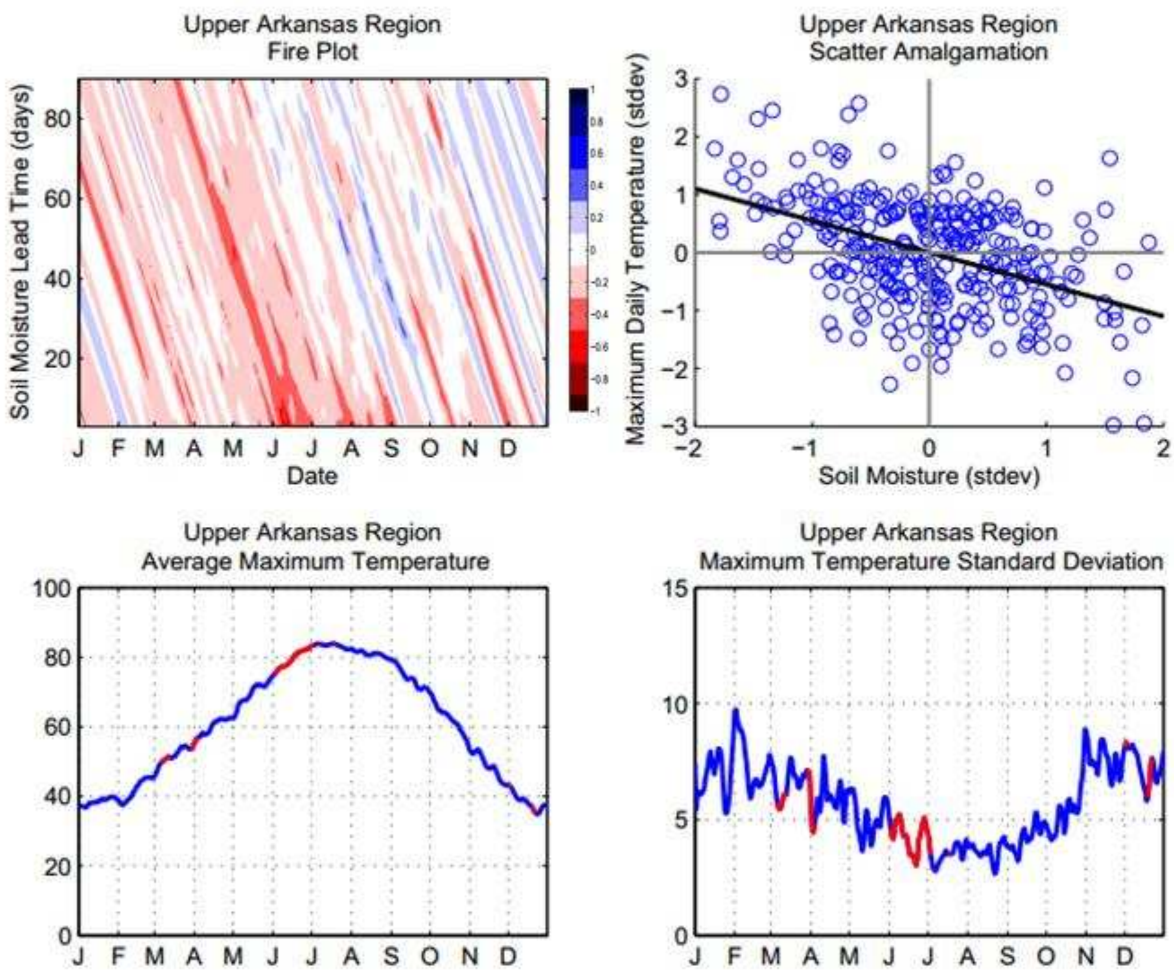

Figure 8.5: Upper Arkansas Region Maximum Temperature Panel

The Upper High Plains Region in southeast and central Wyoming exuded less of a relationship between RZSM and maximum temperature than all over regions except for the South Platte Region. These two regions border one another. Only 2.1% of the area in Julian Day-lag space was found to be statistically significant at 99% confidence. The region-averaged expected decrease in maximum temperature where this magnitude of significance exists is 0.47 standard deviations for every one standard deviation increase in RZSM. There was a small bimodality to where this relationship was most significant which may arise due to not sampling enough years, but it did arise during peak radiation season as expected. Nine-day running average correlation integrated over lead times from 3-90 days was only lower than -0.186 for early to mid-June and again in late June through early July. During these times of year there was an expected decrease in maximum temperatures of -3.61 Fahrenheit for every standard deviation rise in soil moisture.

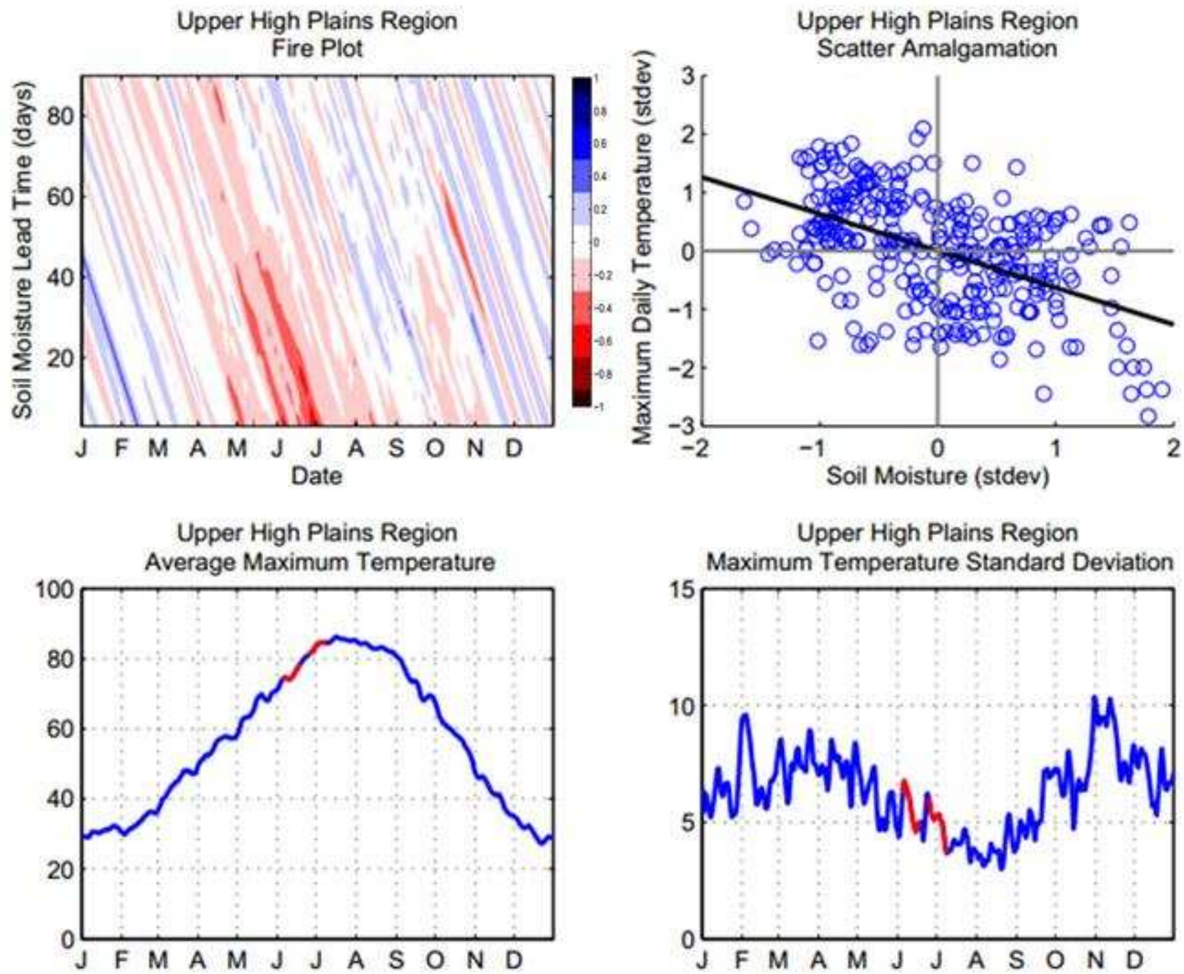

Figure 8.6: Upper High Plains Region Maximum Temperature Panel

The Colorado headwaters region in western and central Colorado shows a very prominent and consistent negative correlation between RZSM and maximum temperatures in the mid warm season months that decreases with lead time. This region does have the highest average elevation of any of the nine regions as well as the lowest summer-time maximum temperatures. Clusters of convection are common in the summer through this region due to high mountains being heated by intense solar radiation and interacting with a cool atmosphere (Henz 1974).

In Texas, it was found that soil moisture impacted warm-season drought primarily by modulating the surface dewpoint, and therefore was a controlling factor of convective inhibition

(Myoung, Nielsen-Gammon 2010). Climate is distinctly different in the Colorado Headwaters than in anywhere in Texas, but applying the findings of this paper to a time of year and a climate region the Colorado Headwaters where the proportion of days that reach convective temperature is high, it is reasonable to think that low soil moisture increase Bowen Ratio, drive up convective temperature, and thereby drive up maximum temperatures. In June 6.4% of the area in Julian Day-lag space was statistically significant at 99% confidence, and a decrease of nearly two thirds (0.619) of a standard deviation in maximum temperature was found on average for every one standard deviation increase in root zone soil moisture. During the parts of the growing season where persistent statistical significance exists this magnitude of slope corresponds to temperature decreases averaging 3.54 degrees Fahrenheit for every standard deviation increase in RZSM. It also merits mention that this expected temperature decrease with increasing soil moisture is higher for the region of significance in late May and early June than later in the growing season because there is more expected variance in maximum temperatures in late May and early June than later in the growing season.

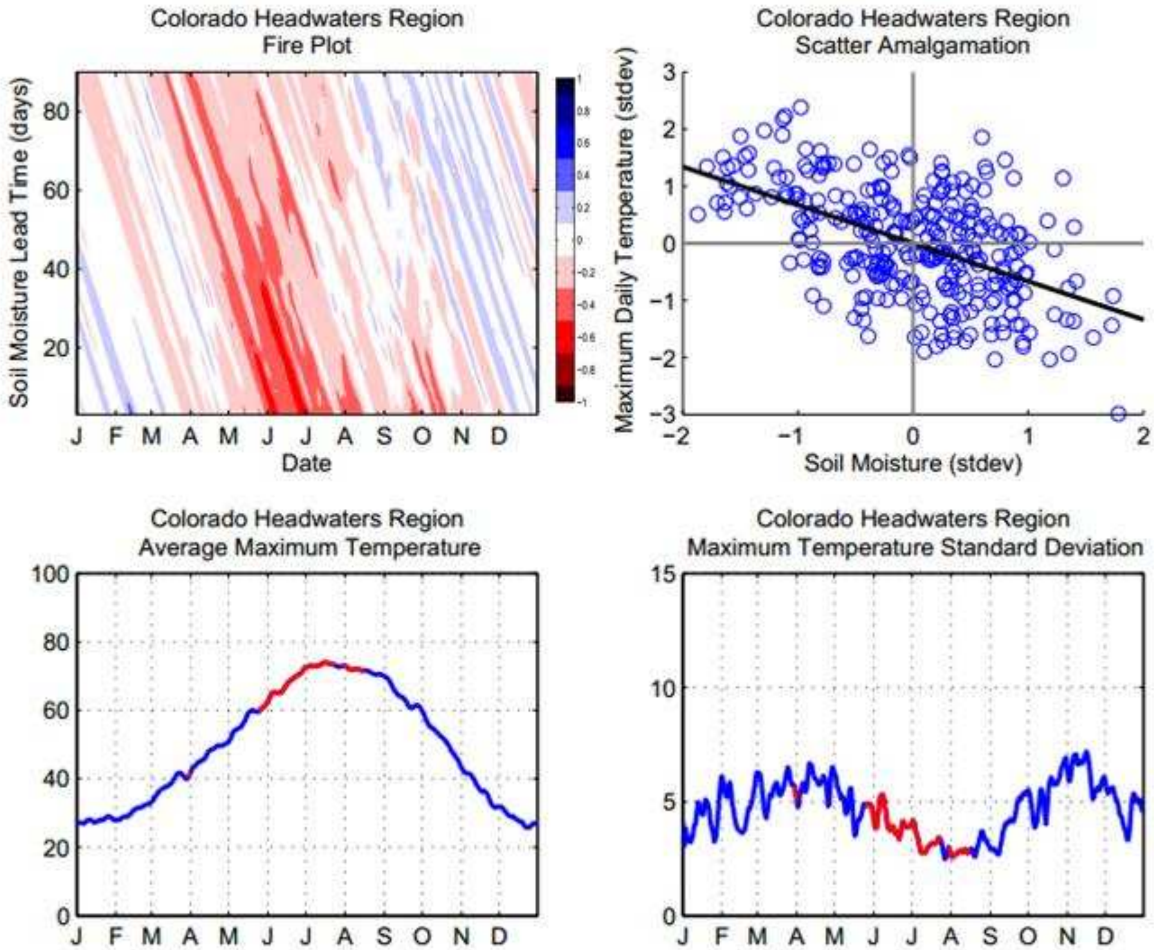

Figure 8.7: Colorado Headwaters Region Maximum Temperature Panel

The low elevations of the San Luis Valley region are climatologically very dry, and this is the smallest region of the nine included, but samples quite a diverse climate as it samples a large chunk of the San Juan Mountain Range in western Colorado. The peak signal of RZSM-max temperature feedback for the San Luis Valley region occurs later in the year than for most other regions peaking in July through mid-August. This corresponds to when monsoonally-driven precipitation climatologically impacts soils in the area. The only region with a later peak in RZSM-maximum temperature feedbacks is the East Great Basin Region.

5.3% of the area in Julian Day-lag space is statistically significant at 99% confidence. In being the smallest region of the nine, it has to overcome the largest threshold in correlation in order to be considered statistically significant. Correlations between late April and early May RZSM and late July and early August maximum temperatures are higher than for most other regions. This can probably be attributed in combination to a smaller effective sample size and to May and June being a dry time of year here relative to other regions. During most of mid-May through mid-August there was an average of a 3.24 degree Fahrenheit decrease in maximum daily temperatures associated with every one standard deviation increase in RZSM.

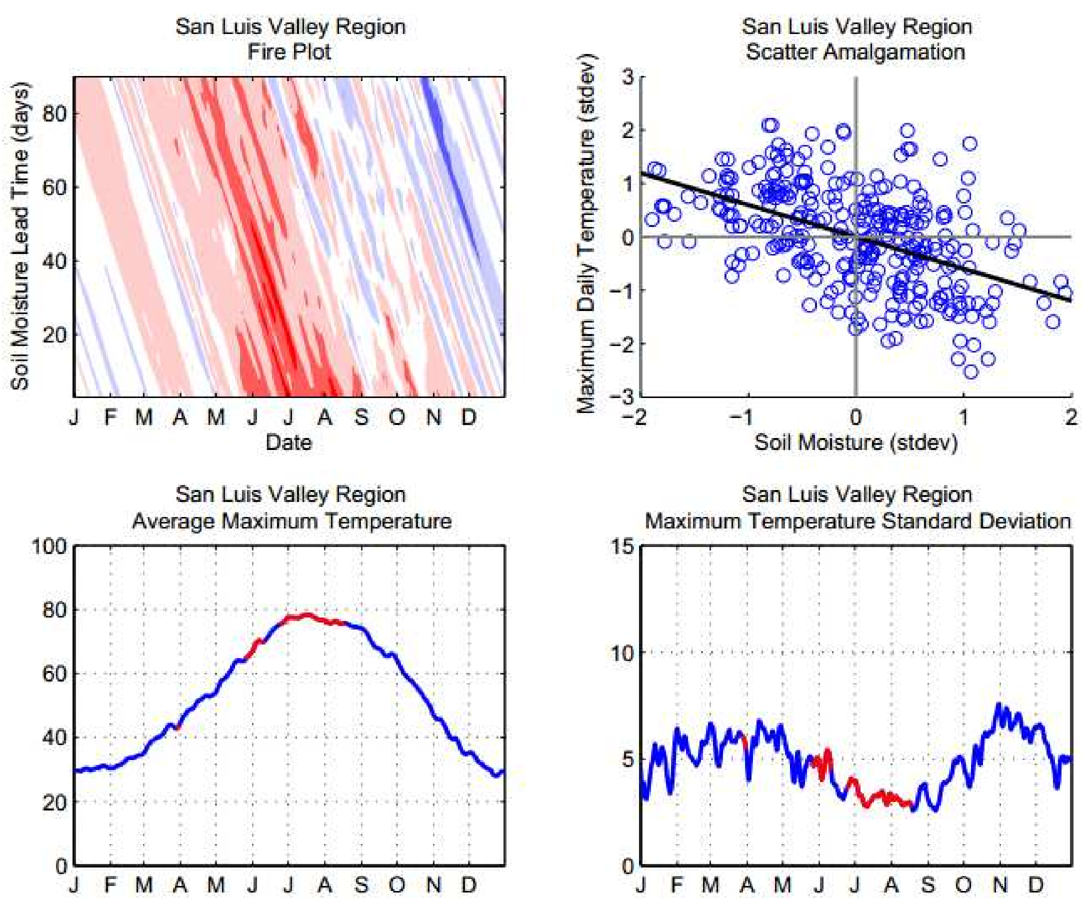

Figure 8.8: San Luis Valley Region Maximum Temperature Panel

Correlations between RZSM and maximum temperature were of consistently-positive sign for the Wasatch to San Juan Region from the beginning of the year through August. After the peak of the warm season non-physical, red-noise behavior appears to dominate. 5.4% of the area in Julian Day-lag space from the upper left plot above exceeded 99% confidence for significance. In these areas maximum temperatures were an average of 0.536 standard deviations lower for every one standard deviation increase in RZSM. In areas where 90% confidence was consistently exceeded maximum daily temperatures fell by 3.39 degrees Fahrenheit for every one standard deviation increase in soil moisture. Perhaps the most interesting feature about this region is how sporadically significance showed up. Most basins indicate one or two clear-cut areas where the feedback between RZSM and maximum temperatures was the strongest whereas in this region there are several little bumps in significance between April and August. This likely means that significance is achieved in areas where red noise combines with a small signal from true land and atmosphere interaction. The highest correlations observed occur in mid-June at small lead times. This is consistent with hypotheses and results from other basins.

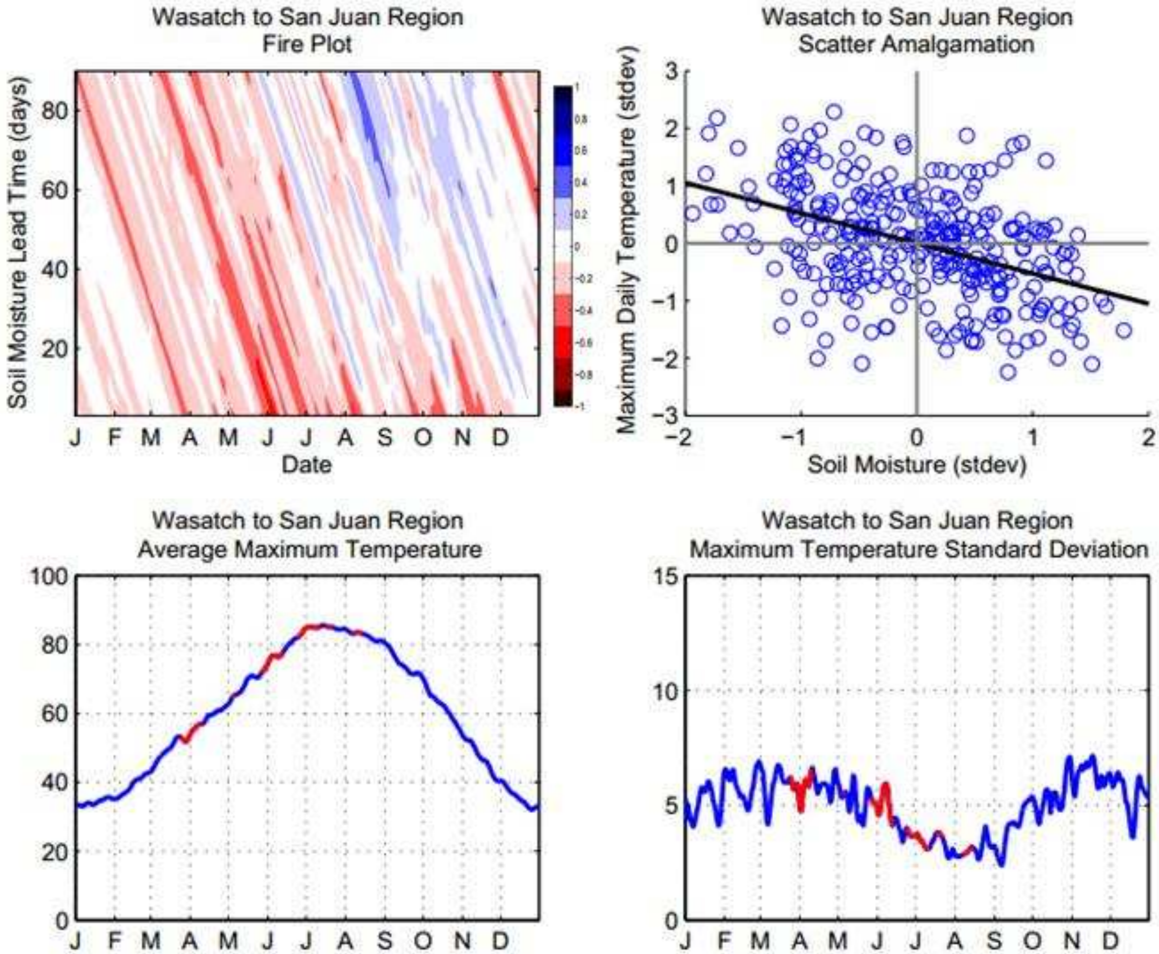

Figure 8.9: Wasatch to San Juan (Colorado Plateau) Region Maximum Temperature Panel

With only 4.1% of the area in Julian Day-lag space exceeding 99% confidence interaction between RZSM and temperature appears to be lower in the Upper Green River Region than most others. There is, however, a clear signal that manifests in June and July that increases in strength at short lead times. There is also a puzzlingly-consistent positive correlation between RZSM and maximum temperature present in mid-January through mid-February. This is thought to be an anomaly in the dataset and no explanation will be sought for it. The relationship between RZSM and maximum temperature is the strongest for this region right during the season with the highest maximum temperatures and on the low side in terms of seasonal temperature variance.

Temperature decreases of 3.16 were realized on average for every standard deviation increase in RZSM for this region over the past 30 years between late June and very early August.

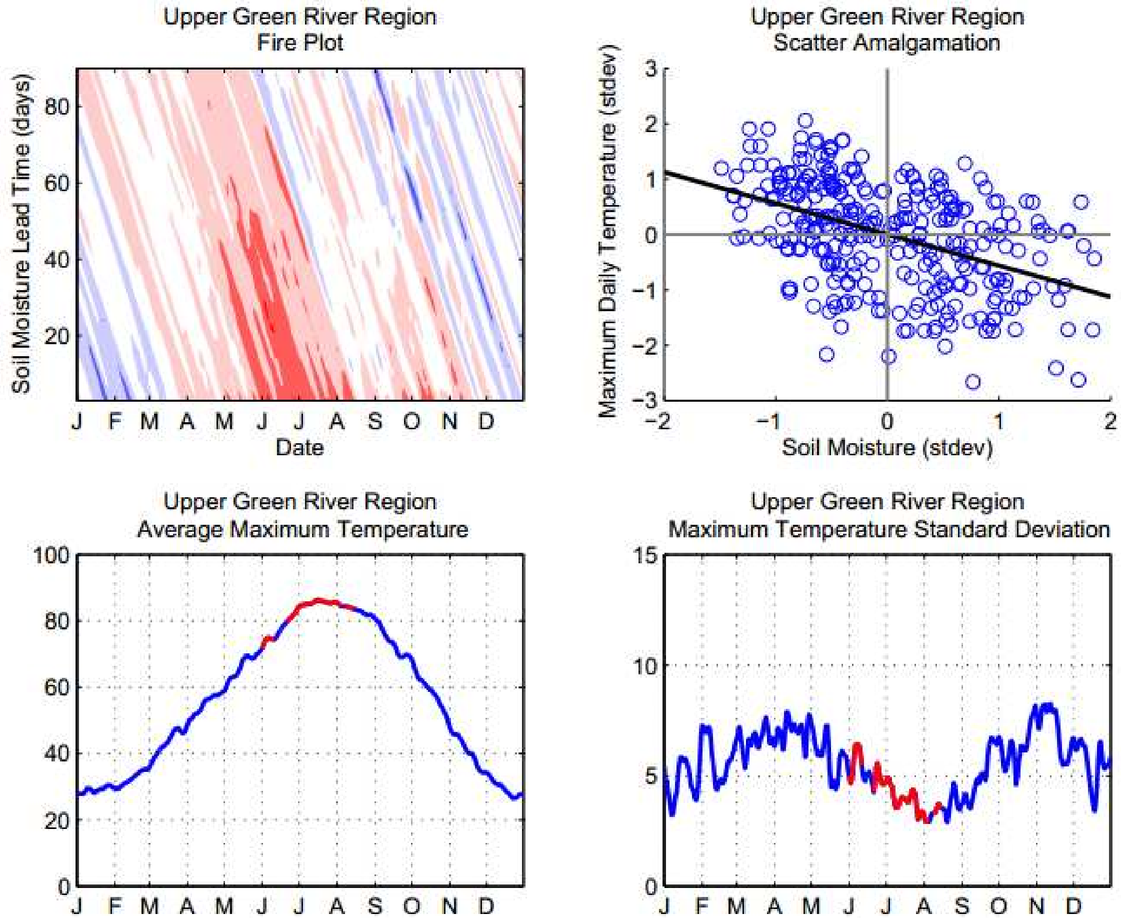

Figure 8.10: Upper Green River Region Maximum Temperature Panel

At 8.8% the East Great Basin Region carried a larger percentage of area significant at 99% confidence in Julian Day-lag space than any other region by far. It is important to note that of the correlations in this area model ensemble RZSM of below 1.5 standard deviations was practically non-existent. This illustrates that the area is typically dry and is characterized by a more skewed-right distribution of soil moisture than most areas. As such, the correlation is strongly driven by the wettest of years being cool in this region. An average of a 3.42 degree drop in maximum temperature is expected for every one standard deviation increase in RZSM. The correlation maximizes in magnitude at well over -0.50 in August at short lead times. This is well beyond the mark needed to achieve 99% confidence in a correlation significantly lower than zero.

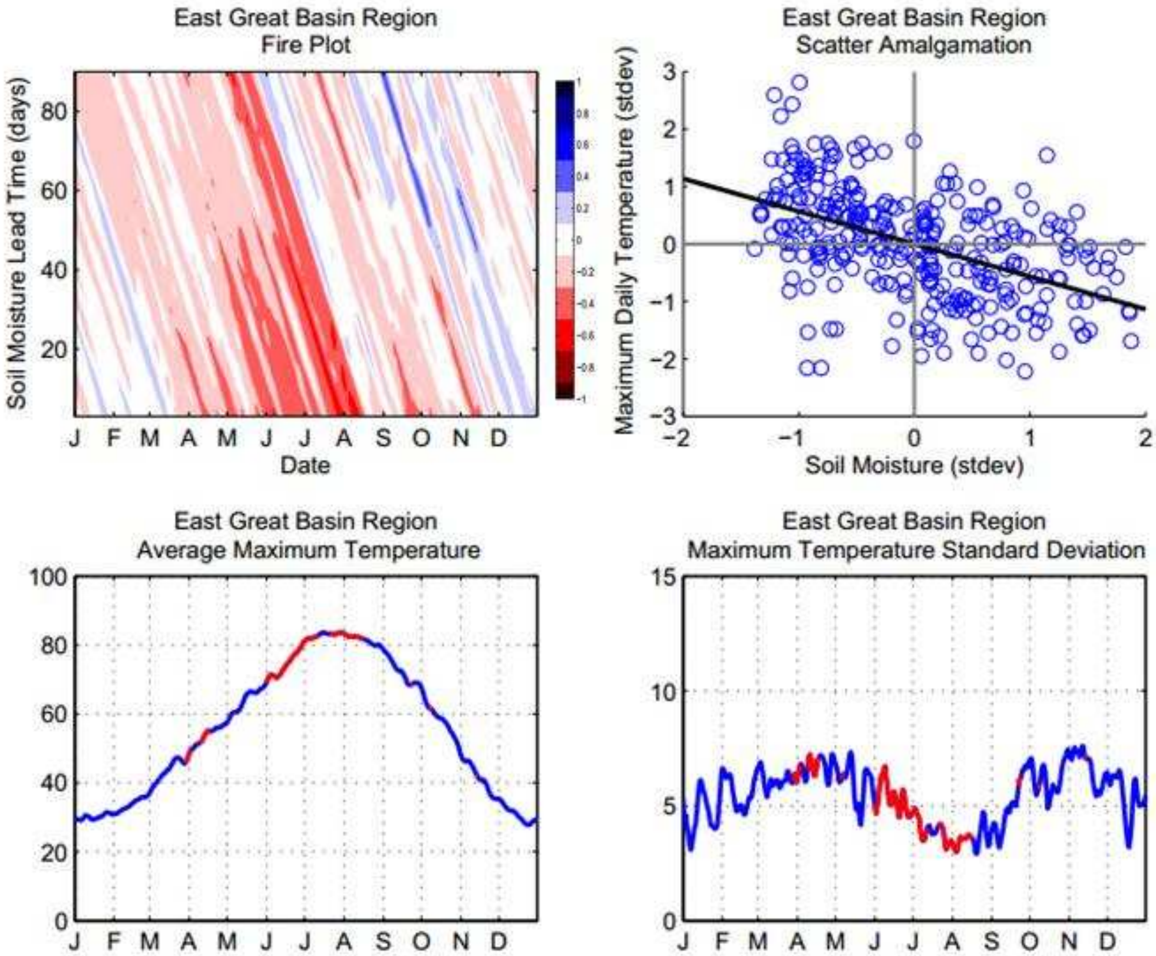

Figure 8.11: East Great Basin Region Maximum Temperature Panel

Earlier experiment results indicated that there was not much significant difference in the RZSM-maximum temperature feedback with elevation other than to suggest that the feedback manifests itself later in the year at higher elevations. In dividing the entire domain into the nine subbasins or sub regions outlined above there was agreement that the subbasins of higher elevation show a signal later in the year. However, there was also a preference in feedback strength towards regions of higher elevation. Signal strength trended positively from low to high elevations, from east to west, and from south to north. The first and third of these three trends correspond to areas that have more intense peaks in incoming solar radiation during the summer (Bonan 2008). The east to west gradient favors regions that are climatologically drier, which could simply illustrate that for times of year and areas where soils are expected to be dry, anomalous wet years have lots of control over the significance of the relationship.

Irrigation has a potentially large role that has not been explored by this study. NLDAS-2 models do include irrigation. Eastern Colorado is the area within the domain with the most farmland, and accounts for some of the weakest feedback strength readings. Particularly the northeast corner of Colorado showed a weaker signal than adjacent regions.

Root Zone Soil Moisture vs Seasonal Precipitation: As has been discussed previously, precipitation patterns are much more heterogeneous than atmospheric temperatures patterns. Furthermore, it is not only possible but likely that water evaporating from soils over one grid box would not fall as precipitation before being advected over another grid box using the full resolution of $1/8^{th}$ lat by $1/8^{th}$ lon, or even at a slightly coarsened resolution such as $3/8^{th}$ lat by $3/8^{th}$ lon. Difficulties that arise in measuring the relationship between RZSM and future precipitation by virtue of precipitation's nature can, however, be mitigated by considering wider regions and longer timescales. The same nine regions from the section above that were used to analyze the relationship between RZSM and future maximum temperatures were used again for measuring the relationship between RZSM and future SPIs.

A correlation analysis was completed finding the best-fitting linear relationship between the standardized model ensemble soil moisture anomaly and Standardized Precipitation Indices (SPIs), which were explained in chapter one. The RZSM anomaly was calculated with respect to Julian Day and subregion for the top meter of soil from the MOS, NOAH, and VIC model ensemble. In order to mitigate error from precipitation falling away from the area where the water was initially evaporated from the soil RZSM and precipitation were aerially-averaged across entire subregions before standardization was applied to the soil moisture field and SPIs were calculated for the precipitation field. This differs from previously-used methods in that cases involving RZSM and the temperature field. In those cases a separate correlation analysis was conducted for each $1/8^{th}$ lat x $1/8^{th}$ lon gird space before region-wide averages were calculated.

As mentioned in chapter one, SPIs are calculated by fitting precipitation totals from a climatological record for the same specific time of year to a Gamma distribution, finding the area to the left of the precipitation value's corresponding cumulative density function, and then transposing this value onto a normal distribution (McKee et al 1993). For example, if the area-averaged precipitation for a region is predicted by its corresponding Gamma distribution for May 1^{st} through May 30^{th} to only eclipse the measured value in 16% of years, that region's corresponding 30-day SPI for May 1-30 would be +1. The specific equation used for Gamma fitting the precipitation data used was based on functions built into MATLAB is reads as $f(x|a,b) = \frac{1}{G(a)b^a} x^{a-1} e^{\frac{-x}{b}}; x > 0$ (MATLAB 2013). This adaptation of the Gamma Distribution may be recognized as problematic since precipitation totals must be larger than zero. For this reason on days where there was no precipitation within a given subregion the average precipitation was adjusted to one gram per m^3, or one micron depth. This allowed for smooth gamma fitting without greatly altering precipitation climatology in the domain. This is especially effective when long windows (say 90 days rather than one day) are used to calculate SPIs. Because standardized RZSM numbers are being correlated with SPIs, which follow a Gamma Distribution, in this exercise there is a non-linearity implicit in each correlation, the extent of which cannot be known without analyzing that specific Gamma distribution.

The figures discussed in this section will follow the same four-panel format as the figures linking RZSM to maximum temperature. In the upper left, correlation between standardized model ensemble RZSM and region-wide SPIs in Julian Day-SPI length space is depicted. In this instance results are only recorded for March 1st-September 30th and SPIs of one to 90 days in length. This is in order to frame areas of statistical significance, since they are hypothesized to be found within the growing season at SPIs longer than several weeks. Figures in the upper right panel will show a blend of scatterplots representative of situations that met qualification for statistical significance at at least 95% confidence. The least squares line depicted represents the average least squares line for all combinations in Julian Day-SPI length space from March through September that were of at least 95% statistical significance.

Figures in the lower left panel in each show average precipitation, or the 0-SPI, for 30, 60, and 90-day timescales with reference to the start date of each period. The start date is being used instead of the end date since it is soil moisture immediately preceding the start that of each SPI that was used for correlation analysis. If the correlation between standardized RZSM anomalies and SPIs for the 30, 60, or 90-day timescales to follow were significantly greater than zero at 95% confidence they are highlighted in red. Once again with reference to the start date, panels in the lower right are quantile plots that depict the 5th, 20th, 50th, 80th, and 95th percentiles for the region's 60-day SPIs. This indicates roughly, but not exactly, how much precipitation is expected over the 60-day time period at -2, -1, 0, 1, and 2 standard deviations from normal.

Studies such as Koster et. al. 2004 have shown strong coupling between RZSM and precipitation across the central plains region as a whole, so, as hypothesized, the strongest correlation between these things was found in the corner of the domain within South Dakota and North Dakota. In this region not only does expected annual precipitation peak in the mid-May through early July time frame, but it is also strongly tied to RZSM as an initial condition. Correlation between standardized RZSM and 80-90-day SPIs peak for the time frame starting the last week of April and ending the last week of July at a region-wide level of over 0.70. After Fischer-Z transformation this correlation is easily significantly greater than zero at 99% confidence.

` 17.8% of the area within the growing season in Julian Day, SPI space above was statistically significant at 99% confidence, 35% at 95% confidence, and 46% and 90% confidence. Of the areas that met the 95% confidence level lines of best fit had slopes spanning from 0.300 to 0.733. There was an average anticipated increase in SPIs of 0.438 standard deviations for every one standard deviation rise in RZSM. Data in the upper right scatter amalgamation indicated that a higher order fit may have been more appropriate as SPIs seem to fall off the table for RZSM < -0.8, and there appears to be diminishing returns to scale for above normal RZSM. There is approximately a spread of 2.5" to 10.0" of precipitation from -2 to 2 SPIs over the mid-April to mid-June time period for the Central Plains Corner region. The spread from -1 to 1 SPIs is approximately 4-8".

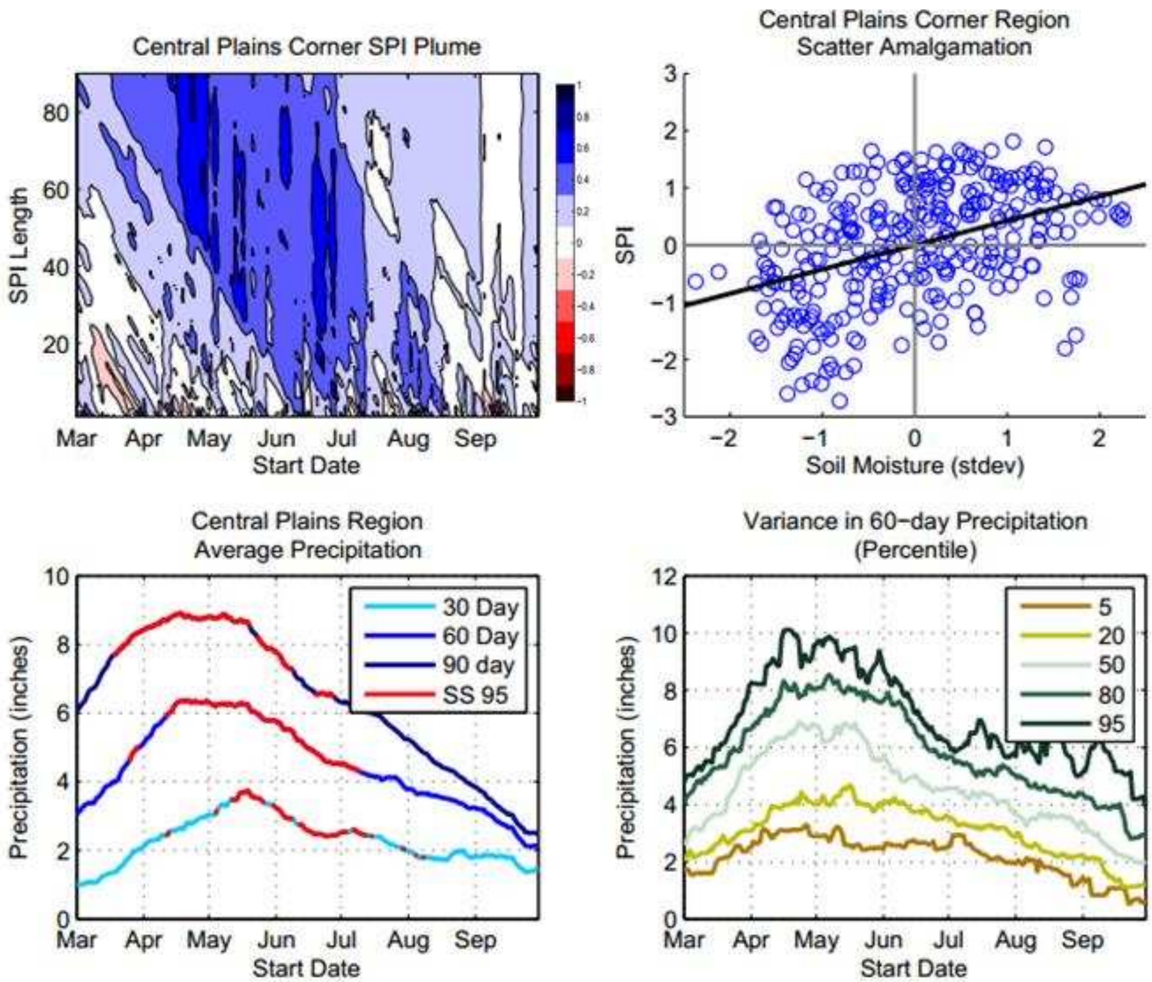

Figure 8.12: Central Plains Corner Region SPI Panel

Impacts of standardized model ensemble RZSM on future precipitation were the lowest in the South Platte Region (northeast Colorado) of any of the nine subregions. Only 2.20% of the area depicted in Julian Day-SPI length space was determined to be significantly higher than zero at 99% confidence. 8.16% of area met the 95% confidence criterion and 15.1% of area was significant at 90% confidence. Much like the relationship between RZSM and maximum temperatures in this area there is a robust peak in the relationship between RZSM and future precipitation in the June time frame. Soil moisture levels in mid-June appear to impact future precipitation levels from timescales from 10-80 or more days. This point corresponds to a temporary minimum in expected precipitation for the region and during peak solar radiation season.

In the time starting in very early June when relationship between RZSM and 60-day SPIs appears to peak based on the last 30 years of record there is a spread of approximately 3.9 to 6" of region-averaged precipitation from the -1 SPI to the +1 SPI. This expands to a spread of approximately 3-7" from the -2 SPI to the +2 SPI. This region averages 18.5" of precipitation annually. The mean slope of best fitting lines for correlations that are statistically significant at 95% confidence is 0.422, so the projected increase or decrease in 60-day SPIs based on early June soil moisture can tilt projected annual precipitation numbers by as much as 20% if soils are very dry (-2 standard deviations) as opposed to very wet (+2 standard deviations). 2012 was a good example of this situation as RZSM was 1.2 standard deviations below normal for the region at the beginning of June and the region averaged 1.53" of precipitation lower than normal over the following 60 days.

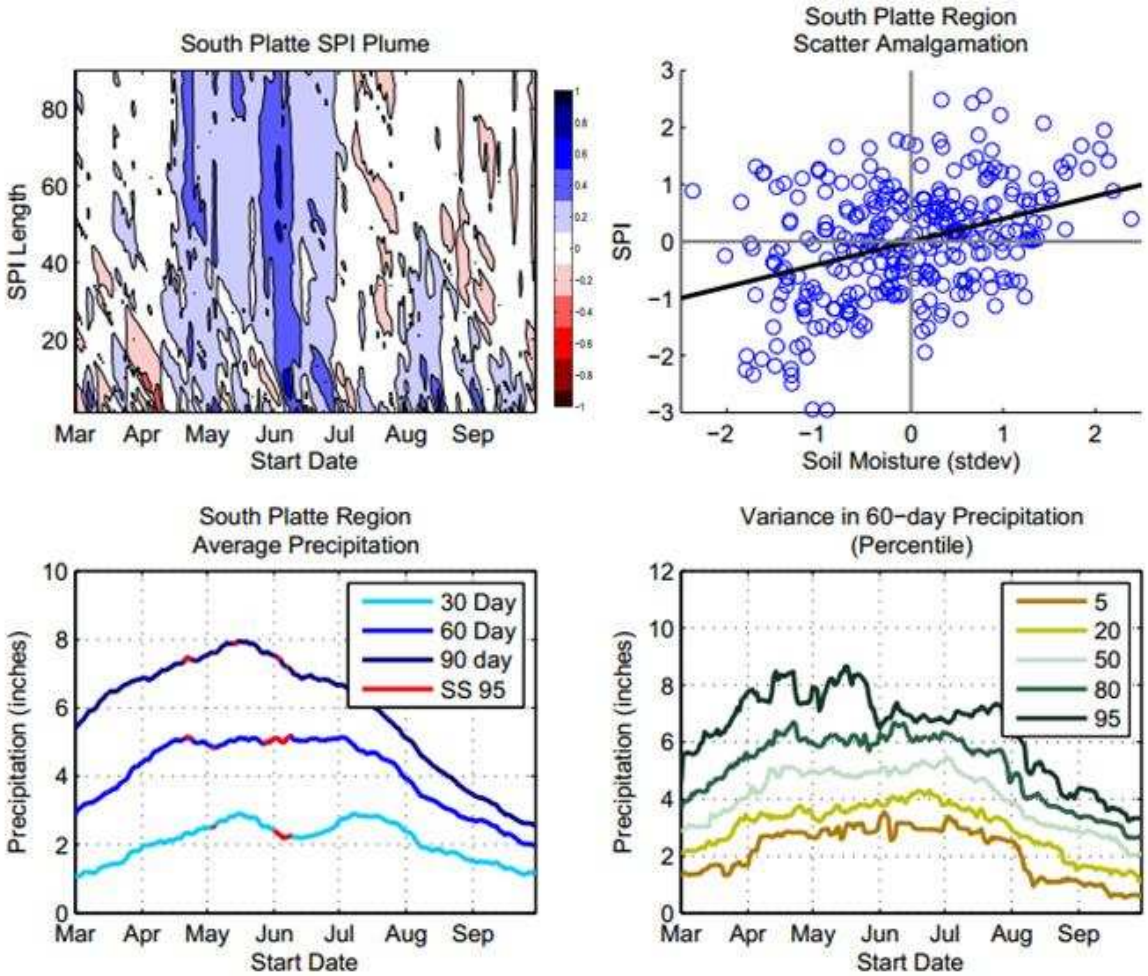

Figure 8.13: South Platte Region SPI Panel

Despite being directly adjacent to the South Platte Region, the Upper Arkansas Region (southeast Colorado) showed statistically significant relationships between RZSM and future precipitation much earlier in the season than its northern counterpart. 30, 60, and 90 SPIs were all significantly higher than zero starting at the beginning of March. For SPIs starting at the beginning of May the signal appears to mostly vanish. Details as to why are not known, but this is nonetheless an interesting result. This region is the beneficiary of monsoonally-advected moisture in the late summer (Douglas et al 1993), hence the seasonal maximum in 60-day precipitation from the end of June to the end of September. It is reasonable to hypothesize that the magnitude of these events is only very weakly-controlled by local RZSM levels. It is also reasonable to hypothesize that soils in this region on average are expected to dry to near-wilting levels by earlier in the season, so the Bowen Ratio heading into peak solar radiation season is typically high.

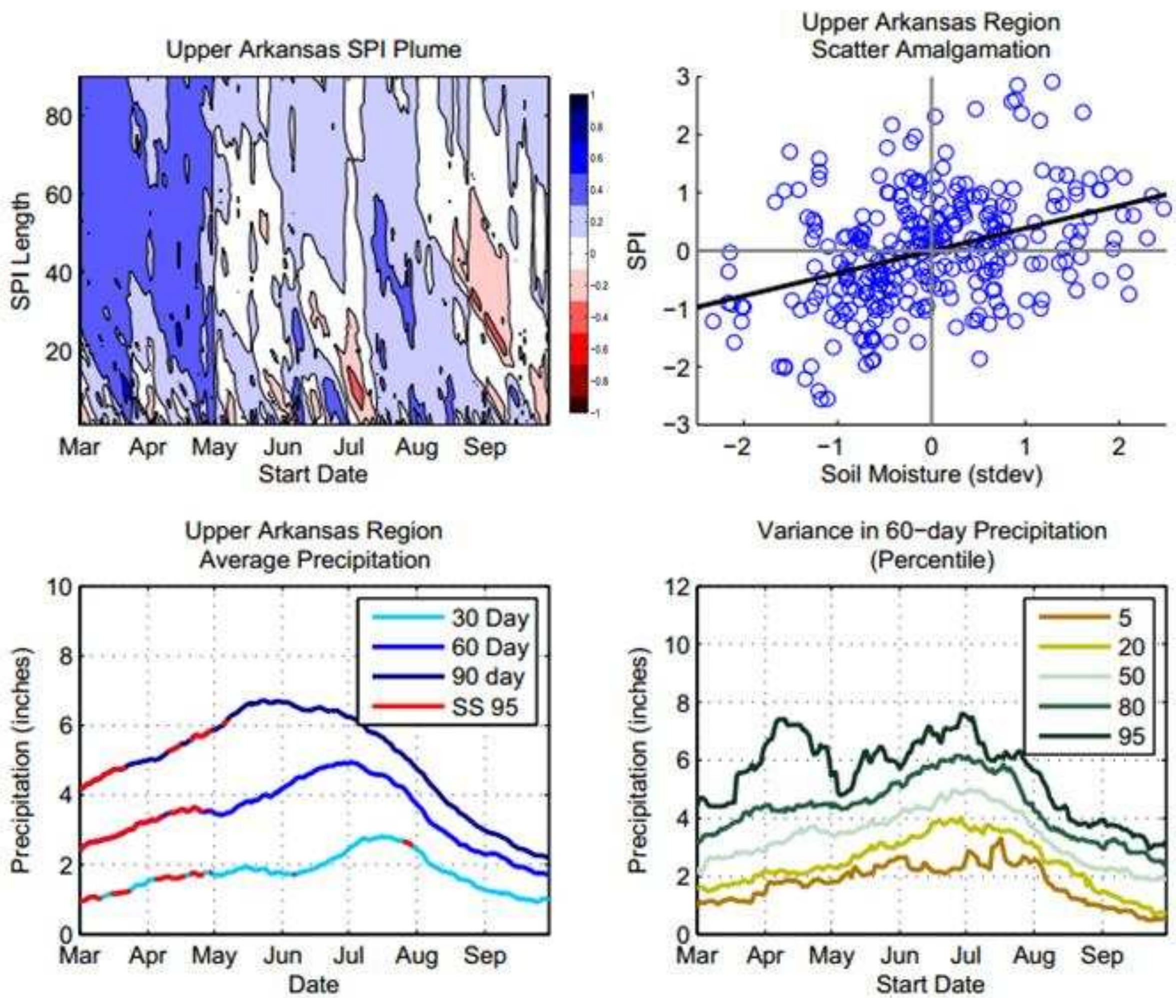

Figure 8.14: Upper Arkansas Region SPI Panel

The Upper High Plains Region in southeast Wyoming is climatologically quite dry with one very clear precipitation maximum expected in April into the early part of June. Through the summer 60-day average precipitation stays remarkably constant right around 3”. It is on the downward side of this anticipated precipitation peak in mid-May through late June that correlation between RZSM and future SPIs maximizes. The maximum appears to be most closely related to SPIs from about 20-70 days in length. Within the Julian Day-SPI length space depicted 6.6% of the area represents correlations that are significantly greater than zero at the 99% confidence level. This is true of 19.8% of area at the 95% confidence level and 28.0% of area at the 90% confidence level. For correlations statistically significant at 95% confidence average slope of the best fit line is 0.412. This slope varies from 0.33 and 0.52 at the 10^{th} to 90^{th} percentile and has units of SPI units/standard deviation. A one standard decrease from normal model ensemble RZSM on May 15^{th} would lead to a projected decrease in mid-May through mid-July precipitation of 0.74”. This is only 4.5% of the region’s average annual precipitation.

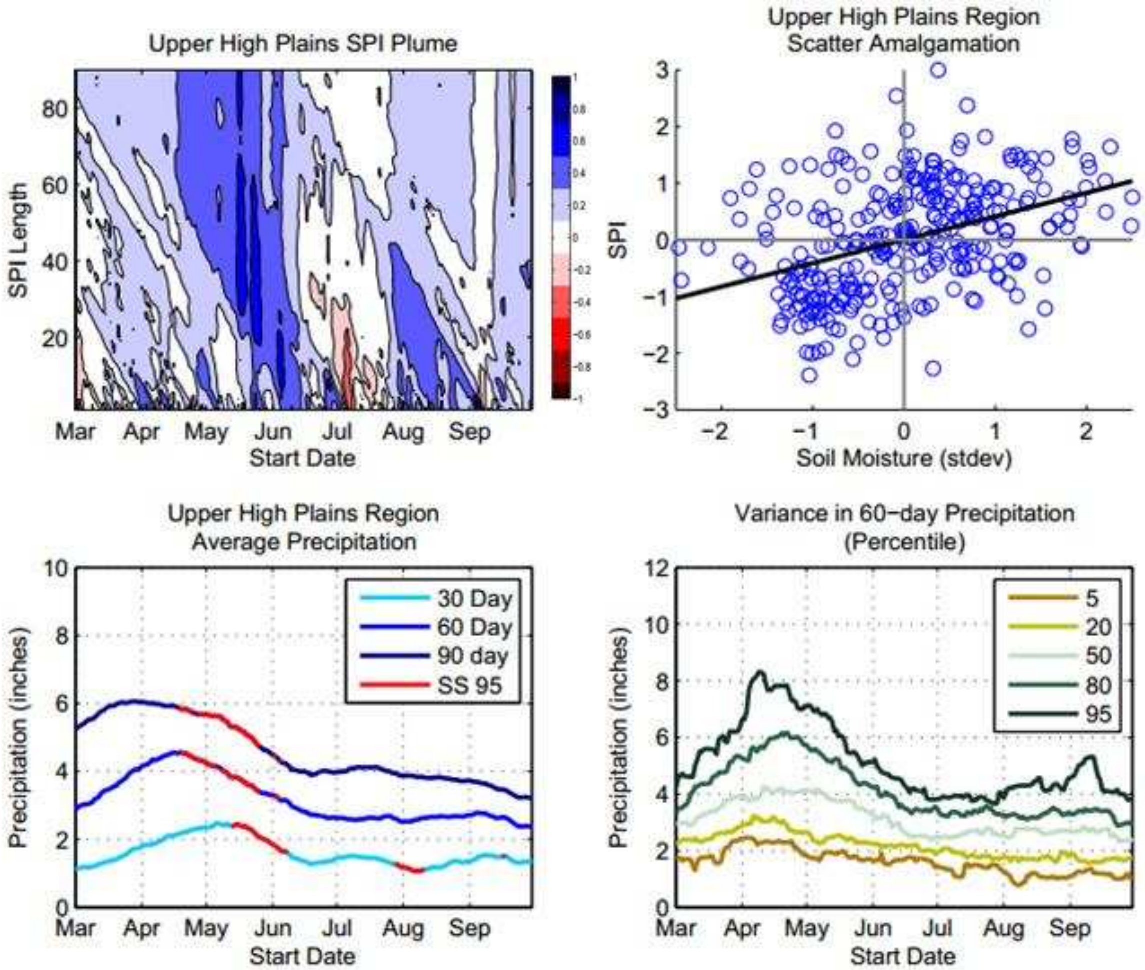

Figure 8.15: Upper High Plains Region SPI Panel

The Colorado Headwaters Region has stood apart as quite distinct in terms of its strong correlations between standardized model ensemble RZSM and both future maximum temperatures and precipitation levels. It is the highest average elevation region within the domain and the wettest. The rather than the late spring and early summer the bulk of the annually-expected 19.38” precipitation in this region comes in the winter. The driest time of year here is May through the middle of July; however during this time the amount of precipitation that falls is significantly influenced by soil moisture levels in the root zone. 14.5% of the area depicted in Julian Day-SPI length space was found to be significantly greater than zero at 99% confidence.

29.6% of the area is significant at 95% confidence. This area is concentrated in the May through June time frame at SPI lengths of 20 to 70 days. The best-fitting trend line for these situations has an average slope of 0.43, and varies from 0.33 to 0.55 at the 10th to 90th percentile. Because this correlation is strongest during the driest time of year a difference in region RZSM from -1 to +1 standard deviation would only lead to a projected increase in precipitation of 4% of the annual mean.

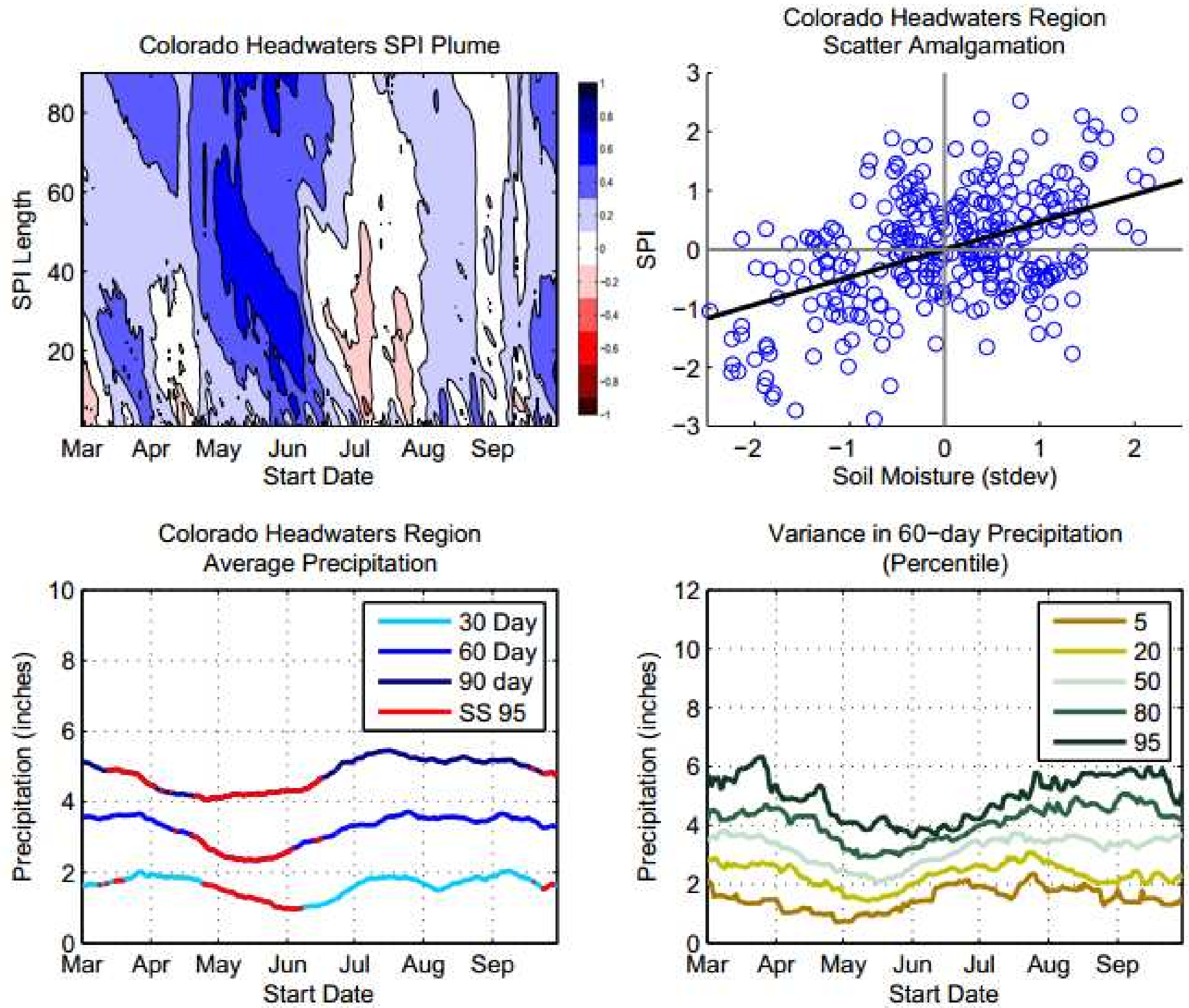

Figure 8.16: Colorado Headwaters Region SPI Panel

Correlations between standardized model ensemble RZSM and SPIs in the San Luis Valley Region are consistently positive for start dates from March through May, but correlation magnitudes are fairly unremarkable relative to adjacent regions. There is a surprising amount of negative correlation between the two variables for start dates from mid-June through mid-July. This region's wet season falls from mid-July through September indicating it is strongly linked to the North American Monsoon (Douglas et al 1993). During this time there is almost no significantly positive correlation between RZSM and SPIs, and what little does exist is quite likely to be spurious. 10.6% of the area depicted in the upper-left panel represents correlations that are significantly greater than zero at 99% confidence. This area is concentrated in the upper-left portion of the figure. 20% of the area is significant at 95% confidence and 40% at 90% confidence.

While this area does include some of the driest land of the entire domain, and the driest area in Colorado (PRISM 2015) it does include quite a bit of high elevation area. As such, the mean annual precipitation from 1985-2014 is 19.18", which ranks it as the third wettest subregion. This region also has the lowest projected increase in SPIs per increase in RZSM for statistically significant regimes averaging 0.381. Soil moisture one standard deviation below normal in the first week of April only predicts a 2% decrease in annual precipitation.

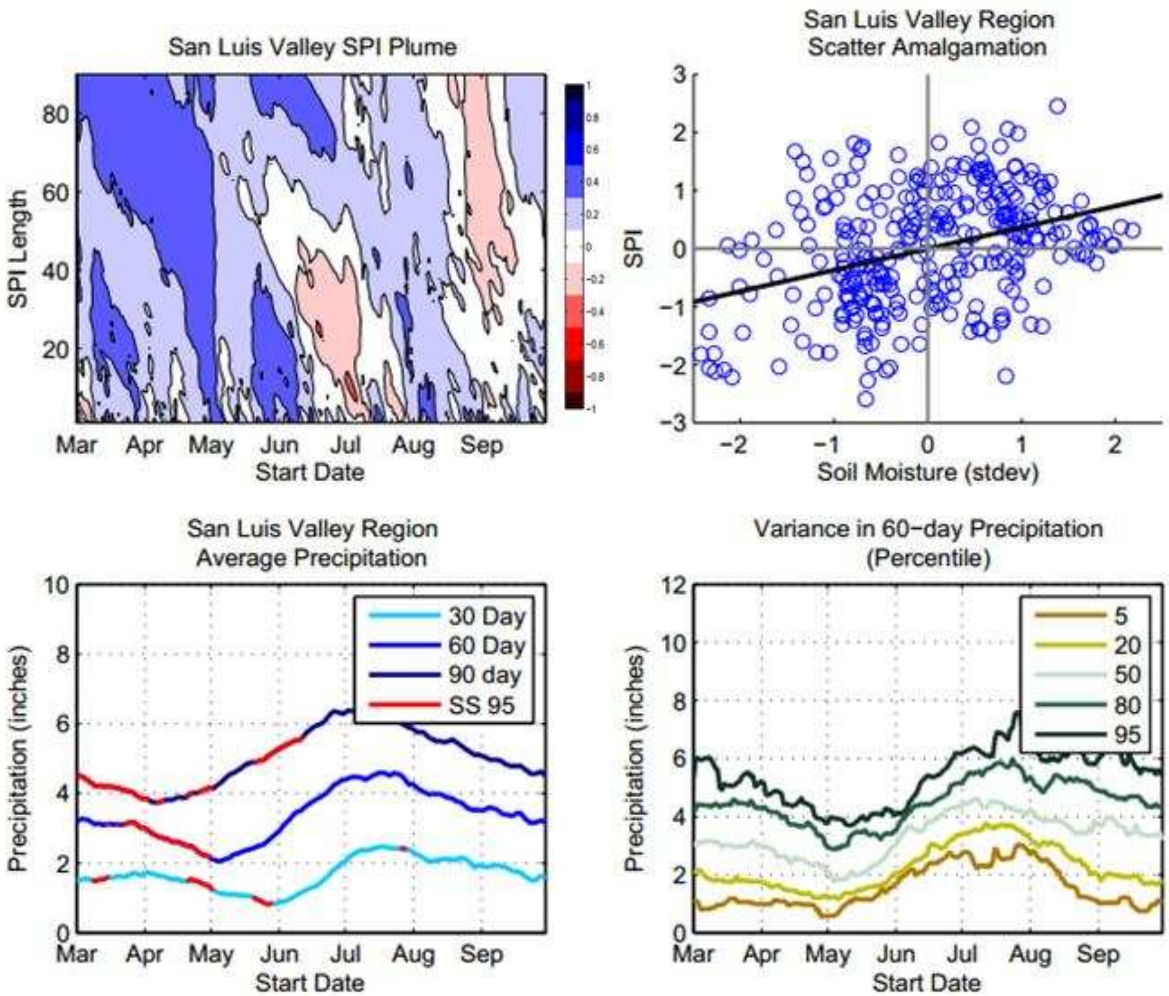

Figure 8.17: San Luis Valley Region SPI Panel

The Upper Green River Region, which includes the Upper Green River, Yampa River, White River, and Duchesne River Basins, shows a very persistent statistically significant relationship between model ensemble RZSM and future SPIs through the early growing season. The most important time of year for these correlations in the Upper Green River Region appears to be late April through early June where significance overlaps SPIs from 30 to 90 days. This region is the second driest of the nine averaging only 14.16” of precipitation annually, but it includes some very wet areas at higher elevations such as the Buffalo Pass and Rabbit Ears Pass area. There are peaks in anticipated precipitation in both late spring and late summer, but not very pronounced peaks.

The average increase in SPIs per standard deviation increase in RZSM is 0.413 with a spread of 0.33 to 0.50 from the 10^{th} to 90^{th} percentile for correlations that are significantly greater than zero at 95% confidence. 38.3% of the area in the upper-left panel represents statistical significance at the 95% confidence level. Again, in the Upper Green River Region RZSM appears to be at its most valuable as a forecast tool for the drier period between climatological spike in precipitation and during peak solar radiation season in June and early July. Top meter RZSM levels one standard deviation below the mean in late May appears to be indicative of a 2.5% loss in annual precipitation over the following 60 days.

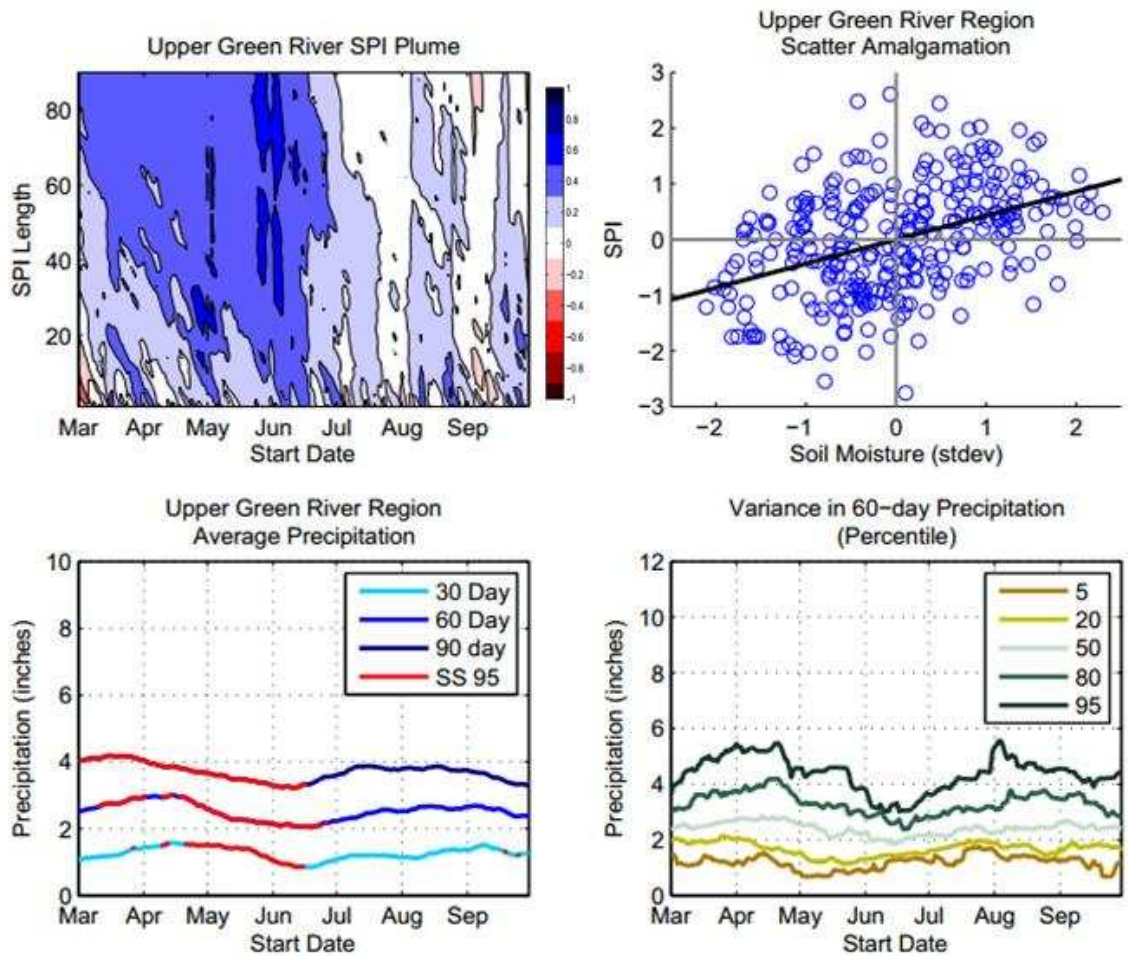

Figure 8.18: Upper Green River Region SPI Panel

The Wasatch to San Juan Region in southeast Utah and southwest Colorado is the driest region of the overall domain with only 12.9" of precipitation anticipated on average annually. Like other regions in the southern portion of the domain such as the Upper Arkansas Region and San Luis Valley Region the seasonal cycle in precipitation peaks in the late summer from mid-July through early September. The driest part of the growing season occurs in early June though early July.

Soil moisture's ability to predict future precipitation is at its highest in early May when there is a correlation between top meter RZSM and SPIs for the days 20 to 80 days to follow of over +0.5. On average, in situations where the correlation between RZSM and future SPIs is significantly higher than zero at 95% confidence or greater SPIs rise by 0.45 for every standard deviation in RZSM. The range for this best fit line is from 0.33 to 0.56 from the 10^{th} to 90^{th} percentile respectively. A difference in RZSM from -1 to +1 standard deviations at the beginning of May would produce an average precipitation deficit for the region of approximately 0.65". That does correspond to 5% of the area's expected annual precipitation.

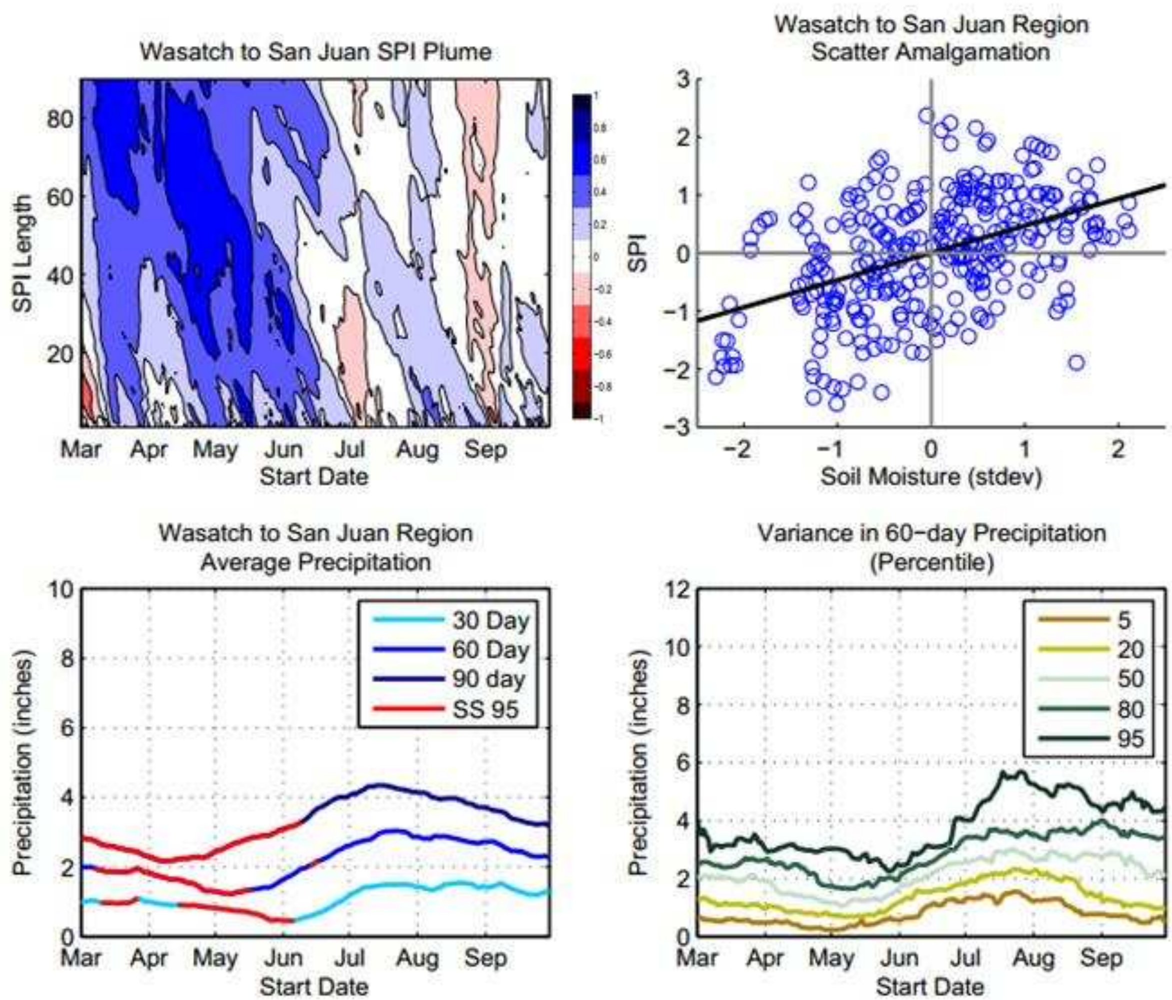

Figure 8.19: Wasatch to San Juan Region SPI Panel

Root Zone Soil Moisture appears to be a very important part of deciphering future precipitation patterns for the East Great Basin Region, which includes central Utah from south to north, part of southeast Idaho, and a little bit of western Wyoming. Similarly to the Central Plains Corner Region this region sees correlation between RZSM and SPIs spike going into the wet season, which is April through mid-June. In late June and July the area dries out considerably. Over 50% of the area depicted in Julian Day-SPI Length space represents correlations significantly greater than zero at 90% confidence. Nearly 20% of the area is significantly greater than zero at 99% confidence. In some situations the influence of RZSM on future precipitation appears to be quite large. Soil moisture that is two standard deviations above normal in the middle of April would yield a projected increase in precipitation of approximately 1.5” on average across the region over the following 60 days. This would correspond to 8.5% of the annual average for the region. Having very dry soils in the region in the middle of April does not have the same magnitude of an impact, but this is in large part due to the way the study was conducted since linear increases in precipitation are non-linear in SPI space.

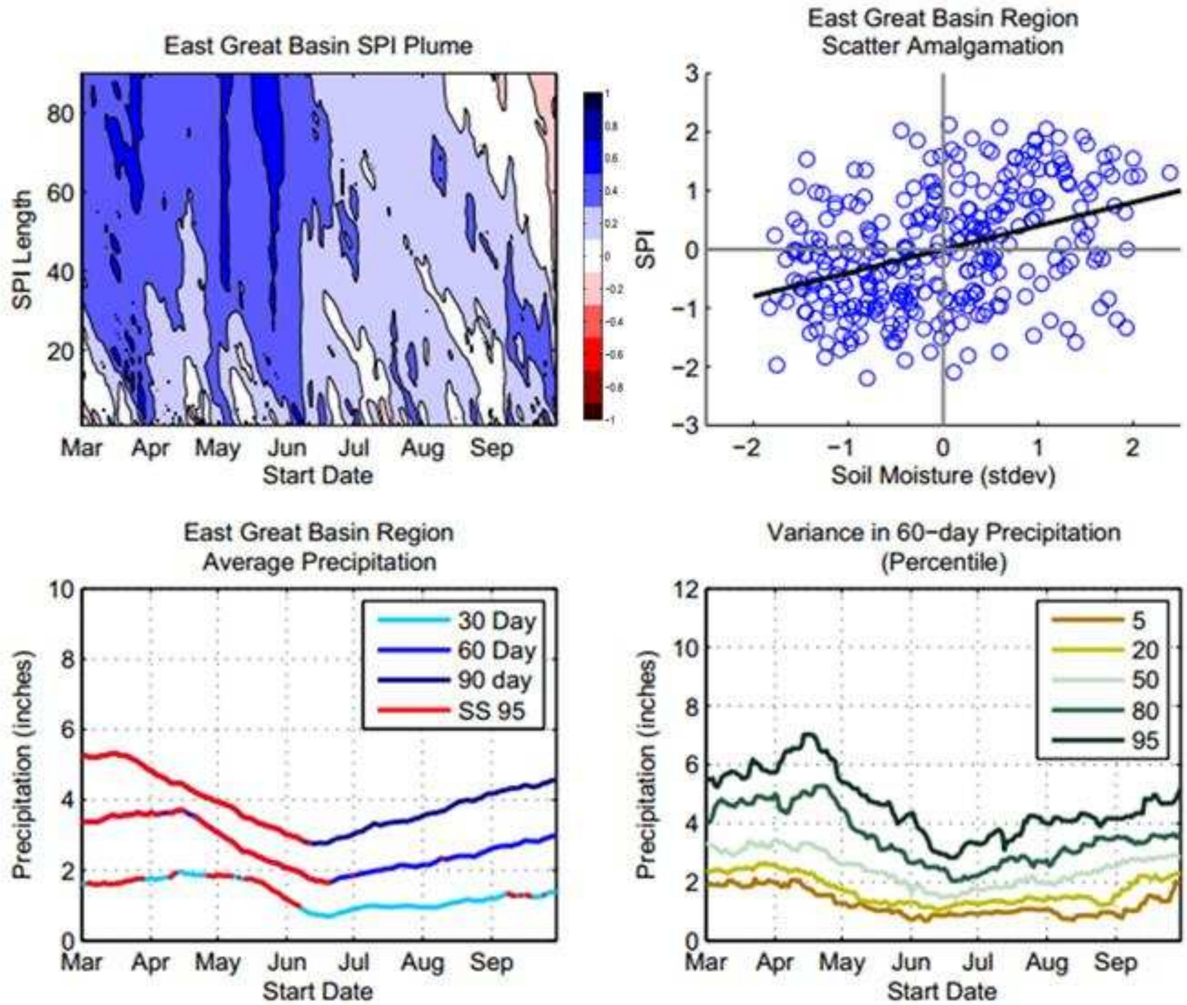

Figure 8.20: East Great Basin Region SPI Panel

Growing season precipitation in all subregions of the domain from the wettest to the driest is influenced by soil moisture levels. Top meter soil moisture in the month of May appears to be especially influential on growing season precipitation for the Upper Colorado River Basin and Western High Plains. Strength of the feedback between RZSM and precipitation exhibited a large amount of latitudinal variation with regions farther south seeing increase in feedback strength earlier in the growing season than areas farther north. The regions with the most consistently-significant feedback in the growing season were the Central Plains Corner Region and the Upper Green River Region. Regions with the least persistence in statistically significant relationship between top meter soil moisture and future SPIs were the South Platte Region, the Upper High Plains Region, and the San Luis Valley Region.

The consistency of the relationship between RZSM and future precipitation levels through the growing season is indicative of the fact that the Upper Colorado River Basin and Western High Plains are reliant on externally-advected moisture in order to maintain equilibrium. This is not a surprising finding for a landlocked domain. While there was a high level of confidence detected in RZSM's ability to modulate future precipitation the increases or decreases associated with RZSM fell within dry times of year for much of the domain. Projected decreases from low top meter soil moisture in late spring can easily be offset though one favorable synoptic-scale event, particularly for areas in the south and west portion of the domain. The main exception to this rule is the Central Plains Corner Region where confidence in the positive relationship between soil moisture and precipitation peaks at the same time that climatological precipitation averages themselves peak.

Perhaps the largest remaining difficulty in capturing the strength of the relationship between RZSM and future precipitation levels is that the relationship is a function of area size. At small sizes the relationship appears to increase as the size of the area analyzed grows as the impact of moisture flux convergence in an out of a given analysis space goes down. At a certain size, which is unknown, and is probably not a constant in space or time, the relationship will appear to decrease with increasing area as climate resolution is lost.

HINDCASTING SEASONAL PRECIPITATION FROM ROOT ZONE SOIL MOISTURE VALUES LEADING INTO RECENT EXTREME DROUGHTS IN COLORADO AND THE UPPER COLORADO RIVER BASIN

One of the largest questions prompting this research was “how much warning can RZSM offer in cases of severe drought onset?” We call on the data of NASA’s Land Data Assimilation Phase-2 data one last time in this chapter to analyze the effectiveness of root zone soil moisture data in the early warning of extreme droughts over recent years in the Upper Colorado River Basin and western High Plains. It has been established from previous chapters that root zone soil moisture in the top meter is of closest relationship to future precipitation leading into the growing season, that there are inter-domain differences in the strength of this relationship, and that for some areas the relationship peaks when conditions are drier than other times of year for the southwest end of the domain while the opposite is true for the northeast sector.

In this section RZSM data and the relationships derived in the chapter eight between RZSM and precipitation will be used to hindcast growing season precipitation. Three specific years will be reviewed in a case-study format. These are theoretical 90-day precipitation hindcasts beginning on May 1st through July 29th of 2002, 2006, and 2012 based on the strength of RZSM-SPI relationships discovered above. These years were chosen because they represent an exacerbated severe drought, a spatially-shifting severe drought, and a flash onset of severe drought respectively. Following these case studies potential for seasonal forecast improvement for all years with soil moisture anomalies less than 0.5 sigma will be reviewed.

Methods: Hindcasts will be made for each region using the whole dataset, and another where data from the year being hindcasted is removed. The reason for generating a hindcast both ways is that each of these two methods contains a notable difference from a seasonal precipitation forecast that would be made for a potential drought onset in a future warm season. Using the whole dataset provides an unfair advantage since the verification is one 30th of the data being used to make the hindcast. Removing the year being hindcasted potentially disadvantages the hindcast with respect to a forecast that would be made for an upcoming drought because the frequency of drought is potentially under-sampled, so future skill of forecasts made using this method would be predispositioned to somewhere in the middle.

For each case study standardized soil moisture anomalies will be reviewed by subbasin leading up to May 1st for each year. Hindcasts will then be based solely on May 1st soil moisture levels at midnight. For hindcasts that do not include precipitation data from the year being hindcasted RZSM on May 1st at midnight will be standardized based upon values from the other 29 years for each subbasin.

Data ingested in each forecast will include data for May 1st as well as points in Julian-Day-SPI space in the ten days before and after May 1st and for SPIs of 80-100 days in length for which the correlation between RZSM and future SPIs differs by no more than 0.03 from the correlation between midnight May 1st soil moisture levels and the subsequent 90-day SPI. The data from all qualifying points in Julian Day-SPI space were added to the same scatterplot. A mean regression line of all qualifying regression slopes was calculated for each year and subbasin Using the mean regression line, all qualifying SPIs were regressed from their actual value to their expected value were the soil moisture at the start of the period an anomaly of the same magnitude as the year being hindcasted. A hindcast range was generated for each subbasin and each of the dry years using the mean regressed SPI as the expected value, and a 10th-90th percentile range based upon the value of the 10th and 90th percentile regressed SPI.

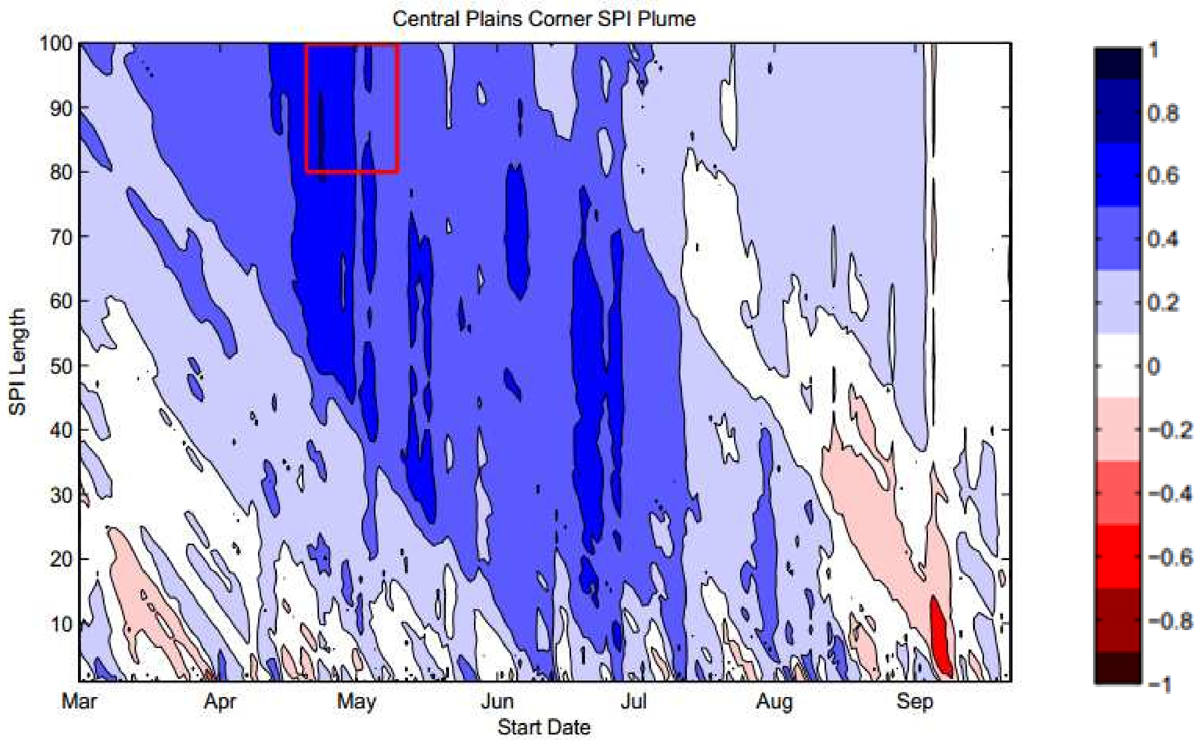

Figure 9.1: As in chapter 8, the correlation between top meter RZSM and future SPIs is shown here as a function of Julian Day and SPI length for the region in the far northeast corner of the domain. The red box here indicates the pool of potential samples drawn on from each year in making a precipitation hindcast based on May 1st SPIs. All points within the box are not necessarily used. Only points were the correlation between RZSM and future SPIs is within 0.03 of its value for 90-day SPIs starting on May 1st were used.

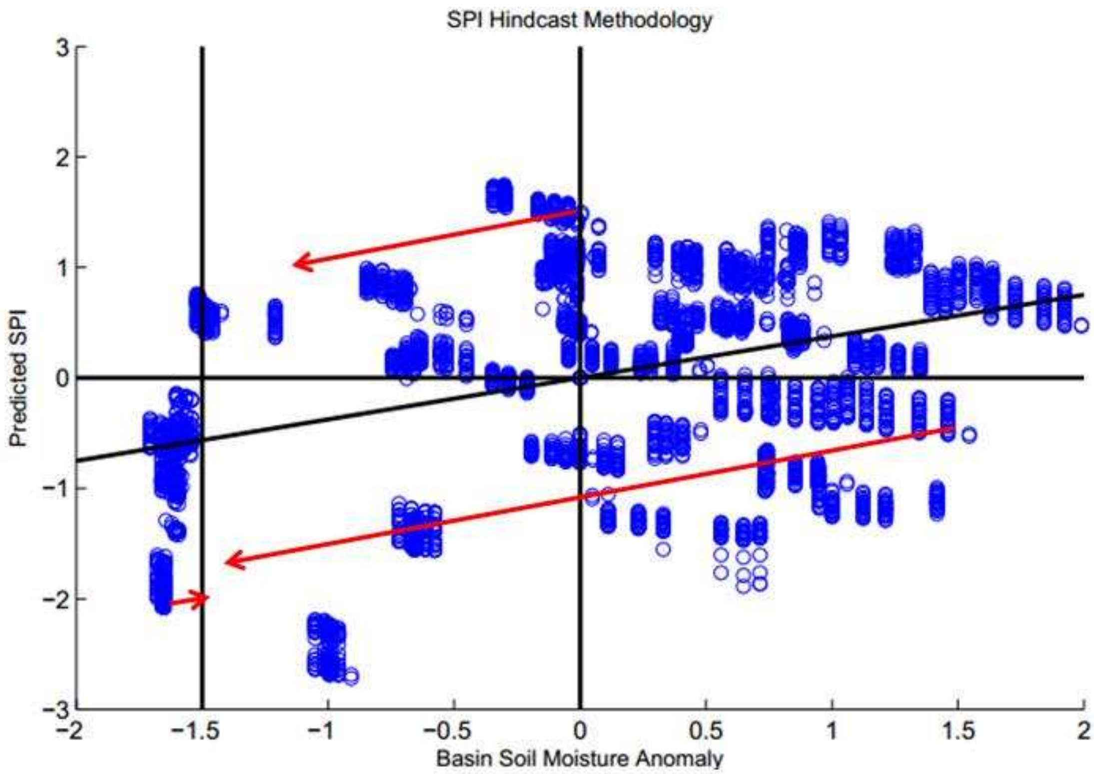

Figure 9.2:A pool of RZSM, SPI combinations used to make a hindcast for the Central Plains Corner Region are shown here. This image depicts an example of how the hindcast would be made if the top meter standardized soil moisture anomaly for the region was -1.5 at midnight on May 1st. The slanted black line is the regression line used, and the red arrows show how SPI values would be changed to fit the low soil moisture situation in order to determine a hindcast value as well as 10 and 90% confidence intervals.

For the case studies to follow seasonal hindcasts for May 1st were chosen in particular because there is high confidence in the relationship between RZSM and seasonal precipitation for all nine sub regions when using the full 30-day dataset. The only sub regions that do not exude a relationship between RZSM and future 90-day SPIs on May 1st that is significantly positive at 95% confidence of the nine are the South Platte and Upper Arkansas Regions. These regions still show a significantly positive relationship at 90% confidence. These upper and lower bounds should not be interpreted as error bars. As discussed in chapter eight there is high confidence in the relationship between RZSM and future SPIs, but there is lots of scatter regardless, so error bounds would be quite large.

90-day precipitation totals were hindcast for each region first by multiplying the region's top meter soil moisture anomaly by its respective regression coefficient to come up with a 90-day SPI value. The inverse cumulative density function of the Gamma distribution used to calculate that SPI value was then used to generate a precipitation hindcast in inches. These numbers were then compared to 90-day average precipitation over the last 30 years for each region.

	CPC	SPB	UAB	UHP	CH	SLV	UGR	CP	EGB
30-Day April 1st	0.071023	-0.01847	0.183376	0.127815	0.085385	0.104971	0.156595	0.179173	0.263043
30-Day May 1st	0.193102	0.152375	0.246278	0.194877	0.376779	0.3983	0.514249	0.455541	0.406641
30-Day June 1st	0.39919	0.317192	0.133558	0.44736	0.560234	0.252493	0.453457	0.548805	0.368498
60-Day April 1st	0.277866	0.051516	0.321077	0.141146	0.252106	0.347096	0.347167	0.431671	0.388221
60-Day May 1st	0.452807	0.220293	0.221431	0.403955	0.538379	0.330008	0.50572	0.581508	0.472298
60-Day June 1st	0.372316	0.436616	0.10417	0.301079	0.370232	0.039773	0.462957	0.211127	0.415517
90-Day April 1st	0.363273	0.04316	0.210392	0.226746	0.348125	0.31455	0.341829	0.478617	0.446625
90-Day May 1st	**0.457478**	**0.242238**	**0.286685**	**0.384438**	**0.4866**	**0.369601**	**0.473389**	**0.47539**	**0.491744**
90-Day June 1st	0.39737	0.302209	0.149335	0.304338	0.530114	0.378523	0.4942	0.363364	0.425694

Figure 9.3: This table illustrates the linear correlation by subbasin between top meter standardized soil moisture and future SPIs. 30, 60, and 90-day SPIs are shown for start dates of April, May, and June 1st. A couple points of reference: thresholds for 90, 95, and 99% confidence in a positive correlation are 0.2417, 0.3072, and 0.4205 respectively. The column abbreviations are as follows: CPC (Central Plains Corner), SPB (South Platte Basin), UAB (Upper Arkansas Basin), UHP (Upper High Plains), CH (Colorado Headwaters), SLV (San Luis Valley), UGR (Upper Green River Basin), CP (Wasatch-to-San Juan), EGB (East Great Basin).

Following the examination of the major case studies of 2002, 2006, and 2012 and more comprehensive overview of hindcasts for dry years was conducted. A hindcast was generated for all combinations of years and subbasins in which a soil moisture anomaly of < -0.5 was present for hindcasts starting on all days from March 1st-June 1st. The average value of a RZSM-based hindcast was calculated for each of the nine regions within the domain. In this overview all 30 years of data were used for each hindcast due to the computational time required to produce a hindcast for one or more basins in almost every year through the period of record. This does give the soil moisture hindcasts a bit of an unfair edge as discussed above, but results below for the three drought case studies lend some confidence to the hypothesis that hindcasts using both methods are typically very similar. Results will be recalculated not using the year being hindcasted before being considered for publication.

2002 Results: Drought impacts were no secret going into the warm and dry summer of 2002 for the Upper Colorado River Basin and western High Plains with impacts being worse yet by the time the summer had finished. Root zone soil moisture levels in the spring of 2002 were generally lowest in the regions farther south such as the San Luis Valley and Colorado Plateau. The Colorado Headwaters region also had especially bad soil moisture at over two standard deviations below normal at the beginning of May 2002.

The incredibly low soil moisture at the start of May in 2002 made for some exceptionally aggressive forecasts for low summer precipitation given the methods used. Precipitation was still lower than even the 10th percentile 90-day hindcast for six of the nine regions even with 2002 included in the data made to use the hindcast. 90-day precipitation from May 1st to July 29th of 2002 verified at less than 50% of average in four of the nine regions, less than 60% in eight of the nine, and less than 70% in all nine making for a truly anomalous large-scale precipitation deficit. Despite still being high, the antecedent soil moisture hindcasts were able to close at least some of the gap between a climate forecast and the verification in every case. In the South Platte Basin and Upper Arkansas Basin hindcasts were still for over 90% of average precipitation. Using the hindcasting method where data from the year being hindcasted are not included still allowed for precipitation hindcasts lower than 90% of normal in six of the nine basins, and lower than 80% of normal in three of the nine basins.

In the Colorado Headwaters Region, where top meter soil moisture was over two standard deviations below normal at the beginning of May, the 10th-90th percentile range for 90-day precipitation was just 50.5-102.1 % of normal. With the region only receiving an area-averaged 1.89" over the following 90 days the actual value was still lower than the 10th percentile hindcast. The RZSM anomaly used to generate hindcasts for the Central Plains Corner Region was not quite as extreme at a value closer to -1.5. Even so, because of the high confidence in the relationship between RZSM anomalies and future precipitation in this region it the 10th-90th percentile range for hindcasts made was for 49.0-102.1 percent of normal not using data from 2002. Even so, precipitation verified lower than the 10th percentile hindcast. It certainly appears from these data that while RZSM does not account for all of the variation in seasonal precipitation it can be used to improve precipitation forecasts for years where soils are dry in the late spring and early summer.

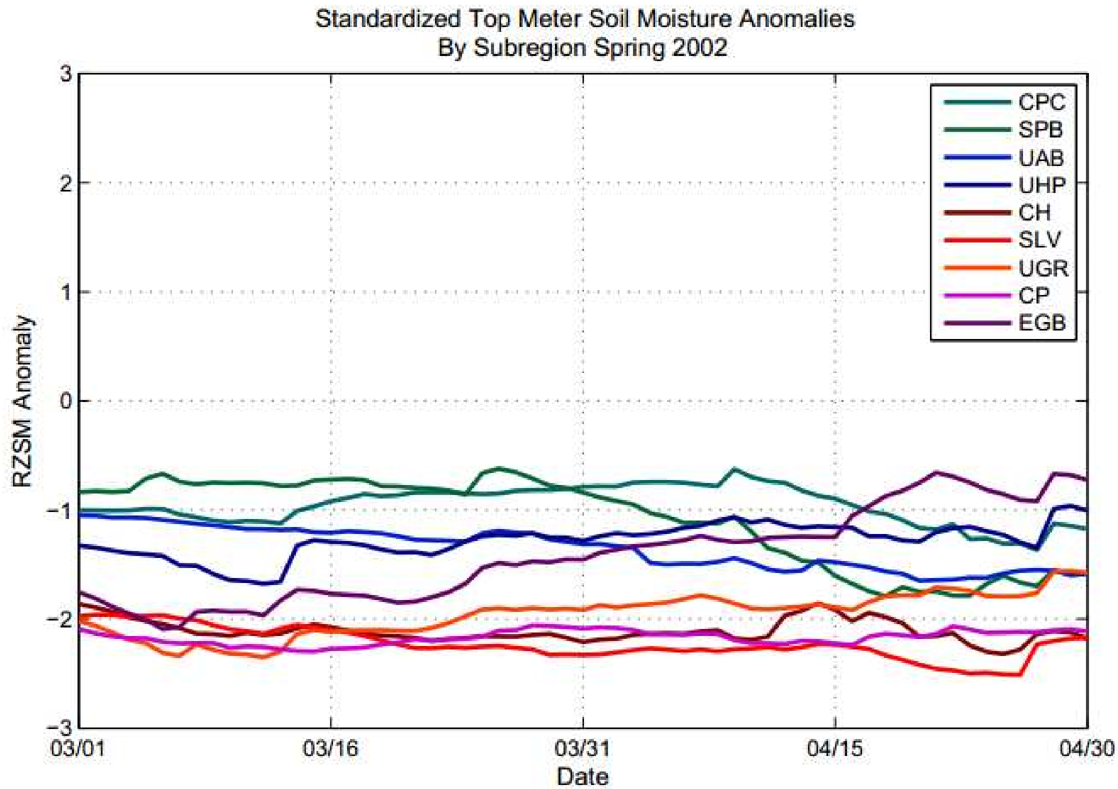

Figure 9.4: Depicted above are standardized top meter soil moisture levels for each region for the early and mid-spring of 2002. The abbreviations in the legend are the same as in figure 9.3

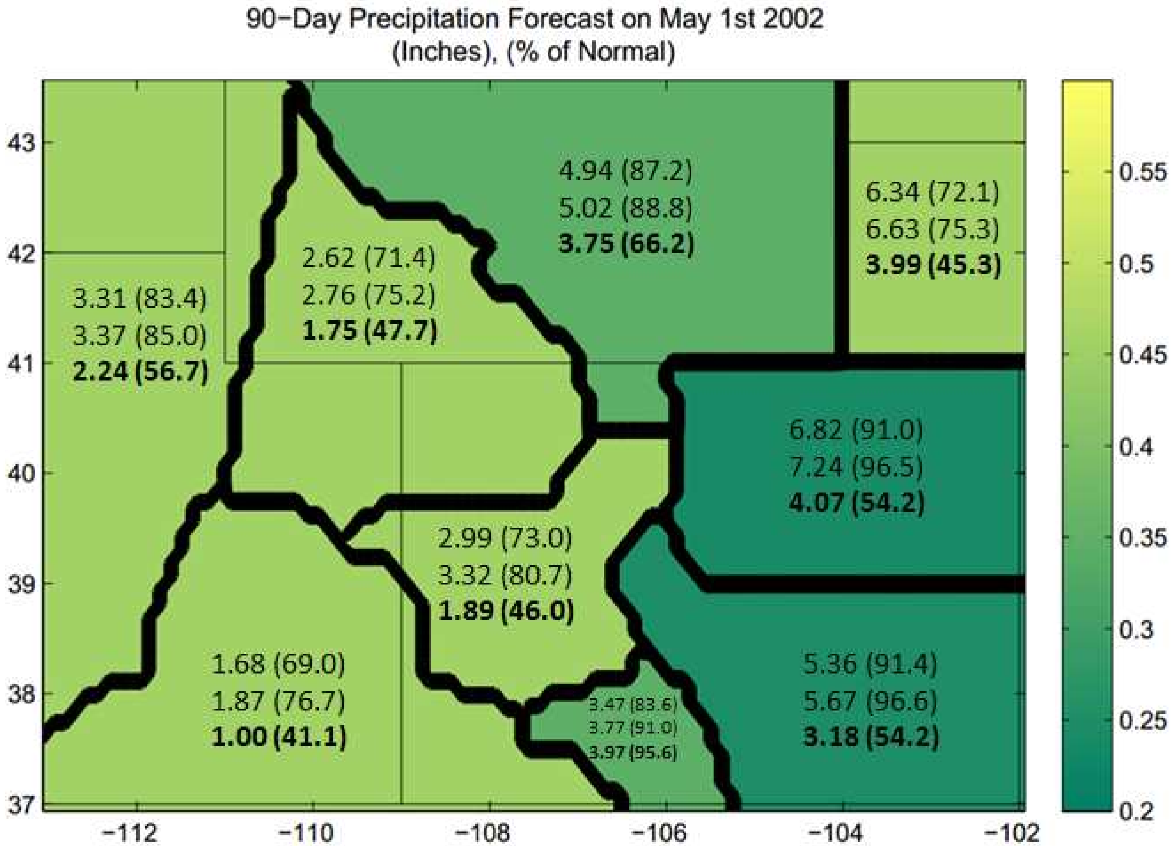

Figure 9.5: Here area-averaged mean precipitation hindcasts for May1st through July 29th of 2002 are depicted (inches, percent of normal). The top number in each basin is the hindcast precipitation amount using the entire dataset. Middle numbers for each basin are the hindcasted precipitation amount with precipitation data from the year being analyzed removed. Bottom numbers are the values that verified. The color bar shows the linear correlation scale that was used to shade the figure. The correlation between midnight May 1st RZSM and the SPI-value for the subsequent 90 days is significantly greater than zero at 90% confidence in dark-shaded regions, 95% confidence in medium-shaded regions, and 99% confidence in lightly-shaded regions. Thicker black lines delineate subbasins whereas thinner ones may just be state boundaries.

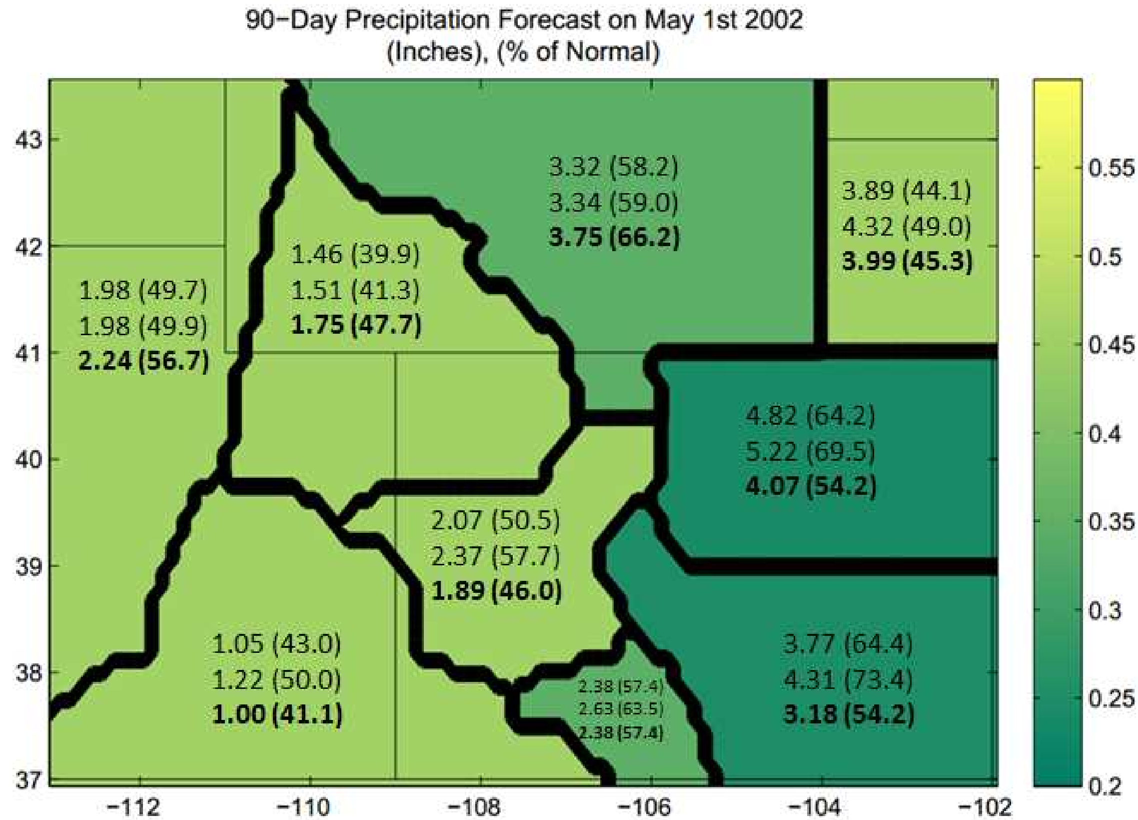

Figure 9.6: Here area-averaged 10th percentile precipitation hindcasts for May1st through July 29th of 2002 are depicted (inches, percent of normal). The top number in each basin is the hindcast precipitation amount using the entire dataset. Middle numbers for each basin are the hindcasted precipitation amount with precipitation data from the year being analyzed removed. Bottom numbers are the values that verified. The color bar shows the linear correlation scale that was used to shade the figure. The correlation between midnight May 1st RZSM and the SPI-value for the subsequent 90 days is significantly greater than zero at 90% confidence in dark-shaded regions, 95% confidence in medium-shaded regions, and 99% confidence in lightly-shaded regions. Thicker black lines delineate subbasins whereas thinner ones may just be state boundaries.

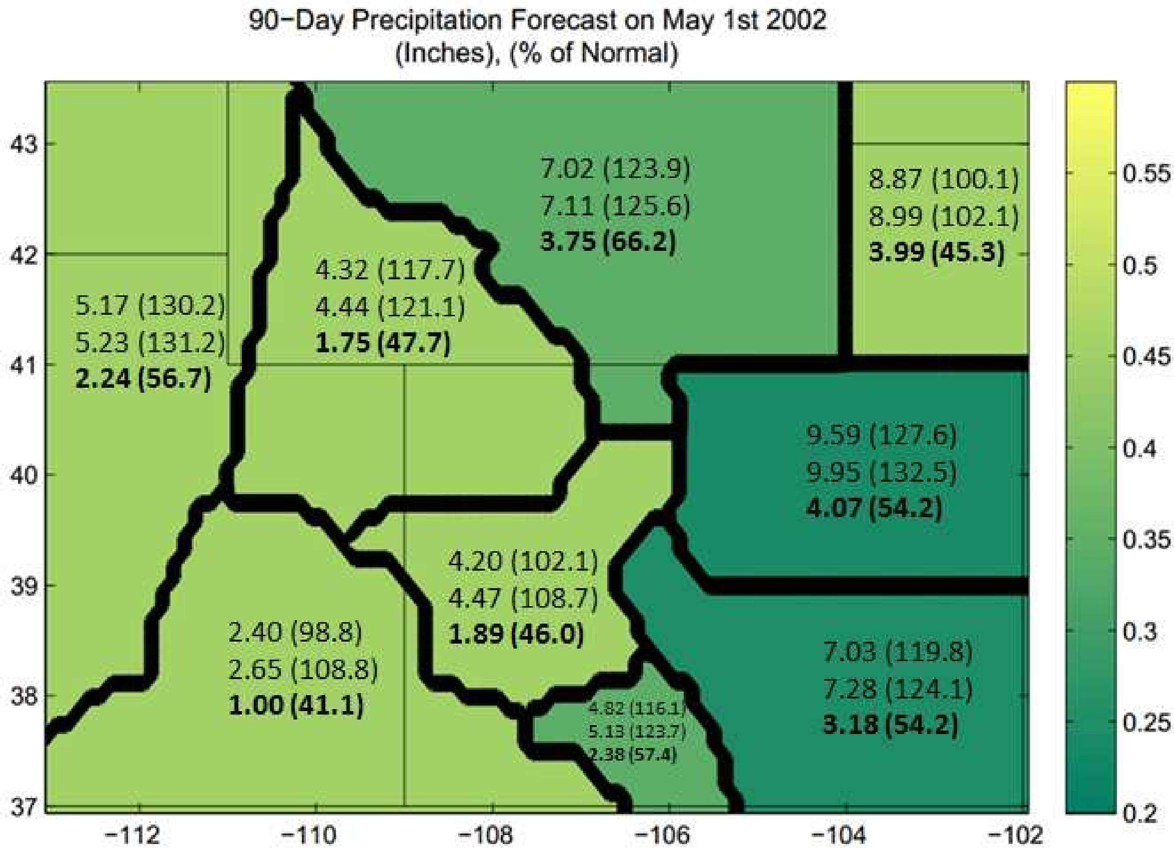

Figure 9.7: Here area-averaged 90th percentile precipitation hindcasts for May1st through July 29th of 2002 are depicted (inches, percent of normal). The top number in each basin is the hindcast precipitation amount using the entire dataset. Middle numbers for each basin are the hindcasted precipitation amount with precipitation data from the year being analyzed removed. Bottom numbers are the values that verified. The color bar shows the linear correlation scale that was used to shade the figure. The correlation between midnight May 1st RZSM and the SPI-value for the subsequent 90 days is significantly greater than zero at 90% confidence in dark-shaded regions, 95% confidence in medium-shaded regions, and 99% confidence in lightly-shaded regions. Thicker black lines delineate subbasins whereas thinner ones may just be state boundaries.

2006 Results: The epicenter of drought was a little bit to the northeast of the domain in 2006 (USDM 2006). Areas farther to the south and west within the domain such as the East Great Basin and Upper Green River Regions were sporting near or above normal soil moisture at the beginning of May. Most regions were below normal, but within one standard deviation of normal. Top meter soil moisture was the lowest farthest east within the domain, including the Central Plains Corner, South Platte, and Upper Arkansas Regions.

The performance of hindcasts for 2006 was quite variable within the domain. Hindcasts for the Colorado Headwaters and Colorado Plateau Regions were accurate within 2%, but especially in the case of the headwaters, did not add much value to a climate average hindcast. In the northeast corner of the domain median hindcasts were above the verification despite dry soils on May 1st, but did constitute large improvements over a climate hindcast, and verifications did fall within the 10th-90th percentile range of the hindcasts. Soils were rather dry turning the corner into late spring of 2006 in the Upper Arkansas Basin and San Luis Valley Regions, but in these regions precipitation actually verified above normal, so considering antecedent soil moisture conditions actually added extra error into the hindcasts. The biggest regional added error for the 2006 season was in the East Great Basin Region where soil moisture was high on May 1st, making it a true outlier. The 10th-90th percentile ranges called for anywhere from 80-180% of normal precipitation based upon having wetter than average soil, but precipitation verified at just 62.5%, proving that drought onset can still occur even when soils are wet entering the portion of the year with the most intense sunlight.

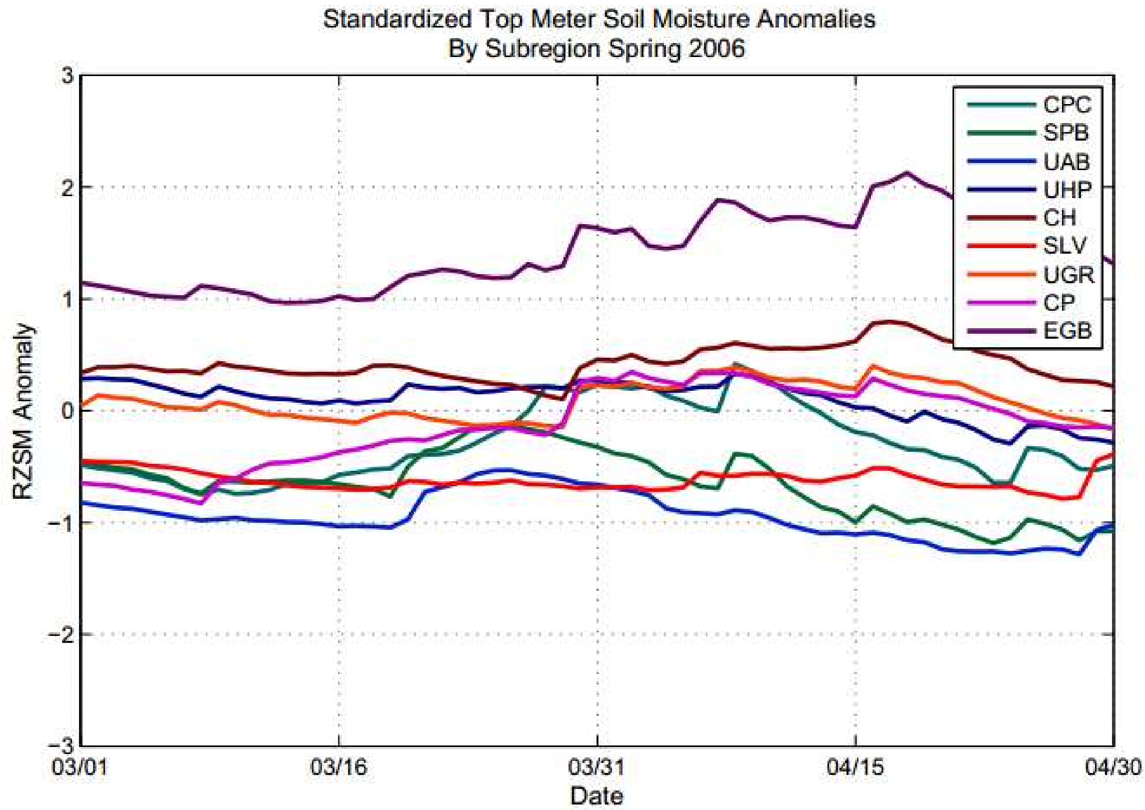

Figure 9.8: Depicted above are standardized top meter soil moisture levels for each region for the early and mid-spring of 2006. The abbreviations in the legend are the same as in figure 9.3

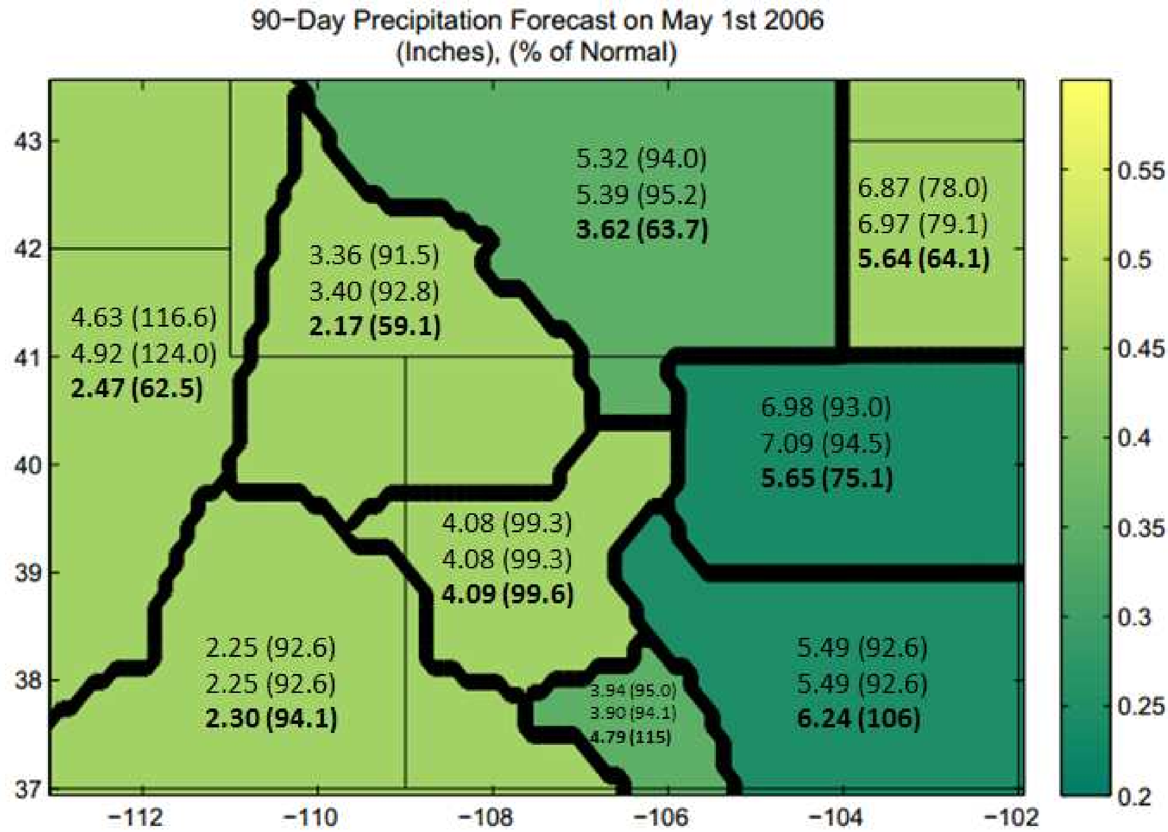

Figure 9.9: Here area-averaged mean precipitation hindcasts for May1st through July 29th of 2006 are depicted (inches, percent of normal). The top number in each basin is the hindcast precipitation amount using the entire dataset. Middle numbers for each basin are the hindcasted precipitation amount with precipitation data from the year being analyzed removed. Bottom numbers are the values that verified. The color bar shows the linear correlation scale that was used to shade the figure. The correlation between midnight May 1st RZSM and the SPI-value for the subsequent 90 days is significantly greater than zero at 90% confidence in dark-shaded regions, 95% confidence in medium-shaded regions, and 99% confidence in lightly-shaded regions. Thicker black lines delineate subbasins whereas thinner ones may just be state boundaries.

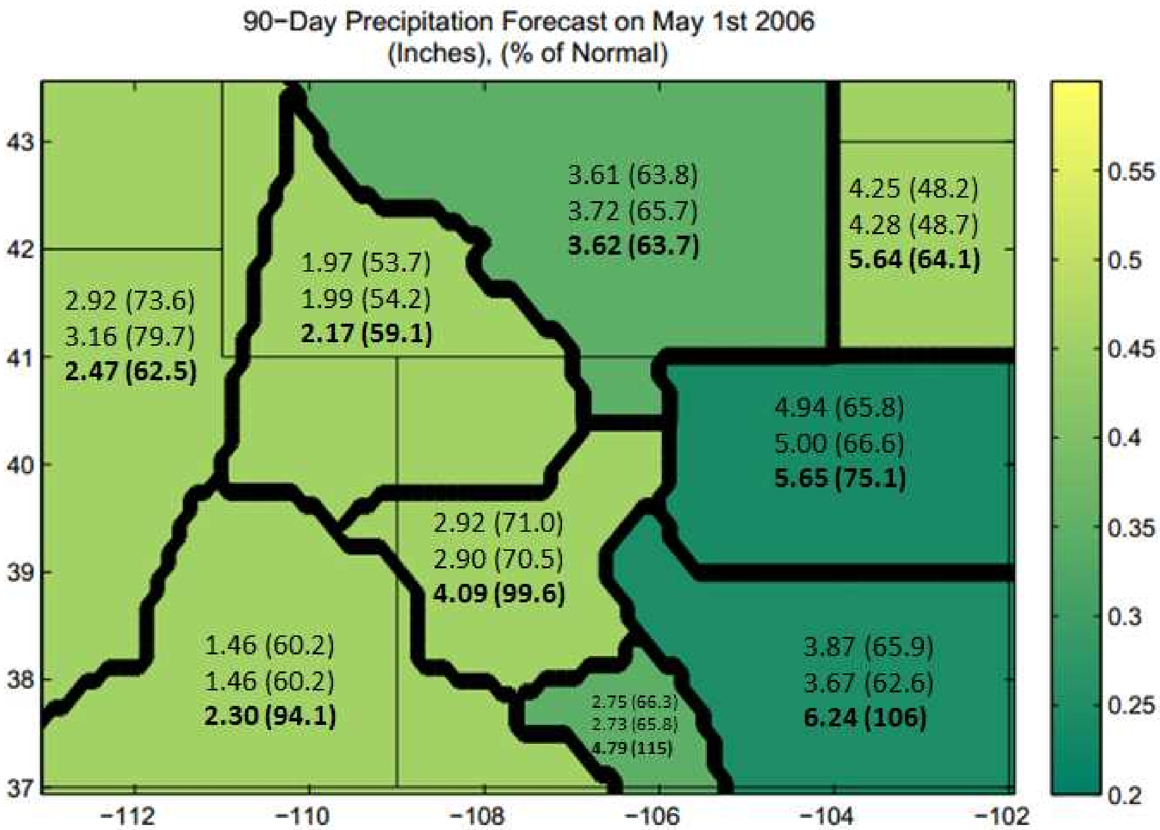

Figure 9.10: Here area-averaged 10th percentile precipitation hindcasts for May1st through July 29th of 2006 are depicted (inches, percent of normal). The top number in each basin is the hindcast precipitation amount using the entire dataset. Middle numbers for each basin are the hindcasted precipitation amount with precipitation data from the year being analyzed removed. Bottom numbers are the values that verified. The color bar shows the linear correlation scale that was used to shade the figure. The correlation between midnight May 1st RZSM and the SPI-value for the subsequent 90 days is significantly greater than zero at 90% confidence in dark-shaded regions, 95% confidence in medium-shaded regions, and 99% confidence in lightly-shaded regions. Thicker black lines delineate subbasins whereas thinner ones may just be state boundaries.

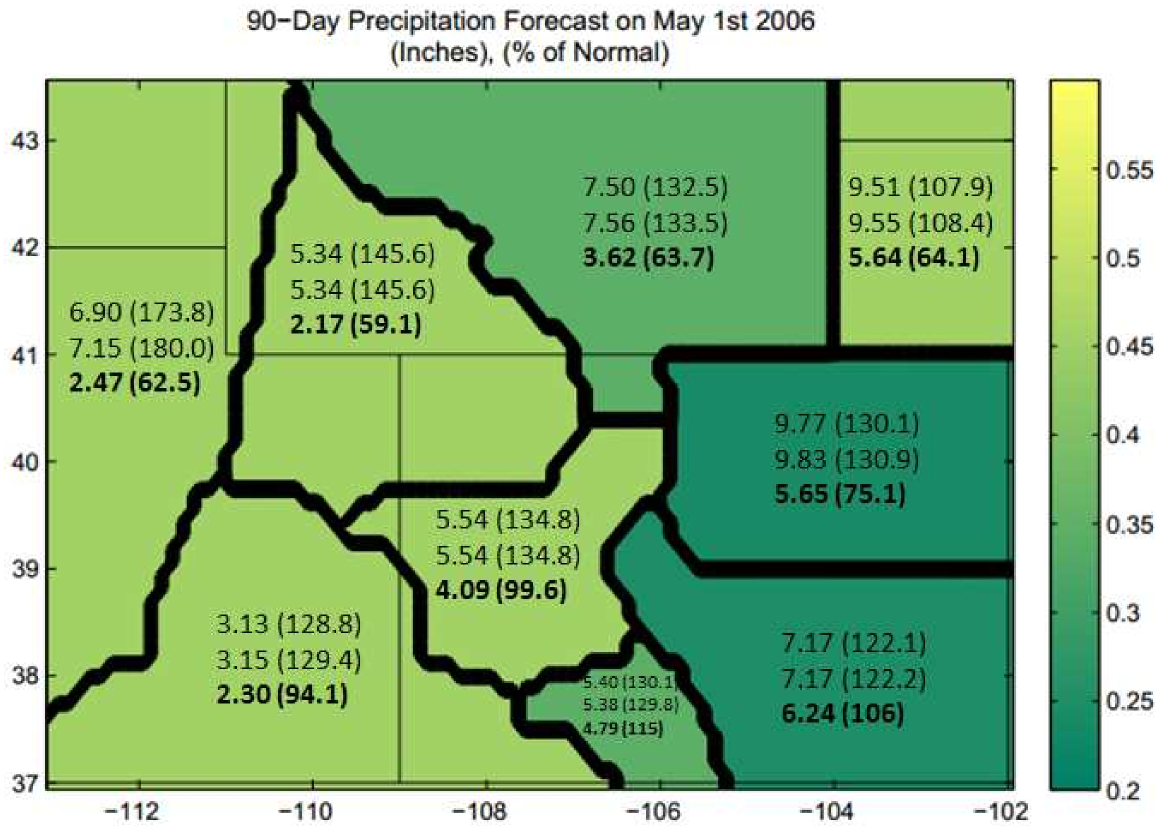

Figure 9.11: Here area-averaged 90th percentile precipitation hindcasts for May1st through July 29th of 2006 are depicted (inches, percent of normal). The top number in each basin is the hindcast precipitation amount using the entire dataset. Middle numbers for each basin are the hindcasted precipitation amount with precipitation data from the year being analyzed removed. Bottom numbers are the values that verified. The color bar shows the linear correlation scale that was used to shade the figure. The correlation between midnight May 1st RZSM and the SPI-value for the subsequent 90 days is significantly greater than zero at 90% confidence in dark-shaded regions, 95% confidence in medium-shaded regions, and 99% confidence in lightly-shaded regions. Thicker black lines delineate subbasins whereas thinner ones may just be state boundaries.

2012 Results: Soil moisture was lower than average across the entirety of the domain at the beginning of May, 2012. The Colorado Headwaters subbasin was in the worst shape within the domain at 1.6 standard deviations below normal. Northeast Colorado and the Nebraska panhandle had seen some beneficial rains in over the last week of April and recovered to near-normal levels by May 1st. The driest regions with respect to May 1st averages as defined by the last 30 years were nearer the south and west corners of the domain.

Despite a soil drying trend in March and April of 2012 soil moisture anomalies were still high enough in regions east of the Continental Divide as to offer very little hint of the severity of the precipitation deficits to come. In the Central Plains Corner Region ten of the 30 standardized RZSM anomalies on May 1st from 1985-2014 were below -0.5. In the South Platte Basin Region this is true for 11 of the 30 years. 2012 was not one of those years in either case. Precipitation verified lower than the 10th percentile hindcast in all regions east of the Continental Divide.

West of the Continental Divide RZSM levels provided a bit stronger of a warning for the dryness to come. In the Colorado Headwaters, Colorado Plateau, East Great Basin, and Upper Green River Regions precipitation verified at lower than 70% of normal across the board, but hindcasts still caught all of these values within the 10th-90th percentile range. In the Colorado Headwaters region an aggressive forecast was made as a result of a very poor snow year. The best forecasts by percent of normal were for the Colorado Plateau, or Wasatch to San Juan Region. Soil moisture in and of itself would not have accurately warned the severity of this drought in advance.

The three cases of drought examined above represent a bad drought that was exacerbated through below normal summer precipitation (2002), a summer where the epicenter of drought conditions shifted (2006), and a rapid drought onset in the early growing season that impacted the entire domain and beyond (2012). Of these three scenarios precipitation hindcasts were best for the 2002 drought where RZSM was already much lower than normal at the start of May, and low precipitation followed suit. The worst performance of the three cases for the northwest and southeast portions of the domain was 2006 where the epicenter of drought shifted northwest from the beginning of May to the end of July. Hindcasts added substantial value to a climate hindcast for the southwest, central, and northeast portions of the domain in 2006. In 2012 antecedent soil moisture was low across the entire domain, but not as low as 2002. This correctly led to domain-wide 90-day hindcasts for than normal (81-99% of average) precipitation. What verified was much lower still (36-63% of average).

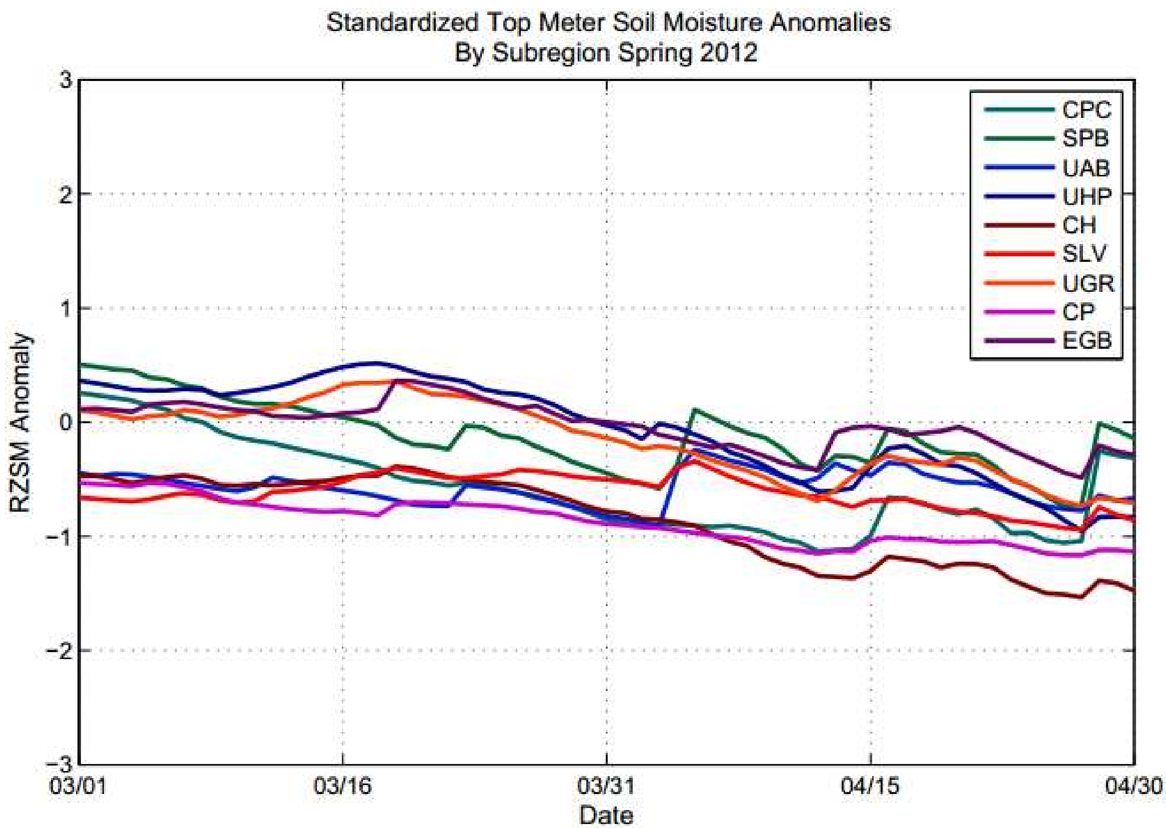

Figure 9.12: Depicted above are standardized top meter soil moisture levels for each region for the early and mid-spring of 2012. The abbreviations in the legend are the same as in figure 9.3

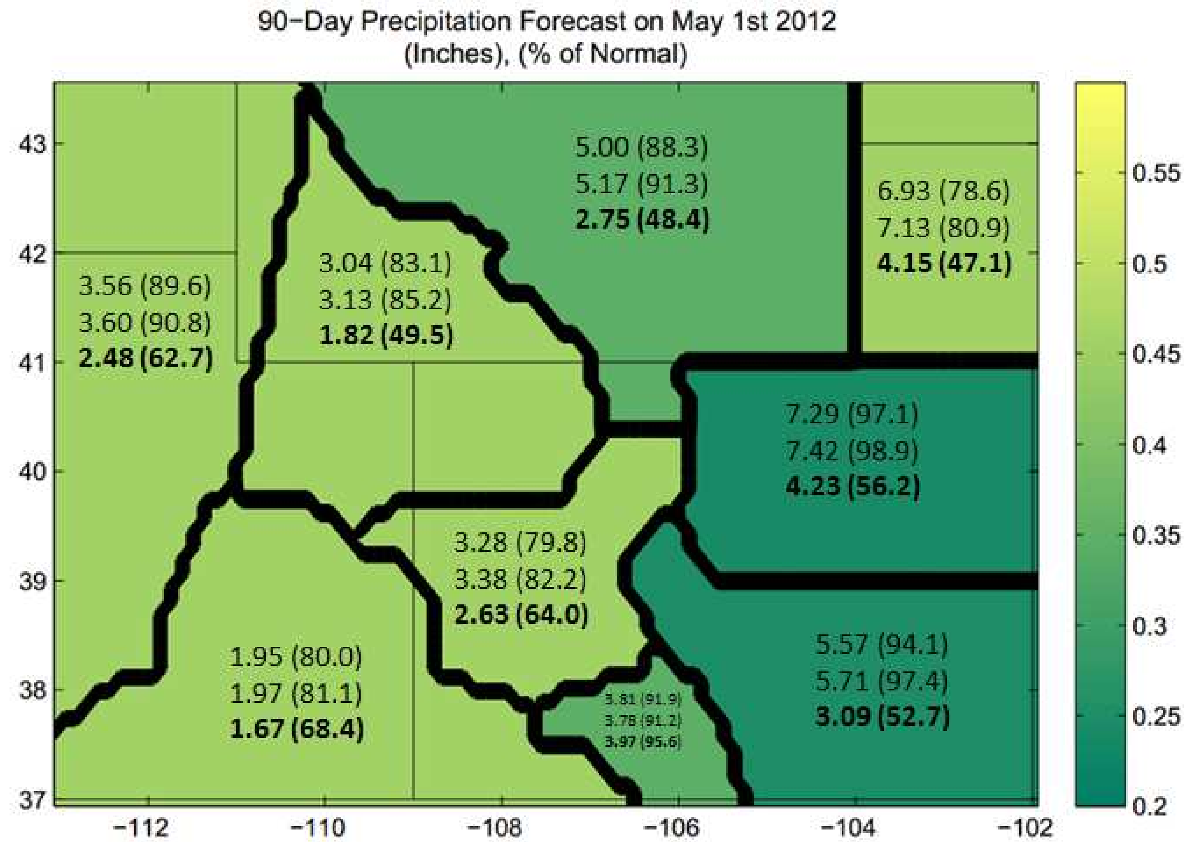

Figure 9.13: Here area-averaged mean precipitation hindcasts for May1st through July 29th of 2012 are depicted (inches, percent of normal). The top number in each basin is the hindcast precipitation amount using the entire dataset. Middle numbers for each basin are the hindcasted precipitation amount with precipitation data from the year being analyzed removed. Bottom numbers are the values that verified. The color bar shows the linear correlation scale that was used to shade the figure. The correlation between midnight May 1st RZSM and the SPI-value for the subsequent 90 days is significantly greater than zero at 90% confidence in dark-shaded regions, 95% confidence in medium-shaded regions, and 99% confidence in lightly-shaded regions. Thicker black lines delineate subbasins whereas thinner ones may just be state boundaries.

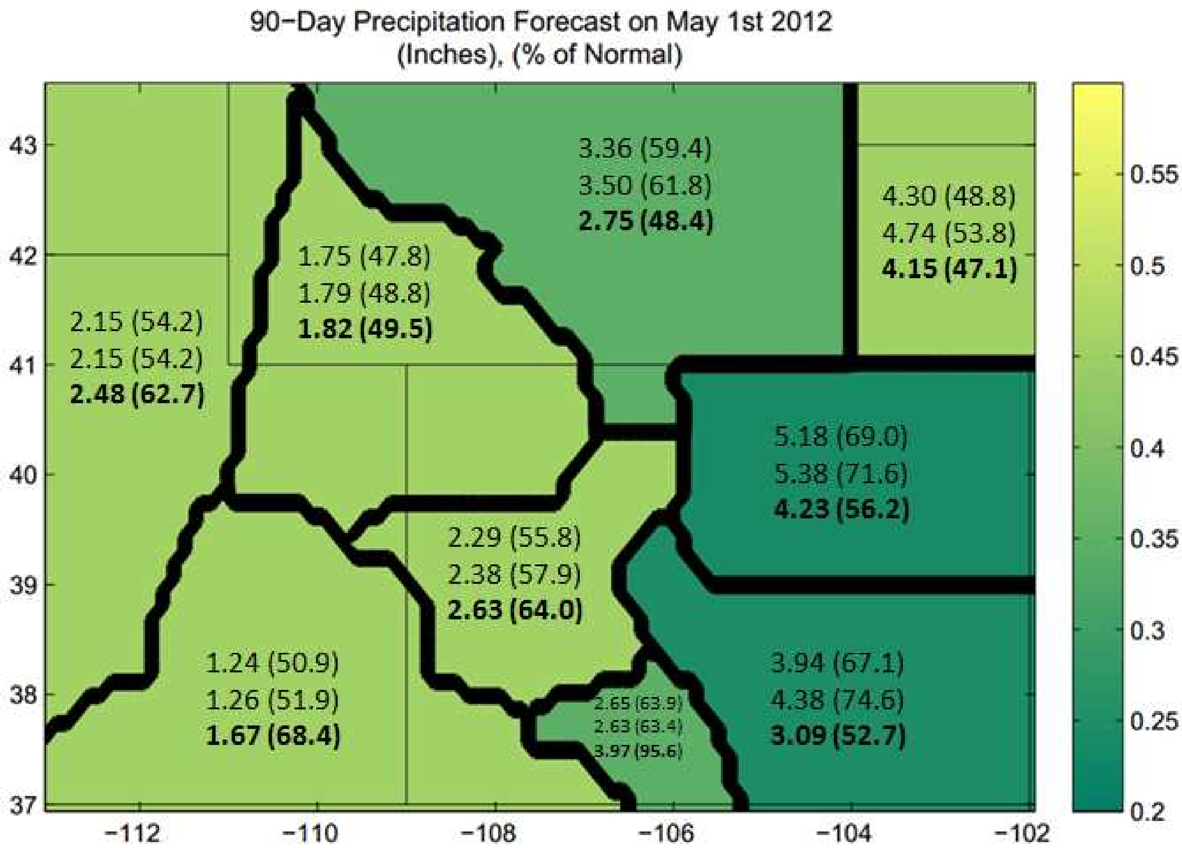

Figure 9.14: Here area-averaged 10th percentile precipitation hindcasts for May1st through July 29th of 2012 are depicted (inches, percent of normal). The top number in each basin is the hindcast precipitation amount using the entire dataset. Middle numbers for each basin are the hindcasted precipitation amount with precipitation data from the year being analyzed removed. Bottom numbers are the values that verified. The color bar shows the linear correlation scale that was used to shade the figure. The correlation between midnight May 1st RZSM and the SPI-value for the subsequent 90 days is significantly greater than zero at 90% confidence in dark-shaded regions, 95% confidence in medium-shaded regions, and 99% confidence in lightly-shaded regions. Thicker black lines delineate subbasins whereas thinner ones may just be state boundaries.

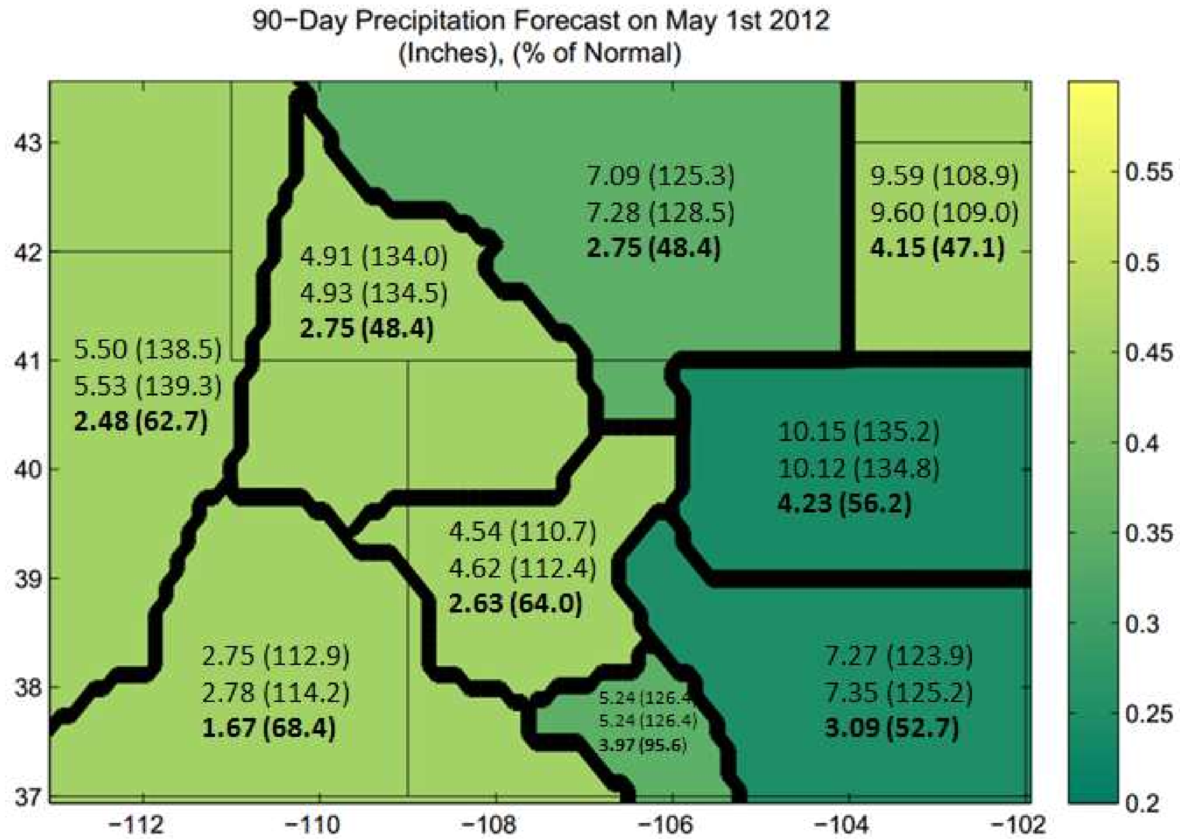

Figure 9.15: Here area-averaged 90th percentile precipitation hindcasts for May1st through July 29th of 2012 are depicted (inches, percent of normal). The top number in each basin is the hindcast precipitation amount using the entire dataset. Middle numbers for each basin are the hindcasted precipitation amount with precipitation data from the year being analyzed removed. Bottom numbers are the values that verified. The color bar shows the linear correlation scale that was used to shade the figure. The correlation between midnight May 1st RZSM and the SPI-value for the subsequent 90 days is significantly greater than zero at 90% confidence in dark-shaded regions, 95% confidence in medium-shaded regions, and 99% confidence in lightly-shaded regions. Thicker black lines delineate subbasins whereas thinner ones may just be state boundaries.

Results (all dry years): Examining case studies that involve drought onset or exacerbation certainly has merit as it can help determine if those droughts could have been warned better using antecedent RZSM conditions. However, it fails to show the folly of forecasting seasonal precipitation using just antecedent soil moisture conditions when so much scatter exists. In considerable percentage of years making a forecast this way would induce extra error over simply forecasting the climate average. In order to more objectively consider the value added the average percent improvement was calculated for each subbasin for 90-day hindcasts initialized at every day from March 1st-June 1st, and is depicted in figure 9.16. This tells us a couple of useful pieces of information: It shows which basins are best suited for seasonal forecast improvement when soils are dry in the spring and by how much, and at what point in the season making forecasts for each region will be most beneficial.

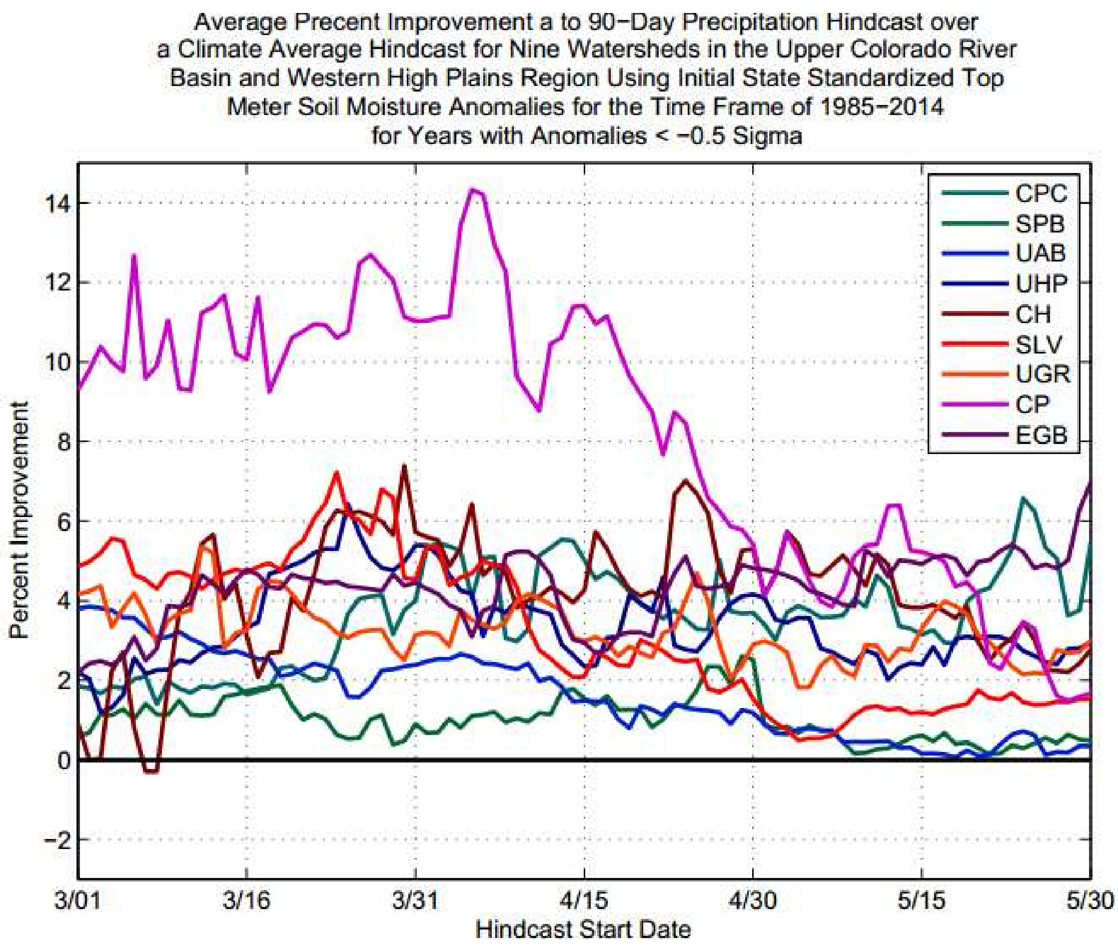

Figure 9.16: Depicted above is the average percent improvement made to precipitation hindcasts over simply predicting 100% of the 1985-2014 average as a function of what day the hindcast is initialized. The abbreviations in the legend are the same as in figure 9.3

The Colorado Plateau Region displayed the most average improvement over a climate average hindcast. Most regions The South Platte Basin and Upper Arkansas Basin scarcely showed any improvement when considering soil moisture anomaly at the beginning of the hindcast. The Upper Arkansas Basin indicates modest improvement ~4% is possible when making a hindcast early (beginning of March). It was surprising to see the value added from considering initial soil moisture anomalies fall off from a hindcast generated in the middle of April to one generated in the middle of May for the Colorado Headwaters Region. It would have been reasonable to hypothesize that post-snowmelt soil moisture values are more indicative of what's to come. 90-day SPI hindcasts based on antecedent soil moisture conditions reveals some latitudinal dependence to when RZSM has the most influence over future precipitation totals. Regions farther north such as the East Great Basin and Central Plains Corner Regions showed increasing value added for hindcasts made starting at the end of May and beginning of June. For farther south regions such as the Upper Arkansas Basin and Colorado Plateau (Wasatch to San Juan) Regions value added decreases for hindcasts made in May versus earlier in the Spring. Likewise, of the two regions of highest elevation the value added to forecasts peaks for the Colorado Headwaters Region later than for the San Luis Valley Region. This offers support for the hypothesis that areas farther north tend to enter a more moisture-limited regime later in the year climatologically.

The relationship between root zone soil moisture and precipitation shines through with great confidence, however RZSM only improves seasonal precipitation forecasts a fraction one way or the other, and is low in comparison with background variation in seasonal precipitation. There is a spread in the magnitude of this fraction within the domain, but in no area can RZSM levels accurately forecast the precipitation deficits necessary to advance into a severe or extreme drought moving into the growing season. RZSM data can be used as a red flag to suggest an increased probability of future degradations, but should not be used to advance drought severity category beyond its current state at any time. There may be lots value to a flagging system that identifies areas in increased danger of slipping into extreme drought, however, advancing current classifications based on high warning of future drought would lead to instances of the drought monitor "crying 'wolf,'" even in the late spring and early meteorologic summer when soil moisture and precipitation are the most strongly coupled.

CONCLUSIONS

Upper Colorado River Basin and eastern Colorado drought monitoring was found to is done by assimilating atmospheric and land surface data from a multitude of sources and assigning a percentile ranking to the hydrologic system to a given area based on how current data compare to climatology. The decision-making process includes assessment of precipitation, soil moisture, snowpack, vegetative health, streamflow, reservoir levels, reference evapotranspiration, surface air temperature, and ground reports from the regional agricultural sector. Drought monitoring was expanded upon in this research through the development of several products intended for future Colorado Climate Center use. In-situ soil moisture timeseries are now being created from select SNOTEL and SCAN measurement sites. Reservoir monitoring graphics are being produced to accompany spatial analyses downloaded from the bureau of reclamation. More soil moisture data is being used, and now come from an ensemble of models rather than just the VIC model.

The NLDAS Phase-2 dataset provides information for a multitude of variables that are of interest to the drought monitoring community that can be standardized in a way similar to precipitation with the SPI assessed with a percentile ranking, and mapped at a resolution appropriate for the process. This dataset should not be the only dataset used for the process, and should be checked against data not assimilated in the NARR for best results.

In-situ SNOTEL soil moisture measurements were analyzed over the 2004 to 2013 period for the Colorado Rockies. A typical seasonal cycle of rocky mountain soil moisture was identified, but any given single station is likely to see large deviations from this seasonal cycle throughout the course of the year. Volumetric water content levels were found to be near-constant during meteorologic winter as well as the beginning of Spring and the end of Fall. This is related to persistent snowpack blocking interaction between the land surface and atmosphere. Volumetric water content values characteristically rose between mid-March and mid-May as this is the time of year in which snowmelt is occurring. This sign reverses in mid-May through early July as high evapotranspiration rates lead to diminishing moisture reserves. In the mean state some recharge of soils is expected during late July and August, but this condition is dependent on receiving favorable moisture in association with a monsoonal circulation. In September precipitation rates are characteristically higher than evapotranspiration rates in a net sense. Some of the largest seasonal anomalies in Rocky Mountain root zone soil moisture over the 2004-2013 period occurred in 2009, 2012, and 2013. These anomalies were associated, with later than average soil moisture depletion, drought, and flooding respectively.

The Christman Field weather station was equipped with both Stevenswater and CS650 reflectometers in order to obtain in-situ measurements of root zone soil moisture, and to compare output from soil moisture measuring stations operated by CoAgMet and SNOTEL. These data will be useful going forward for tracking RZSM locally. Uncalibrated Campbell Scientific 650 Relfectometers do not appear to be suitable for side-by-side comparison with factory LOAM setting Stevens Water Hydra Probes. The uncalibrated reflectometers appear to be more subject to temperature biases as evidenced by the seasonal and diurnal cycles implicit in the readings taken at Christman Field during 2015. There will be follow-up communication with Campbell's Scientific to investigate how best to calibrate these sensors as they are well-reviewed, and should not be discredited based on this research alone.

Replicating soil moisture measurements with a factory loam calibration using gravimetric measuring techniques proved difficult, and consensus between the two does not necessarily imply a correct measurement. Ground validation in terms of both material and opportunity cost will be more expensive/observing station than measurement of rain, hail, or snow, and is subject to large errors that cannot be as easily quality controlled as rain, hail, snow, or reference evapotranspiration due to differences in soil type that change rapidly in space. The pool of potential volunteers is likely only a small subset of the CoCoRaHS community who has the time and unirrigated land available to participate.

A soil moisture protocol is ready to be expanded to aCoCoRaHS volunteer alpha testers around the country. This protocol involves estimating local soil type, using a brass ring to take soil cores of a consistent volume, and oven drying the sample to find its volumetric water content. Assuming alpha testers are already equipped with an oven participation is estimated only to cost $50. Volunteers around the nation are ready to sign up.

It currently appears unlikely that CoCoRaHS will be able to guarantee gravimetric soil moisture measurements within 10% difference of the true volumetric water content as desired for ground validation by the SMAP team if the Stevenswater Hydra Probe relay at Christman Field is used as the standard for accuracy. It does appear to be possible for CoCoRaHS to assemble at least a small, savvy, and ambitious team of volunteers across the country to supply gravimetric measurements using a variation of the final protocol drafted in chapter five that pass the reasonability test. These data can then be made available to end data users such as USDA, SMAP, etc and subject to whatever quality control processes the end data user may have. The measurements taken can be considered as ground truth at the end data users' own risk.

As suggested in the GLACE project (Koster et al 2004) warm season precipitation in North America can be separated into two regimes: a moisture-limited regime in which precipitation is constrained primarily by RZSM, and an energy-limited regime in which precipitation is constrained by solar energy. Areas that are in the relatively narrow transition zone in between the two see the most influence from soil moisture over seasonal precipitation. Within the domain studied from -113.063 to -101.938 degrees in longitude and from 36.938 to 43.563 degrees in latitude relationships between RZSM and future precipitation were not constant with space or with season. There is a climatological expectation that conditions within the domain will advance into the moisture-limited regime mostly within the first half of the warm season starting from the southwest and moving to the northeast, and also starting from low elevations to high elevations.

Data from 1985-2014 do indicate strong confidence in relationships between RZSM and future temperatures, precipitation, and water balance anomalies that peak in the May through July time frame. Projections made based on these relationships are limited by a number of factors: 1. NLDAS-Phase 2 is too coarse a model to fully resolve surface slopes, vegetation coverage, and soil type, so land-atmosphere interaction is subject to error. 2. The magnitude of anomaly that corresponds to a transition between a moisture-limited and energy-limited regime is not spatially or temporally constant. 3. Projections made based on a 30-year climatology are still subject to an over-fitting bias. 4. The relationship between modeled RZSM and future SPIs and SPEIs is largely a function of model resolution. The resolution at which this relationship maximizes is not known, and is unlikely to be spatially or seasonally constant, but it maximizes at a coarse enough resolution that changes to the relationship based on elevation will be largely muted. Despite these limitations, projections made using SPIs and SPEIs did offer improvements over climatology-based hindcasts/forecasts at timescales beyond the reliability of numerical weather prediction models. The findings could be used to help implement a flagging system that identifies locations at greater risk of slipping into more severe drought, but should not be used to advance the drought classification beyond the current appraisal of the hydrologic system due to the amount of scatter in the relationship that exists.

To further improve drought monitoring capabilities it is recommended that future analysis be done between standardized RZSM levels and other atmospheric variables that act as controls on potential evapotranspiration. It is also recommend that more extensive study be conducted on how model and observation RZSM values line up while regressing into drought. It is possible that observations may advance drying trends such as in the spring of 2012 more rapidly than the land data assimilation models used in this study.

Findings from this research will be used to improve the National Integrated Drought Information System early warning process in the Upper Colorado River Basin and eastern Colorado region, and be shared with the drought community at large, hopefully to do the same.

REFERENCES

Al Bitar, Ahmad. "Evaluation of SMOS Soil Moisture Products Over Continental U.S. Using the SCAN/SNOTEL Network. *IEEE Transactions on Geoscience and Remove Sensing ` (Volume 50, Issue 5).* Pages 1572-1586. May 2012.

American Meteorological Society, cited 2015: Drought. Glossary of Meteorology. [Available online at http://glossary.ametsoc.org/wiki/drought

Bailey, R.G. *Ecoregions of the United States*. USDA Forest Service. 1994.

B. J. Cosby, G. M. Hornberger, R. B. Clapp, T. R. Ginn, "A Statistical Exploration of the Relationships of Soil Moisture Characteristics to the Physical Properties of Soils." *Water Resources Research, Vol. 20 NO 6,* Pages 682-690, June 1984

Bjerknes, V. Solberg, H. "Life Cycle of Cyclones and the Polar Front Theory of Atmospheric Circulation." May 1922.

Bonan, Gordon. "Ecological Climatology Concepts and Applications." National Center for Atmospheric Research. Second Edition. 2008.

Brown, Jesslyn F., Wardlow, Brian D., "Drought Monitoring with VegDRI." United States Geological Survey. 2009.

Brown, Peter M., Emily K. Heyerdahl, Stanley G. Kitchen, and Marc H. Weber. "Climate Effects on Historical Firest (1630-1900) in Utah." *International Journal of Wildland Fire* 17.1 (2008); 28-39.

Clapp, Roger B, Hornberger, George M, "Empirical Equations for Some Soil Hydraulic Properites." *Water Resources Research, Vol 14 NO 4.* August 1978

Colorado Climate Center – Drought. ccc.atmos.colostate.edu/~drought. September 14, 2015.

Crosby, B. J., Hornberger, G. M., Clapp, R. B., Ginn, T. R. "A Statistical Exploration of the Relationships of Soil Moisture Characteristics to the Physical Properties of Soils." *Water Resources Research, Vol 20 No 6.* June, 1984.

Darcy, H. Les Fontaines Publiques de la Ville de Dijon, Dalmont, Paris. 1856.

"Dielectric Permittivity." *The Hydra Probe Soil Sensor.* Stevenswater. July, 2007.

Dines, J. S. "Life Cycle of Cyclones and the Polar Front Theory of Atmospheric Circulation. By J. Bjerknes and H. Solberg. Kristiania, Geophysisks Publikationer, 3, 1922, No. 1. Pp. 18. 4°. Price 2 Kr." *Quarterly Journal of the Royal Meteorological Society Q.J.R. Meteorol. Soc.* 49.206 (1923): 140-41.

Douglas, Michael W., Robert A. Maddox, Kenneth Howard, and Sergio Reyes. "The Mexican Monsoon." *Journal of Climate J. Climate* 6.8 (1993): 1665-677.

Fedor Mesinger, Geoff DiMego, Eugenia Kalnay, Kenneth Mitchell, Perry C. Shafran, Wesley Ebisuzaki, Dusan Jovic, Jack Woollen, Eric Rogers, Ernesto H. Berbery, Michael B. Ek, Yun Fan, Robert Grumbine, Wayne Higgins, Hong Li, Ying Lin, Geoff Manikin, and Wei Shi. 2006: North American Regional Reanalysis. Bulletin of the American Meteorological Society: Vol.87, No. 3, pp. 343-360.

Gershunov, Alexander, and Tim P. Barnett. "ENSO Influence on Intraseasonal Extreme Rainfall and Temperature Frequencies in the Contiguous United States: Observations and Model Results." *Journal of Climate J. Climate* 11.7 (1998): 1575-586.

Gochis et al. “The Great Colorado Flood of September 2013.” *Bulletin of the American Meteorological Society volume 96, Issue 9.* September 2015.

“Gravimetric and Volumetric Soil Moisture Protocols.” SMAP – GLOBE.gov. 2014.

Henz, John Francis. “Colorado High Plains Thunderstorm Systems: A Description Radar-synoptic Climatology.” 1974.

“High Plains Regional Climate Center.” *ACIS Climate Maps*. High Plains Regional Climate Center. 16 Sept. 2015.

Hillel, Daniel. “General Physical Characteristics of Soils.” *Fundementals of Soil Physics.* July, 1980.

Hobbins, Mike. “The Evaporative Demand Drought Index, EDDI.” Cooperative Institute for Research in Environmental Sciences. University of Colorado Boulder and NOAA. [Information made available during drought monitor webinar June 8th, 2015].

Holton, James R. *An Introduction to Dynamic Meteorology.* New York: Academic, 1972.

Hualan R., Mocko D. “Readme Document for North American Land Data Assimilation System Phase 2.” Goddard Earth Sciences Data and Information Services Center. Revised March 2014.

“The Hydra Probe Soil Sensor.” Stevens Water Monitoring Systems Inc. July, 2007.

IPCC**,** 2014: *Climate Change 2014: Impacts, Adaptation, and Vulnerability. Part A: Global and Sectoral Aspects. Contribution of Working Group II to the Fifth Assessment Report of the Intergovernmental Panel on Climate Change* [Field, C.B., V.R. Barros, D.J. Dokken, K.J. Mach, M.D. Mastrandrea, T.E. Bilir, M. Chatterjee, K.L. Ebi, Y.O. Estrada, R.C. Genova, B. Girma, E.S. Kissel, A.N. Levy, S. MacCracken, P.R. Mastrandrea, and L.L. White (eds.)]. Cambridge University Press, Cambridge, United Kingdom and New York, NY, USA, 1132 pp.

Jackson, Thomas J. “Measuring Surface Soil Moisture Using Passive Microwave Remote Sensing.” *Hydrological Processes* vol 7. 139-152. 1993.

Justus, C. G., W. R. Hargraves and A. Yaloin,1976: “Nationwide Assessment of Potential Output from Wind-Powered Generators.” *Journal of Applied Meteorology*., 17, 350-353.

Koster, R. D. et al. “Regions of Strong Coupling Between Soil Moisture and Precipitation.” *Science* 305.5687 (2004): 1138-1140.

Lorenzo-Lacruz, J., Sm Vicente-Serrano, Jc González-Hidalgo, Ji López-Moreno, and N. Cortesi. "Hydrological Drought Response to Meteorological Drought in the Iberian Peninsula." *Climate Research Clim. Res.* 58.2 (2013): 117-31.

MATLAB and Statistics Toolbox Release 2013a, The MathWorks, INC., Natrick, Massachusetts, United States

McKee, Thomas B., Doesken, Nolan J., Kleist, John. “The Relationship of Drought Frequency and Duration to Time Scales.” *Eighth Conference on Applied Climatology.* 17-22 January 1993, Anaheim, CA. Colorado State University.

Myong, Boksoon, Nielsen-Gammon, John-W. “The Convective Instability Pathway to Warm Season Drought in Texas. Part: The Role of Convective Inhibition and Its Modulation of Soil Moisture.” *J. Climate*, 23, 4461-4473. 2010

“Overview.” *CS650 and CS655 Water Content Reflectometers.* Campbell Scientific Inc. 2011. Revised May, 2015

“PRISM Climate Group, Oregon State University.” PRISM Climate Group. 2015.

Ramley, F. “Plant Zones in the Rocky Mountains of Colorado.” *Science* 26.671 (1907): 642-43.

Reges, Henry W., Doesken, Nolan J., Tuner, Julian, Newman, Noah, Bergantino, Antony, Schwalbe, Zach. “COCORAHS: The Evolution and Accomplishments of a Volunteer Rain Gauge Network.” *Bulletin of the American Meteorological Society.* 2016.

Rocca, Monique E., Peter M. Brown, Lee H. Macdonald, and Christian M. Carrico. "Climate Change Impacts on Fire Regimes and Key Ecosystem Services in Rocky Mountain Forests." *Forest Ecology and Management* 327 (2014): 290-305.

Ropelewski, C. F., and M. S. Halpert. "North American Precipitation and Temperature Patterns Associated with the El Niño/Southern Oscillation (ENSO)." *Mon. Wea. Rev. Monthly Weather Review* 114.12 (1986): 2352-362.

Seyfried et. al. “Dielectric Loss and Calibration of the Hydra Probe Soil Water Sensor.” *Vadose Zone Journal.* 1070-1079. November 16, 2005.

TAMU North American Soil Moisture Database. Soilmoisture.tamu.edu. 2015.

“Temperature Corrections.” *The Hydra Probe Soil Sensor.* Stevenswater. July, 2007.

Tsakiris, G., D. Pangalou, and H. Vangelis. "Regional Drought Assessment Based on the Reconnaissance Drought Index (RDI)." *Water Resour Manage Water Resources Management* 21.5 (2006): 821-33.

"Upper Colorado Region." Bureau of Reclamation. United States Department of the Interior, 8 June 2010. 19 Aug. 2015.

"U.S. Drought Monitor Background." *Background*. National Drought Mitigation Center, University of Nebraska-Lincoln, United States Department of Agriculture, National Oceanic and Atmospheric Administration, 18 Aug. 2015.

"U.S. Drought Monitor Map Archive." *Map Archive.* National Drought Mitigation Center, University of Nebraska-Lincoln, United States Department of Agriculture, National Oceanic and Atmospheric Administration, 18 Aug. 2015.

Vicente-Serrano, Sergio M., Santiago Beguería, and Juan I. López-Moreno. "A Multiscalar Drought Index Sensitive to Global Warming: The Standardized Precipitation Evapotranspiration Index." *Journal of Climate J. Climate* 23.7 (2010): 1696-718.

Vicente-Serrano, S. M., and J. I. López-Moreno. "Hydrological Response to Different Time Scales of Climatological Drought: An Evaluation of the Standardized Precipitation Index in a Mountainous Mediterranean Basin." *Hydrol. Earth Syst. Sci. Hydrology and Earth System Sciences* 9.5 (2005): 523-33.

"Water Content Reflectometer Method for Measuring Volumetric Water Content." *CS650 and CS655 Water Content Reflectometers.* Campbell Scientific Inc. 2011. Revised May, 2015

":Web Soil Survey." Natural Resources Conservation Services, United States Department of Agriculture. 2015.

Weier, John, Herring, David. "Measuring Vegetation (NDVI & EVI). Earth Observatory/Features. National Aeronautics and Space Administration. 2000.